Getting grip on glucocorticoid-induced metabolic derangements

Anke Jourika Laskewitz

The research described in this thesis was conducted at the Department of Pediatrics, University Medical Center Groningen, University of Groningen, Groningen, The Netherlands.

The research described in this thesis was financially supported by TiPharma, project T1-106 'Glucocorticoid-induced insulin resistance'.

Printing of this thesis was financially supported by:
The University of Groningen
University Medical Center Groningen
Groningen University Institute for Drug Exploration
MSD
Greiner Bio-One B.V.
Astma Fonds
Diabetes Fonds

ISBN (printed): 978-90-367-5351-7
ISBN (digital): 978-90-367-5352-4

Layout: The outsiders
Cover design: M. Daalmans, I. Kuipers & A.J. Laskewitz
Printed by: CPI Wöhrman Print Service

rijksuniversiteit groningen

Getting grip on glucocorticoid-induced metabolic derangements

Proefschrift

ter verkrijging van het doctoraat in de
Medische Wetenschappen
aan de Rijksuniversiteit Groningen
op gezag van de
Rector Magnificus, dr. E. Sterken,
in het openbaar te verdedigen op
woensdag 8 februari 2012
om 16:15 uur

door

Anke Jourika Laskewitz

geboren op 9 februari 1982
te Leeuwarden

Promotores:	Prof. dr. F. Kuipers
	Prof. dr. A.K. Groen
Beoordelingscommissie:	Prof. dr. M. Diamant
	Prof. dr. G. van Dijk
	Prof. dr. J.P. Tuckermann

Voor pap en mam

Paranimfen: Fardau Marije Laskewitz
Annemieke Meijer

Table of contents

1

General Introduction

Anke J. Laskewitz

Scope of the thesis

Synthetic glucocorticoids (GCs), such as prednisolone and dexamethasone, are potent anti-inflammatory drugs that are widely prescribed for the treatment of chronic inflammatory diseases, like rheumatoid arthritis, inflammatory bowel disease and asthma. However, their use is hampered by the serious adverse effects that accompany chronic GC-treatment. These side effects include weight gain due to central adiposity, dyslipidemia, hypertension, osteoporosis, mood disorders, skin thinning, muscle wasting, acne, glucose intolerance and insulin resistance. The endogenous glucocorticoid cortisol plays an essential role in maintaining blood glucose homeostasis. Circulating cortisol levels are under tight control of the hypothalamus-pituitary-adrenal gland axis. To accomplish homeostasis, GCs act on many different tissues and the glucocorticoid receptor is ubiquitously expressed. Therefore, the broad range of side effects when a surplus of GCs is present, as is the case in GC treatment, is not too surprising. Many of the side effects mentioned above constitute components of the metabolic syndrome (metS), a cluster of metabolically interrelated risk factors for cardiovascular disease and diabetes mellitus type 2.

Due to the adverse effects there is a need for novel drugs with improved therapeutic index, *i.e.*, drugs that reduce inflammation with the same efficacy as classical GCs but with less or preferably no adverse effects. In the last two decades, research has focused particularly on the mechanism(s) of GC action: this knowledge is essential for efficient development of improved drugs. These considerable research efforts have led to the discovery of a novel class of potential therapeutics: selective glucocorticoid receptor modulators (SGRM's). Unfortunately, these novel GCs are still in the experimental phase and have not reached approval for clinical use yet. Moreover, in these studies the focus has been mainly on efficacy of the anti-inflammatory effects that were tested predominantly in mouse models of inflammation. Yet, also their potential side effects should directly be taken into account. Side effects like osteoporosis are relatively easy to monitor in rodents by radiographic techniques. Unfortunately, GC-induced metabolic side effects are not as clear in mice as in men and are more difficult to address. Therefore, there is a need for well-defined and extensively validated animal models to test metabolic side effects of GCs; it is well appreciated that separate models will be required for the different side effects mentioned.

The aim of the work described in this thesis is to define and unravel (molecular) mechanisms that underlie side effects of GCs on glucose and lipid metabolism in appropriate mouse models using multiple newly, developed stable isotope methodologies.

General introduction

Glucocorticoids

Already in the beginning of the 20th century it was appreciated that adrenal extracts influenced human physiology, which led Reichstein and Mason in 1936 to the purification of cortisol, the principal hormone produced by the adrenal gland [1,2]. The synthetic form of cortisol, *e.g.*, hydrocortisone, was produced in 1946 and soon the use of hydrocortisone was found to suppress symptoms of rheumatoid arthritis [3]. Cortisol and hydrocortisone are glucocorticoids (also called corticosteroids) and belong to the family of steroid hormones. Other steroid hormones are sex hormones, *i.e.*, estrogen, testosterone and progesterone. These are all synthesized from cholesterol and share the steroid-specific multiple ring structure. The steroid hormones are hydrophobic in nature and therefore are able to diffuse across plasma membranes of cells to reach their intracellular-localized receptors [4].

Cortisol is produced in the adrenal gland upon stimulation of the hypothalamus-pituitary-adrenal gland (HPA)-axis. A stimulus, like stress, causes the release of corticotrophin-releasing hormone (CRH) in the hypothalamus, which travels to the anterior pituitary where it triggers the release of adrenocorticotropic hormone (ACTH) into the bloodstream. ACTH activates the conversion of cholesterol into cortisol in the adrenal gland. Cortisol itself reduces the release of CRH, resulting in a negative feedback circuit [5]. The secretion of cortisol is under the control of the biological clock and shows a circadian rhythm with the highest peak of cortisol secretion early in the morning in humans [6].

The secretion of cortisol by the adrenal gland is only one of the intricate control mechanisms of cortisol availability. Once secreted by the adrenal gland, 90% of cortisol is bound to the plasma protein corticosterone binding globulin (CBG) [7], with a small remainder bound to albumin [8]. After crossing the plasma membrane of cells, free cortisol can bind to glucocorticoid receptors (GR) present in many different tissues, where it may exert various different functions. In addition, intracellular cortisol availability is regulated by the enzyme 11β-hydroxysteroid dehydrogenase type 1 (11β-HSD) [9], that converts the inactive form of cortisol, cortisone, back into cortisol, thereby locally increasing the cortisol concentration. 11β-HSD type 1 acts as a reductase and catalyzes the conversion of cortisone into cortisol, while 11β-HSD type 2 acts predominantly as a dehydrogenase, inactivating cortisol into cortisone. Whereas the GR is ubiquitously expressed, 11β-HSD is distributed in a tissue-specific manner with 11β-HSD-1 mainly present in brain, liver, muscle and adipose tissue and 11β-HSD-2 in kidney and placenta. This specific tissue organization implies that 11β-HSD plays an important role in controlling active intracellular GC levels [10]. Ro-

dents lack the enzyme 17α-hydroxylase in the adrenal gland, hence the main GC hormone in rodents is corticosterone, with 11-dehydroxycorticosterone as its inactive form [11].

Figure 1

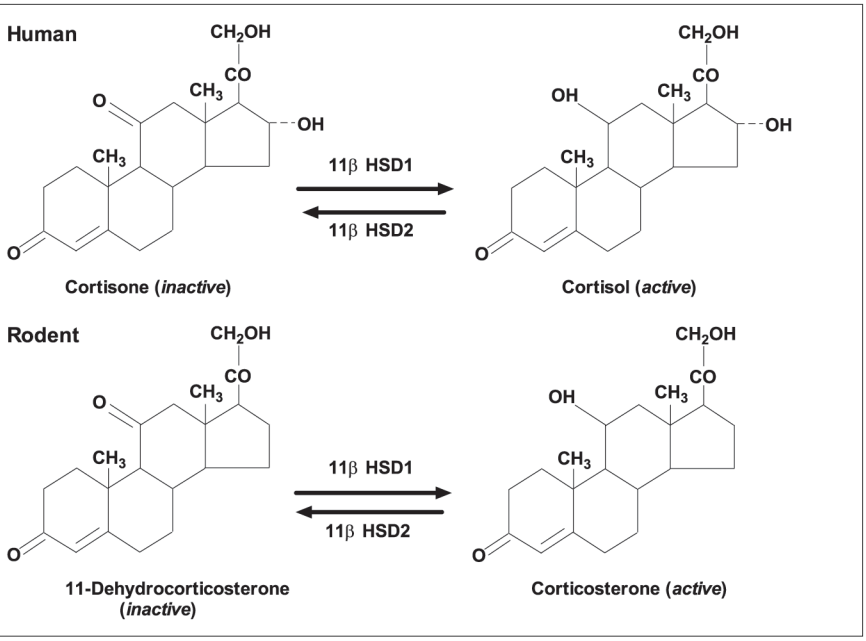

Structures of glucocorticoids. Adapted from [12]

Cortisol is often referred to as a stress hormone, because it is essential for maintaining whole body homeostasis in a stressful situation. It does so by fueling the body in a stressful situation by modulation of lipid and glucose metabolism. In addition, cortisol raises blood pressure, reduces the immune response, improves memory function and reduces sensitivity to pain in order to cope with a stressful situation. These effects are only effective for a short stress response: prolonged or chronic stress may lead to stress-related diseases.

It should be realized that cortisol is not only secreted upon stress but is continuously produced in small amounts, implying that, besides its role as a stress hormone, it has additional functions. One of these functions relates to control of development: cortisol is essential for fetal lung development [13]. Moreover, cortisol has many effects on bone and muscle maturation in young children. The effects of GCs upon the many different target organs and tissues are summarized in figure 2. The role of GCs in control of glucose and lipid metabolism will be more extensively discussed further on.

Figure 2

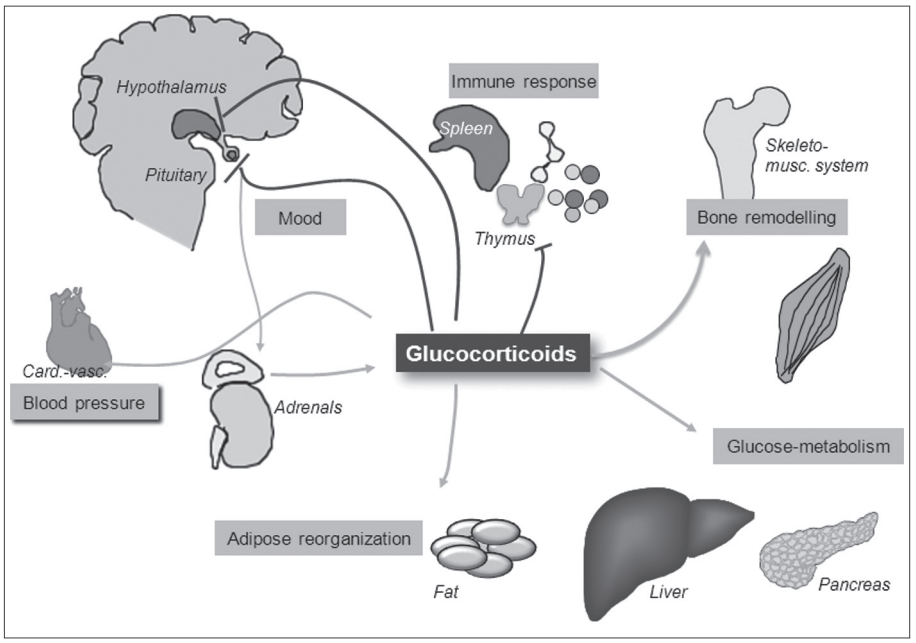

Organs and tissues involved in the glucocorticoid network

The importance of GCs is very clear from two GC-related diseases. In Addison's disease, first described by Thomas Addison in 1855, patients suffer from adrenal insufficiency caused by auto-immunity leading to low levels of cortisol [14]. Some of the symptoms of Addison's disease are weight loss, low blood pressure and hyperpigmentation [15,16]. The 'opposite' of Addison's disease is Cushing's syndrome (Cushing 1912), caused by excess cortisol secretion by the adrenal gland [17]. Cushing's syndrome can either be caused by pituitary or adrenal tumors, but in most cases Cushing's syndrome is due to administration of exogenous GCs to treat various inflammatory diseases. Symptoms of Cushing's syndrome are: weight gain with central adiposity, muscle wasting of extremities leading to a 'lemon on a stick' phenotype, high blood pressure, increased fat pads in the face and neck (called moon face and buffalo hump, respectively), hyperglycemia and insulin resistance, insomnia and many other symptoms. Many of these symptoms also constitute components of the metabolic syndrome [18].

The glucocorticoid receptor

GCs exert their functions via activation of the GR, a member of the nuclear receptor super family of transcription factors (figure 3). GR was identified in 1985 by Weinberger *et al*.

[19]. Like all nuclear receptors, GR contains multiple functional domains. The N-terminal domain contains a transactivation site, whereas the DNA-binding domain lies in the central part of the protein. The C-terminus contains the ligand- binding domain and is involved in receptor dimerization, nuclear translocation and interaction with heat shock proteins [20].

Two forms of GR have been identified; GRα and GRβ [22] (Fig. 3). GRα constitutes the most important receptor in quantitative terms and is widely distributed. Activated GRα is responsible for induction and repression of target genes, while GRβ is only able to repress GRα function. It was long thought that mice only express GRα [20], but a recent paper showed that mice do have GRβ as well [23]. The role of GRβ, however, is still under discussion: therefore when GR is mentioned in this thesis GRα is meant.

Figure 3

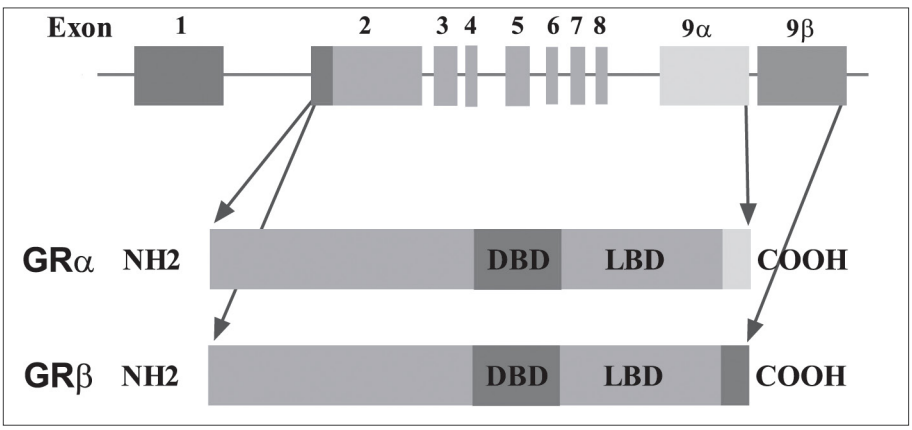

Structures of the two glucocorticoid receptor isoforms. Adapted from [21]

Mechanism of glucocorticoid action

Already in 1974, a 44 page review on GC action citing more than 350 papers [24] was published. Since that review, the expanding availability of cutting-edge technologies has enabled the unraveling of molecular mechanisms of GC action [25]. GR is constitutively present in the cytoplasm, bound by cofactors such as heath shock proteins (HSPs) [26]. When circulating free GCs are taken up by cells, they can bind to cytoplasmic GR (Fig. 4. (1)). Upon binding, the HSPs are removed and the GC-GR complex is channeled to the nucleus by importins [22,27] (2). In the nucleus the GC-GR complex can form a homodimer (Bledsoe 2004) and act as a transcription factor upon binding to GCs response elements (GRE) present in the DNA, hence inducing transcription of target genes (3). This response is generally re-

ferred to as transactivation. However, the GC-GR complex can also bind to other transcription factors like NFκB and AP1, both activators of inflammatory processes (4). It is thought that most anti-inflammatory effects of GCs are being exerted via this pathway. This response is called transrepression [28]. Another form of transrepression is direct binding of the GC-GR complex to a negative GC response element (nGRE) [29], thereby directly repressing gene-transcription. Besides these different roles in the nucleus, the GC-GR complex can also interact with other proteins in the cytoplasm, which is thought to be responsible for rapid effects of GCs (5) [30]. This protein-protein interaction is also referred to as a 'tethering mechanism' [31,32].

Figure 4

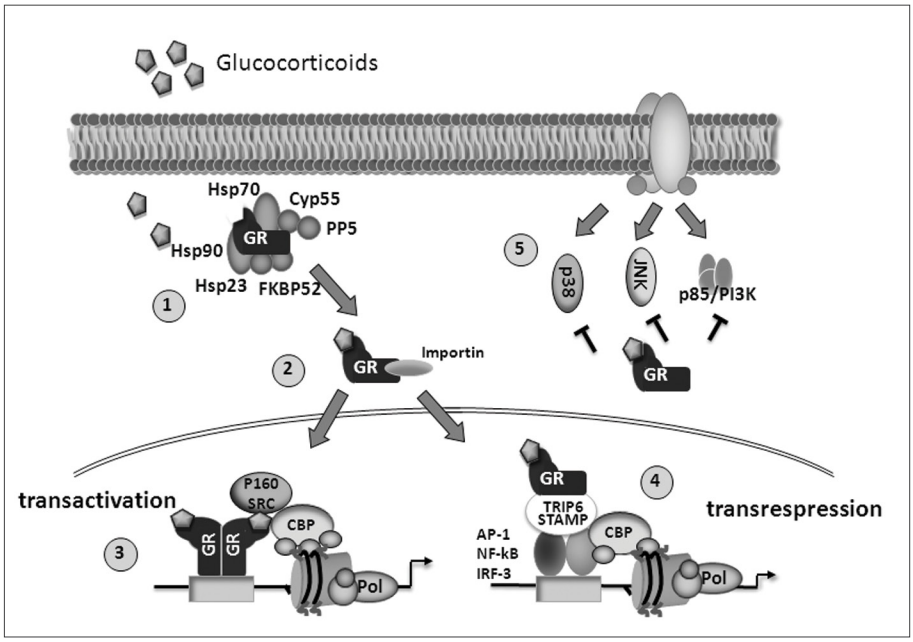

Mechanism of glucocorticoid action. Adapted from [33]

Synthetic glucocorticoids and side effects

GCs are well-known for their principal role in control of the immune system. GCs reduce inflammation by reducing cytokine expression in both dendritic cells and macrophages. GCs can also suppress activity and induce apoptosis of dendritic cells and reduce B-cell numbers. T-cells are most important in adaptive immunity. In these cells, GCs can induce apoptosis, mainly during T-cell development, thereby suppressing T-cell expression and

exert protection from auto-immunity and graft *vs.* host response. The role of GCs in the immune system is extensively described in reviews [32,33].

Since the discovery of hydrocortisone numerous synthetic GCs have been developed as anti-inflammatory and immune suppressive drugs. From the 1960's onwards GCs have been among the most prescribed drugs, particularly prednisolone and dexamethasone. While prednisolone is mostly used in chronic inflammatory disorders, *e.g.*, rheumatoid arthritis, inflammatory bowel disease and asthma, dexamethasone is predominantly used for acute inflammation and in cancer treatment since it has a particularly high affinity for GR (Table 1).

Table 1

Glucocorticoids	Potency	Plasma ½ life h	Biological ½ life h	Binding to CBG	Receptor affinity
Cortisol	1	2	8-12	100	100
Prednisone	3-4	3.2	8-12	59	5
Prednisolone	4	3.2	8-12	Absent	220
Methylprednisolone	5	2.5	18-36	Absent	1190
Dexamethasone	25-30	4	36-54	Absent	710

Characteristics of glucocorticoids. Adapted from [34]

Many differently structured GCs have been developed with different potencies and half lives. GCs were particularly enthusiastically prescribed in the late '60s and the '70s. A plethora of adverse effects soon became apparent that still hamper the use of GCs today. Since GCs are involved in control of a number of important metabolic processes, there is a broad spectrum of side effects that accompanies their application. The adverse effects range from minor, predominantly cosmetic effects, like striae and acne, to very severe ones, such as diabetes and osteoporosis. Table 2 presents an overview of GC-induced side effects. Due to the long history of GC treatment, patients are well aware of these effects, sometimes leading to a so-called 'steroid-phobia'.

Selective Glucocorticoid Receptor Modulators

From the above mentioned adverse effects it is clear that there is a high medical need for new drugs that display the potent anti-inflammatory actions of GCs, without, or with fewer, or less severe side effects. The search for such drugs is actively performed in both the

Table 2

Glucocorticoid-induced side effects

Skin	***Skeleton and muscle***
Delayed wound healing	Muscle atrophy, myopathy
Steroid acne, perioral dermatitis	Osteoporosis
Atrophy, striae rubrae distansae	Bone necrosis
Eye	***Immune system***
Glaucoma	Increased risk of infection
Cataract	Re-activation of latent viruses
CNS	***Cardiovascular system***
Disturbances in mood, memory and cognition	Hypertension
	Dyslipidemia
Steroid psychoses	Thrombosis
Cerebral atrophy	Vasculitis
Electrolytes, metabolism, endocrine system	
Iatrogenic Cushing's Syndrome	Adrenal atrophy
Hypogonadism, delayed puberty	Growth retardation
Increased Na^+ retention and K^+ excretion	Diabetes Mellitus
Gastrointestinal	
Peptic ulcer	Pancreatitis
Gastrointestinal bleeding	

Typical side-effects of glucocorticoid-treatment

pharmaceutical industry and academia. To find new drugs there are different approaches. In the case of GCs, the 'easy' way was followed for many years, by minimally altering the structural conformation of known GCs and by trial-and-error functionality testing of the new drug. This approach has produced quite good drugs, sometimes translating into improved potency and half life compared to the originals, but the side effects were unequivocally present. Systemic side effects were overcome by changing the route of administration, for instance by topical crèmes in the case of dermatitis and by inhalation in asthma. Nevertheless, the 'perfect' GC remains to be found.

After decades of searching new GCs, a more molecular approach is now increasingly being applied. As described before, the mechanisms by which GCs exert their function has been largely defined by now. Especially the ratio between transrepression *vs.* transactivation activities has gained great attention in the development of new GCs since it is thought that transactivation mainly causes the adverse effects, while transrepression is neces-

sary to reduce inflammation. These insights have led to design of a class of compounds called dissociated GCs or selective glucocorticoid receptor modulators (SGRM's)[35,36]. These compounds, in general, aim to target the transrepressing pathway of the GR, without activating the transactivational pathway. A battery of such compounds is currently being developed but so far none of these has made it to the clinic [37-39]. This could be due to side effects occurring in humans, which could not be detected in animal models.

Glucocorticoid-actions on glucose and lipid metabolism

The name 'glucocorticoid' obviously comes from '**glu**cose' relating to its role in control of glucose metabolism, '**cor**tex' from the adrenal cortex where it is synthesized, and 'ster**oid'** from its steroidal structure. As their name implies, GCs play an important role in the control of glucose metabolism, specifically in stress situations. GCs are so-called catabolic hormones and their actions ensure rapid energy supply to tissues in order to be able to react adequately to a stressful event. Glucose production in the liver is up-regulated by induction of gluconeogenesis in order to raise blood glucose levels as a source of energy for the brain. Moreover, glucose uptake in muscle and adipose tissue is reduced, while lipolysis is increased to release free fatty acids as an energy substrate. In addition, stimulation of protein degradation in muscle leads to mobilization of amino acids to serve as additional substrate for gluconeogenesis. Like glucagon, another catabolic hormone, GCs oppose the effects of the anabolic hormone insulin.

Figure 5

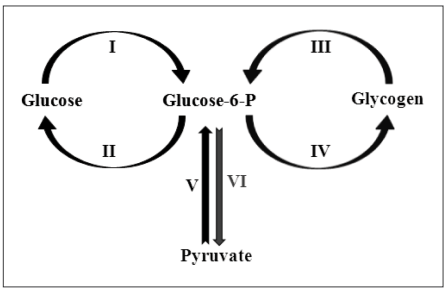

Glucose enters the liver and can be converted to glucose-6-phosphate by glucokinase (GK) (I). Glucose-6-phosphate can either be converted back to glucose by glucose-6-phosphatase (G6Pase) (II) or to glycogen, by glycogensynthase (GS) (IV). Glycogen can be converted back to glucose-6-phosphate by glycogenphosphorylase (GP) (III). In addition, glucose-6-phosphatase can be converted to pyruvate by a number of enzymes including pyruvate kinase (PK) (VI) for use in the TCA cycle or storage. From pyruvate glucose-6-phosphate can be formed by a number of enzymes including phosphoenolpyruvate carboxykinase (PEPCK (Pck1)) (V).

Hepatic glucose metabolism

As mentioned above, one of the main presumed role of GCs is to stimulate hepatic glucose production to provide sufficient glucose for the brain. The liver can be regarded as the metabolic center of the body, adapting metabolic pathways to adequately meet altered energy needs. In case of energy surplus, the liver is able to store glucose in the form of glycogen while in times of energy demand glucose can be produced by liver. The latter can

be achieved either by stimulation of gluconeogenesis or by converting glycogen back into glucose. For these processes, the enzymes phosphoenolpyruvate carboxykinase (PEPCK) and glucose-6-phosphatase (G6Pase), respectively, are essential.

Hepatic gluconeogenesis is stimulated by GCs, the mechanism is generally thought to be due through direct transactivation of *Pck1,* the gene encoding for PEPCK which is one of the enzymes involved in gluconeogenesis. The promoter of *Pck1* contains a classical GRE [40]. However, PEPCK only has a slight control on gluconeogenic flux [41], therefore additional mechanisms must be involved. *G6pase* gene expression is also induced by GC, the *G6pase* was the first gene demonstrated to contain both a GRE and a nGRE. The function of the latter, however, is still under debate [40]. Moreover, GCs can indirectly increase hepatic glucose production by antagonizing the suppressive effects of insulin on hepatic glucose production. Many studies, both in humans and in rodents, have been performed to unravel the molecular mechanisms by which GCs modulate hepatic glucose metabolism. However, all these efforts together have primarily resulted in an enormous amount of (partly) contradicting data. Therefore, the events described above provide a generally accepted mode by which GCs act on the liver, but the actual mechanism of action still remain to be established. Most of the studies showing effects of GCs on hepatic glucose metabolism address short-term, direct effects on gene expression, while long-term effects of GC treatment on gene expression of *Pck1* and *G6pase* under different nutritional and disease conditions are far from clear. Obviously, the fundamental experiments, required to obtain these essential pieces of information cannot be performed in humans.

Peripheral glucose metabolism

While the liver both produces and clears glucose, the peripheral tissues can only utilize or store glucose. The brain, muscle and adipose tissue are the most important tissues involved in glucose utilization.

Muscle tissue can be divided into three main types: skeletal-, cardiac- and smooth muscle. While cardiac and smooth muscle cells are essential for survival, skeletal muscle tissue is of great importance for mobility. Mobility via skeletal muscle activity is a highly energy demanding process, accounting for a major part of glucose consumption. Glucose uptake in the muscle is mainly insulin-dependent and is mediated by the glucose transporter GLUT4 [42]. Insulin stimulates GLUT4 to go to the cell membrane to take up glucose from the circulation. Upon glucose uptake, glucose can be used as a substrate for energy production by conversion into lactate or be stored in the muscle as glycogen. Muscle glycogen can only be used by the muscle itself. Sustained GC treatment may induce muscle wasting due to decreased protein synthesis and/or increased protein breakdown [43]. This phenotype is

also called steroid myopathy. Muscle protein is broken down under influence of GCs, thus mobilizing amino acids to serve as substrate for gluconeogenesis in the liver. In addition, high levels of GCs prevent insulin-mediated glucose uptake in muscle, leaving blood glucose as energy for the brain. Energy coming from protein breakdown can be used in the muscle itself.

The main source of energy in the body is stored in the adipose tissue as fat. In principle GCs have lipolytic effects on adipose tissue, releasing free fatty acids and glycerol [44]. The fatty acids can be taken up and oxidized in tissues in energy need and via mitochondrial β-oxidation yield ATP [45]. At the same time the glycerol released by lipolysis can be used as a substrate for gluconeogenesis in the liver. The lipolytic pathway is activated by GCs mainly by increased protein expression of adipose triglyceride lipase (ATGL) and hormone sensitive lipases (HSL) [46,47]. In addition, GCs reduce glucose uptake in adipose tissue [48] and reduce gene expression of *Pck1*[49,50] thereby preventing the glycerolneogenesis. As a consequence, free fatty acids are released and not esterified back into triglycerides. The role of GCs on adipose tissue will be discussed more extensively later on.

The brain represents only 2% of the human body weight but accounts for about 25% of the bodies glucose utilization [51], because glucose is the main energy substrate for brain tissue. In conditions of glucose-shortage, *e.g.* upon fasting, ketone bodies can also be used as a substrate. Brain glucose uptake is largely insulin-independent and the direct role of GC is minor and not very extensively studied. In patients with Cushing's disease, however, it is thought that reduced glucose uptake by the astrocytes, that surround the blood capillaries of the blood brain barrier, leads to astrocyte atrophy and thereby to cognitive dysfunction [52]. Other brain-related side effects of GCs, such as mood disorders, are more likely to be derived from alterations of HPA-axis activity and hippocampus atrophy [53].

Insulin resistance and diabetes

Insulin is a crucial hormone for adequate regulation of blood glucose homeostasis. It is produced in the pancreas by β-cells in the islets of Langerhans. Insulin is actively secreted by the pancreas in response to high blood glucose levels to stimulate glucose utilization and hence to reduce blood glucose levels [54]. Opposite to GCs, insulin is an anabolic hormone, aiming to store energy, since it promotes the uptake of glucose in target tissues such as the liver, muscle, where it can either be used or stored as glycogen. In adipose tissue insulin promotes glucose uptake after which glucose is converted into acetyl-CoA and *via* lipogenesis into triglycerides. Insulin resistance is a situation characterized by high circulating plasma glucose levels due to an inability of liver, skeletal muscle and adipose tissue to adequately respond to insulin. Insulin resistance precedes diabetes mellitus type 2,

in which the inability of insulin-sensitive tissues to respond to insulin cannot be compensated for by increased insulin secretion of the pancreatic β-cells anymore. As mentioned previously, insulin resistance is one of the major side effects of GC treatment in humans [55-57]. Yet, compared to the incredible amount of GCs that is daily prescribed around the world, the knowledge of adverse events accompanying GC treatment is very limited [58-60].

GC-induced insulin resistance likely involves several tissues. In the liver and peripheral tissues, like muscle and adipose tissue, insulin action appears to be abolished by GCs. Moreover, GCs may have a direct effect on the insulin-secreting β-cells of the pancreas. These effects, however, are controversial since increased insulin secretion [61] as well as decreased insulin secretion [62] upon GC exposure have been reported.

Besides insulin, there are multiple other hormones involved in control of glucose metabolism. Firstly, glucagon produced by the α-cells of the Islets of Langerhans opposes the effects of insulin. Secondly, several hormones secreted by the intestine, like glucagon like peptide-1 (GLP1) and gastric inhibitory polypeptide (GIP) have been recognized as prominent targets for treatment of diabetes [63]. Thirdly, ghrelin, a orexigenic hormone stimulating appetite that is produced by cells of the stomach wall, modulates insulin secretion and sensitivity [64]. The adipose tissue has been discovered to secrete hormones as well, with leptin, resistin and adiponectin all playing prominent roles in glucose metabolism [65]. In addition to these hormones, other proteins also can affect glucose metabolism. Fibroblast growth factor 21 (FGF21), a member of the fibroblast growth factor family, has recently been described to function as an endocrine hormone [66]. FGF21 is produced during fasting [67,68] and has major effects on glucose uptake in adipocytes [69]. Plasminogen activator inhibitor-1 (PAI-1), a serine proteinase secreted by endothelial cells, has been shown to be associated with diabetes [70].

Lipids and cholesterol metabolism

Besides insulin resistance, visceral obesity is another major side effect of GC treatment. Taking into account that GCs are generally described as being lipolytic, the fact that chronic GCs lead to obesity appears to be contradictory. However, GCs have been found to be both lipolytic as well as adipogenic [71] and GC can regulate differentiation, function and distribution of adipocytes [72]. This shows that the effects of excess GCs on adipose tissue are quite complex [44]. Central fat depots (visceral, abdominal, facial and fat in the nape of the neck) are generally increased upon GC stimulation, while peripheral depots, like subcutaneous fat in the legs and arms, become reduced [73]. This could result from differential effects of GCs on lipolysis, or differentiation of pre-adipocytes and on triglyceride synthesis in various fat depots [74]. One reason for this might be the excessive pres-

Figure 6

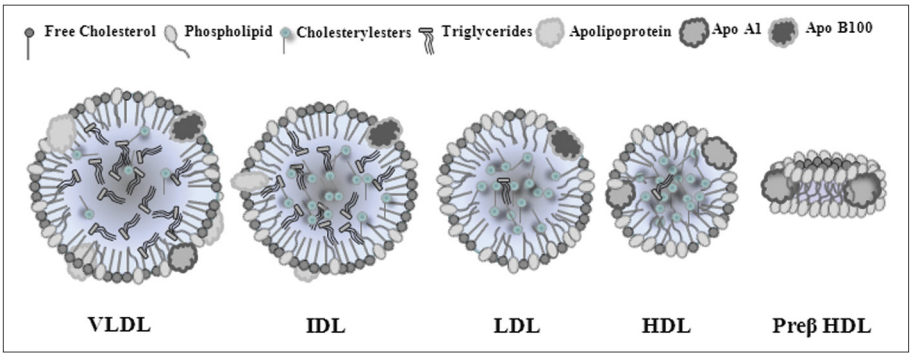

Classification of lipoproteins

Lipoproteins are classified based on their density. Chylomicrons are formed in the intestine and carry mainly triglycerides to the liver. From the liver very low density lipoproteins (VLDL) transports triglycerides to peripheral tissues and is converted into intermediate density lipoproteins (IDL) followed by the conversion to low density lipoproteins (LDL) carrying mainly cholesterol from the liver to the peripheral tissues. The smallelst high dense lipoprotein (HDL) particle transports excess cholesterol from the peripheral cells to the liver.

ence of GRs in visceral fat compared to subcutaneous fat [75]. Moreover, the expression of 11β-hydroxysteroid dehydrogenase type 1 might differ between fat depots [76] and that 11β-HSD type 1 is more active in visceral (omental) fat depots [77].

Although less frequent than other metabolic derangements, GC treatment is also associated with dyslipidemia in humans [45,78]. Lipoproteins function in the body as transporters for lipids and are classified based on their density (Figure 6).

High dose GC treatment has been associated with increased waist circumference, triglycerides, total and LDL-cholesterol levels [79], all symptoms increasing the risk for cardiovascular diseases. However, the effects of GCs on HDL-cholesterol are contradictory; in a study population of 15.000 Americans, GCs were associated with increased HDL-cholesterol ratio in the >60 years population, implying an improved lipid profile [80]. The effects of GCs on lipid metabolism might be due to direct effects of GCs to induce VLDL secretion [44,81] and lipoprotein lipase (LPL) activity. LPL is essential for the release of fatty acids from triglycerides in VLDL particles, in order to be taken up in the adipose tissue and GCs have been shown to increase LPL activity by both transcription as well as posttranslational modifications [44,82,83].

Cholesterol and GCs also interact on another level, *i.e.*, in the adrenal cortex where steroidogenesis takes place in which cortisol is produced from cholesterol. Scavenger receptor B1, is the mediator of HDL-cholesterol uptake in the adrenocortical cells, has been shown to be essential for cortisol production [84].

Animal models for assessment of glucocorticoid actions

Regarding the complexity of GC actions, specific animal models are essential to elucidate the mechanisms of GC-induced metabolic adverse effects. Nevertheless, *the* animal model for GC-induced insulin resistance is currently not available. Several studies on GC-induced adverse effects on glucose metabolism have been performed in rats [85-87]. An experimental model of dexamethasone-induced insulin resistance in rats has first been published by Stojanovska *et al.* [85]. This model has been used in many studies. A daily dose of *ip.* administered dexamethasone (1 mg/kg/day) for several days up to one week induced (fasting) hyperglycemia and hyperinsulinemia [61,86,88]. Dexamethasone is mostly used in rats because prednisolone has poor bioavailability when given orally in rats. Insulin resistance in dex treated rats was studied in more detail by Rafacho *et al.*[61], showing increased AUC in the OGTT, while Venkatesan *et al.*[88] showed an apparent reduction in the glucose infusion rate during the hyperinsulinemic euglycemic clamp (HIEC). This method was developed to study insulin resistance, by infusing insulin to reach high insulin levels in blood (hyperinsulinemic), while simultaneously infusing glucose to maintain glucose levels steady (euglycemic) [89] and is regarded as the gold standard to quantitatively assess insulin resistance. The glucose infusion rate (GIR) in this method is the measure for insulin sensitivity. The ability of dexamethasone to reduce GIR was in rats already apparent after a single injection with dexamethasone [90].

GC-induced insulin resistance has mainly been studied using dexamethasone. Dexamethasone is a very potent GC, 7.5 times more potent than prednisolone, and is mainly used for treatment of severe acute inflammatory conditions in the clinic. Prednisolone, on the other hand, is favoured for chronic treatment in chronic inflammatory diseases, *e.g.*, inflammatory bowel disease (IBD) and rheumatoid arthritis (RA), and hence is of most interest in relation to metabolic side effects.

Although dexamethasone-treatment in rats is an accepted model for GC-induced insulin resistance, such a model is not available for mice. Genetically-modified mice provide powerful models for metabolic research and it would be highly desirable to define a mouse model for full evaluation of GC-related metabolic consequences. Unfortunately, GR knockout mice are not viable which at least demonstrates that GR is essential for development [13]. A transgenic mouse model is available that carries a mutation in the dimerization domain of the GR [91]. In this model, the GR^{dim} mouse, GR is not able to dimerize, leaving all GC-mediated effects restricted to monomeric GR actions. This model is of specific interest when studying trans-activating and trans-repressing effect of GCs.

A limited number of studies on metabolic derangements due to GC treatment involve multiple mouse strains [92-96]. In a study of Gounarides *et al*.[94], C57BL/6J mice were kept

on a high-fat diet for 2 months followed by 5 days of dexamethasone treatment. After this regimen, mice showed a higher HOMA-IR than control mice, indicating the induction of insulin resistance. However, a subsequent oral glucose tolerance test failed to clearly confirm the existence of insulin resistance in this particular model. Bernal-Mizrachi *et. al.* [96] used low density lipoprotein receptor knockout ($LDLR^{-/-}$) mice and an extremely high dose of dexamethasone for prolonged periods of time (5 months) to show decreased glucose tolerance and insulin insensitivity. To our knowledge, studies addressing effects of prednisolone on whole body metabolism in conventional wild-type C57BL/6J mice have not been reported in the literature. All previous mouse studies have been performed with either dexamethasone and/or insulin resistance-prone mouse strains. Moreover, so far no 'gold standard' HIEC studies have been performed to evaluate GC-induced adverse effects on glucose metabolism. Therefore the studies in this thesis focus on the development of a mouse model of prednisolone-induced adverse metabolic effects of glucose and lipid metabolism. For this, conventional C57BL/6J mice were chosen, because this mouse strain is mostly used in metabolic studies and is susceptible to diet-induced obesity. These mice were treated with prednisolone, to resemble the long-term treatment in humans in which prednisolone-induced metabolic adverse effects occur. To detect metabolic derangements, a variety of novel techniques have been applied. For assessment of insulin resistance, the HIEC adapted for mice was combined with stable isotope methodologies in order to quantify hepatic glucose metabolism under fasted, hyperinsulinemic euglycemic and hyperglycemic conditions. In addition, a novel stable-isotope technique to assess basal glucose kinetics was developed, which is also suited for measurements of glucose metabolism in severely ill mice. In addition, we studied the effects of prednisolone in on glucose metabolism in an inflamed mouse model. For this, an experimental model for arthritis was induced in DBA/1J mice, since this strain is the only mouse strain susceptible to collagen induced arthritis. For a more mechanistic insight, we treated GR^{dim} mice with prednisolone. This mouse model had a defective dimerization domain in the GR, thereby discriminating between monomeric effects and dimeric effects of GR. In this model, prednisolone-induced dyslipidemia was studied.

In short, the work described in this thesis aimed at defining and unraveling of molecular mechanism that underlie adverse effects of GCs on glucose and lipid metabolism in appropriate mouse models using multiple newly, developed stable isotope methodologies.

Outline of thesis

The aim of the research described in this thesis was to define the (molecular) mechanism(s) of GC-induced adverse effects on glucose and lipid metabolism in mouse models. For initial experiments, aimed at evaluating GC-induced side effects on glucose metabolism, we monitored fasting blood glucose levels in C57BL/6J mice treated with different doses of prednisolone during a four week period. The C57BL/6J mouse is the most extensively studied mouse strain in metabolic research and is known to be prone to high-fat diet-induced insulin resistance. These mice were subjected to an oral glucose tolerance test (OGTT) once a week for four weeks. Since there were clear effects on fasting glucose levels already after 7 days, but not on outcome of the OGTT, we developed a method to determine blood glucose kinetics in the fasted state; **Chapter 2** describes this method in detail. Blood glucose kinetics was assessed in a fasted, steady state in mice fed a high-fat diet. The main advantage of this method is that due to the relatively small blood volumes required it is possible to perform the test multiple times in an individual animal, thereby enabling monitoring of therapeutic or dietary effects over time.

In **Chapter 3** this method was used in a mouse model employed to evaluate GC-induced insulin resistance. C57BL/6J mice were treated with prednisolone for 7 days. This treatment regime elevated fasting blood glucose and insulin concentrations, *i.e.,* a situation that indicates induction of insulin resistance. However, by the hyperinsulinemic euglycemic clamp (HIEC) technique we showed that these mice actually did not develop a 'classical' insulin resistance. During an HIEC, insulin sensitivity is tested at supraphysiological insulin levels. When blood glucose kinetics were evaluated in a fasted state, prednisolone treatment clearly increased the endogenous glucose production (EGP) at higher insulin levels, suggestive for hepatic insulin resistance. However, we found that the main effect op prednisolone treatment on fasting glucose levels was due to an altered fasting response. Upon fasting, blood glucose levels drop while ketone bodies and fasting hormone fibroblast growth factor 21 (FGF21) increase. In prednisolone-treated mice, FGF21 did increase, but was unable to stimulate ketone body production and to reduce blood glucose levels, resulting in increased fasting blood glucose levels.

In **chapter 4** we examined prednisolone-induced insulin resistance in a state of compromised insulin sensitivity induced by feeding C57BL/6J mice a high-fat diet prior to prednisolone treatment. Like in chow-fed mice, prednisolone treatment increased fasting blood glucose levels and plasma insulin levels in high-fat fed mice, resulting in an increased HOMA-IR. We measured the hepatic glucose fluxes under basal conditions and hyperinsulinemic conditions, again revealing that prednisolone treatment did not aggravate insulin resistance in high-fat fed mice, since the GIR of both groups were similar. Nevertheless,

prednisolone treatment did alter hepatic glucose fluxes in these mice, mainly at the glycogen level, revealing an insulin-independent role for prednisolone on glucose metabolism. A spectrum of hormones and adipokines involved in control of glucose metabolism was analyzed, which showed that prednisolone treatment led to significantly elevated plasma leptin and FGF21 levels, thereby suggesting that prednisolone-induced alterations of glucose metabolism are, at least in part, mediated by other factors than insulin.

In both **chapter 3** and **4** we found evidence for insulin-independent effects of prednisolone on glucose metabolism, which was only detectable in the fasted state. A new class of GCs, called selective glucocorticoids modulators (SGRM), are currently being developed with the aim to reduce inflammation in a partial GC-dependent manner with reduced potential to induce side effects. In **chapter 5** Org-214007, a SGRM, was shown to inhibit collagen-induced arthritis in mice even more efficiently than prednisolone did. When Org-214007 was tested on glucose metabolism by analysis of hepatic glucose fluxes by MIDA, it was shown not to induce adverse effects on hepatic glucose fluxes, whereas prednisolone clearly reduced the glycogen balance.

In **chapter 5** efficacy and adverse effects were evaluated in different animal models. However, the disease can modify GC-induced side effects as well, in **chapter 6** we therefore analysed efficacy and adverse effects in one animal model. For this the blood glucose kinetic model described in **chapter 2** was performed in collagen induced arthritic mice. The resulting model allows the study of effects of (novel) GC compounds on the development of arthritis and on glucose kinetics.

Besides the adverse effects of prednisolone on glucose metabolism, lipid metabolism is also unfavorably affected. In **chapter 7** development of dyslipidemia was studied in a transgenic mouse model, the GR^{dim} mouse. This model was developed to discern the effects of transactivation by dimeric GR and transrepression of monomeric GR. GR^{dim} mice have a mutation in the dimerization part of the GR leading to activation of monomeric GR exclusively. Prednisolone treatment in GR^{dim} mice led to an extreme phenotype of dyslipidemia, with high plasma triglyceride, cholesterol and phospholipid levels, mainly in the very low density lipoprotein (VLDL)-sized fractions. Monomeric GR directly increased mRNA expression of hepatic *Lpl*; future studies should reveal the role of LPL on the development of prednisolone-induced dyslipidemia in GR^{dim} mice.

Finally, in **chapter 8** the work addressed in this thesis is discussed and future implications are given. From the various conclusions of the different chapters it is clear that the effects of GCs on insulin is only one of many components involved in glucose and lipid metabolism and that disturbance of this complex system of multiple organs and opposing

hormones, will lead to serious metabolic side effects.

Reference List

1. van der Laan S. & Meijer, O. C. Pharmacology of glucocorticoids: beyond receptors. *Eur. J. Pharmacol.* **585**, 483-491 (2008).

2. Hillier, S. G. Diamonds are forever: the cortisone legacy. *J. Endocrinol.* **195**, 1-6 (2007).

3. Hench, P. S., Kendall, E. C. & . The effect of a hormone of the adrenal cortex (17-hydroxy-11-dehydrocorticosterone; compound E) and of pituitary adrenocorticotropic hormone on rheumatoid arthritis. *Mayo Clin. Proc.* **24**, 181-197 (1949).

4. Cooper, G. M. *The Cell - A Molecular Approach; Chapter 13, Cell Signaling; Steroid Hormones and the Steroid superfamily*. Sunderland (MA): Sinauer Associates, (2000).

5. Gagner, J. P. & Drouin, J. Opposite regulation of pro-opiomelanocortin gene transcription by glucocorticoids and CRH. *Molecular and Cellular Endocrinology* **40**, 25-32 (1985).

6. Nussey, S. S. a. W. S. A. L. T. &. F. & c2001 *Endocrinology, An integrated approach*. Taylor & Francis, London (2001).

7. Meaney, M. J., Aitken, D. H., Sharma, S. & Viau, V. Basal ACTH, corticosterone and corticosterone-binding globulin levels over the diurnal cycle, and age-related changes in hippocampal type I and type II corticosteroid receptor binding capacity in young and aged, handled and nonhandled rats. *Neuroendocrinology* **55**, 204-213 (1992).

8. Hamrahian, A. H., Oseni, T. S. & Arafah, B. M. Measurements of Serum Free Cortisol in Critically Ill Patients. *New England Journal of Medicine* **350**, 1629-1638 (2004).

9. Chapman, K. E. *et al.* The role and regulation of 11[beta]-hydroxysteroid dehydrogenase type 1 in the inflammatory response. *Molecular and Cellular Endocrinology* **301**, 123-131 (2009).

10. Monder, C. Corticosteroids, receptors, and the organ-specific functions of 11 beta-hydroxysteroid dehydrogenase. *FASEB J* **5**, 3047-3054 (1991).

11. Brock, B. J. & Waterman, M. R. Biochemical Differences between Rat and Human Cytochrome P450c17 Support the Different Steroidogenic Needs of These Two SpeciesGÇá. *Biochemistry* **38**, 1598-1606 (1999).

12. Wolf, G. Glucocorticoids in adipocytes stimulate visceral obesity. *Nutr. Rev.* **60**, 148-151 (2002).

13. Cole, T. J. *et al.* Targeted disruption of the glucocorticoid receptor gene blocks adrenergic chromaffin cell development and severely retards lung maturation. *Genes & Development* **9**, 1608-1621 (1995).

14. Arlt, W. & Allolio, B. Adrenal insufficiency. *The Lancet* **361**, 1881-1893 (2003).

15. Nieman, L. K. & Chanco Turner, M. L. Addison's disease. *Clinics in Dermatology* **24**, 276-280 (2007).

16. Vegiopoulos, A. & Herzig, S. Glucocorticoids, metabolism and metabolic diseases. *Mol. Cell Endocrinol.* **275**, 43-61 (2007).

17. Newell-Price, J., Bertagna, X., Grossman, A. B. & Nieman, L. K. Cushing's syndrome. *The Lancet* **367**, 1605-1617 (2006).

18. Chanson, P. & Salenave, S. Metabolic syndrome in Cushing's syndrome. *Neuroendocrinology* **92 Suppl 1**, 96-101 (2010).

19. Weinberger, C. *et al.* Identification of human glucocorticoid receptor complementary DNA clones by epitope selection. *Science* **228**, 740-742 (1985).

20. Otto, C., Reichardt, H. M. & Schutz, G. Absence of glucocorticoid receptor-beta in mice. *J. Biol. Chem.* **272**, 26665-26668 (1997).

21. McMaster, A. & Ray, D. W. Modelling the glucocorticoid receptor and producing therapeutic agents with anti-inflammatory effects but reduced side-effects. *Experimental Physiology* **92**, 299-309 (2007).

22. Kleiman, A. & Tuckermann, J. P. Glucocorticoid receptor action in beneficial and side effects of steroid therapy: Lessons from conditional knockout mice. *Molecular and Cellular Endocrinology* **275**, 98-108 (2007).

23. Hinds, T. D., Jr. *et al.* Discovery of Glucocorticoid Receptor-{beta} in Mice with a Role in Metabolism. *Mol Endocrinol* (2010).

24. Thompson, E. B. & Lippman, M. E. Mechanism of action of glucocorticoids. *Metabolism* **23**, 159-202 (1974).

25. Schoneveld, O. J., Gaemers, I. C. & Lamers, W. H. Mechanisms of glucocorticoid signalling. *Biochim. Biophys. Acta* **1680**, 114-128 (2004).

26. Pratt, W. B., Gehring, U. & Toft, D. O. Molecular chaperoning of steroid hormone receptors. *EXS* **77**, 79-95 (1996).

27. Freedman, N. D. & Yamamoto, K. R. Importin 7 and importin alpha/importin beta are nuclear import receptors for the glucocorticoid receptor. *Mol. Biol. Cell* **15**, 2276-2286 (2004).

28. Heck, S. *et al.* A distinct modulating domain in glucocorticoid receptor monomers in the repression of activity of the transcription factor AP-1. *EMBO J.* **13**, 4087-4095 (1994).

29. Almawi, W. Y. & Melemedjian, O. K. Negative regulation of nuclear factor-kappaB activation and function by glucocorticoids. *Journal of Molecular Endocrinology* **28**, 69-78 (2002).

30. Jonat, C. *et al.* Antitumor promotion and antiinflammation: Down-modulation of AP-1 (Fos/Jun) activity by glucocorticoid hormone. *Cell* **62**, 1189-1204 (1990).

31. Beato, M., Herrlich, P. & Schütz, G. Steroid hormone receptors: Many Actors in search of a plot. *Cell* **83**, 851-857 (1995).

32. De Bosscher, K., Vanden Berghe, W. & Haegeman, G. The Interplay between the Glucocorticoid Receptor and Nuclear Factor-+¦B or Activator Protein-1: Molecular Mechanisms for Gene Repression. *Endocr Rev* **24**, 488-522 (2003).

33. Baschant, U. & Tuckermann, J. The role of the glucocorticoid receptor in inflammation and immunity. *J. Steroid Biochem. Mol. Biol.* **120**, 69-75 (2010).

34. Longui, C. A. Glucocorticoid therapy: minimizing side effects. *J. Pediatr. (Rio J.)* **83**, S163-S177 (2007).

35. Schacke, H., Docke, W. & Asadullah, K. Mechanisms involved in the side effects of glucocorticoids. *Pharmacology & Therapeutics* **96**, 23-43 (2002).

36. Stahn, C., Lowenberg, M., Hommes, D. W. & Buttgereit, F. Molecular mechanisms of glucocorticoid action and selective glucocorticoid receptor agonists. *Mol. Cell Endocrinol.* **275**, 71-78 (2007).

37. Schacke, H. *et al.* Dissociation of transactivation from transrepression by a selective glucocorticoid receptor agonist leads to separation of therapeutic effects from side effects. *Proc. Natl. Acad. Sci. U. S. A* **101**, 227-232 (2004).

38. Rauner, M. *et al.* Dissociation of Osteogenic and Immunological Effects by the Selective Glucocorticoid Receptor Agonist, Compound A, in Human Bone Marrow Stromal Cells. *Endocrinology* **152**, 103-112 (2011).

39. Schäcke, H. *et al.* Characterization of ZK 245186, a novel, selective glucocorticoid receptor agonist for the topical treatment of inflammatory skin diseases. *British Journal of Pharmacology* **158**, 1088-1103 (2009).

40. Yabaluri, N. & Bashyam, M. D. Hormonal regulation of gluconeogenic gene transcription in the liver. *J. Biosci.* **35**, 473-484 (2010).

41. Burgess, S. C. *et al.* Cytosolic phosphoenolpyruvate carboxykinase does not solely control the rate of hepatic gluconeogenesis in the intact mouse liver. *Cell Metab* **5**, 313-320 (2007).

42. Weinstein, S. P., Wilson, C. M., Pritsker, A. & Cushman, S. W. Dexamethasone inhibits insulin-stimulated recruitment of GLUT4 to the cell surface in rat skeletal muscle. *Metabolism* **47**, 3-6 (1998).

43. Schakman, O., Gilson, H., Kalista, S. & Thissen, J. P. Mechanisms of muscle atrophy induced by glucocorticoids. *Horm. Res* **72 Suppl 1**, 36-41 (2009).

44. Peckett, A. J., Wright, D. C. & Riddell, M. C. The effects of glucocorticoids on adipose tissue lipid metabolism. *Metabolism* (2011).

45. Macfarlane, D. P., Forbes, S. & Walker, B. R. Glucocorticoids and fatty acid metabolism in humans: fuelling fat redistribution in the metabolic syndrome. *J Endocrinol* **197**, 189-204 (2008).

46. Xu, C. *et al.* Direct effect of glucocorticoids on lipolysis in adipocytes. *Mol Endocrinol.* **23**, 1161-1170 (2009).

47. Slavin, B. G., Ong, J. M. & Kern, P. A. Hormonal regulation of hormone-sensitive lipase activity and mRNA levels in isolated rat adipocytes. *J Lipid Res* **35**, 1535-1541 (1994).

48. Buren, J., Lai, Y. C., Lundgren, M., Eriksson, J. W. & Jensen, J. Insulin action and signalling in fat and muscle from dexamethasone-treated rats. *Arch. Biochem. Biophys.* **474**, 91-101 (2008).

49. Olswang, Y. *et al.* Glucocorticoids repress transcription of phosphoenolpyruvate carboxykinase (GTP) gene in adipocytes by inhibiting its C/EBP-mediated activation. *J. Biol. Chem.* **278**, 12929-12936 (2003).

50. Glorian, M., Franckhauser-Vogel, S., Robin, D., Robin, P. & Forest, C. Glucocorticoids repress induction by thiazolidinediones, fibrates, and fatty acids of phosphoenolpyruvate carboxykinase gene expression in adipocytes. *J Cell Biochem.* **68**, 298-308 (1998).

51. Magistretti P.J.Pellerin L., M. J.-L. *Psychopharmacology: The Fourth Generation of Progress*. Bloom, F. E. K. D. J. (ed.) (Nature Publishing Group,2000).

52. Patil, C. G., Lad, S. P., Katznelson, L. & Laws, E. R. Brain atrophy and cognitive deficits in Cushing's disease. *Neurosurgical FOCUS* **23**, 1-4 (2007).

53. Brown, E. S. Effects of glucocorticoids on mood, memory, and the hippocampus. Treatment and preventive therapy. *Ann. N. Y. Acad. Sci.* **1179**, 41-55 (2009).

54. Saltiel, A. R. New Perspectives into the Molecular Pathogenesis and Treatment of Type 2 Diabetes. *Cell* **104**, 517-529 (2001).

55. Stanbury, R. M. & Graham, E. M. Systemic corticosteroid therapy--side effects and their management. *Br. J Ophthalmol.* **82**, 704-708 (1998).

56. Walker, B. R. Cortisol--cause and cure for metabolic syndrome? *Diabet. Med.* **23**, 1281-1288 (2006).

57. Andrews, R. C. & Walker, B. R. Glucocorticoids and insulin resistance: old hormones, new targets. *Clin. Sci. (Lond)* **96**, 513-523 (1999).

58. Munir, A. & Newell-Price, J. Management of diabetes mellitus in Cushing's syndrome. *Neuroendocrinology* **92 Suppl 1**, 82-85 (2010).

59. van Raalte, D. H., Ouwens, D. M. & Diamant, M. Novel insights into glucocorticoid-mediated diabetogenic effects: towards expansion of therapeutic options? *Eur. J Clin Invest* **39**, 81-93 (2009).

60. van der Goes, M. C. *et al.* Monitoring adverse events of low-dose glucocorticoid therapy: EULAR recommendations for clinical trials and daily practice. *Annals of the Rheumatic Diseases* **69**, 1913-1919 (2010).

61. Rafacho, A., Giozzet, V. A., Boschero, A. C. & Bosqueiro, J. R. Functional alterations in endocrine pancreas of rats with different degrees of dexamethasone-induced insulin resistance. *Pancreas* **36**, 284-293 (2008).

62. Shen, C. N., Seckl, J. R., Slack, J. M. & Tosh, D. Glucocorticoids suppress beta-cell development and induce

hepatic metaplasia in embryonic pancreas. *Biochem. J* **375**, 41-50 (2003).

63. Cernea, S. & Raz, I. Therapy in the Early Stage: Incretins. *Diabetes Care* **34**, S264-S271 (2011).

64. Heppner, K. M., Tong, J., Kirchner, H., Nass, R. & Tschop, M. H. The ghrelin O-acyltransferase-ghrelin system: a novel regulator of glucose metabolism. *Curr. Opin. Endocrinol. Diabetes Obes.* **18**, 50-55 (2011).

65. Rabe, K., Lehrke, M., Parhofer, K. G. & Broedl, U. C. Adipokines and insulin resistance. *Mol. Med.* **14**, 741-751 (2008).

66. Kliewer, S. A. & Mangelsdorf, D. J. Fibroblast growth factor 21: from pharmacology to physiology. *The American Journal of Clinical Nutrition* **91**, 254S-257S (2010).

67. Badman, M. K., Koester, A., Flier, J. S., Kharitonenkov, A. & Maratos-Flier, E. Fibroblast growth factor 21-deficient mice demonstrate impaired adaptation to ketosis. *Endocrinology* **150**, 4931-4940 (2009).

68. Inagaki, T. *et al.* Endocrine Regulation of the Fasting Response by PPARalpha-Mediated Induction of Fibroblast Growth Factor 21. *Cell Metab* **5**, 415-425 (2007).

69. Hotta, Y. *et al.* Fibroblast growth factor 21 regulates lipolysis in white adipose tissue but is not required for ketogenesis and triglyceride clearance in liver. *Endocrinology* **150**, 4625-4633 (2009).

70. Grant, P. J. Diabetes mellitus as a prothrombotic condition. *Journal of Internal Medicine* **262**, 157-172 (2007).

71. Campbell, J. E., Peckett, A. J., D'souza, A. M., Hawke, T. J. & Riddell, M. C. Adipogenic and lipolytic effects of chronic glucocorticoid exposure. *Am J Physiol Cell Physiol* **300**, C198-C209 (2011).

72. Arnaldi, G. *et al.* Pathophysiology of dyslipidemia in Cushing's syndrome. *Neuroendocrinology* **92 Suppl 1**, 86-90 (2010).

73. Seckl, J., Morton, N., Chapman, K. & Walker, B. Glucocorticoids and 11beta-Hydroxysteroid Dehydrogenase in Adipose Tissue. *Recent Prog Horm Res* **59**, 359-393 (2004).

74. Samra, J. S. *et al.* Effects of Physiological Hypercortisolemia on the Regulation of Lipolysis in Subcutaneous Adipose Tissue. *Journal of Clinical Endocrinology & Metabolism* **83**, 626-631 (1998).

75. Veilleux, A. *et al.* Expression of genes related to glucocorticoid action in human subcutaneous and omental adipose tissue. *J Steroid Biochem. Mol Biol.* **122**, 28-34 (2010).

76. Livingstone, D. E. W., Grassick, S. L., Currie, G. L., Walker, B. R. & Andrew, R. Dysregulation of glucocorticoid metabolism in murine obesity: comparable effects of leptin resistance and deficiency. *J Endocrinol* **201**, 211-218 (2009).

77. Bujalska, I. J., Kumar, S. & Stewart, P. M. Does central obesity reflect "Cushing's disease of the omentum"? *Lancet* **349**, 1210-1213 (1997).

78. Walker, B. R. Glucocorticoids and cardiovascular disease. *Eur. J. Endocrinol.* **157**, 545-559 (2007).

79. Filipsson, H., Monson, J. P., Koltowska-Häggström, M., Mattsson, A. & Johannsson, G. The Impact of Glucocorticoid Replacement Regimens on Metabolic Outcome and Comorbidity in Hypopituitary Patients. *Journal of Clinical Endocrinology & Metabolism* **91**, 3954-3961 (2006).

80. Choi, H. K. & Seeger, J. D. Glucocorticoid use and serum lipid levels in US adults: the Third National Health and Nutrition Examination Survey. *Arthritis Rheum.* **53**, 528-535 (2005).

81. Reaven, E. P., Kolterman, O. G. & Reaven, G. M. Ultrastructural and physiological evidence for corticosteroid-induced alterations in hepatic production of very low density lipoprotein particles. *J Lipid Res* **15**, 74-83 (1974).

82. Fried, S. K., Russell, C. D., Grauso, N. L. & Brolin, R. E. Lipoprotein lipase regulation by insulin and glucocorticoid in subcutaneous and omental adipose tissues of obese women and men. *J Clin Invest* **92**, 2191-2198 (1993).

83. Appel, B. & Fried, S. K. Effects of insulin and dexamethasone on lipoprotein lipase in human adipose tissue. *Am J Physiol* **262**, E695-E699 (1992).

84. Hoekstra, M. *et al.* Scavenger receptor BI-mediated uptake of serum cholesterol is essential for optimal adrenal glucocorticoid production. *J Lipid Res.* (2009).

85. Stojanovska, L., Rosella, G. & Proietto, J. Evolution of dexamethasone-induced insulin resistance in rats. *Am. J. Physiol* **258**, E748-E756 (1990).

86. Saad, M. J., Folli, F., Kahn, J. A. & Kahn, C. R. Modulation of insulin receptor, insulin receptor substrate-1, and phosphatidylinositol 3-kinase in liver and muscle of dexamethasone-treated rats. *J. Clin. Invest* **92**, 2065-2072 (1993).

87. Guillaume-Gentil, C., ssimacopoulos-Jeannet, F. & Jeanrenaud, B. Involvement of non-esterified fatty acid oxidation in glucocorticoid-induced peripheral insulin resistance in vivo in rats. *Diabetologia* **36**, 899-906 (1993).

88. Venkatesan, N., Lim, J., Bouch, C., Marciano, D. & Davidson, M. B. Dexamethasone-induced impairment in skeletal muscle glucose transport is not reversed by inhibition of free fatty acid oxidation. *Metabolism* **45**, 92-100 (1996).

89. DeFronzo, R. A., Tobin, J. D. & Andres, R. Glucose clamp technique: a method for quantifying insulin secretion and resistance. *Am. J. Physiol* **237**, E214-E223 (1979).

90. Qi, D. *et al.* Single-dose dexamethasone induces whole-body insulin resistance and alters both cardiac fatty acid and carbohydrate metabolism. *Diabetes* **53**, 1790-1797 (2004).

91. Reichardt, H. M. *et al.* DNA binding of the glucocorticoid receptor is not essential for survival. *Cell* **93**, 531-541 (1998).

92. Yen, T. T., Gill, A. M., Powell, J. G. & Sampson, B. M. Ciglitazone prevents and reverses dexamethasone-induced hyperglycemia in female viable yellow mice. *Int. J Obes. Relat Metab Disord.* **16**, 923-933 (1992).

93. Thomas, C. R., Turner, S. L., Jefferson, W. H. & Bailey, C. J. Prevention of dexamethasone-induced insulin resistance by metformin. *Biochem. Pharmacol.* **56**, 1145-1150 (1998).

94. Gounarides, J. S. *et al.* Effect of dexamethasone on glucose tolerance and fat metabolism in a diet-induced obesity mouse model. *Endocrinology* (2007).

95. Couce, M. *et al.* Treatment with growth hormone and dexamethasone in mice transgenic for human islet amyloid polypeptide causes islet amyloidosis and beta-cell dysfunction. *Diabetes* **45**, 1094-1101 (1996).

96. Bernal-Mizrachi, C. *et al*. Dexamethasone induction of hypertension and diabetes is PPAR-alpha dependent in LDL receptor-null mice. *Nat. Med.* **9**, 1069-1075 (2003).

2

A novel approach to monitor glucose metabolism using stable isotopically-labeled glucose in longitudinal studies in mice

Submitted

Anke J. Laskewitz*
Theo H. van Dijk*
Aldo Grefhorst
Theo S. Boer
Vincent W. Bloks
Folkert Kuipers
Albert K. Groen
Dirk-Jan Reijngoud

*Both authors contributed equally

Abstract

The etiology of insulin resistance is still an enigma. Mouse models are frequently employed to solve the underlying pathology. The most commonly used methods to monitor insulin resistance are the HOMA-IR, glucose or insulin tolerance tests or the hyperinsulinemic euglycemic clamp (HIEC). Unfortunately, these tests disturb steady state glucose metabolism. Here we describe a method in which blood glucose kinetics can be determined in fasted mice without noticeably perturbing glucose homeostasis. The method involves an intraperitoneal injection of a trace amount of [6,6-$^{2}H_{2}$]-glucose and can be performed repeatedly in individual mice. The validity and performance of this novel method was tested in mice fed chow or high-fat diet for a period of 5 weeks. After administering the mice with [6,6-$^{2}H_{2}$]-glucose, decay of the glucose label was followed in small volumes of blood collected by tail tip bleeding during a 90 minute period. The total amount of blood collected was less than 120 µl. This novel approach confirmed in detail the well-known increase in insulin resistance induced by a high-fat diet. The mice showed reduced glucose clearance rate, and reduced hepatic and peripheral insulin sensitivity. To compensate for this insulin resistance, β-cell function was slightly increased. We conclude that this refinement of existing methods enables detailed interrogation of glucose homeostasis in mice. Insulin resistance can be accurately determined while mechanistic insight is obtained in underlying pathology. Additionally, this novel approach reduces the number of mice needed for longitudinal studies of insulin sensitivity and glucose metabolism.

Introduction

The metabolic syndrome is one of the most important contemporary disease complexes in western societies [1,2]. The syndrome is defined as a cluster of interrelated risk factors which predict a high incidence of cardiovascular disease and diabetes mellitus type 2. According to the International Diabetes Federation these risk factors include central obesity defined by increased waist circumference, hypertension, increased plasma triglyceride levels, reduced HDL cholesterol, hyperglycemia and insulin resistance [3].

To elucidate the effects of multiple factors, such as gender, heredity and environment on development of the metabolic syndrome, a number of animal models have been introduced. From these models, mouse models are very important, since they can be genetically manipulated and hence offer the possibility to study the role of specific genes in the development of insulin resistance and/or changes in glucose metabolism independent from other circumstances [4-6]. In addition, mice have a high reproduction rate and a relatively short lifespan which is essential for studies on parental effects (*e.g.,* in metabolic programming) and healthy aging [7]. Due to their small size, however, mouse experiments are limited by the amount of blood that can be taken, which is restricted to 8 ml/kg/14 days [8] by most animal ethical committees. In addition, infusion rates during complex stable isotope infusion protocols have to be adjusted to the high metabolic rate of mice and (surgical) handling of mice is complicated and requires specific skills. Therefore, some of the published mouse experiments are performed under restrained or even anaesthetized conditions which strongly influences rates of glucose turnover, making it difficult to interpret the results [9].

Simple parametric models like the homeostatic model assessment (HOMA-IR) are most commonly used to assess the degree of insulin resistance and glucose intolerance. These models are solely based on measurements of insulin and glucose concentration and are therefore not suited to study the (patho)physiology of inter organ relationships that could underlie perturbed insulin sensitivity [10]. Moreover, methods need to be developed to allow for longitudinal studies in individual mice to evaluate changes in tissue-specific insulin sensitivity. For this purpose, the kinetic or steady-state flux experiments are a good approach. To study insulin resistance in more detail, *e.g.*, tissue-specific insulin sensitivity, a number of techniques are available from which the hyperinsulinemic euglycemic clamp (HIEC) is regarded as the 'gold standard' [11,12]. The HIEC can not be used for longitudinal studies of tissue-specific insulin sensitivity in individual mice, since the HIEC is invasive and can only be performed once in an individual mouse [13]. Less invasive techniques are glucose tolerance tests and insulin tolerance test [14], but these tests only evaluate effects on whole body glucose metabolism under perturbing conditions and are not tissue-specific.

Longitudinal studies on changes in insulin sensitivity and glucose tolerance with sequential testing in individual mice depend on the ability to accurately perform measurements in small blood samples. We developed a blood sampling method by taking bloodspots via tail tip bleeding on filter paper as starting material for analyses of stable isotopically-labeled compounds by gas chromatography-mass spectrometry (GC-MS). Hereby, we were able to minimize the volume of blood to be drawn [15] that allowed us to follow the concentrations of labeled compounds over time in very small blood volumes. This approach can be implemented in other published methods. Galvin and colleagues, for instance, estimated glucose kinetics and insulin sensitivity from glucose and insulin data during an intravenous glucose tolerance test (IVGTT) [16]. This method, however, perturbs the glucose and insulin concentrations due to the high amount of glucose given. Pacini *et al.* introduced a similar method for mice, in which data were analyzed using the minimum model technique, according to a two-compartment model [17]. During this experiment, mice were kept under anesthesia on a heating pad and 7 blood samples were taken of 75µl each. The large volume of blood withdrawn in this method perturbs the circulation severely which makes interpretation of the data difficult.

We hypothesized that the combination of a trace amount of stable isotopically-labeled glucose, combined with collection of small blood samples on filter paper and GC-MS analysis, would enable us to obtain the necessary data to calculate glucose kinetics at prevailing glucose and insulin concentrations during fasting. In this study, we present a method to calculate glucose kinetics and correlate these kinetic data with parameters of the HOMA-IR under prevailing glucose and insulin concentrations. To this purpose, a small amount of stable isotopically-labeled [6,6-^{2}H]-glucose was administrated intraperitoneally to mice fed a standard laboratory chow diet or a high-fat diet for 5 weeks. High-fat diet fed mice were included as a well-documented model for insulin resistance. Since basal blood glucose and plasma insulin concentrations were not disturbed during the experimental protocol, glucose kinetics can be approximated by single-pool first-order kinetic model [20-22]. Furthermore, several parameters describing insulin sensitivity and β-cell function were assessed using a HOMA-IR adapted for mice [10].

Materials and Methods

Animals

Male C57BL/6J mice (25.3 ± 1.4 g), aged 8-12 weeks, were included (n=40). The animals were obtained from Harlan Laboratories (Horst, The Netherlands). After arrival, animals

were allowed to recover for 1 week in groups of 6 animals in plexiglas cages, receiving a commercially available lab chow (RMH-B, Arie Blok Diervoeding, Woerden, The Netherlands). Mice were subsequently housed individually for 1 week after which the first blood glucose kinetics test (day 0) was performed. Next, mice remained on lab chow or received a high-fat diet (36% (wt/wt) bovine tallow, *i.e.*, 60% energy from fat) [23] for 5 weeks after which the blood glucose kinetics test was repeated. During the whole experiment mice were housed under a controlled 12 h light-dark cycle and temperature (21°C) regime. The experiments were approved by the Ethical Committee for Animal Experiments of the University of Groningen.

Blood glucose kinetics

After 9 hour fast (23:00 h – 8:00 h), at time point 0, mice received a small volume of 2.0 mg D-[6,6-$^2H_2$]glucose in 0.20 ml by intraperitoneal injection (~450 µmol kg^{-1} BW). Blood glucose concentrations were determined and blood spots obtained by tail tip bleeding were collected on filter paper just before (time point 0) and at 10, 20, 30, 40, 50 60, 75 and 90 minutes after glucose administration. At the end of the test, a blood sample of ~30 µl was taken for insulin measurements. This represents a total volume of ~120 µl of blood which is less than 7% of the total blood volume. Blood samples were centrifuged immediately and plasma was stored at -20°C until analysis. Blood spots were air-dried and stored at room temperature until analysis. In an additional group of mice (n=12) the effect of the experimental procedure on insulin levels was measured. To study the influence of the administrated glucose on insulin levels, in a separate experiment, blood glucose levels were measured and blood samples of ~30 µl were taken for insulin measurements before and at 15, 30 and 90 minutes after D-[6,6-$^2H_2$]glucose injection.

Metabolite concentrations

Blood glucose concentrations were determined with a handheld OneTouch Ultra Blood Glucose Meter (LifeScan Benelux, Beerse, Belgium). Plasma insulin concentrations were determined using enzyme-linked immunosorbent assay adapted for measurements in 10 µl plasma (Ultrasensitive Mouse Insulin kit, Mercodia, Uppsala, Sweden). HOMA-IR was calculated by a formula adapted to Mathews *et al.* [10]. For mice, reference values were calculated using average fasting glucose (6.4 mM) and plasma insulin (2.2 $mU.l^{-1}$) concentrations from the control group at the start of the experiment (Table 1, eq.9 to eq. 15).

Derivatization and GC-MS measurements of glucose

Fractional distributions of D-[6,6-$^2H_2$]glucose in bloodspot were measured according to Van Dijk *et al*. [15]. In short, glucose was extracted from bloodspots by punching out a disk

(6.5 mm in diameter), transferred to a reaction vial and wetted with 50 µl water for 10 min followed by the addition of 500 µl ethanol after which the mixture was incubated overnight at room temperature. Subsequently, the solution was centrifuged in a centrifuge for 5 min after which 400 µl supernatant was removed and transferred to a Teflon-capped reaction vial and dried at 60°C under a stream of nitrogen. Glucose was converted to its pentaacetate derivative by adding 300 µl pyridine/acetic anhydride (1:2) to the residue, incubating it overnight at room temperature, followed by drying at 60°C under a stream of nitrogen. The residue was dissolved in 200 µl ethylacetate and transferred into injection vials for analysis. All samples were analyzed by gas chromatography mass spectrometry (Agilent 9575C inert MSD; Agilent Technologies, Amstelveen, The Netherlands). Derivatives were separated on AT-1701 30 m x 0.25 mm ID (0.25 µm film thickness) capillary column (Alltech, Breda, The Netherlands). The separation for glucose pentaacetate was as follows: the oven temperature started at 150°C for 0.5 min, increased to 280°C at a rate of 80°C min^{-1}, and remained at 280°C for 4.4 min. Mass spectrometric analyses were performed by positive chemical ionization with ammonia. Ions monitored, *m/z* 408-414 (m_0 - m_6), were corrected for the fractional distribution due to natural abundance of ^{13}C by multiple linear regression as described by Lee *et al.* [24] to obtain the excess fractional distribution of mass isotopomers (M_0 - M_6) due to the dilution of administered labelled glucose, *i.e.*, M_2 represents the fractional contribution of D-[6,6-$^2H_2$]glucose in blood glucose. This fractional contribution was used in the calculations of blood glucose kinetics.

Calculation of blood glucose kinetics

Whole body glucose turnover and clearance were calculated by kinetic analysis from the wash-out of injected D-[6,6-$^2H_2$]-glucose from the circulation. Formulas used for calculations of the kinetic parameters are given in Table 1. Since there is no dynamic insulin action under these conditions, we used a single-pool first-order kinetic model for basal glucose kinetics as described previously [22,25,26]. This was confirmed by comparison of the results on glucose turnover and metabolic clearance rates obtained from a two-compartment model with those obtained from a single compartment model, which resulted in similar turnover and clearance rates. To fit the model, the average time course was constructed for each of the studied groups using SAAMII. The values obtained were used as Bayesian values in the fitting of the model to the data points for individual mice. Next, averages of the parameter values of the individual mice were calculated for each of the studied groups and compared to the initial parameter values extracted from the average time-course. The estimates of parameters for each individual mouse were accepted when no significant difference remained between both sets of values. Otherwise, the procedure was repeated with adjusted Bayesian values.

Statistics

Deming regression was used for comparisons of different methods. Data were plotted as median values in a Tukey box-plot, showing 2x SD with its outliers. Two group comparisons were done by the Wilcoxon signed-rank test or Mann-Whitney U test for related and unrelated groups, respectively. Differences were considered statistically significant when $p<0.05$. (Prism 5.00, Graph-Pad Software, Inc. La Jolla, USA)

Table 1

Formulas for calculation of blood glucose kinetics

Eq. 1	Tracer Concentration at t	$C_t = M_t \times [glc]_t$
Eq. 2	Single-pool first-order kinetics	$C_t = C_0^{el} e^{-k^{el}t} - C_0^{ab} e^{-k^{ab}t}$
Eq. 3	Bioavailability	$F = 1 - \left(\frac{C_0^{ab} \times k^{el}}{k^{ab} \times C_0^{el}} \right)$
Eq. 4	Area under the curve	$AUC = \frac{C_0^{el}}{k^{el}} - \frac{C_0^{ab}}{k^{ab}}$
Eq. 5	Metabolic clearance rate	$MCR = \frac{F \times D}{AUC}$
Eq. 6	Apparent volume of distribution	$V = \frac{MCR}{k^{el}}$
Eq. 7	Turnover rate	$Ra = MCR \times BG$
Eq. 8	Pool size	$A = \frac{Ra}{k^{el}}$
Eq. 9	Insulin Sensitivity	$\%S = \frac{(PI_c \times BG_c)_{median}}{PI \times BG} = \frac{14.1}{PI \times BG}$
Eq. 10	Hepatic Insulin Sensitivity	$\%H = \frac{(PI_c \times Ra_c)_{median}}{PI \times Ra} = \frac{308}{PI \times Ra}$
Eq. 11	Peripheral Insulin Sensitivity	$\%P = \frac{MCR / PI}{(MCR_c / PI_c)_{median}} = \frac{MCR / PI}{0.0098}$
Eq. 12	100% β-cell function	$PI_c = a \times BG_c - b = 0.66 \times BG_c - 2.18$
Eq. 13	β-cell function	$\%B = \frac{1/a \times PI}{(BG - b/a)} = \frac{1.52 \times PI}{(BG - 3.30)}$
Eq. 14	Disposition Index	$\%DI = \%B \times \%S$
Eq. 15	Homeostatic model	$HOMA - IR = \frac{BG \times PI}{14.1}$

Legend Table 1

Formulas for the calculated parameters for the single-pool first order glucose kinetics

Relevant equations in blood glucose kinetics and HOMA-IR are shown. M_t represents the fractional contribution of the tracer in blood at time point t and $[glc]_t$ the blood glucose level at time point t. C^{el}_0 and C^{ab}_0 represent the extrapolated concentrations of tracer at time point 0 in the elimination and absorption curve, respectively. k^{el} and k^{ab} represent rate constants of elimination and absorption, respectively, which were calculated using SAAM II software (Version 1.2.1 Compartmental, SAAM Institute, University of Washington). D represents the dose of tracer in $\mu mol^{-1}.kg^{-1}$ given to the mice at time point 0. BG is the mean blood glucose level during the experiment and PI the plasma insulin level at time point 90 min. %S represents whole body insulin sensitivity, however, blood glucose kinetics in combination with plasma insulin levels were used to distinguish between hepatic (%H) and peripheral (%P) insulin sensitivity. %H was calculated as a constant divided by the product of blood glucose and plasma insulin.

The clearance of the administrated glucose tracer (MCR) was assumed to be independent from endogenous glucose production the relation to plasma insulin levels (PI) was used to estimate peripheral insulin sensitivity (%P), which was calculated as the ratio of MCR and PI of individual mice divided by the median of these ratios of the control group. Note; for these calculations a linear relationship between PI and MCR was assumed. Because kinetics of glucose tracer were identical to the kinetics of glucose tracee (3) the calculations were also valid for blood glucose metabolism.

To deduce the line of representing 100% β-cell function (%B) in the control group as shown in Fig. 3A we used an empirical approach. It was assumed that this line intersects the median data point of the control group, *i.e.* 6.4 mM and 2.2 $mU.l^{-1}$ for blood glucose and plasma insulin, respectively. Additionally, it was assumed that median β -cell function of the group equals 100%. The optimal result was obtained for this line is described by eq. 12. From this equation it can be deduced that %B for the individual mice can be calculated by eq. 13. It has been shown that in normal situations changes in %S are adjusted by inverse effects in %B so that the relation between %B and %S can be described by a hyperbolic function (eq. 14). Eq. 15 gives the adjusted HOMA-IR for mice for this study, in which fasting BG is blood glucose in mM and fasting ins is fasting insulin in $mU.l^{-1}$.

RESULTS

To investigate the effect of this experimental protocol on glucose metabolism, a small amount (2.0 mg per mouse) of D-[6,6-$^2H_2$]-glucose was injected intraperitoneally into 9 hours-fasted mice (n=40) and the effect on glucose concentration was measured (Fig. 1A). Due to handling of the animals, blood glucose concentrations increased from 4.6 mM at t=0 min to 6.6 mM at t=30 min (Fig. 1A). Subsequently, blood glucose concentration declined slightly to 5.9 mM at t=90 min. The wash-out of stable isotopically-labeled glucose from the circulation was determined by analyzing the isotopic enrichment of glucose eluted from bloodspots collected consecutively on filter paper obtained by tail tip bleeding (Fig 1B). The concentration of [6,6-$^2H_2$]-glucose tracer in blood was calculated according to eq. 1 (Table 1). The influence of tracer injection on insulin levels was tested in a second group of mice (n=12) that also received D-[6,6-$^2H_2$]-glucose intraperitoneally. Since insulin measurement requires a relatively large amount of blood, glucose and insulin levels were measured at four time points during a separate experiment to avoid large blood volume to be drawn from each individual animal (Fig. 1C-D). Figure 1C shows the blood glucose curve during this experiment, which was very similar to the curve shown in figure 1A. There was no change in plasma insulin levels (p=0.4) during the experiment (Fig. 1D), which confirms that the amount of glucose tracer injected, did not trigger insulin secretion. This indicates that the insulin level measured at the end of the experiment is representative for the insulin level during the experiment.

Figure 1

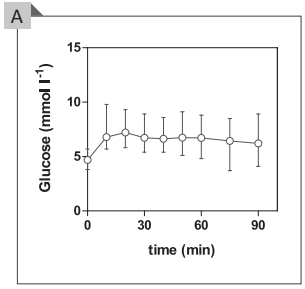

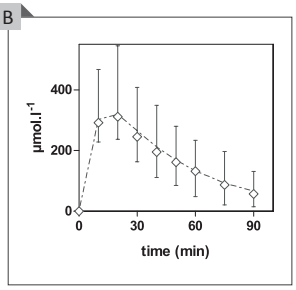

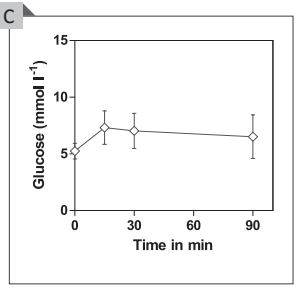

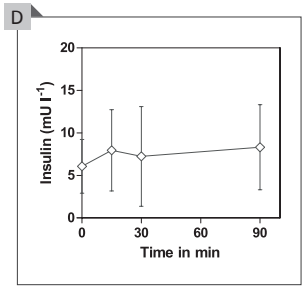

Glucose and insulin levels during experiment

Blood concentrations of glucose, tracer D-[6,6-^{2}H]glucose and insulin after a intraperitoneal bolus of D-[6,6-^{2}H]glucose from two separate experiments. Two parallel experiments were carried out; the first experiment focused on actual blood glucose kinetics, while the second experiment focused on analysis of insulin concentrations during the experiment.

A, Concentrations of glucose in blood **B,** Concentration of [6,6-^{2}H]glucose in blood. **C,** Blood glucose concentrations during second experiment. **D,** Plasma insulin concentrations during second experiment.

A high-fat diet increases HOMA-IR and reduces insulin sensitivity

Next the performance of the blood glucose kinetics test was investigated in a group of mice fed either a chow or a high-fat diet for 5 weeks. Both groups had similar median values of fasting blood glucose levels on day 0 of the experiment (Fig. 2A). Fasting blood glucose levels increased significantly when mice received a high-fat diet for 35 days, *i.e.*, from a median of 6.5 mM to 11.9 mM, while it remained almost unchanged in the chow-fed group. Plasma insulin levels showed a very similar course (Fig. 2B): plasma insulin levels only increased in mice fed a high-fat diet for 35 days, *i.e.*, from 2.3 mU.l^{-1} to 10.3 mU.l^{-1}. The values measured in mice at day 0 of the experiment (*i.e.* 6.4 mM for glucose and 2.2 mU.l^{-1} for insulin) were used to calculate the basal values of the HOMA-IR, which allowed for adjustment of the HOMA-IR for mice. High-fat feeding of mice resulted in a significantly increased HOMA-IR (Fig. 2C). Additionally, the insulin sensitivity (%S) and β-cell function (%B) were calculated, according to eq. 9 and eq. 13 from Table 1, respectively, for which the values of day 0 represents 100% insulin sensitivity (%S) and 100% β-cell function (%B). After 35 days %S was slightly but significantly reduced in the chow-fed group (Fig. 2D), *i.e.*, from 97% to 79%. In contrast, the high-fat fed group had a very strong reduction of 88% in %S. In contrast, β-cell function (%B) was increased in the high-fat fed group (Fig. 2E), *i.e.*, median 91% to 177%, implying compensation for reduced insulin sensitivity by increasing β-cell activity. Subsequently, the relationship was studied between β-cell function and insulin sensitivity in mice (Fig. 2F-G). In figure 2G the relationship between %B and %S is shown. Like in humans, the relationship can be described by a hyperbolic function in mice

Figure 2

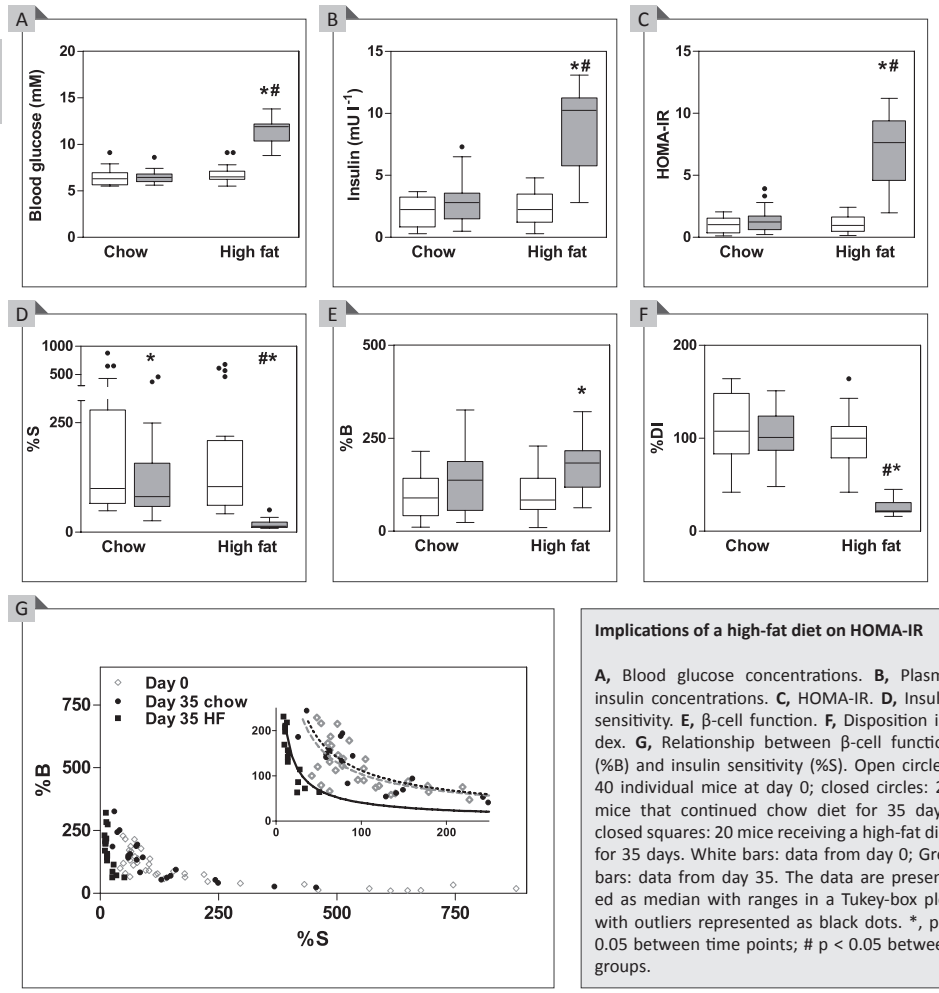

Implications of a high-fat diet on HOMA-IR

A, Blood glucose concentrations. **B,** Plasma insulin concentrations. **C,** HOMA-IR. **D,** Insulin sensitivity. **E,** β-cell function. **F,** Disposition index. **G,** Relationship between β-cell function (%B) and insulin sensitivity (%S). Open circles: 40 individual mice at day 0; closed circles: 20 mice that continued chow diet for 35 days; closed squares: 20 mice receiving a high-fat diet for 35 days. White bars: data from day 0; Grey bars: data from day 35. The data are presented as median with ranges in a Tukey-box plot with outliers represented as black dots. *, $p < 0.05$ between time points; # $p < 0.05$ between groups.

as well. The disposition index (%DI), a measure for the ability of β-cells to compensate for reduced insulin sensitivity, was calculated according to eq. 14 (Table 1). It was clear that %DI at the end of the experiment in chow fed animals was very comparable to that calculated for the start of the experiment (Fig. 2F). In contrast, the %DI of high-fat fed mice was greatly reduced at the end of the experiment when compared to the value of %DI observed at the start of the experiment.

A high-fat diet reduces metabolic clearance rate and apparent volume of distribution of glucose in mice

Glucose kinetics was studied in chow-fed and high-fat fed mice at the start and end of

the experiment (Fig. 3A-H). Chow-fed mice slightly gained bodyweight over time, from 25.3 ± 1.1 g at the start of the experiment to 28.0 ± 1.7 g at day 35. Mice fed a high-fat diet showed a more pronounced increase in bodyweight, *i.e.*, from 25.2 ± 1.1 g to 31.0 ± 2.3 g. The increase in bodyweight of the mice over time in combination with an identical amount of administered tracer resulted in a significantly lower dose of tracer per kg bodyweight on day 35 compared to day 0 for both groups (Fig. 3A).

Metabolic clearance of glucose (MCR), *i.e.*, the volume of blood completely cleared from glucose in by peripheral tissue, *i.e.*, muscle, brain and adipose tissue, is an important pa-

Figure 3

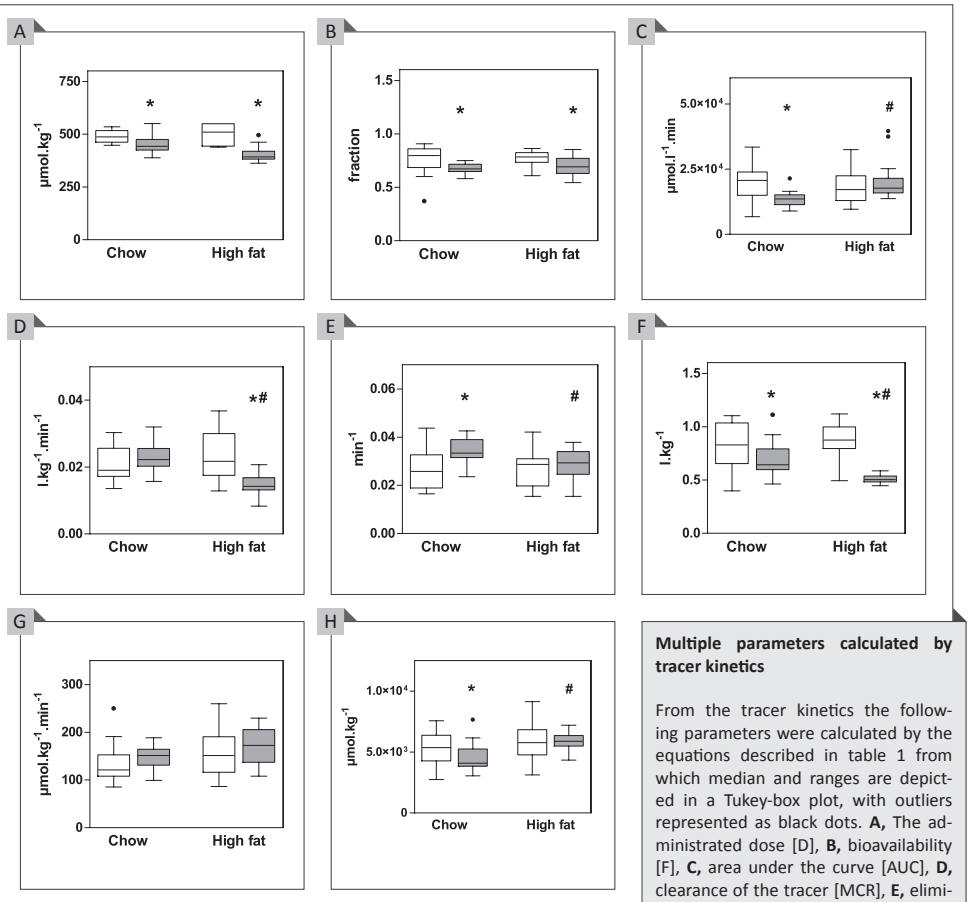

Multiple parameters calculated by tracer kinetics

From the tracer kinetics the following parameters were calculated by the equations described in table 1 from which median and ranges are depicted in a Tukey-box plot, with outliers represented as black dots. **A,** The administrated dose [D], **B,** bioavailability [F], **C,** area under the curve [AUC], **D,** clearance of the tracer [MCR], **E,** elimination rate [k_{el}], **F,** apparent volume of distribution [V], **G,** turnover rate [Ra] (HGP) and **H,** pool size [A] from mice on a chow diet or high-fat diet are shown with white bars representing day 0 and grey bars after 35 days of diet. *, $p < 0.05$ between time points; # $p < 0.05$ between groups.

rameter in blood glucose kinetics. Equation 5 from Table 1 shows that MCR depends on the dose of D-[6,6-$^2H_2$]glucose administrated, the bioavailability of D-[6,6-$^2H_2$]glucose (F) (eq. 3) and the area under the concentration curve of D-[6,6-$^2H_2$]glucose (AUC) (eq. 4). The bioavailability of the tracer, *i.e.*, the fraction of administered tracer that enters the sampled pool, was significantly lower on day 35 compared to day 0 in both the chow and high-fat diet group (Fig. 3B). After 35 days of high-fat feeding the AUC was considerably higher as compared to a 35-day chow diet (Fig. 3C) which resulted in significant differences in AUC between both groups on day 35. The calculated MCR of the tracer (Fig. 3D) was similar in both groups on day 0 and did not change in the chow-fed group over time, but was reduced in the high-fat fed mice MCR, *i.e.*, from 0.022 $l.kg^{-1}.min^{-1}$ to 0.014 $l.kg^{-1}.min^{-1}$, resulting in a significant difference in MCR after 5 weeks between both groups.

According to eq. 6 from Table 1, the apparent volume in which glucose is distributed (V) depends on the MCR of glucose and the elimination rate k_{el} (Fig. 3E). After 35 days of chow diet median k_{el} was significantly changed from 0.026 min^{-1} to 0.033 min^{-1}, yet, k_{el} remained unchanged in the high-fat fed group over the same period of time. The apparent volume of distribution (Fig. 3F) was slightly decreased after 35 days in the chow-fed group, *i.e.*, from median 0.83 $l.kg^{-1}$ to 0.64 $l.kg^{-1}$. However, in the high-fat fed group, V was more reduced, *i.e.*, from 0.87 $l.kg^{-1}$ to 0.50 $l.kg^{-1}$.

Other relevant parameters in blood glucose kinetics, *i.e.*, turnover rate (Ra) and pool size (A) were calculated according to eq. 7 and eq. (Table 1), respectively (Fig. 3G-H). The pool size was slightly reduced in chow-fed mice after 35 days, while there were no differences in mice fed a high-fat diet. Although Ra was slightly increased on day 35 in both groups, no significant difference was observed between either group or time point. Since the mice were fasted prior to the study of glucose kinetics, the turnover rate of glucose can be regarded as the endogenous glucose production rate, which implicated that high-fat diet feeding did not alter hepatic glucose production.

HOMA-IR and glucose kinetics

Matsuda *et al.* [18] and Færch *et al.* [19] presented arguments to merge certain kinetic parameter of whole body glucose metabolism with the HOMA-IR such that changes in tissue-specific insulin sensitivity can be evaluated. In their discussion the authors related insulin levels to the endogenous glucose production to evaluate hepatic insulin sensitivity (%H, eq. 10, Table 1). In fasted mice the turnover of glucose (Ra) in the circulation reflects this production. We assumed that peripheral insulin sensitivity (%P, eq. 11, Table 1) could be reflected by the relation between MCR and insulin concentration. Since both turnover and MCR can be derived from the data of the wash-out of a tracer amount of stable isotopic

Figure 4

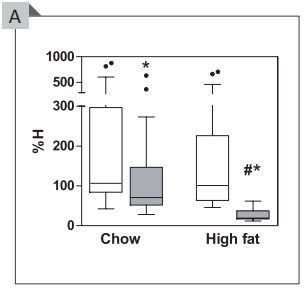

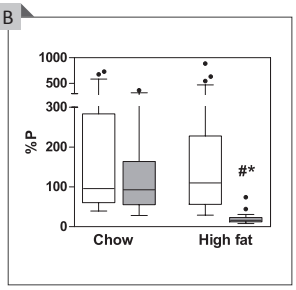

Implications of a high-fat diet on insulin related glucose kinetics

A, Hepatic insulin sensitivity (%H). **B,** Peripheral insulin sensitivity (%P). White bars: day 0; grey bars: day 3. The data are presented in a Tukey-box plot, with outliers represented as black dots. *, $p < 0.05$ between time points; # $p < 0.05$ between groups.

labeled glucose after injection, %H and %P were calculated for individual mice both at the start and the end of the experiment. After 35 days, %H was decreased slightly in the chow-fed group, while the reduction of %H in the high-fat fed group was 5-fold, *i.e.*, from 101% to 22% (Fig. 4A). In addition, the high-fat fed group showed an almost 7-fold reduction in %P, *i.e.*, from a median of 110% to 16% after 35 days of high-fat feeding (Fig. 4B), implying that a high-fat diet reduces both peripheral and hepatic insulin sensitivity.

Discussion

In this paper, we present a novel approach to assess interorgan relationships determining insulin and glucose action in small laboratory animals. The approach is a combination of the application of HOMA-IR to assess insulin resistance and analysis of a glucose tracer wash-out by a single-pool, first-order kinetic model to assess whole body glucose metabolism. The merging of both methods makes evaluation of tissue-specific insulin sensitivity possible during fasting at prevailing insulin an glucose concentration in a fasted steady-state condition. By collecting bloodspots on filter paper by tail tip bleeding, this approach allows for sequential application in individual mice in order to document time-dependent changes in insulin action and whole body glucose metabolism in small laboratory animals,

The approach starts with an intraperitoneal injection of 2 mg D-[6,6-$^{2}H_{2}$]glucose per animal. Subsequently, blood glucose is measured and bloodspots are taken at nine time points (~10 µl per time point). At the final time point a larger sample (~30 µl blood) is taken to measure insulin levels. In total, about 120 µl of blood is taken per animal during the experiment. This very small volume of blood drawn is an important *refinement* in mice studies, compared to, for instance, Pacini *et al.* [17] who collected as much as 525 µl during a comparable experiment. In addition, our novel procedure can be repeated (within limits of time) in the same animal and therefore *reduces* the number of animals needed to study effects of different dietary protocols and pharmacological treatments. The validity

of the single-compartment first-order kinetic model used to calculate glucose kinetics was compared with results calculated from the generally used two-compartment model. No differences were observed between both models (data not shown), which confirmed our hypothesis that the single-compartment first-order kinetic model is valid under fasted insulin and glucose concentrations. Since Matthews *et al.* [10] presented their model to asses insulin action for humans, the model parameters they derived are only applicable for humans. In mice a new set of parameters needed to be established. To do so, we assumed that all data measured and calculated at the start of the experiment in young, wild-type, chow fed mice reflects 100% insulin sensitivity and β-cell function. Subsequently, model parameters for insulin sensitivity and β-cell function could be calculated [27,28]. To calculate hepatic insulin sensitivity (%H) we used the product of endogenous glucose production and plasma insulin level as presented by Matsuda *et al.* [18], which was discussed by Færch *et al.* [19], and for peripheral insulin sensitivity (%P) the ratio of clearance rate and plasma insulin level was used. Note that the values given in this study adapting the HOMA-IR for use in mice is only applicable for mice of this particular mouse strain, in which glucose and insulin concentration are measured using the same methods.

We investigated the performance of our approach in a large group of young C57BL/6J mice at the start and after a period of 5 weeks in which they received either a high-fat diet or continued their habitual chow diet. It is well-known that feeding mice a high-fat diet induces insulin resistance [29]. An important observation was that in young mice on a chow diet (day 0) fasting insulin concentrations vary highly in combination with almost identical blood glucose concentrations, indicating that insulin plays a minor role in regulation of glucose homeostasis under fasting conditions. Thus other hormones, like glucagon might be more important in regulation of glucose homeostasis during fasting. The broad range in fasted insulin concentrations resulted in large ranges in the calculated overall and tissue specific insulin sensitivities, *i.e.*, %S, %H, and %P. High-fat feeding significantly increased both fasting insulin and glucose levels, resulting in an increased HOMA-IR, a decreased disposition index (%DI) and a reduction in all three insulin sensitivity indices, *i.e.*, overall insulin sensitivity (%S), hepatic insulin sensitivity (%H) and peripheral insulin sensitivity (%P). In contrast, the animals that continued the chow diet over the same period showed hardly any changes in fasting glucose and insulin levels, resulting in no changes in %S and %P and only a minor reduction in %H.

In addition, using HIEC, we have previously shown that feeding mice the same high-fat diet as used in the present paper resulted in peripheral insulin resistance accompanied by a reduced disposal of glucose by 40% [30], which was also seen in this study (see values for MCR in Fig. 2D). It should be realized, however, when comparing HIEC and the combined HOMA-glucose kinetic models that during HIEC supraphysiological concentrations of in-

sulin were applied, while for the HOMA-glucose kinetic model the measurements were done under prevailing concentrations of insulin. The Ra remained unchanged over time in both groups. The calculated turnover rate (which during fasting equals HGP) and metabolic clearance rate (MCR) were in the same order of magnitude as calculated by Mass Isotopomer Distribution Analysis as previously published [31-33], and thus show the validity of the presented kinetic analysis of the wash-out of stable isotopic labeled glucose after injection of a tracer amount.

The median apparent volume of distribution of 0.67 $l.kg^{-1}$ calculated on day 0 was higher than the extracellular fluid volume (0.22 $l.kg^{-1}$) often used in non-steady-state calculations [34,35] implicating that intracellular fluid volume is involved in the distribution of the administrated glucose. High-fat feeding reduced this volume to 0.46 $l.kg^{-1}$, most likely the result of a reduction in involved intracellular volume. The effect of high-fat feeding on the apparent distribution volume of glucose has not been reported before, although it is known that high-fat feeding reduces GLUT4 concentration and translocation form intracellular stores to the plasma membrane [36-38]. Furthermore, high-fat feeding impairs central insulin stimulation of blood flow [39], adding to the already perturbed glucose disposal in peripheral tissue and therefore in a reduced volume of distribution.

In conclusion, we describe a refined approach to evaluate blood glucose metabolism with a minimum level of inconvenience for the mice, which can be used in longitudinal studies in individual mice. This represents an opportunity for a major reduction in the number of animals necessary for these metabolic studies. It combines known protocols for calculation of insulin sensitivity and blood glucose kinetics under basal situations and can be repeated over time. In our view, the single pool kinetic analysis of intraperitoneally injected D-[6,6-$^2H_2$]-glucose offers a valuable alternative to estimate whole body glucose metabolism without perturbing its metabolism.

Acknowledgements

Grants: This research was performed within the framework of project TI-106 of the Dutch Top Institute Pharma.

Reference List

1. Sprott, R. L. Introduction: animal models of aging: something old, something new. *ILAR. J.* **52**, 1-3 (2011).
2. Despres, J. P. & Lemieux, I. Abdominal obesity and metabolic syndrome. *Nature* **444**, 881-887 (2006).

3. Eddy, D. M., Schlessinger, L. & Heikes, K. The metabolic syndrome and cardiovascular risk: implications for clinical practice. *Int. J. Obes. (Lond)* **32 Suppl 2**, S5-10 (2008).

4. Yuan, R., Peters, L. L. & Paigen, B. Mice as a mammalian model for research on the genetics of aging. *ILAR. J.* **52**, 4-15 (2011).

5. Blasco, M. A. Mice with bad ends: mouse models for the study of telomeres and telomerase in cancer and aging. *EMBO J.* **24**, 1095-1103 (2005).

6. Martin, G. M. Genetic engineering of mice to test the oxidative damage theory of aging. *Ann. N. Y. Acad. Sci.* **1055**, 26-34 (2005).

7. Gallou-Kabani, C. *et al.* Resistance to high-fat diet in the female progeny of obese mice fed a control diet during the periconceptual, gestation, and lactation periods. *Am. J. Physiol Endocrinol. Metab* **292**, E1095-E1100 (2007).

8. Van Zutphen, L. F. M., Baumans, V. & Beynen, A. C. *Handboek Proefdierkunde*. Elsevier Gezondheidszorg, Maarssen (2001).

9. Constantinides, C., Mean, R. & Janssen, B. J. Effects of isoflurane anesthesia on the cardiovascular function of the C57BL/6 mouse. *ILAR. J.* **52**, 22-32 (2011).

10. Matthews, D. R. *et al.* Homeostasis model assessment: insulin resistance and beta-cell function from fasting plasma glucose and insulin concentrations in man. *Diabetologia* **28**, 412-419 (1985).

11. DeFronzo, R. A., Tobin, J. D. & Andres, R. Glucose clamp technique: a method for quantifying insulin secretion and resistance. *Am. J. Physiol* **237**, E214-E223 (1979).

12. Bergman, R. N., Prager, R., Volund, A. & Olefsky, J. M. Equivalence of the insulin sensitivity index in man derived by the minimal model method and the euglycemic glucose clamp. *J. Clin. Invest* **79**, 790-800 (1987).

13. Grefhorst, A. *et al.* Differential effects of pharmacological liver X receptor activation on hepatic and peripheral insulin sensitivity in lean and ob/ob mice. *Am. J Physiol Endocrinol Metab* **289**, E829-E838 (2005).

14. Antuna-Puente, B. *et al.* How can we measure insulin sensitivity/resistance? *Diabetes & Metabolism* **37**, 179-188 (2011).

15. van Dijk, T. H. *et al.* Quantification of hepatic carbohydrate metabolism in conscious mice using serial blood and urine spots. *Anal. Biochem.* **322**, 1-13 (2003).

16. Galvin, P. *et al.* A simple method for quantitation of insulin sensitivity and insulin release from an intravenous glucose tolerance test. *Diabet. Med.* **9**, 921-928 (1992).

17. Pacini, G., Finegood, D. T. & Bergman, R. N. A minimal-model-based glucose clamp yielding insulin sensitivity independent of glycemia. *Diabetes* **31**, 432-441 (1982).

18. Matsuda, M. & DeFronzo, R. A. Insulin sensitivity indices obtained from oral glucose tolerance testing: comparison with the euglycemic insulin clamp. *Diabetes Care* **22**, 1462-1470 (1999).

19. Faerch, K., Brons, C., Alibegovic, A. C. & Vaag, A. The disposition index: adjustment for peripheral vs. hepatic insulin sensitivity? *J Physiol* **588**, 759-764 (2010).

20. Best, J. D. *et al.* Role of glucose effectiveness in the determination of glucose tolerance. *Diabetes Care* **19**, 1018-1030 (1996).

21. Ader, M., Ni, T. C. & Bergman, R. N. Glucose effectiveness assessed under dynamic and steady state conditions. Comparability of uptake versus production components. *J Clin Invest* **99**, 1187-1199 (1997).

22. Pacini, G., Thomaseth, K. & Ahren, B. Contribution to glucose tolerance of insulin-independent vs. insulin-dependent mechanisms in mice. *Am J Physiol Endocrinol. Metab* **281**, E693-E703 (2001).

23. Oosterveer, M. H. *et al.* High fat feeding induces hepatic fatty acid elongation in mice. *PLoS. One.* **4**, e6066 (2009).

24. Lee, W. N., Byerley, L. O., Bergner, E. A. & Edmond, J. Mass isotopomer analysis: theoretical and practical considerations. *Biol. Mass Spectrom.* **20**, 451-458 (1991).

25. Ader, M., Ni, T. C. & Bergman, R. N. Glucose effectiveness assessed under dynamic and steady state conditions. Comparability of uptake versus production components. *J Clin Invest* **99**, 1187-1199 (1997).

26. Best, J. D. *et al.* Role of glucose effectiveness in the determination of glucose tolerance. *Diabetes Care* **19**, 1018-1030 (1996).

27. Bergman, R. N., Phillips, L. S. & Cobelli, C. Physiologic evaluation of factors controlling glucose tolerance in man: measurement of insulin sensitivity and beta-cell glucose sensitivity from the response to intravenous glucose. *J Clin Invest* **68**, 1456-1467 (1981).

28. Kahn, S. E. *et al.* Quantification of the relationship between insulin sensitivity and beta-cell function in human subjects. Evidence for a hyperbolic function. *Diabetes* **42**, 1663-1672 (1993).

29. Surwit, R. S., Kuhn, C. M., Cochrane, C., McCubbin, J. A. & Feinglos, M. N. Diet-induced type II diabetes in C57BL/6J mice. *Diabetes* **37**, 1163-1167 (1988).

30. Schreurs, M. *et al.* Soraphen, an inhibitor of the acetyl-CoA carboxylase system, improves peripheral insulin sensitivity in mice fed a high-fat diet. *Diabetes Obes Metab* **11**, 987-991 (2009).

31. van Dijk, T. H. *et al.* Quantification of hepatic carbohydrate metabolism in conscious mice using serial blood and urine spots. *Analytical Biochemistry* **322**, 1-13 (2003).

32. Herrema, H. *et al.* Disturbed hepatic carbohydrate management during high metabolic demand in medium-chain acyl-CoA dehydrogenase (MCAD)-deficient mice. *Hepatology* **47**, 1894-1904 (2008).

33. Derks, T. G. *et al.* Inhibition of mitochondrial fatty acid oxidation in vivo only slightly suppresses gluconeogenesis but enhances clearance of glucose in mice. *Hepatology* **47**, 1032-1042 (2008).

34. Mari, A. Estimation of the rate of appearance in the non-steady state with a two-compartment model. *Am J Physiol* **263**, E400-E415 (1992).

35. van Dijk, T. H. *et al.* An Increased Flux through the Glucose 6-Phosphate Pool in Enterocytes Delays Glucose Absorption in Fxr-/- Mice. *J. Biol. Chem.* **284**, 10315-10323 (2009).

36. Miura, S. *et al.* Regulatory sequence elements of mouse GLUT4 gene expression in adipose tissues. *Biochem. Biophys. Res Commun.* **312**, 277-284 (2003).

37. Zierath, J. R., Houseknecht, K. L., Gnudi, L. & Kahn, B. B. High-fat feeding impairs insulin-stimulated GLUT4 recruitment via an early insulin-signaling defect. *Diabetes* **46**, 215-223 (1997).

38. Wright, J. J. *et al.* Mechanisms for increased myocardial fatty acid utilization following short-term high-fat feeding. *Cardiovasc Res* **82**, 351-360 (2009).

39. Cabou, C. *et al*. Central insulin regulates heart rate and arterial blood flow: an endothelial nitric oxide synthase-dependent mechanism altered during diabetes. Diabetes **56**, 2872-2877 (2007).

3

Chronic prednisolone treatment reduces hepatic insulin sensitivity while perturbing the fed-to-fasting transition in mice

Endocrinology 2010 May;151(5):2171-8

Anke J. Laskewitz
Theo H. van Dijk
Vincent W. Bloks
Dirk-Jan Reijngoud
Marie-José van Lierop
Wim H. Dokter
Folkert Kuipers
Albert K. Groen
Aldo Grefhorst

Abstract

Chronic glucocorticoid use for treatment of inflammatory diseases is accompanied by severe side effects in humans, *e.g.*, hyperglycemia and insulin resistance. The present studies were conducted to characterize consequences of chronic treatment with the synthetic glucocorticoid prednisolone on insulin sensitivity and blood glucose kinetics in mice. Prednisolone treatment increased fasting blood glucose and plasma insulin concentrations, but this apparent reduced insulin sensitivity could not be confirmed in hyperinsulinemic euglycemic clamp studies. Therefore, a novel method to study whole-body glucose kinetics was used. This revealed that prednisolone-treated mice had an increased hepatic glucose production (HGP). The increased HGP was accompanied by elevated plasma insulin concentrations, indicating reduced insulin sensitivity of hepatic glucose metabolism in prednisolone-treated mice. Compared to vehicle-treatment, prednisolone-treated mice had lower blood glucose concentrations, higher plasma free fatty acids and higher plasma FGF21 concentration in the fed condition, mimicking a fasting situation. Next, the effects of 24-h fasting on energy metabolism were studied. Compared to controls, fasted prednisolone-treated mice had higher blood glucose concentrations and a hampered induction of plasma β-hydroxybutyrate concentrations. In conclusion, these results indicate that chronic prednisolone treatment reduces insulin sensitivity of hepatic glucose production, induces a fasting-like phenotype in fed mice and perturbs the fed-to-fasting transition.

Introduction

The human steroid hormone cortisol and its rodent variant corticosterone are endogenous glucocorticoids that control a plethora of processes such as bone formation, blood pressure, stress response, blood glucose homeostasis, and the immune response [1]. When a glucocorticoid binds to the glucocorticoid receptor (GR), the formed complex can bind to glucocorticoid response elements (GREs) located in promoter regions of GR-target genes [2], hence activating or repressing gene transcription. In addition, the activated GR can also bind to cytosolic proteins, *e.g.*, nuclear factor-kappa B and activator protein-1, to perform immune suppressive roles via protein-protein interactions [3].

Synthetic glucocorticoids such as prednisolone and dexamethasone are widely used as anti-inflammatory and immunosuppressive drugs in the treatment of (chronic) inflammatory diseases. Side effects of synthetic glucocorticoids are widespread and include hypertension, hypertriglyceridemia, central obesity, and insulin resistance [4]. These side effects are all components of the metabolic syndrome, a cluster of metabolically interrelated risk factors for diabetes mellitus and cardiovascular diseases in which insulin resistance is thought to be of key relevance [5]. Insulin resistance, for instance, is a very common metabolic disturbance found in rheumatic patients treated chronically with glucocorticoids [3,6]. Interestingly, insulin resistance has also been reported to occur in a disorder characterized by elevated cortisol levels, Cushing's syndrome [7].

Studies in humans have provided evidence for increased hepatic gluconeogenesis (GNG) and reduced peripheral glucose uptake upon glucocorticoid treatment [8-12]. Stimulation of GNG might be the result of increased activity of phospho*enol*pyruvate carboxykinase (PCK1), a direct GR-target [13].

Although most studies suggest a role of hepatic PCK1 and disturbed GNG in the development of glucocorticoid-induced insulin resistance, the exact mechanism of action remains unclear. Animal models might help to unravel these mechanisms. Indirect and direct evidence is available that glucocorticoids affect insulin sensitivity and GNG in animal studies. However, most animal studies were conducted with rats [14-16] or special mouse strains, *e.g.,* low density lipoprotein receptor knockout (*Ldlr*$^{-/-}$) mice [17], or diet induced obese mice [18], and/or involved the extreme chronic use of high dose of dexamethasone for very long periods [17,19]. In these studies, whole body insulin resistance has been assessed on the basis of fasting glucose and insulin levels or by performing oral glucose tolerance tests (OGTTs) and insulin tolerance tests (ITTs). These tests, however, do not distinguish between hepatic and peripheral insulin sensitivity, i.e., the ability of insulin to suppress hepatic glucose production and stimulate peripheral glucose uptake, respectively.

The studies presented in this paper were performed to obtain more insight in the mechanisms by which the commonly used glucocorticoid prednisolone affects insulin sensitivity of blood glucose kinetics in mice. For this purpose, mice received 10 mg/kg/day prednisolone for 7 days. Hepatic and peripheral insulin sensitivity were determined using the hyperinsulinemic euglycemic clamp and with an intraperitoneal D-[6,6-$^2H_2$]-glucose injection. Our data revealed that chronic prednisolone treatment reduces insulin sensitivity of hepatic glucose production, induces a fasting-like phenotype in fed mice and perturbs the fed-to-fasting transition.

Materials and Methods

Animals

Male C57Bl/6J mice were obtained from Harlan (Horst, the Netherlands) and housed under conventional conditions, in a 12 hour-12 hour light-dark cycle (lights on 6 am-6 pm). Before start of the treatments, mice were allowed to adjust to the environment for at least one week. Prednisolone (10 mg/kg/day) or vehicle (gelatin (5 g/l)/mannitol (5g/l)) was administered by gavage at 1 pm for 7 days. Except for the fed and 24 hour fasting, all experiments started at 8 am after an overnight fast (food removed at 11 pm the day before) on the day following the last treatment. All experiments were approved by the Ethics Committee for Animal Experiments of the State University Groningen. Prednisolone and vehicle were kindly provided by Schering Plough, Oss, the Netherlands.

Basal values

Blood glucose concentrations were measured in awake mice in blood drops collected by tail tip bleeding with a Lifescan EuroFlash glucose meter (Lifescan Benelux Beerse, Belgium). Mice were sacrificed by cardiac puncture under isoflurane anesthesia. Blood samples obtained were centrifuged and the retrieved plasma samples were stored at -20 °C until analyzed. Organs were quickly removed and snap frozen in liquid nitrogen for RNA isolation and determination of metabolite concentrations.

Hyperinsulinemic euglycemic clamp experiments

To determine insulin sensitivity of glucose metabolism under high insulin concentrations, mice were subjected to a hyperinsulinemic euglycemic clamp as previously described [20] with minor adjustments. Five days before the experiment, *i.e.*, at day 2 of treatment, mice were equipped with a permanent jugular vein catheter, with a two-way entrance

attached to the skull with acrylic glue [21]. Treatment was continued during the recovery period. Mice were individually housed in small plexiglas cages during the experiment, allowing frequent collection of blood samples in freely moving mice. The mice were infused for 6 hours with an insulin solution containing insulin (110 mU/ml, Actrapid, Novo Nordisk, Bagsvaerd, Denmark), somatostatin (40 μg/ml, UCB, Breda, The Netherlands), glucose (18%) and 2% [U-^{13}C]-glucose (99% ^{13}C atom %excess; Cambridge Isotope Laboratories, Andover, MA)) and 1% BSA (Sigma, St. Louis, MO, USA) at a constant rate of 0.135 ml/h. The second solution that contained 27% glucose and 3% [U-^{13}C]-glucose was infused with an adjustable rate to maintain plasma glucose levels at ~7 mM. For this, blood glucose levels were measured every 15 minutes in blood drops collected by tail tip bleeding with a Lifescan EuroFlash glucose meter. Every hour, blood spots for GC-MS analysis were taken by tail bleeding on filter paper, air-dried and stored at room temperature until further analysis.

Blood glucose kinetics

To determine blood glucose kinetics without inducing hyperinsulinemia, 9-h fasted mice were injected intraperitoneally with a low dose of D-[6,6-$^{2}H_2$]-glucose (100 mg/kg). Before and at the indicated time points after injection, blood glucose concentrations were measured in blood collected by tail tip bleeding. At the same time points, a small blood spot was taken on filter paper, in which the fractional contribution of D-[6,6-$^{2}H_2$]-glucose to the whole blood glucose pool was measured by GC-MS. Whole body glucose turnover and clearance were calculated by kinetic analysis of the wash-out of injected D-[6,6-$^{2}H_2$]-glucose from the circulation. A blood sample was taken by orbital puncture after the test for insulin measurements.

24 hours fasting experiment

Food was removed one hour after the last treatment and mice were fasted for 24 hours. Blood glucose levels were measured every 6 hours by tail tip bleeding. At the same time points, a small amount of blood was obtained by orbital puncture under light anesthesia. In the dark period, a red light was used to facilitate the procedure. After 24 hours of fasting, mice were sacrificed by cardiac puncture under isoflurane anesthesia. The blood sample was centrifuged and the retrieved plasma was aliquoted and stored at -20 °C until analyzed. Organs were quickly removed, snap frozen in liquid nitrogen for RNA isolation and metabolite concentrations.

Metabolite analysis

Plasma insulin, corticosterone and fibroblast growth factor-21 (FGF21) concentrations

were measured using commercially available ELISA kits (Mercodia ultrasensitive mouse insulin ELISA, Orange Medical, Tilburg, the Netherlands; Diagnostic System Laboratories Benelux, Assendelft, The Netherlands; and Phoenix secretomics, Burlingame, CA, respectively). The HOMA-score was calculated adjusted for basal mouse values taken from vehicle-treated group. Plasma non-esterified fatty acid (NEFA) concentrations were determined with a commercially available kit *(*Diasys, Holzheim, Germany*).* Plasma β-hydroxybutyrate concentrations were measured using a total ketone body kit (Wako Chemicals, Neuss, Germany). Liver homogenates for lipid and protein measurements were made in ice-cold PBS. Hepatic lipids were extracted from the liver homogenates according to Bligh and Dyer [22]. Commercially available kits were used for determination of hepatic and plasma triglycerides (Roche Diagnostics, Mannheim, Germany), free and total cholesterol (Wako chemicals, Neuss, Germany). Hepatic glycogen and glucose-6-phosphate concentrations were determined as described before previously [23,24].

Gene expression

Total liver RNA was isolated using the TRI Reagent method (Sigma) according to manufactures protocol. Integrity and concentration of RNA was determined spectrophotometrically using the Nanodrop spectrophotometer (NanoDrop™ 1000 Spectrophotometer, Thermo Scientific, Waltham, MA). cDNA was obtained using the reverse transcription procedure with Moloney Murine Leukemia Virus-RT (Sigma) with random primers according to the protocol of the manufacturer. cDNA levels were measured in real-time quantitative PCR amplification using an ABI PRISM 7700 sequence detector (Applied Biosystems, Foster City, USA) against a calibration curve of pooled cDNA solutions. Expression levels were normalized for *RPLP0* levels. The sequences of the used primers and probes for *Gr* (NR3C1; Acc. No. NM_008173) are GGA TAT TCA AGC CCT GGA ATG A (foreward primer), ACG TCA GCA CCC CAT AAT GG (reverse primer), and ACC ACC TCC CAA ACT CTG CCT GGT GT (probe); for *Tat* (Acc. No. NM_146214) are CAG CCA CGT GCT TCG AGT AC (foreward primer), AAC TCC TGG ATC CGG CTA CAA G (reverse primer), and CAT CAC AGT CCC CGA GGT GAT GAT GC (probe); for *Per1* are (Acc. No. NM_011065): CTT CTG GCA ATG GCA AGG ACT (foreward primer), TGG GCT CTG TGA GTT TGT ACT CTT (reverse primer), and CTG CTC TCAG TGG TCT CCA GCA GAG CT (probe); for *Acox1* (Acc. No. NM_015729) are GCC ACG GAA CTC ATC TTC GA (foreward primer), CCA GGC CAC CAC TTA ATG GA (reverse primer), and CCA CTG CCA CAT ATG ACC CCA AGA CCC (probe); for *Foxo1* (Acc. No. NM_019739) AGA TCT ACG AGT GGA TGG TGA AGA G (foreward primer), GGA CAG ATT GTG GCG AAT TGA AT (reverse primer), and CAG CCC GCC GAG CTG TTG CT (probe). The sequence of the primers and probes that were used before can be found on www.labpediatricsrug.nl and are deposited at RTPrimerDB (www.rtprimerdb.org).

Measurement of mass isotopomer distribution by GC-MS

Extraction of glucose from blood spots on filter paper from the hyperinsulinemic-euglycemic clamp and blood glucose kinetics test, derivatization of the extracted compounds, and GC-MS measurements of derivatives was done according to the analytical procedure described by van Dijk *et al.* [25]. In short, a disk was punched out of the blood spots, glucose was extracted from the disk by incubating it in ethanol/water (10:1 v/v) and glucose was derivatized to its pentaacetate-ester. Samples were analyzed by GC-MS with positive ion chemical ionization with methane. The fractional isotopomer distribution measured by GC-MS (m_0-m_6) was corrected for the fractional distribution due to natural abundance of ^{13}C by multiple linear regression as described by Lee *et al.* [26] to obtain the excess fractional distribution of mass isotopomers (M_0-M_6) due to dilution of infused labeled compounds.

Calculation of blood glucose metabolism

Formulas for calculating the endogenous glucose production (EGP) and metabolic clearance rate (MCR) under hyperinsulinemic euglycemic clamped conditions were previously described [20]. For the blood glucose kinetics test a single-pool, first-order kinetic model was assumed. The excess fractional distribution of mass isotopomers was used to calculate the first order absorption process in an one-compartment model using SAAM-II software (version 1.2.1; SAAM Institute, University of Washington, Seattle, WA) [27]. The formulas

Table 1

Parameter	Formula
D-[6,6-^{2}H]-glucose blood concentration	$C_t = M_2 \times [glc]$
D-[6,6-^{2}H]-glucose in blood over time	$C_t = C(0)^{el} \times e^{-k(el) \times t} - C(0)^{ab} \times e^{-k(ab) \times t}$
Lag time	$t_{lag} = (\ln(C(0)^{ab} - \ln(C(0)^{el}))/(k^{ab} - k^{el})$
D-[6,6-^{2}H]-glucose in blood at t_{lag}	$C_{lag} = C(0)^{el} \times e^{-k(el) \times t(lag)} = C(0)^{ab} \times e^{-k(ab) \times t(lag)}$
Bioavailability	$F = 1 - ((C(0)^{ab} \times k^{el})/(k^{ab} \times C(0)^{el}))$
Volume of distribution	$V_D = F \times D / C_{lag}$
Total amount of D-[6,6-^{2}H]-glucose	$A = V_D \times [glc]$
Metabolic clearance rate of glucose	$MCR = k^{el} \times V_D$
Glucose turnover rate, EGP	$R_a = EGP = k^{el} \times A$

The formulas used to calculate the concentration vs. time curves and the kinetic parameters in a first order absorption process in an one-compartment model.
$C(0)^{ab}$, initial concentration by extrapolation of the absorption period; $C(0)^{el}$, concentration by extrapolation of the elimination period; C_{lag}, concentration at lag time calculated from elimination or absorption curve; D, dose D-[6,6-^{2}H]-glucose administrated; [glc], total blood glucose concentration; k^{ab}, absorption rate constant; k^{el}, elimination rate constant; M_2, mole percent enrichment of blood glucose; t_{lag}, time between administration and appearance in sampled compartment; EGP, endogenous glucose production.

used to calculate the concentration *vs.* time curves and the kinetic parameters are given in Table 1.

Statistics

All data are represented as mean ± SEM. Statistical analysis for two independent groups was performed using Mann-Whitney-U tested with SPSS for Windows software (SPSS, Chicago, IL, USA). For multiple comparison statistical analysis were performed by Kruskal-Wallis test, when this was positive ($p<0.05$) a pair wise comparison of subgroups according to Conover was performed using Brightstat [28]. Significance was considered at a level of $p<0.05$.

Results

Chronic prednisolone treatment increased the HOMA-score in mice

The first experiments were performed to test the consequences of a chronic, 7 day prednisolone treatment in mice. Activation of the hypothalamic-pituitary-adrenal axis (HPA-axis) by prednisolone results in a reduction of plasma corticosterone levels [29] and glucocorticoid-induced apoptosis of thymocytes results in a severely reduced thymus weight [30]. The 85% decrease in thymus weight and severely reduced plasma corticosterone levels in prednisolone-treated mice (Table 2) are therefore indicative for an efficient prednisolone treatment.

Blood glucose levels in 9 hour fasted mice tended to be higher upon prednisolone treatment (Table 2). In addition, prednisolone treatment elevated plasma insulin levels. Consequently, the HOMA-score was increased upon chronic prednisolone treatment, suggesting insulin resistance.

Surprisingly, the hepatic expression of the classic GR-target genes *Tat* (encoding for tyrosine aminotransferase) [31] and *Per1* (encoding for the clock-gene Period-1) [32] was reduced upon prednisolone treatment in the 9-h fasted mice (Figure 1). The expression of genes encoding proteins involved in gluconeogenesis, *e.g.*, *Pck1*, *G6pc*, and *Pdk4*, was also significantly reduced in the livers of 9 hour fasted prednisolone-treated mice.

Table 2

	Vehicle	Prednisolone
Bodyweight (g) day 0	25.9 ± 0.8	25.9 ± 0.9
Bodyweight (g) day 7	25.1 ± 0.7	24.0 ± 0.6
Thymus weight (mg)	24.2 ± 1.9	3.6 ± 0.3 *
Plasma		
Glucose (mM)	7.4 ± 0.5	8.8 ± 0.7
Insulin (mU/l)	1.7 ± 0.1	3.4 ± 0.5 *
HOMA	1.0 ± 0.1	2.3± 0.3 *
Cholesterol (mM)	3.0 ± 0.1	3.4 ± 0.2
Triglycerides (mM)	0.74 ± 0.07	1.03 ± 0.1 *
NEFA (mM)	0.55 ± 0.16	0.38 ± 0.13
β-hydroxybutyrate (mM)	0.56 ± 0.07	0.26 ± 0.04 *
Corticosterone (µg/l)	889 ± 74	167 ± 44 *
FGF21 (µg/l)	3.05	3.65
Liver		
Cholesterol (µmol/g liver)	10.8 ± 0.3	9.6 ± 0.7
Triglycerides (µmol/g liver)	19.4 ± 3.2	17.2 ± 2.4
Glycogen (µmol/g liver)	180 ± 17	212 ± 39

Treatment parameters of 9 hour fasted vehicle- and prednisolone-treated mice.
Values represent means ± SEM; n = 7 (vehicle); n = 8 (prednisolone); *, $p < 0.05$. The values for plasma FGF21 are from pooled plasma samples.

Figure 1

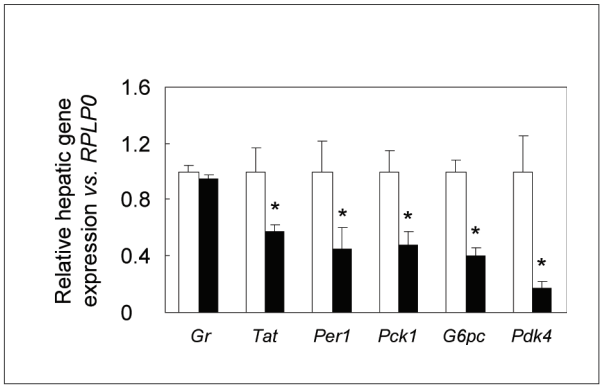

Hepatic gene expression of 9 hours fasted mice treated with vehicle (white bars) or prednisolone (black bars).

Results were normalized to *Rplp0* (ribosomal protein, large, P0 (36B4)) with data from vehicle treated mice defined as '1'. Values are means ± SEM; n = 6 (prednisolone); n = 7 (vehicle); *****, $p < 0.05$; *Gr*, glucocorticoid receptor; *Tat*, tyrosine amino transferase; *Per1*, period-1; *Pck1*, phosphoenolpyruvate carboxykinase 1; *G6pc*, glucose-6-phosphatase, catalytic; *Pdk4*, pyruvate dehydrogenase kinase, isozyme 4.

Figure 2

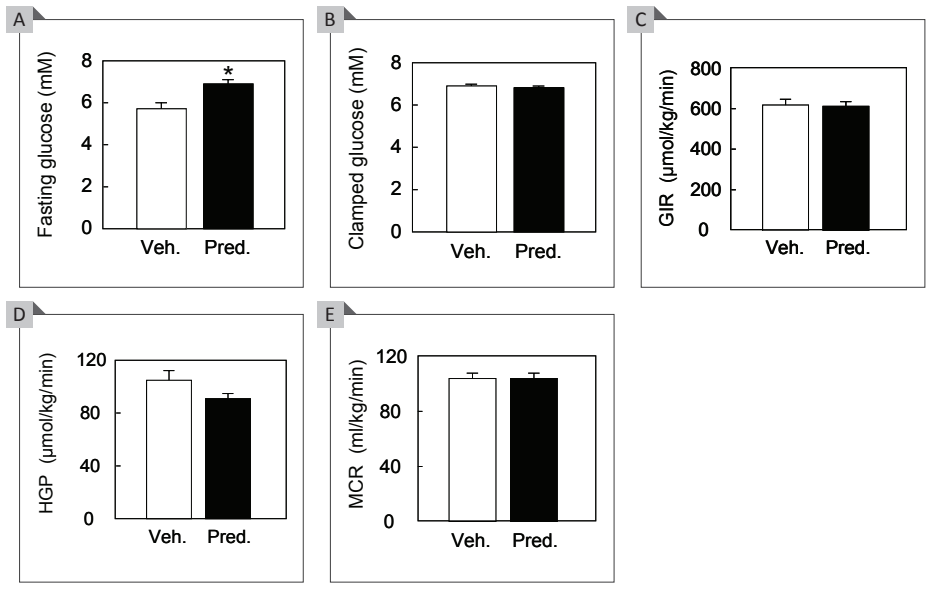

Parameters of the hyperinsulinemic euglycemic clamp experiment performed in mice treated with vehicle (white bars) or prednisolone (black bars).

A, Fasting blood glucose concentration; **B**, Average blood glucose concentration during the steady-state period of the experiment (3-6 hours); **C**, Average Glucose Infusion Rate (GIR) needed to maintain euglycemic conditions during the steady-state period of the experiment (3-6 hours); **D**, Hepatic glucose production (HGP) during the steady-state period of the experiment; **E**, Metabolic clearance rate (MCR) of glucose during the steady-state period of the experiment. Values are means ± SEM; n = 6; *, $p<0.05$.

Prednisolone-induced insulin resistance was detectable with a D-[6,6-$^2H_2$]-glucose injection

In order to evaluate the characteristics of the reduced insulin sensitivity upon prednisolone treatment in more detail, a hyperinsulinemic euglycemic clamp was performed. Again, mice treated with prednisolone and fasted for 9 hours had increased blood glucose concentrations (Figure 2A). Surprisingly, the Glucose Infusion Rate (GIR) needed to maintain euglycemic conditions during the clamping period did not differ between treated and non-treated mice (Figure 2C). Prednisolone treatment affected neither the metabolic clearance rate (MCR) nor hepatic glucose production (HGP) (Figures 2D and 2E) under the hyperinsulinemic conditions. Altogether, these data indicate that the hyperinsulinemic euglycemic clamp is not the preferred method to study prednisolone-induced insulin resistance, probably due to the artificially high plasma insulin concentrations.

To determine hepatic and peripheral insulin sensitivity of glucose kinetics without inducing the high plasma insulin concentrations, 9 hour fasted mice were intraperitoneal in-

Figure 3

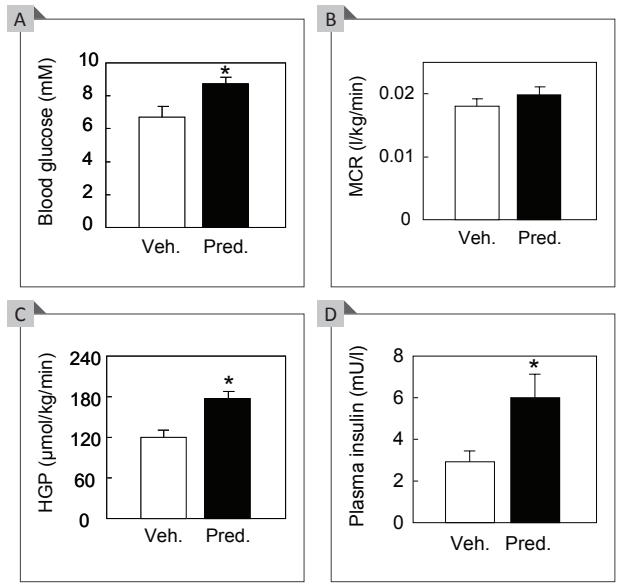

Parameters of the blood glucose kinetics test performed in mice treated with vehicle (white bars) or prednisolone (black bars).

A, Blood glucose concentrations during the test; **B**, Metabolic clearance rate (MCR) of glucose during the test; **C**, Hepatic glucose production (HGP) during the test; **D**, Plasma insulin concentrations after the test. Values are means ± SEM; n = 6-8; *****, $p < 0.05$.

jected with a tracer amount of D-[6,6-$^2H_2$]-glucose. This injection did not affect the blood glucose levels (Figure 3A). From the decay of the blood D-[6,6-$^2H_2$]-glucose *vs.* time curve, MCR was calculated and this parameter did not differ between vehicle- and prednisolone-treated mice (Figure 3B). The HGP was calculated using the MCR and blood glucose concentrations and was increased in prednisolone-treated mice (Figure 3C), despite increased plasma insulin concentrations (Figure 3D). The increased HGP at higher plasma insulin concentrations indicates hepatic insulin resistance.

Prednisolone treatment induced a fasting-like phenotype in fed mice and hampered the effects of fasting on energy metabolism

The hyperinsulinemic euglycemic clamp induced a state with supraphysiological insulin concentrations and therefore mimics a fed situation but the HOMA and blood glucose kinetics were calculated under fasted situations with low plasma insulin concentrations. We therefore investigated the effects of prednisolone and fasting on glucose metabolism. Mice were fasted for 24 hours after the seventh day of treatment. At the start of the fasting period, one hour after the last treatment, prednisolone-treated mice had significantly reduced blood glucose levels (Figure 4A). In vehicle-treated mice blood glucose concentration showed a clear fasting-induced reduction, but this effect was less clear in prednisolone treated mice (Figure 4B). Moreover, the prednisolone-treated mice showed a hampered induction of β-hydroxybutyrate levels upon fasting (Figure 4C). Metabolic parameters from a different 24 hour fasting experiment are shown in Table 3. In the fed

Figure 4

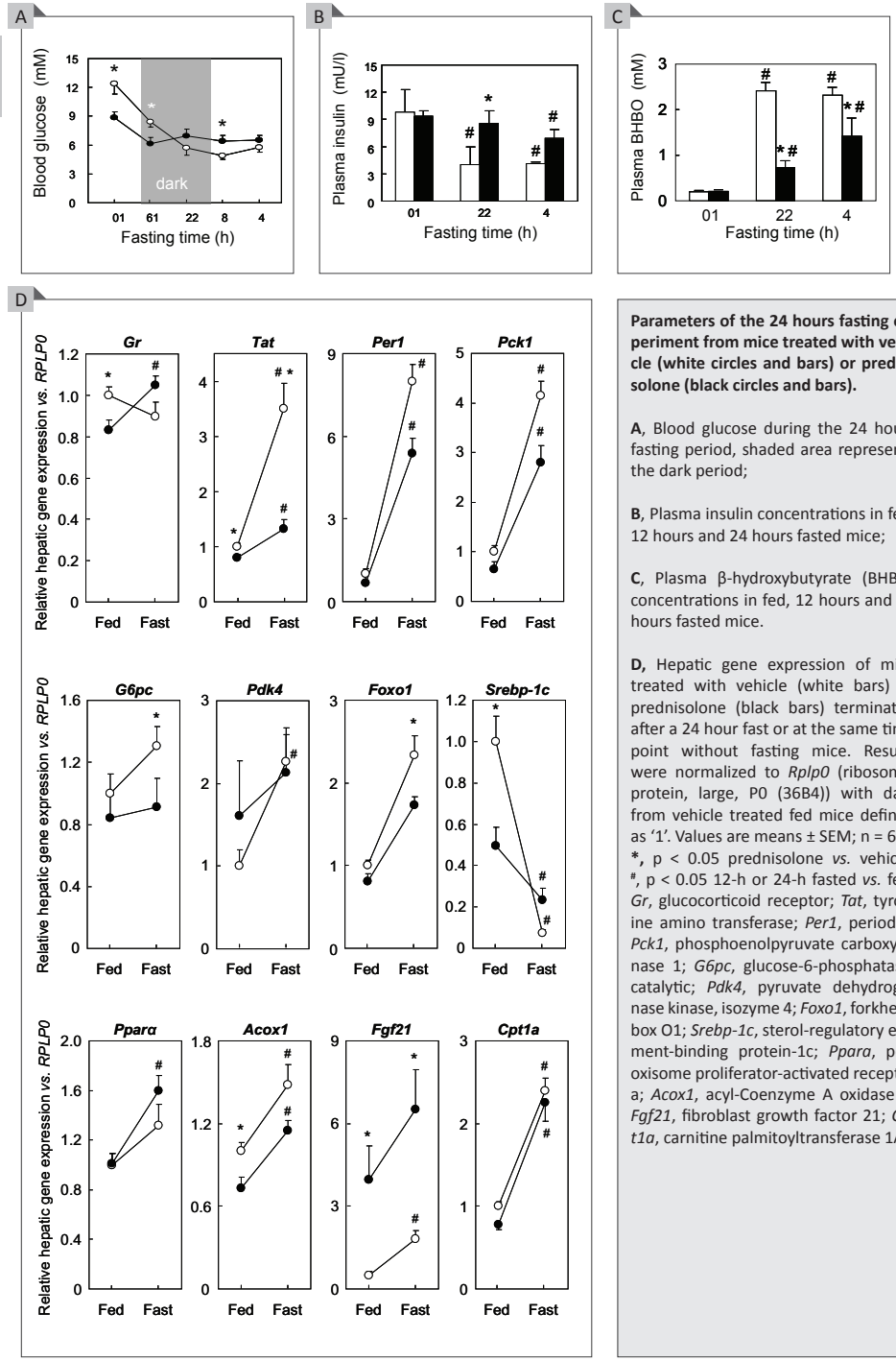

Parameters of the 24 hours fasting experiment from mice treated with vehicle (white circles and bars) or prednisolone (black circles and bars).

A, Blood glucose during the 24 hours fasting period, shaded area represents the dark period;

B, Plasma insulin concentrations in fed, 12 hours and 24 hours fasted mice;

C, Plasma β-hydroxybutyrate (BHBO) concentrations in fed, 12 hours and 24 hours fasted mice.

D, Hepatic gene expression of mice treated with vehicle (white bars) or prednisolone (black bars) terminated after a 24 hour fast or at the same time point without fasting mice. Results were normalized to *Rplp0* (ribosomal protein, large, P0 (36B4)) with data from vehicle treated fed mice defined as '1'. Values are means ± SEM; n = 6-8; *, $p < 0.05$ prednisolone *vs.* vehicle; #, $p < 0.05$ 12-h or 24-h fasted *vs.* fed; *Gr*, glucocorticoid receptor; *Tat*, tyrosine amino transferase; *Per1*, period-1; *Pck1*, phosphoenolpyruvate carboxykinase 1; *G6pc*, glucose-6-phosphatase, catalytic; *Pdk4*, pyruvate dehydrogenase kinase, isozyme 4; *Foxo1*, forkhead box O1; *Srebp-1c*, sterol-regulatory element-binding protein-1c; *Pparα*, peroxisome proliferator-activated receptor a; *Acox1*, acyl-Coenzyme A oxidase 1; *Fgf21*, fibroblast growth factor 21; *Cpt1a*, carnitine palmitoyltransferase 1A.

state, the prednisolone-treated mice had higher plasma NEFA concentrations than the vehicle treated mice. During fasting, these concentrations remained unchanged in the prednisolone-treated mice, but they rose in the mice that received the vehicle. Prolonged fasting in vehicle-treated mice resulted in increased hepatic TG and reduced hepatic glycogen concentrations. In prednisolone-treated mice, neither liver TG nor liver glycogen concentrations were affected..

Fasting resulted in an increased *Pck1* expression (Figure 4D), but *Pck1* expression was lower in prednisolone compared to vehicle-treated mice in both fed and fasted condition. Expression of *Srebp-1c* was reduced in fed prednisolone-treated mice compared to fed control mice. The induction of *Foxo1*, *Pdk4*, and *G6pc* upon fasting was reduced in prednisolone-treated mice compared to controls. Again, prednisolone treatment reduced the expression of the GR-target genes *Tat* and *Per1*.

Because the results so far suggested a hampered response to fasting upon prednisolone treatment, we investigated the hepatic mRNA expression of target genes of peroxisomal proliferator activated receptor α (PPARα), the major regulator of gene expression upon fasting [33] (Figure 4D). Fasting increased the expression of *Ppar*α and its target genes *Acox1* and *Cpt1a* but this was not affected in prednisolone-treated mice. *Fgf21,* on the contrary, was strongly induced in prednisolone-treated mice in the fed state. This is in line with the fact that fed prednisolone-treated mice had a ~2 fold increase in plasma FGF21 compared to fed vehicle-treated mice and that fasting strongly induced plasma FGF21 concentrations in the vehicle-treated but not in prednisolone-treated mice (Tables 2 and 3).

Table 3

	Fed		Fasted	
(μg/ml)	**Vehicle**	**Prednisolone**	**Vehicle**	**Prednisolone**
Insulin	5.2 ± 1.8	10.2 ± 3.8*	ND	ND
Glucagon	0.70 ± 0.14	0.79 ± 0.22	0.38 ± 0.06$^{\#}$	0.38 ± 0.11$^{\#}$
Leptin	22.2 ± 4.3	44.5 ± 7.9*	7.72 ± 2.96$^{\#}$	13.93 ± 3.04$^{*\#}$
Resistin	261.7 ± 72.3	229.6 ± 64.4	217.1 ± 43.1	227.7 ± 57.4
GLP-1	0.19 ± 0.05	0.17 ± 0.08	0.11 ± 0.02$^{\#}$	0.09 ± 0.03$^{\#}$
GIP	1.16 ± 0.35	1.47 ± 0.54	0.40 ± 0.07$^{\#}$	0.37 ± 0.10$^{\#}$
PAI1	0.82 ± 0.07	1.45 ± 0.28*	1.08 ± 0.32	1.04 ± 0.34
Ghrelin	3.58 ± 1.25	2.41 ± 1.39	6.95 ± 2.37	4.78 ± 2.00

Plasma concentrations of diabetes biomarkers
Fed samples were taken at 23:00 h, fasted samples at 08:00 h after a 9 hours fast. Values represent means ± SD; n=6.
* p<0.05 prednisolone *vs.* vehicle, $^{\#}$ p<0.05 fed *vs.* fasted, ND – not detectable.

Discussion

Insulin resistance is a well known side effect of glucocorticoid treatment [3,4]. As early as 1983, it was shown that 7 day administration of prednisolone induced insulin resistance in healthy human subjects [9]. The 'gold' standard to study insulin sensitivity is the hyperinsulinemic euglycemic clamp. To our surprise, we were not able to detect reduced insulin sensitivity in prednisolone-treated mice using this technique (Figure 2). In sharp contrast, however, the fasting blood glucose and plasma insulin concentrations (Table 2) suggested that prednisolone-treatment *did* reduce insulin sensitivity in mice. Apparently, induction of hyperinsulinemia during the clamp masked the effects of prednisolone on mouse glucose metabolism. We therefore used a less perturbing method to investigate glucose kinetics in this study. By carefully modeling the decay of injected D-[6,6-$^2H_2$]-glucose, a reduced hepatic insulin sensitivity was detected in prednisolone-treated mice: enhanced HGP and unchanged MCR despite elevated plasma insulin concentrations (Figure 3).

The clearly distinct conclusions generated with the hyperinsulinemic euglycemic clamp and the injections with D-[6,6-$^2H_2$]-glucose about prednisolone's effect on insulin sensitivity can be related to the feeding status they symbolize. While the hyperinsulinemic euglycemic clamp induces a state of supraphysiological insulin concentrations, the small amount of D-[6,6-$^2H_2$]-glucose is injected in the blood glucose kinetic experiment did not perturb the fasting state. To investigate whether prednisolone affected the response to fasting, we performed feeding-fasting transition experiments.

The increased hepatic *Fgf21* expression (Figure 4D), reduced plasma glucose concentrations (Figure 4A), and increased plasma NEFA concentrations (Table 3) in prednisolone-treated mice in the fed state mimic a fasted condition. The plasma β-hydroxybutyrate levels, in contrast, were not increased under these conditions (Figure 4C), but the relatively high plasma insulin levels in the fed prednisolone-treated mice (Figure 4B) might be held responsible for reduced ketogenesis. One might expect that the increased plasma NEFA in the fed mice upon prednisolone-treatment were the result of the actions of FGF21 on adipose tissue. Plasma FGF21 concentrations were also higher in fed prednisolone-treated mice compared to fed vehicle-treated mice (compare Tables 2 and 3). Also the reduced blood glucose concentrations do fit with the actions of FGF21 [34]. Studies with *Fgf21* transgenic and *Fgf21* knockdown mice showed that FGF21 is not required for ketogenesis [35], exactly mimicking the fed prednisolone-treated mice in our study: high plasma FGF21 without elevated plasma β-hydroxybutyrate concentrations (Table 4 and Figure 4C). In general, prednisolone-treated mice in the fed state showed a fasting-like metabolic profile and fasting did not affect the measured parameters.

The effects of fasting on the measured parameters of energy metabolism all seem to be hampered in the prednisolone-treated mice. The fasting-mediated reductions in blood glucose (Figure 4A) and plasma insulin (Figure 4B) and the fasting-mediated induction in plasma β-hydroxybutyrate (Figure 4C) and plasma NEFA (Table 3) were all severely hampered in the prednisolone-treated mice. The effects of fasting on the hepatic expression of *Pck1*, *G6pc*, and *Pdk4* were also reduced in the prednisolone-treated mice (Figure 4D). PPARα plays an important role in both fasting response and fatty acid metabolism [33]. Bernal-Mizrachi *et al.* [17] showed that *Pparα*$^{-/-}$ *Ldlr*$^{-/-}$ mice are protected from dexamethasone-induced insulin resistance. In our hands, prednisolone had no effects on the expression of PPARα target genes (Figure 4D), apart from a major increase in the aforementioned *Fgf21* in the fed state. So far, no GRE has been found in the promoter of *Fgf21*, suggesting that the effects of prednisolone on *Fgf21* could be indirect. A recent study by Bougarne *et al.* showed that the enhanced expression of *G6pase* in HepG2 cells upon dexamethasone is reduced when the cells were co-treated with a PPARα agonist [36]. Elegant binding studies confirmed that the transcriptional activity of the GR-GRE complex was reduced when PPARα was also activated. In the light of the surprising findings on the *Fgf21* expression, the interaction between GR and PPARα requires more research

At the gene expression level, many of the effects of chronic prednisolone treatment on GR target genes are in contrast to reported effects (Figure1). Although it has repeatedly been shown that GR activation leads to up-regulation of *Tat* [31], *Pck1* [13], and *Per1* [32], hepatic mRNA levels of these three genes were decreased upon chronic prednisolone treatment in the current study. Previous experiments with methylprednisolone in rodents showed that hepatic *Pck1* was increased in a fast and transient manner [37]. Therefore, the reduced *Pck1* expression in our experiments was very likely a consequence of the chronic treatment protocol, reflecting a compensatory mechanism for the acute effects of prednisolone on GR target genes. The half-life of *iv* injected prednisolone in blood is ~35 minutes in mice [38] and the effects on gene expression were studied ~18 hours after the last oral prednisolone dose. Therefore, the reduced expression of GR-target genes (Figure 1) might be due to the low plasma corticosterone concentrations (Table 2). In addition, preliminary data from GR-DNA binding studies showed different effects of chronic and acute prednisolone treatment.

Insulin affects transcription of *Srebp-1c* [39] and the reduction of its expression in fed prednisolone-treated mice compared to fed control mice suggest reduced insulin sensitivity of lipid metabolism (Figure 4D). Via reduction of nuclear FoxO1, insulin reduces the expression of *Pdk4* and *G6pc*. Hence, the reduced induction of these genes upon fasting might also suggest that the insulin or fasting-mediated flexibility of this system is hampered upon chronic prednisolone-treatment.

In conclusion, this study revealed that 7 day prednisolone treatment in normal, lean mice reduced hepatic insulin sensitivity in fasted mice. Because high insulin concentrations mask this effect, the hyperinsulinemic euglycemic clamp is not applicable in this animal model. In addition, prednisolone-treated mice in the fed state showed a fasting-like metabolic profile and fasting-mediated changes in energy metabolism are severely hampered upon chronic prednisolone treatment.

Acknowledgements

The authors would like to thank Theo Boer, Rick Havinga and Monique van Vleuten for their skilful technical assistance.

Reference List

1. Schoneveld OJ, Gaemers IC, Lamers WH 2004 Mechanisms of glucocorticoid signalling. *Biochim Biophys Acta* **1680**:114-128
2. Giguère V, Hollenberg SM, Rosenfeld MG, Evans RM 1986 Functional domains of the human glucocorticoid receptor. *Cell* **46**:645-652
3. Schacke H, Docke W, Asadullah K 2002 Mechanisms involved in the side effects of glucocorticoids. *Pharmacology & Therapeutics* **96**:23-43
4. Stanbury RM, Graham EM 1998 Systemic corticosteroid therapy--side effects and their management. *Br J Ophthalmol* **82**:704-708
5. Walker BR 2006 Cortisol--cause and cure for metabolic syndrome? *Diabet Med* **23**:1281-1288
6. Dessein PH, Joffe BI, Stanwix AE, Christian BF, Veller M 2004 Glucocorticoids and insulin sensitivity in rheumatoid arthritis. *J Rheumatol* **31**:867-874
7. Bowes SB, Benn JJ, Scobie IN, Umpleby AM, Lowy C, Sonksen PH 1991 Glucose metabolism in patients with Cushing's syndrome. *Clin Endocrinol (Oxf)* **34**:311-316
8. Nicod N, Giusti V, Besse C, Tappy L 2003 Metabolic adaptations to dexamethasone-induced insulin resistance in healthy volunteers. *Obes Res* **11**:625-631
9. Pagano G, Cavallo-Perin P, Cassader M, Bruno A, Ozzello A, Masciola P, Dall'omo AM, Imbimbo B 1983 An in vivo and in vitro study of the mechanism of prednisone-induced insulin resistance in healthy subjects. *J Clin Invest* **72**:1814-1820
10. Tappy L, Randin D, Vollenweider P, Vollenweider L, Paquot N, Scherrer U, Schneiter P, Nicod P, Jequier E 1994 Mechanisms of dexamethasone-induced insulin resistance in healthy humans. *J Clin Endocrinol Metab* **79**:1063-1069
11. Rizza RA, Mandarino LJ, Gerich JE 1982 Cortisol-induced insulin resistance in man: impaired suppression of glucose production and stimulation of glucose utilization due to a postreceptor detect of insulin action. *J Clin Endocrinol Metab* **54**:131-138
12. Binnert C, Ruchat S, Nicod N, Tappy L 2004 Dexamethasone-induced insulin resistance shows no gender difference in healthy humans. *Diabetes Metab* **30**:321-326

13. Friedman JE, Yun JS, Patel YM, McGrane MM, Hanson RW 1993 Glucocorticoids regulate the induction of phosphoenolpyruvate carboxykinase (GTP) gene transcription during diabetes. *J Biol Chem* **268**:12952-12957

14. Saad MJ, Folli F, Kahn JA, Kahn CR 1993 Modulation of insulin receptor, insulin receptor substrate-1, and phosphatidylinositol 3-kinase in liver and muscle of dexamethasone-treated rats. *J Clin Invest* **92**:2065-2072

15. Stojanovska L, Rosella G, Proietto J 1990 Evolution of dexamethasone-induced insulin resistance in rats. *Am J Physiol* **258**:E748-E756

16. Guillaume-Gentil C, Assimacopoulos-Jeannet F, Jeanrenaud B 1993 Involvement of non-esterified fatty acid oxidation in glucocorticoid-induced peripheral insulin resistance in vivo in rats. *Diabetologia* **36**:899-906

17. Bernal-Mizrachi C, Weng S, Feng C, Finck BN, Knutsen RH, Leone TC, Coleman T, Mecham RP, Kelly DP, Semenkovich CF 2003 Dexamethasone induction of hypertension and diabetes is PPAR-alpha dependent in LDL receptor-null mice. *Nat Med* **9**:1069-1075

18. Gounarides JS, Korach-Andre M, Killary K, Argentieri G, Turner O, Laurent D 2008 Effect of dexamethasone on glucose tolerance and fat metabolism in a diet-induced obesity mouse model. *Endocrinology* **149**:758-766

19. Thomas CR, Turner SL, Jefferson WH, Bailey CJ 1998 Prevention of dexamethasone-induced insulin resistance by metformin. *Biochem Pharmacol* **56**:1145-1150

20. Grefhorst A, van Dijk TH, Hammer A, van der Sluijs FH, Havinga R, Havekes LM, Romijn JA, Groot PH, Reijngoud DJ, Kuipers F 2005 Differential effects of pharmacological liver X receptor activation on hepatic and peripheral insulin sensitivity in lean and ob/ob mice. *Am J Physiol Endocrinol Metab* **289**:E829-E838

21. Kuipers F, Havinga R, Bosschieter H, Toorop GP, Hindriks FR, Vonk RJ 1985 Enterohepatic circulation in the rat. *Gastroenterology* **88**:403-411

22. Bligh EG, Dyer WJ 1959 A rapid method of total lipid extraction and purification. *Can J Biochem Physiol* **37**:911-917

23. Hohorst HJ 1970 D-Glucose-6-phosphat und D-fructuse-6-phosphat. In: Bergmeyer HU, eds. Methoden der Enzymatischen Analyse. Weinheim, Germany: *Verlag Chemie*; 1200-1204

24. Keppler D, Decker K 1970 Glykogen. Bestimmung mit amyloglucosidase In: Bergmeyer HU, eds. Methoden der Enzymatischen Analyse. Weinheim, Germany: *Verlag Chemie*; 1089-1094

25. van Dijk TH, Boer TS, Havinga R, Stellaard F, Kuipers F, Reijngoud DJ 2003 Quantification of hepatic carbohydrate metabolism in conscious mice using serial blood and urine spots. **Anal Biochem 322**:1-13

26. Lee WN, Byerley LO, Bergner EA, Edmond J 1991 Mass isotopomer analysis: theoretical and practical considerations. *Biol Mass Spectrom* **20**:451-458

27. van Dijk TH, Grefhorst A, Oosterveer MH, Bloks VW, Staels B, Reijngoud DJ, Kuipers F 2009 An increased flux through the glucose-6-phosphate pool in enterocytes delays glucose Absorption in $Fxr^{-/-}$ mice. *J. Biol. Chem.* **284**: 10315-10323

28. Stricker D 2008 BrightStat.com: Free statistics online. *Computer Methods and Programs in Biomedicine* **92**:135-143

29. Brattsand R, Thalén A, Roempke K, Källström L, Gruvstad E 1982 Influence of 16 alpha, 17 alpha-acetal substitution and steroid nucleus fluorination on the topical to systemic activity ratio of glucocorticoids. *Journal of Steroid Biochemistry* **16**: 779-786

30. Compton M, Cidlowski J 1986 Rapid in vivo effects of glucocorticoids on the integrity of rat lymphocyte genomic deoxyribonucleic acid. *Endocrinology* **118**: 38–45

31. Beato M, Chalepakis G, Schauer M, Slater EP 1989 DNA regulatory elements for steroid hormones. *Journal of Steroid Biochemistry* **32**:737-747

32. Balsalobre A, Brown SA, Marcacci L, Tronche F, Kellendonk C, Reichardt HM, Schutz G, Schibler U 2000 Resetting of circadian time in peripheral tissues by glucocorticoid signaling. *Science* **289**:2344-2347

33. Kersten S, Seydoux J, Peters JM, Gonzalez FJ, Desvergne B, Wahli W 1999 Peroxisome proliferator-activated receptor alpha mediates the adaptive response to fasting. *J Clin Invest* **103**:1489-1498

34. Kharitonenkov A, Shiyanova TL, Koester A, Ford AM, Micanovic R, Galbreath EJ, Sandusky GE, Hammond LJ, Moyers JS, Owens RA, Gromada J, Brozinick JT, Hawkins ED, Wroblewski VJ, Li DS, Mehrbod F, Jaskunas SR, Shanafelt AB 2005 FGF-21 as a novel metabolic regulator. *J Clin Invest* **115**:1627-16

35. Hotta Y, Nakamura H, Konishi M, Murata Y, Takagi H, Matsumura S, Inoue K, Fushiki T, Itoh N 2009 Fibroblast growth factor 21 regulates lipolysis in white adipose tissue but is not required for ketogenesis and triglyceride clearance in liver. *Endocrinology* **In Press**

36. Bougarne N, Paumelle R, Caron S, Hennuyer N, Mansouri R, Gervois P, Staels B, Haegeman G, De Bosscher K 2009 PPARalpha blocks glucocorticoid receptor alpha-mediated transactivation but cooperates with the activated glucocorticoid receptor alpha for transrepression on NF-kappaB. *Proc Natl Acad Sci USA* **106**:7397-7402

37. Jin JY, Dubois DC, Almon RR, Jusko WJ 2004 Receptor/gene-mediated pharmacodynamic effects of methylprednisolone on phosphoenolpyruvate carboxykinase regulation in rat liver. *J Pharmacol Exp Ther* **309**:328-339

38. Hashida N, Ohguro N, Arakawa Y, Kurokawa N, Tano Y 2006 Intraocular concentration of intravenous prednisolone in experimental autoimmune uveoretinitis mice. *Jpn J Ophthalmol.* **50**:561-562

39. Hegarty BD, Bobard A, Hainault I, Ferre P, Bossard P, Foufelle F 2005 Distinct roles of insulin and liver X receptor in the induction and cleavage of sterol regulatory element-binding protein-1c. *Proc Natl Acad Sci USA* **102**:791-796

4

Chronic prednisolone treatment aggravates hyperglycemia in mice fed a high-fat diet but does not enforce dietary fat-induced insulin resistance

Conditionally accepted

Anke J. Laskewitz
Theo H. van Dijk
Aldo Grefhorst
Marie-José van Lierop
Rick Havinga
Marijke Schreurs
Vincent W. Bloks
Dirk-Jan Reijngoud
Wim H. Dokter
Folkert Kuipers
Albert K. Groen

Abstract

Synthetic glucocorticoids such as prednisolone have potent anti-inflammatory actions. Unfortunately these drugs induce severe adverse effects in patients, many of which resemble features of the metabolic syndrome, such as insulin resistance. In this study we investigated whether adverse effects of prednisolone on glucose homeostasis are aggravated in mice with compromised insulin sensitivity due to a high-fat diet applying various methods to analyze changes in insulin sensitivity in mice. C57BL/6J mice were fed a high-fat diet for six weeks and treated with either prednisolone (10 mg/kg/d) or vehicle for the last 7 days. Insulin sensitivity and blood glucose kinetics were analyzed with state-of-the-art stable isotope procedures in different experimental conditions. Prednisolone treatment aggravated fasting hyperglycemia and hyperinsulinemia caused by high-fat feeding, resulting in a higher HOMA-IR. In addition, prednisolone-treated high-fat diet fed mice appeared less insulin sensitive by detailed analysis of fasted blood glucose kinetics. Remarkably, using hyperinsulinemic-euglycemic or hyperglycemic clamp techniques, neither hepatic nor peripheral insulin resistance was worsened in the group that was treated with prednisolone. Yet, analysis of hepatic glucose metabolism revealed that prednisolone did alter glycogen balance by reducing glycogen synthase flux, under hyperinsulinemic as well as hyperglycemic conditions. In addition to elevated insulin levels, prednisolone-treated mice showed a major rise in plasma leptin and FGF21 levels. Our data indicate that prednisolone-induced adverse effects on glucose metabolism in high-fat diet fed mice do not reflect impaired insulin sensitivity but may be caused by other changes in the hormonal regulatory network controlling glucose metabolism such as FGF21 and leptin.

Introduction

Glucocorticoids are steroid hormones produced by the adrenal gland under control of the hypothalamic-pituitary-adrenal axis (HPA-axis) [1]. Cortisol and corticosterone are the major endogenous glucocorticoids in humans and rodents, respectively. Cortisol is regarded as a stress hormone and is involved in regulation of a plethora of processes that modulate blood pressure, salt and water balance, immune response, energy metabolism and glucose homeostasis [1,2]. Related to their effects on the immune response, synthetic glucocorticoids, (*e.g.,* prednisolone) are widely used as anti-inflammatory and immunosuppressive drugs [3,4]. Unfortunately, chronic glucocorticoid treatment is accompanied by many adverse effects in humans, among which central obesity, hypertension, hyperlipidemia, hyperglycemia and insulin resistance, commonly referred to as Cushing's Syndrome [5,6]. These adverse effects also represent components of the metabolic syndrome, a condition defined by a combination of symptoms that increase the risk of cardiovascular disease and diabetes. The metabolic syndrome is strongly associated with the 'western' lifestyle, *i.e.*, low physical activity and excess caloric intake. Stress and elevated cortisol levels have been reported to contribute to development of the metabolic syndrome [7].

Induction of insulin resistance by prednisolone in humans was established by Pagano *et al.* in 1982 [8]. A more recent study showed that prednisolone readily induces insulin resistance in humans at a low-dose [9]. To be able to overcome the undesired adverse effects of glucocorticoids, the underlying mechanisms of their modes of action must be resolved. Several studies to this end have been performed in rats, *e.g.* after treatment with dexamethasone [10-13]. Reported effects of glucocorticoids in conventional mice, however, are highly variable. This is of relevance since genetically-modified mouse models offer great possibilities to dissect molecular mechanisms of insulin resistance [14]. Orland *et al.* showed strain-specific effects of dexamethasone in *db/db* mice on either a C57BL/KsJ or C57BL/6J background, but four days of dexamethasone treatment did not affect blood glucose levels in the control mice of either strain while serum insulin levels were minimally increased [15]. Dexamethasone-treatment increased plasma blood glucose levels in female A^{vy}/a (viable yellow) mice, but did not further increase plasma glucose levels in (hyperglycemic) male A^{vy}/a mice [16]. In C57BL/6J mice 5 days of alternate dexamethasone treatment did not affect fasting plasma glucose and insulin levels under conditions of high-fat diet-induced obesity, although these mice did have a perturbed muscle lipid metabolism [17].

We have recently shown that chronic prednisolone treatment for 7 days in C57BL/6J mice kept on a standard laboratory chow does affect hepatic glucose production (HGP) in the fasted state in a very subtle manner [18]. When the 'gold standard' to determine insulin sensitivity, *i.e.*, the hyperinsulinemic-euglycemic clamp (HIEC), was applied, we were not able

to demonstrate effects of chronic prednisolone treatment on insulin sensitivity. In fact, apparent insulin resistance was only detectable under conditions characterized by physiologically relevant insulin concentrations. A high-fat diet has been shown to induce insulin resistance in mice [19] and used for evaluation of glucocorticoid-induced adverse effects on insulin sensitivity [17]. Feeding mice a high-fat diet compromises insulin sensitivity and we hypothesized that this more closely resembles the human situation.

In the present study we therefore investigated whether prednisolone affects insulin sensitivity in mice fed a high-fat diet (36 energy% from lard) and whether we could discern effects of prednisolone on hepatic glucose metabolism under these conditions. For this purpose, we used state-of-the-art stable isotope techniques to monitor glucose metabolism under three different experimental conditions. First, fasting glucose metabolism was evaluated using a novel blood glucose kinetics model. Secondly, hepatic glucose metabolism was studied in more detail using Mass Isotopomer Distribution Analysis (MIDA) [20] before and during a hyperinsulinemic-euglycemic conditions (HIEC). Thirdly, a similar technique was used under hyperglycemic (HGC) conditions to study glucose metabolism in a state of elevated glucose concentrations and physiological insulin concentrations. The data reported in this paper revealed that prednisolone further increased high-fat diet-induced insulin resistance as estimated by means of the Homeostatic Model Assessment (HOMA-IR) [21] and by a kinetic model of glucose metabolism. Subsequent HIEC and HGC studies, however, did not indicate changes in insulin sensitivity, while prednisolone did influence hepatic glucose metabolism. These effects of prednisolone on glucose metabolism were associated with markedly elevated plasma leptin and FGF21 levels. Altogether, our data indicate that prednisolone alters hepatic glucose metabolism by bringing about selective changes in the complex network of hormones that control glucose metabolism.

Material and methods

Animals, treatments and diets

Male C57BL/6J mice were obtained from Harlan (Horst, the Netherlands) and housed under conventional conditions. Mice were fed a high-fat diet (beef tallow, rich in saturated fat) [22] for six weeks (Arie Blok Diervoeding, Woerden, The Netherlands). After five weeks of diet, the mice received prednisolone (10 mg/kg/d) or vehicle (gelatin (0.5 g/l)/mannitol (5g/l)) daily by gavage at 13:00 h for 7 days (n=7-8). All experiments were approved by the Ethics Committee for Animal Experiments of the University of Groningen. Prednisolone and vehicle were kindly provided by MSD (Oss, the Netherlands). For the infusion studies,

mice were equipped with a permanent jugular vein catheter, with a two-way entrance attached to the skull with acrylic glue as previous described [23]. Plasma levels of diabetes biomarkers were measured in fed (at 23:00 h) and 9 hours fasted (from 23:00 h till 08:00 h) mice.

Blood glucose kinetics

To determine blood glucose kinetics in mice multiple times during the high-fat diet mice were fasted for 9 hours (23:00 h – 08:00 h). Like previously described [24-26], we used a single-pool first-order kinetic model since there is no dynamic insulin action under these conditions. After the fasting period the mice were injected intraperitoneally at the start of the experiment, after 5 weeks and after 6 weeks with a low dose of D-[6,6-$^{2}H_{2}$]glucose (100 mg/kg) without inducing hyperinsulinemia. Before (at t=0) and at time points 10, 20, 30, 40, 50, 60, 75 and 90 minutes after injection, blood glucose concentrations were measured in blood collected by tail tip bleeding with a Lifescan EuroFlash (Lifescan Benelux, Beerse, Belgium) glucose meter. At the same time points, small blood samples were collected on filter paper, in which the fractional contribution of D-[6,6-$^{2}H_{2}$]glucose to the whole blood glucose pool was measured by GC-MS. Whole body glucose turnover and clearance were calculated by kinetic analysis of the wash-out of injected D-[6,6-$^{2}H_{2}$] glucose from the circulation (supplemental table 1). At the end a blood sample was taken by tail tip bleeding for insulin measurements.

Determination of hepatic carbohydrate fluxes before and during HIEC and HGC

For the HIEC and HGC two separate groups of C57BL/6J mice were operated for jugular vein catheterization at day 2 of the treatment with prednisolone. After surgery, mice were allowed to recover for 5 days before they were subjected to experiments, resulting in 7 days of prednisolone treatment. Before the experiments, mice were fasted for a 9 hours-(23:00 h– 08:00 h) or a 4-hours period (04:00 h – 08:00 h), for HIEC and HGC, respectively. During the experiment, mice were kept in small Plexiglas cages, with a wired floor to allow urine sampling and frequent collection of blood samples in freely moving mice [20]. To determine hepatic carbohydrate fluxes under basal conditions mice were infused for a four hours basal period with a solution containing [U-^{13}C]glucose (2.5 mg/ml), [2-^{13}C]glycerol (15 mg/ml), [1-^{2}H]galactose (6 mg/ml) (Cambridge Isotope Laboratories, Andover, MA) and paracetamol (1 mg/ml) at an infusion rate of 0.54 ml/h as previously described [20,27]. For the HIEC, solutions were changed after four hours and mice were subjected to a four hour hyperinsulinemic period by infusing a solution containing insulin (44 mU/ml, Actrapid, Novo Nordisk, Bagsvaerd, Denmark), somatostatin (40 μg/ml, UCB, Breda, the Netherlands), [2-^{13}C]glycerol (60 mg/ml), [1-^{2}H]galactose (24 mg/ml), paracetamol (4 mg/

ml) and 1% BSA (Sigma, St. Louis, MO) at a constant rate of 0.135 ml/h. During hyperinsulinemia, euglycemia was kept by infusion a second solution which contained 27% glucose (291 mg/ml) and 3% [U-^{13}C]glucose (9 mg/ml) at an adjustable rate to maintain plasma glucose levels at 7 mM. For the second experiment, the HGC, infusions were changed after four hours and mice were subjected to a four hour hyperglycemic period by infusion of a solution containing [U-^{13}C]glucose (10 mg/ml), [2-^{13}C]glycerol (60 mg/ml), [1-^{2}H]galactose (24 mg/ml) and paracetamol (4 mg/ml) and 1% BSA at a constant rate of 0.135 ml/h. A second solution which contained 27% glucose (291 mg/ml) and 3% [U-^{13}C]glucose (9 mg/ml) was infused with an adjustable rate to maintain plasma glucose levels at a hyperglycemic level of ~17 mM, comparable to the peak blood glucose level measured in control mice during an oral glucose tolerance test. During both experiments, blood glucose levels were measured every 15 minutes in blood drops collected by tail tip bleeding with a Lifescan EuroFlash glucose meter. Every hour, blood spots for GC-MS analysis were taken by tail tip bleeding on filter paper, air-dried and stored at room temperature until further analysis. Urine samples were collected on filter paper at hourly intervals. Hepatic carbohydrate fluxes as well as whole body glucose turnover and clearance rates during the experiment were calculated using MIDA as previous described [27,28]. Additionally, after the hyperglycemic period a blood sample was taken for insulin measurements.

Indirect calorimetry

Mice fed a high-fat diet for almost 5 weeks were subjected to indirect calorimetry for 7 days with free access to water and a high-fat diet, while food intake was measured (TSE systems GmbH, Bad Homberg, Germany). Three days before the start of the prednisolone treatment mice were placed in the calorimetric cages to acclimatize and for basal measurement. Upon start of the treatment mice were tracked for the 4 following days. For prednisolone treatment by gavage, measurements were shortly interrupted daily between 12:00 and 13:00 h. Oxygen and carbon dioxide flow rates were measured every 13 minutes. The respiratory exchange ratio (RER) was calculated using the following equation: $RER = VO_2 / VCO_2$ in which the VO_2 represents the volume rate of oxygen consumption and the VCO_2 is the volume rate carbon dioxide production.

Measurement of Mass Isotopomer Distribution by GC-MS

The fractional contributions of stable isotopically-labeled carbohydrates from blood and urine samples collected during the HIEC, HGC and during the blood glucose kinetics study were extracted, derivatized and measured by GC-MS as previously described by van Dijk *et al.* [20].

Metabolite analysis

Basal values of blood glucose concentrations were measured in conscious mice in blood drops collected by tail tip bleeding with a Lifescan EuroFlash glucose meter. Plasma insulin, corticosterone and fibroblast growth factor-21 (FGF21) concentrations were measured using commercially available ELISA kits (Mercodia ultrasensitive mouse insulin ELISA, Orange Medical, Tilburg, the Netherlands; Diagnostic System Laboratories Benelux, Assendelft, The Netherlands and Millipore, Amsterdam, The Netherlands, respectively). The HOMA-IR was calculated adjusted for basal mouse values taken from a chow-fed vehicle-treated group as previously described [18] . Plasma non-esterified (or free) fatty acid (NEFA) and 3-hydroxybutyrate concentrations were determined with commercially available kits (Diasys, Holzheim, Germany, Wako Chemicals, Neuss, Germany, respectively). Hepatic lipids were extracted from the liver homogenates according to Bligh and Dyer [29] . Hepatic and plasma triglycerides were measured using a kit from Roche Diagnostics (Mannheim, Germany), and free and total cholesterol levels were measured with a kit from Wako chemicals (Neuss, Germany). Hepatic glycogen concentrations were determined as described [30]. Plasma diabetes biomarkers were measured by a commercially available multiplex (Bio-plex Pro™ Mouse Diabetes, Bio-Rad, Veenendaal, the Netherlands) measuring insulin, leptin, glucagon, ghrelin, glucagon like peptide-1 (GLP-1), gastric inhibitory peptide (GIP), resistin and plasminogen activator inhibitor-1 (PAI1).

Gene expression analysis

RNA was isolated from liver and white adipose tissue and gene-expression was measured as previously described [18]. Expression levels were normalized for *RPLP0* levels. The sequence of the primers and probes that were previously used can be found are deposited at RTPrimerDB (http://www. rtprimerdb.org). The sequences of the primers and probes used for *Leptin* are (Acc. No. NM_008493.3) AAG ACC ATT GTC ACC AGG ATC AA (forward primer) GGT CCA TCT TGG ACA AAC TCA GA (reverse primer) and CAC ACA CGC AGT CGG TAT CCG CC (probe).

Statistics

All data are represented as mean ± SEM. Statistical analysis for two independent groups was performed using Mann-Whitney U tested with SPSS for Windows software (SPSS 16, Chicago, IL, USA). For multiple comparison statistical analysis were performed by Kruskal-Wallis test, followed by a Mann-Whitney U test corrected for multiple comparisons. For paired measurements statistical analysis was performed using a Wilcoxon signed-rank test. Significance was considered at a level of $p<0.05$ and adjusted for multiple comparisons.

Results

Chronic prednisolone treatment aggravates the high-fat diet-induced increase in HOMA-IR

To assess whether chronic prednisolone treatment aggravates high-fat diet-induced insulin resistance, we first examined the effect of prednisolone-treatment on body parameters and metabolite concentrations (Table 1). Effective prednisolone treatment was confirmed by a severe reduction of thymus weight and a reduction of plasma corticosterone concentration by almost 90% due to activation of the HPA-axis. Prednisolone treatment did not further affect the increase in body weight in mice fed a high-fat diet for 6 weeks.

After 9h of fasting blood glucose levels were higher upon prednisolone treatment in mice fed a high-fat diet, while fasting insulin levels were slightly increased as well, resulting in

Table 1

	Vehicle	Prednisolone
Body weight (g) day 0	25.2 ± 0.57	25.4 ± 0.42
Body weight (g) day 42	29.1 ± 1.2	29.8 ± 0.5
Thymus weight (mg)	25.1 ± 2.8	4.1 ± 0.23 *
Plasma		
Glucose (mM)	7.6 ± 0.3	11.1 ± 0.6*
Insulin (mU/liter)	7.4 ± 2.6	10.3 ± 1.7
HOMA-IR	3.6 ± 1.3	7.3 ± 1.3*
Cholesterol (mM)	5.9 ± 0.1	7.9 ± 0.4*
Free Cholesterol (mM)	1.5 ± 0.08	1.9 ± 0.11*
Triglycerides (mM)	1.3 ± 0.07	1.9 ± 0.15*
NEFA (mM)	0.58 ± 0.03	0.44 ± 0.02*
Corticosterone (µg/liter)	820 ± 37	96 ± 17*
β-Hydroxybutyrate (mM)	1.07 ± 0.27	0.11 ± 0.01*
FGF21 fasted (µg/liter)	1.41 ± 0.30	2.77 ± 0.98*
Liver		
Cholesterol (µmol/g liver)	11.8 ± 0.76	13.6 ± 0.53
Triglycerides (µmol/g liver)	43.7 ± 6.39	57.8 ± 4.99
Glycogen (µmol/g liver)	111 ± 29	154 ± 31

Treatment parameters of 9 hours fasted mice
mice fed a high-fat diet for six weeks and treated with either vehicle (control) or prednisolone (10 mg/kg/d) during the last seven days. Data are represented as means ± SEM; N=8; * p<0.05. The HOMA-IR was calculated adjusted for basal mouse values taken from a chow-fed, vehicle-treated group.

a 2-fold higher HOMA-IR (Table 1). The high-fat diet itself also increased the HOMA-IR to 3.6 ± 1.3 compared to mice on a chow diet, which had a HOMA-IR of 1.0 ± 0.1 (p= 0.003) [18]. Prednisolone-treatment in mice fed a high-fat diet increased plasma cholesterol and triglyceride levels, while plasma NEFA concentration dropped. Remarkably, prednisolone-treatment resulted in a 10-fold decrease in plasma 3-hydroxybutyrate concentrations and almost doubled plasma fibroblast growth factor 21 (FGF21) levels in the fasted state (Table 1), but did not influence hepatic cholesterol and triglyceride levels.

In order to evaluate if the prednisolone-induced increase HOMA-IR influenced fasting glucose production and clearance, we analyzed fasting blood glucose kinetics in whole body from the wash-out of intraperitoneal injected D-[6,6-$^2H_2$]glucose from the circulation. To follow the effects of both the high-fat diet and prednisolone treatment in time, mice were subjected to this test three times; 1) at the start of the experiment (week 0) before start of the diet, 2) after 5 weeks of diet before start of the prednisolone treatment, and 3) after 6 weeks of diet and one week of prednisolone treatment. This experimental setup allows for sequential analysis of glucose metabolism under basal conditions throughout the 6 weeks of diet in the same animals. After 5 weeks on a high-fat diet, blood glucose levels were significantly elevated in high-fat fed mice compared to mice on a normal chow diet (Fig. 1A). One-week prednisolone-treatment resulted in an additional increase of blood glucose levels compared to mice fed a high-fat diet for 6 weeks. Plasma insulin levels followed a similar pattern over time (Fig. 1B), showing that plasma insulin levels were elevated upon feeding a high-fat diet. Yet, in mice fed a high-fat diet combined with

Figure 1

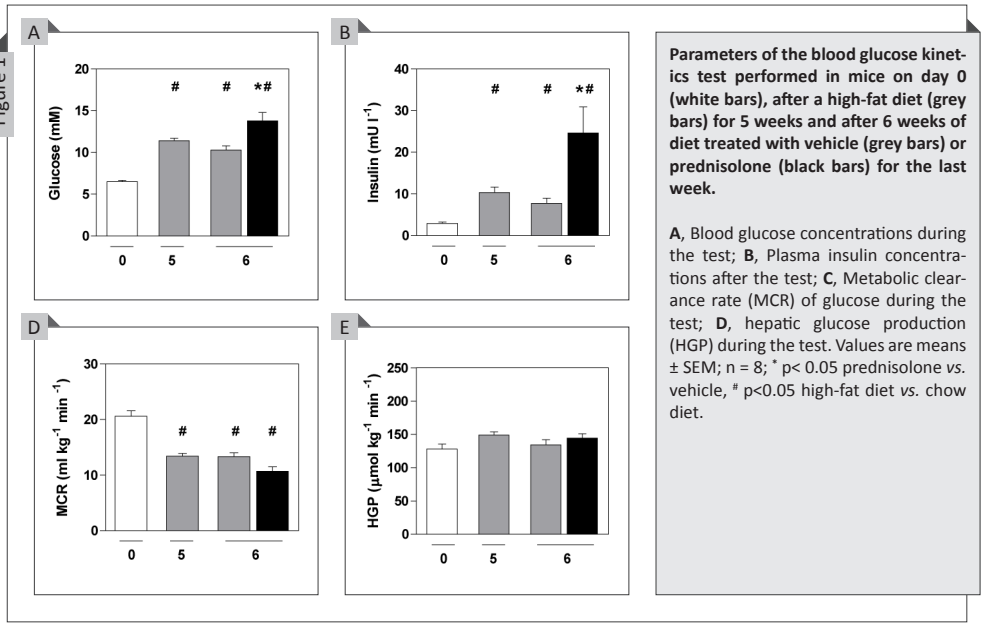

Parameters of the blood glucose kinetics test performed in mice on day 0 (white bars), after a high-fat diet (grey bars) for 5 weeks and after 6 weeks of diet treated with vehicle (grey bars) or prednisolone (black bars) for the last week.

A, Blood glucose concentrations during the test; **B**, Plasma insulin concentrations after the test; **C**, Metabolic clearance rate (MCR) of glucose during the test; **D**, hepatic glucose production (HGP) during the test. Values are means ± SEM; n = 8; * p< 0.05 prednisolone *vs.* vehicle, # p<0.05 high-fat diet *vs.* chow diet.

prednisolone-treatment plasma insulin levels were even more strongly induced.

The high-fat diet induced a distinct reduction of metabolic clearance rate (MCR) of glucose after 35 days and 42 days compared to a chow diet at the start of the experiment (Fig. 1C). Treatment with prednisolone had no significant additional effect on MCR. Neither the high-fat diet nor prednisolone-treatment changed the hepatic glucose production (HGP; Fig. 1D). Nevertheless, note that plasma insulin levels were extremely high in prednisolone-treated mice fed a high-fat diet. Therefore, when HGP and MCR were related to the prevailing insulin levels, mice treated with prednisolone upon a high-fat diet appeared insulin resistant which was in line with the increased HOMA-IR.

Prednisolone does not induce insulin resistance according to the HIEC and HGC

To study whether increased blood glucose and plasma insulin concentration in high-fat fed mice treated with prednisolone was actually caused by insulin resistance, we combined the HIEC to the MIDA technique to measure hepatic glucose metabolism during hyperinsulinemia. Again prednisolone treatment led to increased fasting glucose levels (6.1 ± 0.4

Figure 2

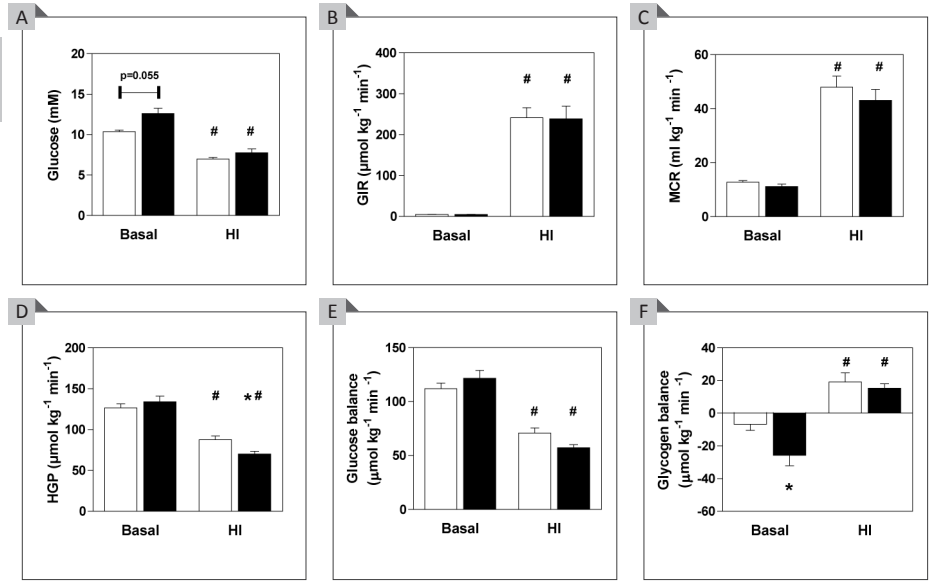

Parameters of the basal and hyperinsulinemic euglycemic (HI) clamp experiment performed in mice on a high-fat diet treated with vehicle (white bars) or prednisolone (black bars).

A, Average blood glucose concentration during the steady-state periods of the experiment (2-4 hours and 6-8 hours); **B**, Glucose Infusion Rate (GIR) needed to maintain euglycemic conditions; **C**, Metabolic Clearance Rate (MCR); **D**, Hepatic Glucose Production (HGP); **E**, glucose balance and **F**, Glycogen balance. Values are means ± SEM; n = 8; * p<0.05.

vs. 8.8 ± 0.6, veh *vs*. pred, p=0.004) and glucose levels during the basal period of the test tended to be higher (p=0.055) (Fig. 2A). During the basal period glucose infusion rate (GIR) was kept at a steady, very low level in both groups for it represents the infusion of the stable isotopes solution, as is evident from Fig. 2B. During the hyperinsulinemic period, the GIR was adjusted to keep a euglycemic state at a blood glucose level of 7 mM in both groups. Surprisingly, prednisolone-treatment on top of a high-fat diet did not influence the magnitude of the GIR (Fig. 2B).

Even though blood glucose levels in the basal state tended to be higher in prednisolone-treated mice compared to controls, both the MCR (Fig. 2C) and HGP (Fig. 2D) were similar during this period. Upon hyperinsulinemia, the well-documented stimulatory effect of insulin on the uptake of glucose in the peripheral tissues and inhibitory effect on the hepatic production of glucose were observed in both groups. Prednisolone treatment did not further alter the MCR but, strikingly, resulted in a more pronounced suppression of the HGP by insulin.

By means of MIDA the relevant hepatic fluxes constituting hepatic glucose metabolism were measured and these are presented in table 2A. Prednisolone treatment reduced

Table 2

A

Fluxes	Basal period		Hyperinsulinemic period	
	Vehicle	Prednisolone	Vehicle	Prednisolone
G6Pase	170.4 ± 5.9	190.3 ± 8.3	122.2 ± 9.7$^{\#}$	102.5 ± 6.9$^{\#}$
GK	58.5 ± 4.2	68.6 ± 8.1	51.4 ± 10.2	45.2 ± 5.4$^{\#}$
GS	59.1 ± 5.8	39.4 ± 1.5*	56.8 ± 5.3	36.8 ± 1.2*
GP	65.9 ± 4.5	65.1 ± 5.5	37.6 ± 2.7$^{\#}$	21.5 ± 2.0$^{*\#}$
GNG	105.1 ± 1.9	95.9± 2.9*	90.0 ± 5.4$^{\#}$	72.5 ± 1.2$^{*\#}$

B

Fluxes	Basal period		Hyperglycemic period	
	Vehicle	Prednisolone	Vehicle	Prednisolone
G6Pase	199.1 ± 16.3	178.7 ± 1.5	187.7 ± 25.2	189.3 ± 14.5
GK	75.5 ± 9.6	54.7 ± 2.5	105.0 ± 16.3$^{\#}$	84.9 ± 6.2$^{\#}$
GS	42.4 ± 5.5	32.1 ± 2.5	56.5 ± 4.7	34.0 ± 2.4*
GP	81.9 ± 10.1	76.0 ± 3.4	70.5 ± 8.9	63.7 ± 4.3
GNG	84.1 ± 3.4	80.1 ± 1.8	68.7 ± 4.3$^{\#}$	74.7 ± 4.3

Hepatic glucose fluxes during the basal and hyperinsulinemic (A) and hyperglycemic period (B)
The hepatic carbohydrates fluxes trough glucose-6-phosphatase (G6Pase), glucokinase (GK), Glycogen synthase (GS), glycogen phosphorylase (GP) and gluconeogenesis (GNG). Fluxes are shown in µmol/kg/min. Values represent means ± SEM; n=7-8. * p<0.05 prednisolone *vs.* vehicle, $^{\#}$ p<0.05 hyperinsulinemic *vs.* basal period within treatment.

both the glycogen synthase (GS) flux and the gluconeogenic (GNG) flux in the basal period. The hyperinsulinemia reduced the glucose-6-phosphatase (G6Pase), the glycogen phosphorylase (GP) and GNG flux in both groups. Strikingly, even though GNG has repeatedly been reported to be up regulated by GCs [31], it was slightly reduced upon prednisolone treatment in both the basal and hyperinsulinemic state in mice on a high-fat diet. In addition prednisolone treatment led to a reduced GS and GP flux in the hyperinsulinemic period, resulting in a similar glycogen balance compared to the vehicle-treated group in the hyperinsulinemic period compared to the basal period. From these fluxes, the glucose and glycogen balances were calculated (Fig. 2E and F). The glucose balance was reduced in both groups during the hyperinsulinemic period, mainly due to a reduction in G6Pase flux. This was even more pronounced in the prednisolone-treated group. The initially negative glycogen balance, which was more negative in prednisolone-treated mice, turned positive upon hyperinsulinemia, even more pronounced in prednisolone-treated mice. The differences in glycogen balance upon hyperinsulinemia were mainly due to reductions in the GP flux, whereas the GS flux was not affected by hyperinsulinemia, but was reduced by prednisolone treatment in both periods.

Figure 3

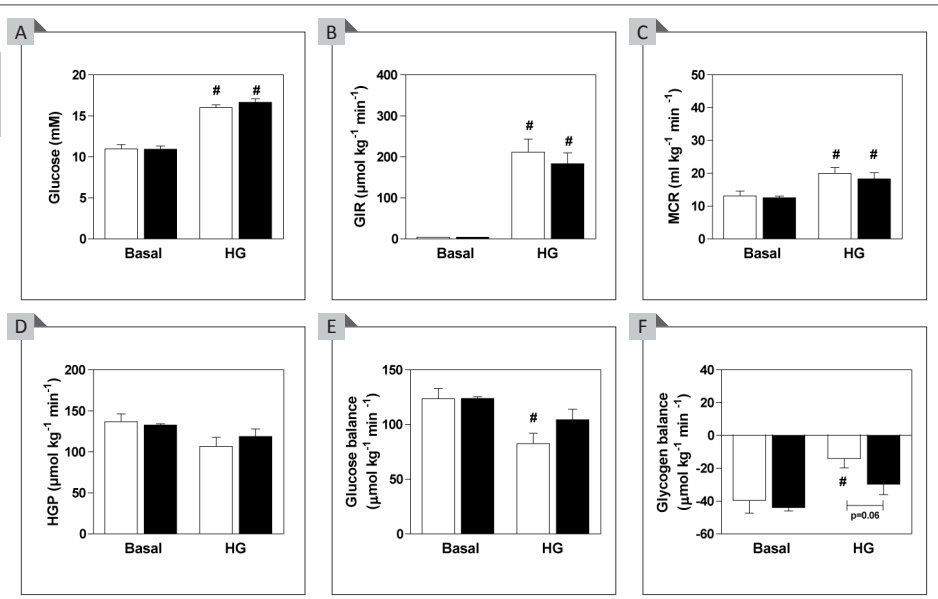

Parameters of the basal and hyperglycemic (HG) clamp experiment performed in mice on a high-fat diet treated with vehicle (white bars) or prednisolone (black bars).

A, Average blood glucose concentration during the steady-state periods of the experiment (1-3 hours and 4-6 hours); **B**, Average Glucose Infusion Rate (GIR) needed to maintain hyperglycemic conditions; **C**, Metabolic Clearance Rate (MCR); **D**, Hepatic Glucose Production (HGP); **E**, glucose balance and **F**, Glycogen balance. Values are means ± SEM; n = 7; * p<0.05.

So far, these data suggest that prednisolone treatment of mice receiving a high-fat diet did not decrease insulin sensitivity as measured with the 'gold standard' HIEC, although blood glucose and plasma insulin levels as well as hepatic glucose metabolism were clearly affected. To evaluate regulation of glucose metabolism during stimulation of endogenous insulin production at elevated glucose levels, a HGC combined with hepatic glucose metabolism analysis was performed. To this purpose, mice were fasted for 4 hours, after which the groups did not show difference in fasted blood glucose levels (8.6 ± 0.3 *vs.* 8.2 ± 0.4, means ± SEM in mM, veh. *vs.* pred, ns) and in blood glucose levels in the basal period (Fig. 3A). To induce hyperglycemia with blood glucose levels up to 17 mM, very similar glucose infusion rates (GIR) were necessary in both groups (Fig. 3B), indicating no differences in insulin response since insulin levels during the HGC were similar in both groups (41.8 mU/L [11.7 – 73.1] *vs.* 25.9 mU/L [11.6 – 74.0] (after the hyperglycemic period, median and ranges, veh. *vs.* pred, ns).

In the basal period MCR and HGP were similar in both groups, as expected from the former experiment. Upon hyperglycemia MCR was increased in both groups, while HGP showed a slight decrease in vehicle-treated mice (Fig. 3C and D). Prednisolone treatment had no effect on either MCR or HGP. Nevertheless, analysis of hepatic glucose fluxes revealed that the GS-flux was clearly reduced in the hyperglycemic period by prednisolone treatment (Table 2B). This resulted in a minor effect on glycogen balance (Fig. 3F). The glucose balance was reduced in the vehicle group during the hyperglycemic period (Fig. 3E), which was mainly due to an increase in the GK-flux, which remained unchanged in the prednisolone-treated group. We checked for hepatic mRNA expression levels of genes crucially involved in glucose metabolism (Fig. 4); phosphoenolpyruvate carboxykinase 1 (*Pck1)* and glucose-6-phosphatase (*G6pc)* were reduced by a high fat diet as compared

Figure 4

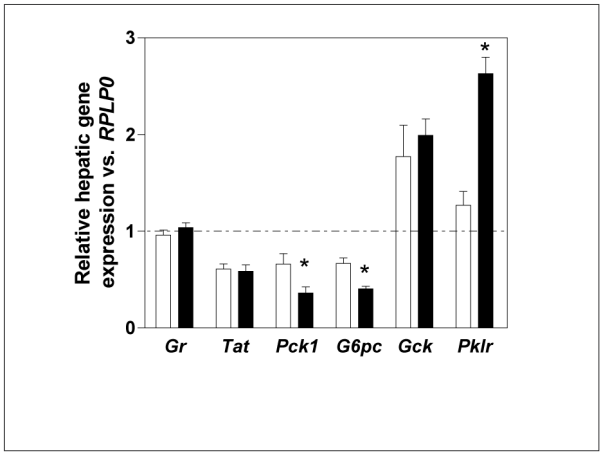

Hepatic gene expression of 9 hours fasted mice on a high-fat diet treated with vehicle (white bars) or prednisolone (black bars).

Results were normalized to *Rplp0* (ribosomal protein, large, P0 (*36b4*)) with data from vehicle-treated mice on a chow diet defined as '1' (dotted line). Values are means ± SEM; n = 8; * p < 0.05 prednisolone *vs.* vehicle, *Gr*, glucocorticoid receptor (N*r1c3,* nuclear receptor subfamily 3, group C, member 1); *Tat*, tyrosine aminotransferase; *Pck1*, phosphoenolpyruvate carboxykinase 1 (cytosolic); *G6pc*, glucose-6-phosphatase (catalytic); *Gck*, glucokinase; *Pklr*, pyruvate kinase (liver and red blood cell).

to chow and combined with prednisolone even more so. Glucokinase *(Gck)* and pyruvate kinase (*Pklr*) mRNA levels were increased by the high-fat diet or prednisolone treatment, respectively. Glucorticoid target genes were checked to confirm prednisolone activation. Surprisingly, the classical GC target gene tyrosine aminotransferase *(Tat)* was reduced by a high-fat diet and unaltered by prednisolone while *Pck1*, another classic target gene, was even reduced by prednisolone treatment.

Prednisolone alterations on blood glucose metabolism are insulin independent

The apparent insulin resistance as indicated by an increased HOMA-IR and blood glucose kinetics under prevailing insulin concentrations was not revealed when insulin sensitivity was more thoroughly studied by the HIEC and the HGC. This suggested that prednisolone treatment in mice fed a high-fat diet did not induce a classical insulin resistance measured according to generally accepted methods. These findings could imply that other metabolic factors might be involved. As shown in Table 1, plasma FGF21 levels were increased upon prednisolone treatment, which was confirmed by hepatic gene expression levels of *Fgf21* (Fig. 5A). The main regulator of FGF21 expression PPARα [18] showed no increase in gene expression levels and target genes of *Pparα*, like *Acox1* and *Cpt1a*, were not elevated by prednisolone.

Figure 5

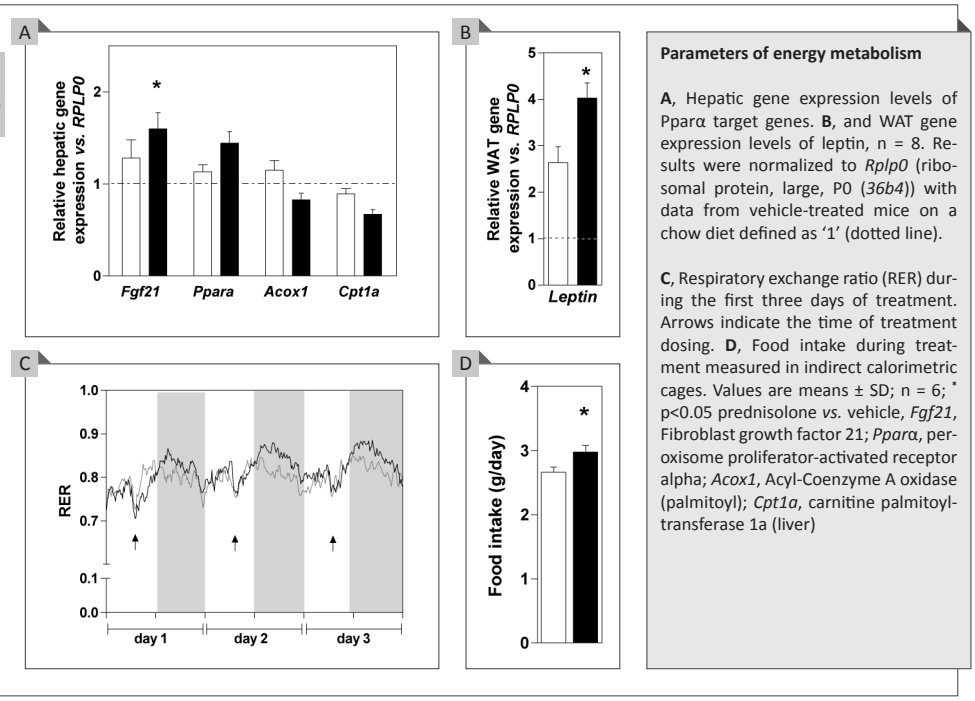

Parameters of energy metabolism

A, Hepatic gene expression levels of Pparα target genes. **B**, and WAT gene expression levels of leptin, n = 8. Results were normalized to *Rplp0* (ribosomal protein, large, P0 (*36b4*)) with data from vehicle-treated mice on a chow diet defined as '1' (dotted line).

C, Respiratory exchange ratio (RER) during the first three days of treatment. Arrows indicate the time of treatment dosing. **D**, Food intake during treatment measured in indirect calorimetric cages. Values are means ± SD; n = 6; * p<0.05 prednisolone *vs.* vehicle, *Fgf21*, Fibroblast growth factor 21; *Pparα*, peroxisome proliferator-activated receptor alpha; *Acox1*, Acyl-Coenzyme A oxidase (palmitoyl); *Cpt1a*, carnitine palmitoyltransferase 1a (liver)

Finally, we analyzed multiple hormones and hormone-like factors in plasma from fed and 9 hours fasted mice. Table 3 shows that prednisolone-induced plasma leptin levels, both in the fed and fasted state, in addition to inducing plasma insulin levels. Other analyzed hormones were not affected by prednisolone treatment in the fasted state, but PAI1 was increased upon prednisolone treatment in the fed state only. Fasting itself reduced plasma leptin, GLP-1 and GIP. Increased plasma leptin levels were confirmed by *leptin* gene expression levels in white adipose tissue (Fig. 5B). Leptin plays a major role in energy expenditure and as a satiety factor; therefore energy expenditure in mice fed a high-fat diet was measured in indirect calorimetry cages. Figure 5C shows a slight increase in respiratory exchange ratio (RER) at night in prednisolone-treated mice, indicating that at night glucose utilization is increased in mice fed a high-fat diet treated with prednisolone compared to vehicle-treated mice. Food intake, however, was slightly increased upon prednisolone treatment (Fig. 5D)

Discussion

In an earlier study [18] we showed that, under chow-fed conditions, sustained treatment of C57BL/6J mice with prednisolone reduced insulin sensitivity only in a very subtle manner under fasting conditions. In this subsequent study we show that in mice challenged with a high-fat diet, prednisolone treatment did not aggravate insulin resistance induced by a high-fat diet as measured by a HIEC, even though these mice appeared insulin resistant since HOMA-IR was increased and whole body glucose kinetics at basal prevailing insulin

Table 3

	Fed		Fasted	
(μg/ml)	**Vehicle**	**Prednisolone**	**Vehicle**	**Prednisolone**
Insulin	5.2 ± 1.8	10.2 ± 3.8*	ND	ND
Glucagon	0.70 ± 0.14	0.79 ± 0.22	0.38 ± 0.06$^{\#}$	0.38 ± 0.11$^{\#}$
Leptin	22.2 ± 4.3	44.5 ± 7.9*	7.72 ± 2.96$^{\#}$	13.93 ± 3.04$^{*\#}$
Resistin	261.7 ± 72.3	229.6 ± 64.4	217.1 ± 43.1	227.7 ± 57.4
GLP-1	0.19 ± 0.05	0.17 ± 0.08	0.11 ± 0.02$^{\#}$	0.09 ± 0.03$^{\#}$
GIP	1.16 ± 0.35	1.47 ± 0.54	0.40 ± 0.07$^{\#}$	0.37 ± 0.10$^{\#}$
PAI1	0.82 ± 0.07	1.45 ± 0.28*	1.08 ± 0.32	1.04 ± 0.34
Ghrelin	3.58 ± 1.25	2.41 ± 1.39	6.95 ± 2.37	4.78 ± 2.00

Plasma concentrations of diabetes biomarkers
Fed samples were taken at 23:00 h, fasted samples at 08:00 h after a 9 hours fast. Values represent means ± SD; n=6. * p<0.05 prednisolone *vs.* vehicle, $^{\#}$ p<0.05 fed *vs.* fasted, ND – not detectable.

concentrations were perturbed. This study clearly shows a disengagement of the HOMA-IR with outcome of the HIEC and HGC and also documents that prednisolone-induced alterations of glucose metabolism in these mice are not directly linked to insulin sensitivity.

Insulin resistance is a well-known side effect of glucocorticoid treatment in humans [8,9,32]. In addition, it has been shown repeatedly that dexamethasone treatment also induces insulin resistance in rats [11,13,33,34]. In mice, however, glucocorticoid-induced insulin resistance is not as evident. Most studies on glucocorticoid-induced insulin resistance in mice involve specific transgenic mouse strains [15,35] usually in combination with long-term, or high doses, of dexamethasone administration [36,37]. Since prednisolone is routinely used for chronic treatment in humans [38], we have evaluated prednisolone-induced insulin resistance in conventional C57BL/6J mice fed a high-fat diet known to compromise the physiological actions of insulin. In order to analyze insulin resistance, which is defined as a decreased sensitivity or responsiveness to metabolic actions of insulin [39], in conventional C57BL/6J mice, we subjected them to different methods available to assess insulin resistance, including the HOMA-IR, HIEC, HGC, basal blood glucose kinetics and analyzed hepatic glucose metabolism by MIDA.

Like in chow-fed mice [18], we confirmed that chronic, 7 days of prednisolone treatment increased the HOMA-IR, in high-fat fed mice while, as expected, the high-fat diet by itself already caused an increased HOMA-IR in comparison to chow-fed mice. Note that for the calculations of HOMA-IR, the values were adjusted for basal values of glucose and insulin concentrations in mice. In addition, when the MCR and HGP calculated from basal whole body blood glucose kinetics were related to prevailing insulin levels, prednisolone-treated mice appeared to have reduced insulin sensitivity. Yet, similar to our earlier study in chow-fed animals, when insulin sensitivity was evaluated by the HIEC, the 'gold standard' to evaluate insulin action on glucose metabolism, prednisolone treatment was found not to alter insulin sensitivity since GIR values were similar with and without prednisolone treatment. This clearly shows that, although HOMA-IR and HIEC were shown to be well correlated in humans [40], there is a disengagement between the HOMA-IR with the HIEC in mice, which has previously been reported for rodents [39,41]. Nevertheless, assessment of hepatic carbohydrate metabolic fluxes by stable isotope techniques under basal, hyperinsulinemic-euglycemic as well as hyperglycemic conditions revealed that prednisolone treatment did alter hepatic glucose metabolism in high-fat fed mice, mainly by reducing the glycogen synthase flux. These effects of prednisolone on glucose metabolism are not mediated by insulin, as infusion of since insulin infusion during HIEC did not affect the GS-flux, but in contrast reduced the GP-flux.

In our former study [18], we showed that nutritional status has to be taken into account

when evaluating prednisolone-induced insulin resistance. In order to accurately assess effects of prednisolone on glucose metabolism in mice fed the high-fat diet, we studied hepatic glucose metabolism under different nutritional conditions, *i.e.*, after four and nine hours of fasting and under hyperglycemic and hyperinsulinemic euglycemic conditions. First 9-h fasted state was assessed by measuring blood glucose kinetics by modeling the wash-out of *ip* injected D-[6,6-$^{2}H_{2}$]glucose, since this method allows repeated measurements over time in the same animals. This is not possible with the HIEC and HGC, because these are complex and laborious experiments which require invasive surgery. However, to quantitatively assess hepatic glucose metabolism and hepatic and peripheral insulin resistance both the HIEC and HGC were combined with a method to study hepatic glucose metabolism with stable isotopically-labeled glucose by MIDA [20,27,28]. By adapting these state-of-the-art methods, both hepatic carbohydrate fluxes and insulin sensitivity could be measured at the same time. During the HIEC supra-physiological insulin levels were introduced, which can be regarded as a post-prandial condition. Importantly, during the HIEC the pancreas is blocked by somatostatin, thereby overruling part of the bodies' natural reaction. As a consequence subtle changes might not be detected under these conditions. To aim for a more physiological approach with a normal pancreatic response at high glucose levels, the HGC was used. The basal periods of the HIEC and the HGC both symbolize a different nutritional status; for the HIEC mice were fasted for 9 hours, while for the HGC mice were fasted for only 4 hours. During the basal periods of both experiments the sum fluxes from both hepatic glucose sources, *i.e.*, glycogen phosphorylase and gluconeogenesis, was identical. However, there is a switch from the glycogen phosphorylase to gluconeogenesis with prolonged fasting. This shows that upon fasting, first glycogen breakdown takes place after which gluconeogenesis takes over. Note that the magnitudes of HGP and MCR in the basal period of both clamp experiments are in the same order of magnitude as the HGP and MCR from the fasting blood glucose kinetics, confirming the relevance of this experimental procedure. During the HIEC, GIR were equal between the groups, however, the HGP was slightly reduced during the hyperinsulinemic period in prednisolone-treated mice. Because this was at similar infusion rates of insulin the reduced HGP may be explained as increased hepatic insulin sensitivity.

Relating hepatic gene expression levels of the genes encoding enzymes that catalyze the reactions that constitute the hepatic carbohydrate fluxes to the quantitatively measured hepatic glucose fluxes is complex; fluxes were measured over a period of time under a specific nutritional status, while samples for gene expression levels measurements were taken at fixed time points after fasting and treatment. In addition, regulation of metabolic fluxes largely depends on the substrate availability and enzyme activity. The observed effects of the chronic prednisolone treatment in the current study on mRNA levels of GR

target genes are partly contrasting reported effects. *Tat* [42] and *Pck1* [43,44] have been shown to be classical GR target genes, being up-regulated when GCs are present, but prolonged prednisolone treatment, like in our study, resulted in decreased hepatic mRNA levels of both genes, as previously reported [18]. Up-regulatory effects of GCs on *Pck1* have been shown to be fast and transient [45]. Thus, the reduced *Pck1* expression likely reflects the reduced plasma GC concentration in prednisolone-treated mice 18-h after the last dose. In addition, a study by Magnusson *et al.* showed actually that major changes in gene expression of *Pck1* do not alter GNG-flux *per se* [46].

As previously shown in mice receiving a chow diet, also on a high-fat diet plasma FGF21 levels were elevated by prednisolone [18]. Together with the low plasma 3-hydroxybutyrate levels, high FGF21 levels imply a perturbed feeding-to-fasting transition [47,48] also in mice fed a high-fat diet. Possibly prednisolone-treated mice might be FGF21 resistant, like in obesity [49]. In addition, FGF21 has been shown to reduce *G6pc* and glycogenolysis through *Ppargc1a* [50]; prednisolone-treated mice in this study had a reduction in hepatic *G6pc* gene expression levels, which could be mediated *via* FGF21-*Ppargc1a*.

During fasting leptin is reduced, thereby reducing satiety and promoting food intake [51]. In mice on a high-fat diet, prednisolone treatment increased plasma leptin levels both in the fed and the fasted state, but did not reduce food intake. Leptin and glucocorticoids are counter regulatory and control satiety and appetite mainly via the hypothalamus [52]. Moreover, together with insulin, leptin and glucocorticoids are important factors in an expanding hormonal network regulating glucose metabolism which, in turn, is tightly connected to energy homeostasis. It was thought that hepatic leptin signaling did not affect hepatic glucose metabolism [53,54], yet, a recent paper showed that the hepatic leptin receptor is involved in diet- and age-related insulin resistance [55], thereby opening a direct role for leptin on hepatic glucose metabolism. These data demonstrate that prednisolone, which caused a subtle phenotype on glucose metabolism in C57BL/6J mice, closely interacts with members of a complex hormonal network influencing glucose metabolism other than insulin.

Although glucocorticoids have been shown to induce insulin resistance in humans and rats measured by HIEC, prednisolone treatment in C57BL/6J mice fed a high-fat diet did not lead to such a clear insulin resistance phenotype. Nevertheless, fasting glucose and insulin levels, fasting blood glucose kinetics and hepatic glucose fluxes during both hyperinsulinemic and hyperglycemic states showed clear signs of an adapted glucose metabolism after prednisolone treatment. Thus, this study shows that prednisolone treatment did not aggravate high-fat diet-induced insulin resistance, but does alter hepatic glucose fluxes independent of insulin action, presumably due to adaptations in the hormonal networks regulating glucose control, involving leptin and FGF21.

Acknowledgements

The authors would like to thank Rick Havinga, Aycha Bleeker, Theo Boer and Monique van Vleuten for their excellent skillful technical assistance.

Reference List

1. Rhen, T. & Cidlowski, J. A. Antiinflammatory action of glucocorticoids--new mechanisms for old drugs. *N. Engl. J Med.* 353, 1711-1723 (2005).
2. Walker, B. R. Glucocorticoids and cardiovascular disease. *Eur. J. Endocrinol.* 157, 545-559 (2007).
3. Barnes, P. J. Anti-inflammatory actions of glucocorticoids: molecular mechanisms. *Clin Sci. (Lond)* 94, 557-572 (1998).
4. Baschant, U. & Tuckermann, J. The role of the glucocorticoid receptor in inflammation and immunity. *J. Steroid Biochem. Mol. Biol.* 120, 69-75 (2010).
5. Schacke, H., Docke, W. & Asadullah, K. Mechanisms involved in the side effects of glucocorticoids. *Pharmacology & Therapeutics* 96, 23-43 (2002).
6. van Raalte, D. H., Ouwens, D. M. & Diamant, M. Novel insights into glucocorticoid-mediated diabetogenic effects: towards expansion of therapeutic options? *Eur. J Clin Invest* 39, 81-93 (2009).
7. Walker, B. R. Cortisol--cause and cure for metabolic syndrome? *Diabet. Med.* 23, 1281-1288 (2006).
8. Pagano, G. *et al.* An in vivo and in vitro study of the mechanism of prednisone-induced insulin resistance in healthy subjects. *J. Clin. Invest* 72, 1814-1820 (1983).
9. van Raalte, D. H. *et al.* Acute and 2-week exposure to prednisolone impair different aspects of beta-cell function in healthy men. *Eur. J Endocrinol* 162, 729-735 (2010).
10. Saad, M. J., Folli, F., Kahn, J. A. & Kahn, C. R. Modulation of insulin receptor, insulin receptor substrate-1, and phosphatidylinositol 3-kinase in liver and muscle of dexamethasone-treated rats. *J. Clin. Invest* 92, 2065-2072 (1993).
11. Severino, C. *et al.* Low-dose dexamethasone in the rat: a model to study insulin resistance. *Am. J. Physiol Endocrinol. Metab* 283, E367-E373 (2002).
12. Stojanovska, L., Rosella, G. & Proietto, J. Dexamethasone-induced increase in the rate of appearance in plasma of gut-derived glucose following an oral glucose load in rats. *Metabolism* 40, 297-301 (1991).
13. Venkatesan, N., Lim, J., Bouch, C., Marciano, D. & Davidson, M. B. Dexamethasone-induced impairment in skeletal muscle glucose transport is not reversed by inhibition of free fatty acid oxidation. *Metabolism* 45, 92-100 (1996).
14. Clee, S. M. & Attie, A. D. The genetic landscape of type 2 diabetes in mice. *Endocr. Rev.* 28, 48-83 (2007).
15. Orland, M. J. & Permutt, M. A. Genetic susceptibility to diabetes in inbred strains of mice: measurements of proinsulin mRNA and response to dexamethasone. *Diabetologia* 30, 934-939 (1987).
16. Gill, A. M., Leiter, E. H., Powell, J. G., Chapman, H. D. & Yen, T. T. Dexamethasone-induced hyperglycemia in obese Avy/a (viable yellow) female mice entails preferential induction of a hepatic estrogen sulfotransferase. *Diabetes* 43, 999-1004 (1994).
17. Gounarides, J. S. *et al.* Effect of dexamethasone on glucose tolerance and fat metabolism in a diet-induced obesity mouse model. *Endocrinology* (2007).

18. Laskewitz, A. J. *et al.* Chronic Prednisolone Treatment Reduces Hepatic Insulin Sensitivity while Perturbing the Fed-to-Fasting Transition in Mice. *Endocrinology* 15, 2171-2178 (2010).

19. Surwit, R. S., Kuhn, C. M., Cochrane, C., McCubbin, J. A. & Feinglos, M. N. Diet-induced type II diabetes in C57BL/6J mice. *Diabetes* 37, 1163-1167 (1988).

20. van Dijk, T. H. *et al.* Quantification of hepatic carbohydrate metabolism in conscious mice using serial blood and urine spots. *Anal. Biochem.* 322, 1-13 (2003).

21. Matthews, D. R. *et al.* Homeostasis model assessment: insulin resistance and beta-cell function from fasting plasma glucose and insulin concentrations in man. *Diabetologia* 28, 412-419 (1985).

22. Oosterveer, M. H. *et al.* High fat feeding induces hepatic fatty acid elongation in mice. *PLoS. One.* 4, e6066 (2009).

23. Kuipers, F. *et al.* Enterohepatic circulation in the rat. *Gastroenterology* 88, 403-411 (1985).

24. Best, J. D. *et al.* Role of glucose effectiveness in the determination of glucose tolerance. *Diabetes Care* 19, 1018-1030 (1996).

25. Ader, M., Ni, T. C. & Bergman, R. N. Glucose effectiveness assessed under dynamic and steady state conditions. Comparability of uptake versus production components. *J Clin Invest* 99, 1187-1199 (1997).

26. Pacini, G., Thomaseth, K. & Ahren, B. Contribution to glucose tolerance of insulin-independent vs. insulin-dependent mechanisms in mice. *Am J Physiol Endocrinol. Metab* 281, E693-E703 (2001).

27. Grefhorst, A. *et al.* Differential effects of pharmacological liver X receptor activation on hepatic and peripheral insulin sensitivity in lean and ob/ob mice. *Am. J Physiol Endocrinol Metab* 289, E829-E838 (2005).

28. van Dijk, T. H. *et al.* Acute inhibition of hepatic glucose-6-phosphatase does not affect gluconeogenesis but directs gluconeogenic flux toward glycogen in fasted rats. A pharmacological study with the chlorogenic acid derivative S4048. *J. Biol. Chem.* 276, 25727-25735 (2001).

29. BLIGH, E. G. & DYER, W. J. A rapid method of total lipid extraction and purification. *Can. J. Biochem. Physiol* 37, 911-917 (1959).

30. Keppler D & Decker K. Glykogen. Bestimmung mit amyloglucosidase. In: Methoden der Enzymatischen Analyse, edited by Bergmeyer HU. Weinheim, Germany: Verlag Chemie. 1089-1094. 1970. Ref Type: Generic

31. Inagaki, T. *et al.* Endocrine Regulation of the Fasting Response by PPARalpha-Mediated Induction of Fibroblast Growth Factor 21. *Cell Metab* 5, 415-425 (2007).

32. Rizza, R. A., Mandarino, L. J. & Gerich, J. E. Cortisol-induced insulin resistance in man: impaired suppression of glucose production and stimulation of glucose utilization due to a postreceptor detect of insulin action. *J. Clin. Endocrinol. Metab* 54, 131-138 (1982).

33. Okumura, S. *et al.* Effects of troglitazone on dexamethasone-induced insulin resistance in rats. *Metabolism* 47, 351-354 (1998).

34. Ruzzin, J. & Jensen, J. Contraction activates glucose uptake and glycogen synthase normally in muscles from dexamethasone-treated rats. *Am. J Physiol Endocrinol Metab* 289, E241-E250 (2005).

35. Yen, T. T., Gill, A. M., Powell, J. G. & Sampson, B. M. Ciglitazone prevents and reverses dexamethasone-induced hyperglycemia in female viable yellow mice. *Int. J Obes. Relat Metab Disord.* 16, 923-933 (1992).

36. Bernal-Mizrachi, C. *et al.* Dexamethasone induction of hypertension and diabetes is PPAR-alpha dependent in LDL receptor-null mice. *Nat. Med.* 9, 1069-1075 (2003).

37. Thomas, C. R., Turner, S. L., Jefferson, W. H. & Bailey, C. J. Prevention of dexamethasone-induced insulin resistance by metformin. *Biochem. Pharmacol.* 56, 1145-1150 (1998).

38. Buttgereit, F. *et al.* Standardised nomenclature for glucocorticoid dosages and glucocorticoid treatment

regimens: current questions and tentative answers in rheumatology. *Annals of the Rheumatic Diseases* 61, 718-722 (2002).

39. Muniyappa, R. *et al.* Comparison between surrogate indexes of insulin sensitivity/resistance and hyperinsulinemic euglycemic clamp estimates in rats. *American Journal of Physiology - Endocrinology And Metabolism* 297, E1023-E1029 (2009).

40. Katz, A. *et al.* Quantitative insulin sensitivity check index: a simple, accurate method for assessing insulin sensitivity in humans. *J. Clin Endocrinol. Metab* 85, 2402-2410 (2000).

41. Lee, H. W. *et al.* Comparison between Surrogate Indexes of Insulin Sensitivity/Resistance and Hyperinsulinemic Euglycemic Glucose Clamps in Rhesus Monkeys. *Endocrinology* 152, 414-423 (2011).

42. Hashimoto, S., Schmid, W. & Schütz, G. Transcriptional activation of the rat liver tyrosine aminotransferase gene by cAMP. *Proceedings of the National Academy of Sciences of the United States of America* 81, 6637-6641 (1984).

43. Friedman, J. E., Yun, J. S., Patel, Y. M., McGrane, M. M. & Hanson, R. W. Glucocorticoids regulate the induction of phosphoenolpyruvate carboxykinase (GTP) gene transcription during diabetes. *J. Biol. Chem.* 268, 12952-12957 (1993).

44. Imai, E. *et al.* Characterization of a complex glucocorticoid response unit in the phosphoenolpyruvate carboxykinase gene. *Mol. Cell Biol.* 10, 4712-4719 (1990).

45. Jin, J. Y., Dubois, D. C., Almon, R. R. & Jusko, W. J. Receptor/gene-mediated pharmacodynamic effects of methylprednisolone on phosphoenolpyruvate carboxykinase regulation in rat liver. *J. Pharmacol. Exp. Ther.* 309, 328-339 (2004).

46. Magnuson, M. A., She, P. & Shiota, M. Gene-altered Mice and Metabolic Flux Control. *J. Biol. Chem.* 278, 32485-32488 (2003).

47. Kharitonenkov, A. *et al.* FGF-21 as a novel metabolic regulator. *J Clin Invest* 115, 1627-1635 (2005).

48. Badman, M. K., Koester, A., Flier, J. S., Kharitonenkov, A. & Maratos-Flier, E. Fibroblast growth factor 21-deficient mice demonstrate impaired adaptation to ketosis. *Endocrinology* 150, 4931-4940 (2009).

49. Fisher, f. M. *et al.* Obesity Is a Fibroblast Growth Factor 21 (FGF21)-Resistant State. *Diabetes* 59, 2781-2789 (2010).

50. Potthoff, M. J. *et al.* FGF21 induces PGC-1alpha and regulates carbohydrate and fatty acid metabolism during the adaptive starvation response. *Proc. Natl. Acad. Sci. U. S. A* 106, 10853-10858 (2009).

51. Friedman, J. M. & Halaas, J. L. Leptin and the regulation of body weight in mammals. *Nature* 395, 763-770 (1998).

52. Sánchez-Lasheras, C., Könner, A. C. & Brüning, J. C. Integrative neurobiology of energy homeostasis-neurocircuits, signals and mediators. *Frontiers in Neuroendocrinology* 31, 4-15 (2010).

53. Denroche, H. C. *et al.* Leptin therapy reverses hyperglycemia in mice with streptozotocin-induced diabetes, independent of hepatic leptin signaling. *Diabetes* 60, 1414-1423 (2011).

54. Cohen, P. *et al.* Selective deletion of leptin receptor in neurons leads to obesity. *J Clin Invest* 108, 1113-1121 (2001).

55. Huynh, F. K. *et al.* Disruption of hepatic leptin signaling protects mice from age- and diet-related glucose intolerance. *Diabetes* 59, 3032-3040 (2010).

Supporting Information

Table s1

Formulas for calculation of blood glucose kinetics

Eq. 1	Tracer Concentration at t	$C_t = M_t \times [glc]_t$
Eq. 2	Single-pool first-order kinetics	$C_t = C_0^{el} e^{-k^{el}t} - C_0^{ab} e^{-k^{ab}t}$
Eq. 3	Bioavailability	$F = 1 - \left(\frac{C_0^{ab} \times k^{el}}{k^{ab} \times C_0^{el}} \right)$
Eq. 4	Area under the curve	$AUC = \frac{C_0^{el}}{k^{el}} - \frac{C_0^{ab}}{k^{ab}}$
Eq. 5	Metabolic clearance rate	$MCR = \frac{F \times D}{AUC}$
Eq. 6	Apparent volume of distribution	$V = \frac{MCR}{k^{el}}$
Eq. 7	Turnover rate	$Ra = MCR \times BG$
Eq. 8	Pool size	$A = \frac{Ra}{k^{el}}$

The formulas used to calculate the concentration vs. time curves and the kinetic parameters in a first order absorption process in an one-compartment model.

C_t, D-[6,6-^{2}H]glucose concentration at time point t; M_t, fractional contribution of D-[6,6-^{2}H]glucose at time point t; $[glc]_t$, blood glucose concentration at time point t. $C(0)^{ab}$, initial concentration of D-[6,6-^{2}H]glucose determined by extrapolation of the absorption period; $C(0)^{el}$, initial concentration of D-[6,6-^{2}H]glucose determined by extrapolation of the elimination period; k^{ab}, absorption rate constant; k^{el}, absorption rate constant. D, dose D-[6,6-^{2}H]glucose administrated; BG, average blood glucose concentration during the test; Ra = HGP

5

Chronic prednisolone treatment aggravates hyperglycemia in mice fed a high-fat diet but does not enforce dietary fat-induced insulin resistance

Under revision

Marie-José C. van Lierop*
Wynand Alkema*
Anke J. Laskewitz
Rein Dijkema
Hans M. van der Maaden
Martin J. Smit
Ralf Plate
Paolo G.M. Conti
Christan G.J.M. Jans
C. Marco Timmers
Stan C.A.A. van Boeckel
Scott J. Lusher
Ross McGuire
Rene C. van Schaik
Jacob de Vlieg
Ruben L. Smeets
Claudia L. Hofstra
Annemieke M.H. Boots
Marcel van Duin
Benno A. Ingelse
Willem G.E.J. Schoonen
Aldo Grefhorst
Theo H. van Dijk
Folkert Kuipers
Wim H.A. Dokter

*First two authors share first author-ship

Abstract

Glucocorticoids (GCs) such as prednisolone are potent immunosuppressive drugs but suffer from severe adverse effects, including the induction of insulin resistance due to a very broad spectrum of GC target genes. Therefore, development of so-called Selective Glucocorticoid Receptor Modulators (SGRM) is highly desirable. Here we describe a non-steroidal Glucocorticoid Receptor (GR)-selective compound (Org 214007-0) with a binding affinity to GR similar to that of prednisolone. Using various cell lines and primary human cells, we show here that Org 214007-0 acts as a partial GC agonist, since it repressed inflammatory genes and was less effective in induction of metabolic genes. More importantly, *in vivo* studies in mice indicated that Org 214007-0 retained full efficacy in acute inflammation models as well as in a chronic collagen-induced arthritis (CIA) model. Gene expression profiling of muscle tissue derived from arthritic mice showed a partial activity of Org 214007-0 at an equi-efficacious dosage of prednisolone, with an increased ratio in repression versus induction of genes. Finally, in mice Org 214007-0 did not show induced fasting glucose and a shift in the glucose / glycogen balance in the liver as seen with an equi-efficacious dose of prednisolone. All together, our data demonstrate that Org 214007-0 belongs to the new class of SGRMs with an increased therapeutic index compared to prednisolone that could contribute to effective anti-inflammatory therapy with a lower risk for metabolic side effects.

Introduction

Synthetic glucocorticoids (GCs), like prednisolone, are among the most widely prescribed anti-inflammatory drugs for diseases like rheumatoid arthritis, inflammatory bowel disease and asthma. However, prolonged and/or high dosage GC treatment is associated with severe side effects such as insulin resistance, osteoporosis, skeletal muscle wasting, mood disorders and many others [1, 2]. The wide range of side effects is not surprising giving the essential role of the natural glucocorticoid cortisol in survival. For example, cortisol has a major role in blood glucose homeostasis and is essential for induction of stress-coping mechanisms. Effects of GCs are mediated via the ubiquitously expressed glucocorticoid receptor (GR), a member of the nuclear receptor super family. The small lipophilic GC molecule diffuses across the plasma membrane and binds to cytoplasmic GR that, upon binding of its ligand, alters its conformation and translocates to the nucleus. Within the nucleus, ligand-bound GR acts as a transcription factor that regulates expression of a set of target genes directly or indirectly. Direct regulation occurs via binding of activated GR homodimers to GC-response elements (GRE) in promoter regions of genes, thereby suppressing or inducing gene expression, the latter often termed "transactivation" (TA). Indirect regulation occurs by binding of activated GR to other transcription factors, hence facilitating or suppressing the action of these transcription factors, the latter often referred to as "transrepression" (TR) [3]. It has long been thought that the anti-inflammatory activity of GCs was mainly linked to TR activity, via interference with the two most important pro-inflammatory transcription factors, *i.e.*, NFκB and AP-1 [4,5]. The induction of metabolic side effects by GCs was thought to be mainly related to TA activity via the induction of many genes encoding enzymes that are active in metabolic pathways like glucose-6-phosphatase (*G6pc*) and phosphoenolpyruvate carboxykinase (*Pck1*). Because of these two clearly separated GC mechanisms of action it has long been hypothesized that it should be possible to design a GC molecule with preserved TR actions and reduced TA effects, resulting in an improved therapeutic index [6,7,8,9]. This type of compounds has been referred to as dissociated GCs, selective GR agonists (SEGRAs), dissociated agonists of the GR (DAGRs) or selective GR modulators (SGRMs). However, selection of novel SGRMs with dissociating TA from TR activities *in vitro*, have so far only resulted in a few compounds with improved therapeutic profiles in animal models [6,10,11,12]. To date, proof of concept in human remains to be obtained.

Due to a better understanding of the molecular interactions between the ligand-bound GR and its target molecules, awareness is growing that the concept of dissociation, based solely on TA *vs*. TR, is too simplistic. For example, the anti-inflammatory activity of GCs is also partly driven by TA [3,7,13,14,15]. Furthermore, besides interference with NFκB and AP-1,

GC-bound GR also interacts with less known transcription factors involved in immune responses like IRF3, NFAT, STATs, GATA3, T-bet and CREB1 [11,16]. Of note, a recent publication indicates that a large number of genes involved in GC-induced side effects is regulated via a functional negative GRE in their promoter region [15]. Furthermore, a series of studies has shown that even subtle changes in the GR-ligand may alter conformation of the ligand-receptor complex with consequences for co-factor recruitment and hence for function of the receptor [9,17,18,19,20,21]. Many studies indeed have shown that different ligands result in differential co-activator and co-repressor recruitment by GR [12,22,23]. However, the final activity of agonists, partial agonists and antagonists is also determined by the sequence of the target-gene promoter itself [24,15] and the involvement of other components of the transcriptional machinery, such as chromatin-remodeling proteins or RNA polymerase II [9,20,15,25]. Finally, the wide array of diverse posttranslational modifications (phosphorylation, acetylation, sumoylation) of GR, as well as the interacting factors and, reversibly, the GR-mediated modulations of kinases (*e.g.*, MAP kinases) and phosphatases involved in inflammatory responses, all contribute to the final outcome of cellular activity [3].

Here we describe a novel non-steroidal, low-molecular weight GR ligand, Org 214007-0, with characteristics of a partial GR agonist *in vitro* that shows sustained full anti-inflammatory activity *in vivo* in mice, without adverse effects on hepatic glucose metabolism.

Materials and Methods

Glucocorticoid receptor binding assay

The glucocorticoid receptor (GR) fluorescence polarisation (FP) binding assay was performed using the commercially available kit from Panvera (Glucocorticoid receptor competitor assay, Green Cat# P2816) (for more detailed information see SI text).

Assay in U2OS cells

To determine the repressive activity of GR ligands, cell line U2OS GR.G9, the human osteoblastic cell line U2OS, stably transfected with human GR, was used. Cells (10^4 cells/well) were incubated in 384-wells plates, in the presence of 50 ng/ml TNFα (R&D systems) / 100 ng/ml IFNγ (Peprotech) and compound, for 18 hours. Hereafter, a mixture of two different antibodies to hMCP-1, one Eu-labeled and one APC-labeled, were added. One hour later the time-resolved fluorometric resonance energy transfer (TR-FRET) signal was measured (for more detailed information see SI text).

Assay in CHO cells

For monitoring both human steroid receptor agonistic as well as antagonistic activity of compounds, Chinese hamster ovary (CHO) K1 cells stably co-transfected with the specific human steroid receptor and its respective reporter construct were used (as previously described [45]).

For human glucocorticoid receptor (GR)-specific activity CHO-GR B4.8 cells containing both recombinant human GR as well as a reporter construct consisting of the mouse mammary tumor virus (MMTV) promotor and the luciferase reporter gene, were used. Compound was incubated alone (in the agonistic setup) or with 50 nM dexamethasone (in the antagonistic setup) overnight. Hereafter, 200 µl medium was removed and 50 µl luciferine substrate solution from the LucLite luminescence kit (Packard, Meriden, USA) was added. After 10 minutes luminescence of each sample was counted and percentage maximal agonistic efficacy was related to the maximal efficacy of prednisolone. Percentage maximal antagonistic efficacy was related to the maximal antagonistic efficacy of reference GR antagonist Org 34116. Similar procedures were followed for the other human steroid receptor assays (for more detailed information see SI text).

Gene expression profiling in HepG2 cells

HepG2-8/97-WS.5 cells, deprived from serum for 18 hours, were stimulated with glucocorticoid and 0.5 mM cAMP for 6 hours. RNA was isolated and used for double stranded cDNA synthesis using the One-Cycle Target Labeling Kit (Affymetrix Santa Clara, CA). This cDNA was used as a template for the preparation of biotin-labeled cRNA using the GeneChip IVT Labeling Kit (Affymetrix Santa Clara, CA). Biotin-labeled cRNA was fragmented and hybridized at 45°C for 16-17 hours to the Human Genome U133A 2.0 Array or the Human Genome U133 Plus 2.0 Array (Affymetrix, Santa Clara, CA) (for more detailed information see SI text). Arrays were stained with phycoerythrin-streptavidin conjugate (Molecular Probes, Eugene, OR), and the signals were amplified by staining the array with biotin-labeled anti-streptavidin antibody (Vector Laboratories, Burlingame, CA) followed by phycoerythrin-streptavidin. The arrays were laser scanned with a GeneChip Scanner 3000 6G (Affymetrix, Santa Clara, CA) according to the manufacturer's instructions. Data was saved as raw image file and quantified using GCOS (Affymetrix).

For Q-PCR, cDNA was synthesized and diluted 125 times in milliQ and 5 µL was added to 12.5 µL of SYBR green mix (Applied Biosystems cat. No. 4309155) , 2.5 µL of each primer (~20 ng/µl) and 2.5 µL of milliQ. The following primer-pairs were used: for GAPDH: 5'-CCACATCGCTCAGACACCAT-3' and 5'-CCAGGCGCCCAATACG-3'; for PEPCK: 5'-TCCCATTGAAGGCATTATCTTTG-3' and 5'-GCCAGCTGAGAGCTTCATAGACT-3'; for TAT: 5'-TACAGAC-

CCTGAAGTTACCCAG-3' and 5'-TAAGAAGCAATCTCCTCCCGA-3'; for G6Pase: 5'-TGCTGCT-CAAGGGACTG-3' and 5'-GAATGGGAGCCACTTGCTG-3'. Quantitative PCR was performed on an ABI7900HT real time thermo cycler (Applied Biosystems) and results were analyzed by SDS2.1 software (for more detailied information in SI text).

Gene expression profiling in THP-1 cells

THP-1 cells were incubated with glucocorticoid in the presence of either DMSO (control) or IFNγ/TNFα (220ng/ml / 375 ng/ml). After 6 hours total RNA was isolated and further processed for micro-array hybridization as described before for the HepG2 cells. Expression of FKBP51, DUSP1 and GILZ was confirmed by Q-PCR according to the same procedure as described for the HepG2 cells. In this case THP1 cells were stimulated with 40 ng/ml IFNγ and 60 ng/ml TNFα and a whole dose range of prednisolone and Org 214007-0 was tested. Besides the GAPDH primers (described above) the following primer-pairs were used: for FKBP51: 5'-AAAAGGCCAAGGAGCACAAC-3' and 5'-TTGAGGAGGGGCC-GAGTTC-3'; for DUSP1: 5'-GTACATCAAGTCCATCTGAC-3' and 5'-GGTTCTTCTAGGAGTAGA-CA-3'; for GILZ: 5'-AGTGCCTCCGGAGCCAGC-3' and 5'-ATGATTCTTCACCAGATCC-3'. Expression of MCP-1, IL-6 and IL-8 was measured by specific AlphaLISAs (PerkingElmer; #AL244C [MCP-1], #AL223C [IL-6] and #AL224C [IL-8]) according to the manufacturer manual. (for more detailed information see SI text)

ChIP-SEQ analysis

From the THP1 samples that were used for gene expression analysis after 6 hours, samples were drawn after 1 hour and used for ChIP – Seq analysis at Genpathway (Carlsbad, CA). For precipitation of genomic DNA regions antibody against GR (Santa Cruz sc-8992) was used. Details are provided in SI Text. The obtained amplified DNA libraries were sent to Illumina Sequencing Services (San Diego, CA) for sequencing on a Genome Analyzer II. Sequence files were analyzed with the Genomatix Genome Analyzer Workbench from Genomatix (Genomatix Software GmbH, Munich). Sequences were clustered using default parameter settings and aligned against the human genome version GRCh37/hg19. Clusters from the three conditions, DMSO, Prednisolone and Org 214007-0 treated THP-1 were merged using the Replicate Analysis module from the Workbench package. In short, this results in a file with chromosomal coordinates with new merged clusters for each position in which a cluster is found for one or more conditions. For each of these merged clusters, the reads and normalized enrichment for each of the conditions is given. Additionally, for each merged clusters P-values for each pairwise comparison of the three conditions were also calculated.

Human whole blood LPS- or PMA/anti-CD28-induced cytokine release

Peripheral blood from healthy volunteers was collected into lithium heparinised tubes, diluted with RPMI 1640 medium (without phenol red) (Gibco BRL) and used within 3 hours after collection. Diluted blood (final dilution 5x) was pre-incubated in cell culture 96-wells flat-bottom plates (Nunc) together with compound for 1 hour and further incubated with 1 µg/ml Lipopolysaccharide (E. coli serotype 0111:B4, Sigma) or 100 ng/ml phorbol 12-myristate 13-acetate (PMA, Sigma) / 100 ng/ml mouse anti-human CD28 antibody (Sanquin, The Netherlands) for 24 hours in an incubator at 37°C, 6% CO2 and 95% humidity. Hereafter, supernatant was carefully collected and tested at the most optimal dilution (predetermined by a titration study on control samples) in a human TNFα-specific ELISA (for the LPS stimulated samples) or in a human IL-5-specific or human G-CSF-specific ELISA (for the PMA / anti-CD28 stimulated samples) (Duoset, R&D systems USA).

Animals

All animal procedures and experiments received ethics approval and were according to the recognized guidelines. Female Balb/c mice (Charles River, Sulzfeld, Germany), male C57BL/6J OlaHsd (Harlan, Zeist, the Netherlands) and male DBA/1J/BOM mice (Bomholtgard, Ry, Denmark) were group-housed under controlled conditions with a constant temperature (19–21°C), a 12-h light/dark cycle and *ad libitum* access to water and standard laboratory chow pellets. For MIDA analysis, C57Bl6 mice were equipped with a permanent right jugular vein catheter afterwhich mice were allowed to recover.

Acute inflammation mouse models

For both the LPS-induced TNFα as well as the anti-CD3 induced IL-2 model, female Balb/c mice of 8-12 week old were used. Mice were treated orally with 0.2 ml compound or vehicle (water / mannitol (5%) with 5% DMSO / 5% chremophore for the LPS model or with 0.5% gelatine for the anti-CD3 model). One hour after oral treatment animals were challenged i.p. with 0.2 ml of either 20µg/mouse LPS (Sigma, E. coli serotype 055:B5) or 5 µg/mouse hamster anti-CD3 monoclonal (BD Biosciences Pharmingen, art. nr. 553057, clone 145-2C11). Ninety minutes after LPS injection or 3 hours after anti-CD3 challenge, blood samples were collected and serum levels of TNFα or IL-2 were determined via specific ELISAs (BD Biosciences Pharmingen, San Diego, CA, USA). In the experiment that included treatment with RU486 to block GR, mice were dosed subcutaneously with 50 mg/kg RU486 30 minutes before the oral compound dosing. ED50 and % efficacy (maximal percentage inhibition of TNFα or IL-2 release) are determined using a 3 parameter sigmoidal curve calculation. Statistical analysis of the results was performed using an one-way ANOVA (log) test.

Mouse CIA model

The experiment was essentially performed as described previously [46]. At day 0 mice were immunized at the base of the tail with 100µg bovine type II collagen (UMC Nijmegen, The Netherlands) in Complete Freund's Adjuvant (CFA, Difco) enriched with 2 mg/ml *Mycobacterium tuberculosis* H37RA (Difco). At day 21 mice were boosted by an i.p. injection of 100 µg bovine type II collagen dissolved in saline. After disease onset, mice with an arthritis score ranging from 0.25 to 1.25 were divided into matched groups (n=12). Animals were orally treated once daily with vehicle (0.5% gelatin / 5% mannitol in water) or compound for 21 to 23 days. The clinical severity of arthritis (arthritis score) was graded and scored as described [47]. To assess the effects of treatments, the area under the curve (AUC) of arthritis score (subtracting baseline AUC of arthritis score on day 0) was used. One day after the final treatment animals were sacrificed and the knee and ankle joints were imaged using a Faxitron X-ray, Modl MX-20 digital imaging system and analysed using Specimen (Version 2.0.1). The bone destruction was scored on a scale of 0-5 as described previously [47]. The cumulative scores of 2 joints (right ankle and knee) were used as radiological scores. From H&H-stained sections, articular cartilage destruction and inflammatory infiltrate in the right knee joint were scored on a scale of 0 – 3. The whole study was carried out in a blinded fashion. Statistical analysis was performed using one-way ANOVA.

Micro array on muscle tissue mRNA from mice

Two and a half hours after the final treatment animals were sacrificed and samples were collected from the thigh muscle (*musculus tensor fasciae latae* and *musculus rectus femoris*). Samples were stored immediately at -80 ºC and send to Covance (Princeton, New Jersey) for RNA extraction and subsequent analysis of gene expression on the Mouse Genome 430A 2.0 array. For statistical analysis, the .CEL files obtained after hybridization were analyzed with the R (www.r-project.org) and the BioConductor software package (www.bioconductor.org) as described previously [35]. Normalization was done using gcrma. Building of the experimental design and calculation of the ratios was done with the limma package. Differentially expressed probe sets were selected on basis of the fold change and the adjusted p-value (Benjamini-Hochberg correction). Multivariate data analysis and clustering was done with standard methods in the R software package (www.r-project.org).

Mouse fasting glucose and MIDA model for liver glucose metabolism

For fasting blood glucose levels, male C57Bl/6J OlaHSD mice (n=8 per group, ~25 g) were treated daily by oral gavage for 28 days with either prednisolone (1.5 or 10 mg/kg/day), an equipotent dose of Org 214007-0 (0.17 or 0.5 mg/kg/day), vehicle (0.5% gelatin / 5%

mannitol in water) or no treatment as a stress control. Eighteen hours after the last oral treatment and 9 hours after start of starvation, blood samples were taken from the tail vein and directly used for glucose measurements using "One touch Ultra" glucose meter from Lifescan EuroFlash (Lifescan Benelux Beerse, Belgium). The mouse MIDA study was performed as described previously by van Dijk *et al.* [40,48]. Briefly, individually housed C57Bl/6J mice (n=8) were treated orally with prednisolone (10 mg/kg/day), Org 214007-0 (0.5 mg/kg/day) or vehicle (0.5% gelatin / 5% mannitol in water) daily for 7 days. On the third day, mice were cannulated in the right jugular vein. After 7 days of treatment, mice were placed in small Plexiglas cages, which allowed collection of blood samples frequently in freely moving mice. Twenty four hours after the final dose and after a 9 hours starving period, a tail vein blood sample was used for a glucose measurement after which mice were shortly anesthetized to attach the infusion lines before the experiment. Filter paper was placed under the wired floor cages to collect urine samples and replaced hourly. Mice received an infusion of a sterilized aqueous solution containing [U-^{13}C]glucose (13 µmol/ml), [2-^{13}C]glycerol (160 µmol/ml), [1-^{2}H]galactose (33 µmol/ml) and paracetamol (1 mg/ml) at a rate of 0.54 ml/hr for 6 hours. During the experiment blood glucose was measured and blood spots for GC-MS measurements were collected from tail tips just before the start of the infusion and at hourly intervals. Blood spots and urine filter papers were air-dried and stored at room temperature until analysis. Glucose and paracetamol-glucuronic acid (Par-GLcUa) were extracted from blood spot and urine filter papers, respectively, derivatised, and measured by GC-MS, essentially as described previously [40,48]. The fractional isotopomer distribution according to GC-MS was corrected for fractional distribution due to the natural abundance of ^{13}C by multiple linear regression to obtain the excess mole fraction of mass isotopomers M_0-M_6 due to incorporation of infused labeled carbohydrates. From isotope dilution and infusion rates, the flux rates of the following metabolic pathways could be calculated: 1) *de novo* synthesis of G6P, 2) glucokinase, 3) glucose-6-phosphatase, 4) glycogenolysis, and 5) glycogen synthesis. The method of calculation was performed as described before [40,48,49].

Results

In vitro studies

Org 214007-0, [(-)-N-(2S,10S,14bS)]-N-(8-cyano-1,2,3,4,10,14b-hexahydro-10-methyl dibenzo *[c,f]*pyrido[1,2-*a*]azepin-2-yl)-4-methyl-1,2,3-thiadiazole-5-carboxamide], the structure of which is shown in Figure 1, has a molecular weight of 430 g/mole ($C_{24}H_{23}N_5OS$). Synthesis of Org 214007-0 was performed as described elsewhere [26]. Org 214007-0 was found to bind to GR as efficient as prednisolone (Ki of 2.2 nM *vs.* 3.8 nM for prednisolone) (Table 1, row A). In spite of this, in comparison to prednisolone, Org 214007-0 showed a

Figure 1

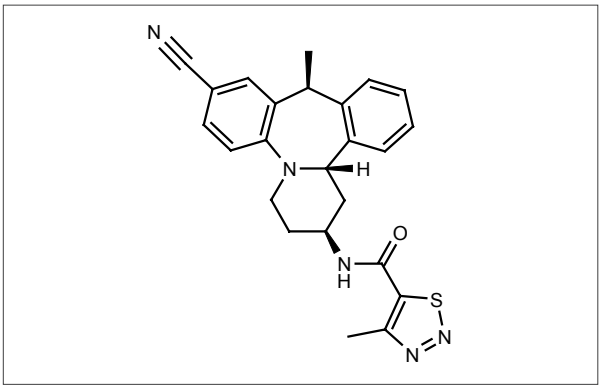

The structure of ORG 214007-0.

This compound,

[(-)-N-(2S,10S,14bS)]-N-(8-cyano-1,2,3,4,10,14b-hexahydro-10-methyl dibenzo*[c,f]*pyrido[1,2-*a*]azepin-2-yl)-4-methyl-1,2,3-thiadiazole-5-carboxamide]

has a molecular weight of 430 g/mole ($C_{24}H_{23}N_5OS$)

stronger potency (5-fold lower EC50), but a clearly lower efficacy (34%, agonistic mode) in GRE-mediated induction of gene expression in a human GR transfected cell line (CHO) (Table 1, row B), indicative for a partial GR agonistic activity. GR-selectivity of Org 214007-0 was shown by the absence of any detectable agonistic activity for other human steroid receptors. Org 214007-0 only possessed minor antagonistic activity for the human progestagen (B) and mineralocorticoid receptor (data in SI Table S1).

To investigate whether in comparison to prednisolone the partial activity of Org 214007-0 would be sustained in cells that express endogenous GR, the human hepatocyte cell line HepG2 was used. Instead of focusing on a limited set of genes the genome-wide effect of both GCs was investigated by micro-array analysis on total mRNA from these cells. As shown in Table 1, row C, Org 214007-0 was found to induce expression of a much lower number of genes than prednisolone did. The genes regulated by Org 214007-0 represent a subset of the genes regulated by prednisolone, confirming partial agonistic activity of Org 214007-0 in these cells. For a few genes, *i.e.*, tyrosine aminotransferase (TAT), glucose 6-phosphatase (G6Pase) and phosphoenolpyruvate carboxykinase (PEPCK, *Pck1*), the partial induction by Org 214007-0 in comparison to prednisolone was confirmed for a whole dose-range of the compounds using Q-PCR (Fig. S1).

The anti-inflammatory activity of Org 214007-0 in comparison to predisolone was quantified in a stably human GR transfected cell line (U2OS) stimulated to elicit an inflammatory response. Org 214007-0 was shown to inhibit this response with a potency comparable to that of prednisolone, while its efficacy was somewhat less compared to prednisolone (81%) (Table 1, row D). To determine in one cell system both activities, *i.e.* the induction of gene expression as well as the repression of gene expression under an inflammatory condition, Org 214007-0 and prednisolone were tested in the human monocytic THP1 cell line. The set of genes induced was defined as genes that were up-regulated at least 2-fold

by either compound compared to vehicle in the non-triggered cells. The set of repressed genes was defined as genes that were up-regulated at least 2-fold by the inflammatory stimulus and subsequently down-regulated at least 2-fold by either prednisolone or Org 214007-0. For both sets, the numbers of genes regulated by Org 214007-0 were much

Table 1

	Cells / Assay	Stimulus	Read-out	Parameter		PRED	ORG 214007-0
A	**GR-binding**	-	competitive binding	Ki	nM	3.8 (± 0.8)	2.2 (± 1.3)
B	**CHO-ind**	-	MMTV-luc	EC50 Max. eff.	nM %	26.2 (± 7.5) 100	5.1 (± 1.6) 32 (± 8.1)
C	**HepG2-ind**	-	micro-array	regulated genes	n	310	106
D	**U2OS- rep**	IFNγ/TNFα	MCP-1	IC50 Max. eff.	nM %	0.74 (± 2.3) 100 (± 9.6)	0.36 (± 0.19) 81 (± 16)
E	**THP-1**	-	micro-array	up-regulated	n	166	8
		IFNγ/TNFα	micro-array	down-regulated	n	120	4
F	**THP-1- rep**	IFNγ/TNFα	MCP-1	IC50 Max. eff.	nM %	69.9 (± 30.4) 100	23.5 (± 9.3) 44 (± 8)
			IL-6	IC50 Max. eff.	nM %	34.1 (± 6.6) 100	9.3 (± 2.1) 78 (± 9)
			IL-8	IC50 Max. eff.	nM %	36.9 (± 11.3) 100	11.0 (± 3.1) 74 (± 10)
G	**THP-1 - ind**	-	FKBP51	EC50 Max. eff.	nM %	65.8 (± 22.4) 100	8.0 (± 5.3) 42 (± 8)
			GILZ	EC50 Max. eff.	nM %	60.2 (± 19.6) 100	13.7 (± 11.8) 13 (± 5)
			DUSP1	EC50 Max. eff.	nM %	67.4 (± 8.4) 100	6.4 (± 4.1) 41 (± 6)
H	**hWB - rep**	LPS	TNFα	IC50 Max. eff.	nM %	27 (± 5.7) 100	50 (± 19) 68 (± 8.7)
		PMA/CD28	IL-5	IC50	nM	6.76 (± 1.5)	14.45 (± 3.2)
				Max. eff.	%	100	64 (± 11)
	- ind	PMA/CD28	G-CSF	EC50 Max. eff.	nM %	67.61 (± 3.8) 100	186.2 (± 63) 39 (± 7.8)
I	**CASM3C -rep**	IL1/IFNγ/ TNFα	MCP-1	Max. eff.	%	100	98
	-ind	-	SAA	Max. eff.	%	100	58
J	**HDF3CGF -rep**	IL1/IFNγ/ TNFα	MMP-1	Max. eff.	%	100	120
	-ind	-	PAI-1	Max. eff.	%	100	55

Prednisolone (PRED) and Org 214007-0 *in vitro* studies , for legend see next page.

lower than those regulated by prednisolone as shown in Table 1, row E. In both cases, all genes that were regulated by Org 214007-0 were also regulated by prednisolone. Shown in Figure 2A are the gene sets ranked on basis of the magnitude of up- or down-regulation by prednisolone. The top 30 genes from each set were used for further comparison. These data show that, in this cell system, Org 214007-0 possesses on average a two-fold lower gene repression activity and an eight-fold lower gene induction activity than prednisolone does. To illustrate this, examples of one gene induced (FKBP51) and one gene repressed (CCL8) are shown in Figure 2B. For a small selection of genes, these differences in expression levels were confirmed, comparing a whole dose range of Org 214007-0 and prednisolone by either Q-PCR (FKBP51, GILZ and DUSP) or by specific AlphaLISAs (MCP1, IL6 and IL8) (Table 1, rows F and G). This data shows that Org 214007-0, in comparison to prednisolone, has a preference for repressing gene expression rather than activating gene expression.

In order to define in more detail the molecular mechanism that underlies the differential effects of Org 214007-0 compared to prednisolone on gene expression, we performed ChIP-Seq analysis on DNA from these THP-1 cells. Compared to vehicle, the numbers of clusters found for Org 214007-0 versus prednisolone under the non-stimulated condition were 2080 *vs.* 9413, respectively. An example of these clusters in the FKBP51 gene is shown in Figure 3B. Under the inflammatory condition, the numbers of clusters were

Legend Table 1

Prednisolone (PRED) and Org 214007-0 *in vitro* studies

A) *GR binding*: binding to recombinant human glucocorticoid receptor (GR) assessed by a fluorescence polarization competitor binding assay. Ki = inhibition constant or concentration of compound in the competitive binding assay which would occupy 50% of GR if no ligand was present. B) *CHO – ind*: Induction of gene expression measured in CHO cells stably co-transfected with human GR and a MMTV promoter – luciferase construct. C) *HepG2 – ind*: Induction of gene expression measured by micro-array analysis of mRNA isolated from HepG2 cells incubated with either 1 µM prednisolone or 1 µM Org 214007-0; n= number of genes that were up-regulated at least 2-fold in comparison to cells incubated with vehicle only. D) *U2OS – rep*: Repression of gene expression in U2OS cells overexpressing human GR. INFγ/TNFα - MCP-1 = IFNγ (100 ng/ml) / TNFα (50 ng/ml) induced MCP-1 release. E) *THP-1*: Micro-array analysis of mRNA isolated from THP-1 cells incubated for 6 hours with either 1 µM prednisolone or 1 µM Org 214007-0 without or with IFNγ (220 ng/ml) / TNFα (374 ng/ml) (=IFNγ/TNFα), n= number of genes that were up-regulated at least 2-fold in comparison to cells incubated with vehicle only or number of genes that were up-regulated at least 2-fold by INFγ/TNFα and at least 2-fold down-regulated by either prednisolone or Org 214007-0. F) *THP-1 – rep:* Repression of gene expression in THP-1 cells. INFγ/TNFα – MCP-1, IL-6, IL-8 = TNFα (60 ng/ml) / IFNγ (40 ng/ml) induced MCP-1, IL-6 or IL-8 release. G) *THP-1 – ind:* Induction of FK506 binding protein 51 (FKBP51), glucocorticoid induced leucine zipper (GILZ) and dual specificity phosphatase 1 (DUSP1) in THP-1 cells. H) *hWB - rep:* Inhibition of LPS-induced TNFα release or PMA / anti-CD28 induced IL-5 release by primary human whole blood cells and *hWB – ind:* enhancement of PMA / anti-CD28 / compound induced G-CSF release by primary human whole blood cells. I) *CASM3C – rep*: Inhibition of MCP-1 release of coronary artery smooth muscle cells stimulated with a cytokine mixture of IL-1β (1 ng/ml), TFNα (5 ng/ml) and IFNγ (100 ng/ml) (=CASM3C) by 1 µM prednisolone or 1 µM Org 214007-0. *CASM3C – ind*: Induction of serum amyloid A (SAA) of the cells mentioned above by 1 µM prednisolone or 1 µM Org 214007-0. J) *HDF3CGF – rep*: inhibition of matrix metalloproteinase (MMP-1) release of human neonatal foreskin fibroblasts stimulated with the cytokine mixture mentioned above plus required growth factors (=HDF3CGF). *HDF3CGF – ind*: Activation of plasminogen activator inhibitor-1 (PAI-1) by cells mentioned above by 1 µM prednisolone or 1 µM Org 214007-0.

IC50 or EC50 values represent the mean concentration of compound (±SD) required to resp. inhibit or effect the response to 50%. Maximal efficacy (Max. eff.) is expressed as the mean relative maximal effect (±SD) compared to the maximal effect by prednisolone (set at 100%). All assays (except for the micro array experiments) are performed at least two times.

Figure 2

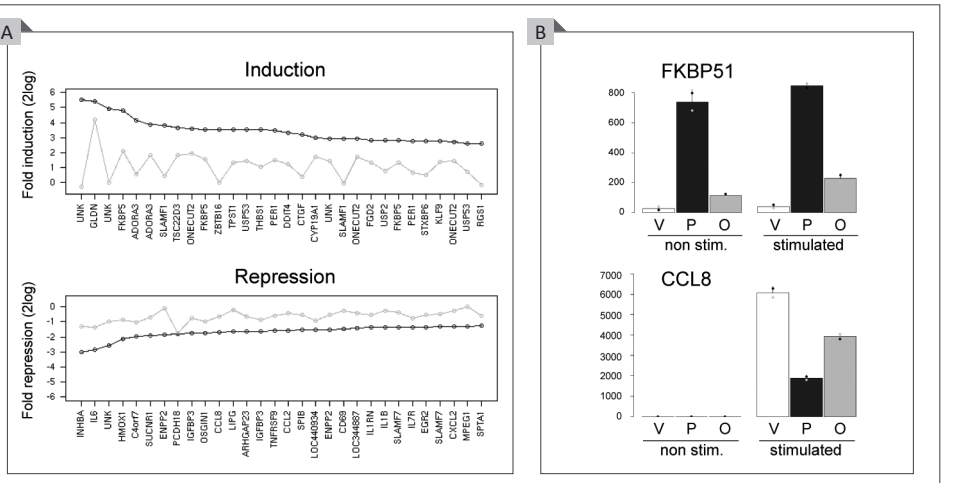

Org 214007-0 has a relatively lower impact on induction than on respression of genes in THP-1 cells as measured by micro-array analysis.

A, Fold changes for the top 30 induced genes (upper figure) and repressed genes (bottom figure) by prednisolone (black) and Org 214007-0 (grey). NB. Scales are in 2log. **B**, Example of an induced gene, FK506 binding protein 51 (FKBP51, top) and a repressed gene, chemokine [C-C motif] ligand 8 (CCL8, bottom) by prednisolone (black bars) and Org 214007-0 (grey bars) in comparison to the vehicle control (white bars) under either non-stimulated (left part, control) or stimulated (right part, IFNγ/TNFα) condition.

2502 *vs.* 3471. So, under both conditions, Org 214007-0, causes less binding of GR to the DNA than prednisolone does. Comparison of the set of 2080 putative binding sites of Org 214007-0 with the 9413 binding sites of prednisolone showed that 99.5 % of the binding sites in the Org 214007-0 set were also contained within the prednisolone set, indicating that Org 214007-0 is a genuine GC that does not lead to binding of GR on sites that are not targeted by prednisolone. This is in close agreement with the micro-array data in which a similar large overlap was shown between the 2 gene sets. The ratio of the read count for clusters induced by prednisolone or Org 214007-0 is shown in Figure 3A as a histogram. Clearly, most clusters have a ratio greater than 0, indicating that prednisolone leads to more GR occupancy than Org 214007-0.

The activity of Org 214007-0 in cell lines needed to be confirmed in human primary cells. The effect of Org 214007-0 was tested on the cytokine release of primary human whole blood cells treated with either LPS or anti-CD28/PMA. As depicted in Table 1, row H, under all conditions the EC50 values for the inhibitions by Org 214007-0 were more or less comparable to those of prednisolone, while on maximal efficacies Org 214007-0 again showed partial activities in comparison to prednisolone (additional data shown in SI Table S2). In addition, Org 214007-0 and prednisolone were compared in some of the Biologically Multiplexed Activity Profiling (BioMAP) assays at BioSeek, Inc. (Burlingame, CA, USA). These

Figure 3

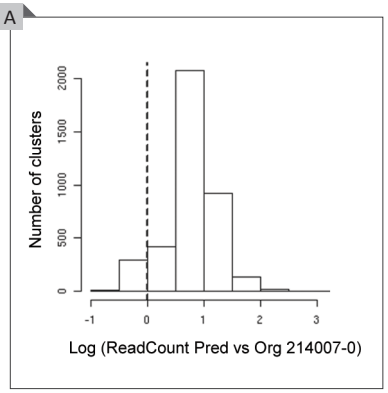

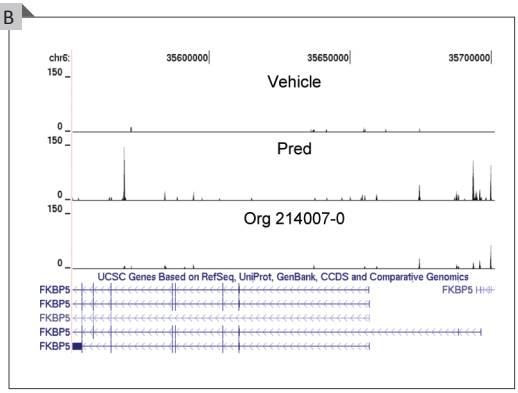

GR binding profile of Org 214007-0

A, Ratio of the read count for clusters induced by prednisolone or Org 214007-0. If Org 214007-0 and prednisolone would induce an equal number of reads, the histogram would be centered on 0, indicated by the dotted line. There is a clear shift to the right from this line (P-value (mean = 0) <0.000001), indicating that prednisolone leads to more GR occupancy than Org 214007-0. **B**, Example profile of the tag clusters in the GR response gene FKBP51. Multiple binding sites are found within this gene, each showing denser clusters after treatment with prednisolone than after treatment with Org 214007-0.

assays make use of different types of primary human cells, in this case coronary artery smooth muscle cells and neonatal foreskin fibroblasts, in an inflammatory environment [27, 28]. As can be seen in Table 1, rows I and J, Org 214007-0 showed full efficacies in the two cell systems, *i.e.*, 98% and 120% repression of MCP1 (*Ccl2*) and MMP1, respectively. Also in these cells, partial induction of protein expression by Org 214007-0 in comparison to prednisolone was observed, *i.e.* 58% for serum amyloid A and 55% for plasminogen activator inhibitor-1. Consistently, these data in primary human cells show a relatively stronger impact of Org 214007-0 on repression versus induction of gene expression.

In vivo studies

To evaluate how the *in vitro* profile of Org 214007-0 would translate *in vivo* with regard to both anti-inflammatory efficacy and induction of side effects, the compound was tested head-to-head to prednisolone in different *in vivo* models. Since pharmacokinetic studies in mice showed good oral bio-availability of Org 214007-0 and prednisolone (data in SI table S3), both compounds were dosed orally in all preclinical mouse models. Firstly, Org 214007-0 was tested in an acute inflammation model for its potency to inhibit the LPS-induced raise in serum TNFα. As can be seen in Figure 4A, the potency of Org 214007-0 in this model was stronger than that of prednisolone (ED50 0.5 mg/kg *vs*. 1 mg/kg). Surprisingly, and in contrast to its *in vitro* repression efficacy on LPS-induced TNFα, the maximal efficacy of Org 214007-0 in this model was as good as that of prednisolone, reaching a

90% inhibition of the LPS-induced TNFα release. Administration of GR antagonist RU486 (mifepristone) to the mice just prior to oral treatment with either Org 214007-0 or prednisolone fully antagonized this inhibition (Fig. S2), confirming that inhibition of the TNFα response was indeed mediated via GR. The effect of Org 214007-0 was also tested in a T-cell-driven inflammation model using anti-CD3-induced IL-2 release as readout. As can be seen in Figure 4B, Org 214007-0 dose-dependently reduced the anti-CD3 induced IL-2 serum levels with a similar efficacy as prednisolone (75% inhibition) but with a stronger potency than prednisolone (ED50 0.3 mg/kg *vs.* ca. 10 mg/kg). This again indicates that,

Figure 4

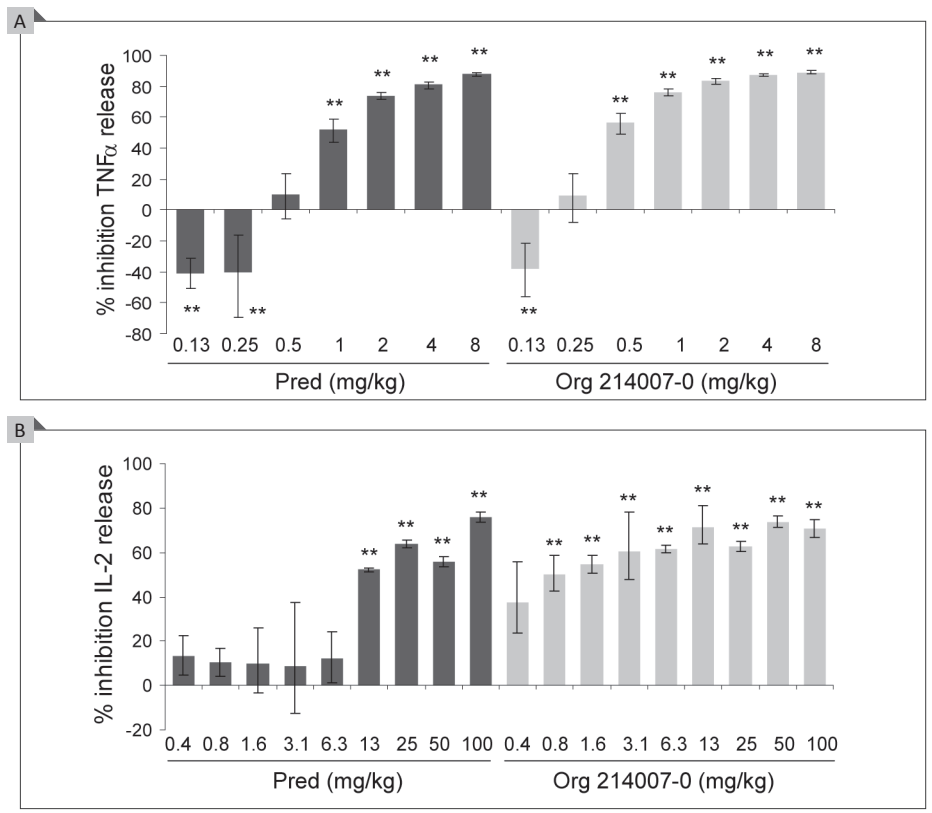

Inhibitory properties of Org 214007-0 on TNFα and IL-2 secretion

A, Org 214007-0 and prednisolone are equally effective in inhibiting acute inflammation in the LPS-induced TNFα mouse model. Mean percentage inhibition (of each group of n=8) (± SEM) of the LPS-induced TNFα release by the vehicle treated group is shown (no TNFα is detectable without LPS injection). ** = significantly different from placebo ($p < 0.01$; ANOVA-test). **B** Org 214007-0 and prednisolone are equally effective in inhibiting acute T cell-driven inflammation in the anti-CD3-induced IL-2 mouse model, although Org 214007-0 shows a more potent activity in this model. Mean percentage inhibition (of each group of n=2) (± SEM) of the anti-CD3-induced IL-2 release relative to a positive control group (treated with 10 mg/kg A420983, a pan-SRC inhibitor from Abbott) (set at 100%) is shown (no IL-2 is detectable without anti-CD3 injection). ** = significantly different from placebo ($p < 0.01$; ANOVA-test).

although Org 214007-0 behaves as a true partial GR agonist *in vitro*, it shows full anti-inflammatory activity as good as prednisolone *in vivo*.

We next tested the efficacy of the compound in a more relevant chronic disease model in which the classical glucocorticoids have proven efficacy. The murine collagen-induced arthritis (CIA) model is a well-accepted model of human rheumatoid arthritis, encompassing inflammation of synovial joints, destruction of cartilage and bone erosion. Org 214007-0 and prednisolone were dosed once daily orally during 3 weeks in a therapeutic manner, *i.e.*, treatment started when disease was already established. Both prednisolone and Org 214007-0 caused a dose-dependent reduction of the disease score (Fig. 5A). Org 214007-0 was found to be about 3-fold more potent than prednisolone in this model, leading to a total suppression of the disease symptoms at a dose of 1.5 mg/kg/day. Besides the clinical score of the paws, the two highest doses of Org 214007-0 (0.5 and 1.5 mg/kg/day) also showed a significant reduction in bone damage as determined by X-ray on knees and paws at the end of the study (Fig. 5B). Finally, histopathologic examination of the inflamed knee joints also showed a significant reduction of inflammatory infiltrates, cartilage destruction and bone apposition in mice treated with the two highest doses of Org 214007-0 (Fig. S3). Altogether these results demonstrate that the anti-inflammatory *in vivo* efficacy of Org 214007-0 is as good as or even better than that of prednisolone.

Figure 5

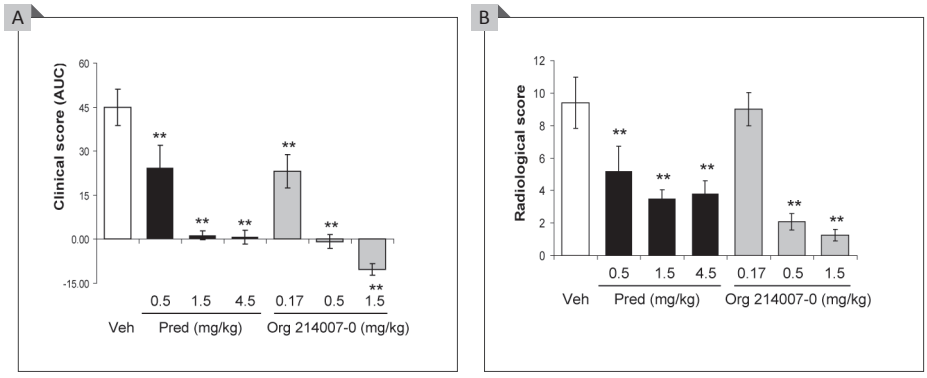

Arthritis reducing properties of Org 214007-0

A, Org 214007-0 is equally effective as prednisolone in inhibiting arthritis in CIA model. Mean clinical score of each group (n=12), shown as area under the curve (AUC) of the arthritis score monitored every other day during 3 weeks, corrected for baseline, is indicated (± SEM). ** = significantly different from placebo ($p < 0.01$; ANOVA-test). **B**, Org 214007-0 significantly reduces bone destruction at 0.5 and 1.5 mg/kg in the CIA model as measured by X-ray. Mean radiological score (sum of the X-ray scores of left and right hindpaws and knees) of each group of mice (n=12) at the end of the CIA experiment is indicated (± SEM). ** = significantly different from placebo ($p < 0.01$; ANOVA-test).

Figure 6

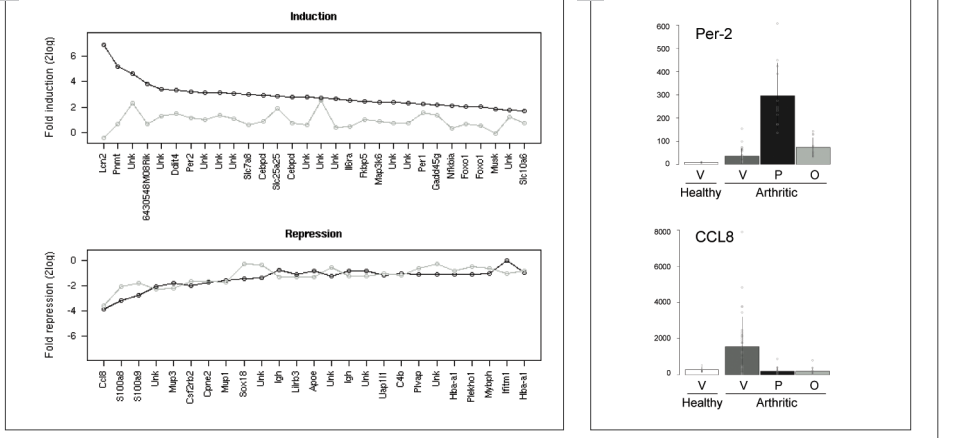

Org 214007-0 has a relatively lower impact on induction of genes as measured by micro-array analysis on muscle tissue mRNA from CIA mice.

A, Fold changes for the top 30 induced genes (upper figure) and 25 repressed genes (bottom figure) by prednisolone (black) and Org 214007-0 (grey). NB. Scales are in 2log. **B,** Examples of an induced gene (Per-2, top) and a repressed gene (CCL8) regulated in CIA mice treated with prednisolone (P) or Org 214007-0 (O) in comparison to the vehicle treated CIA mice (V) and naïve healthy mice (V, white bars)

In the same chronic disease model we wanted to test whether the partial activity of Org 214007-0 on induction of gene expression, as observed *in vitro*, would be conserved *in vivo*. For this purpose, muscle tissue was collected from arthritic mice that were treated for 3 weeks with either vehicle only or with dosages of Org 214007-0 and prednisolone that were equally effective in inhibiting arthritis. Besides these groups of mice, one group of healthy mice was included. Collected tissue was used to isolate mRNA for microarray analysis. All genes that were at least 2-fold up-regulated by the disease induction (vehicle treated arthritic *vs.* healthy mice) and that were down-regulated at least 2-fold by either Org 214007-0 or prednisolone are shown in Figure 6A (bottom). Among the genes are some well-known inflammatory markers as *S100A8*, *S100A9* and *Ccl8*, the latter shown as an example in Figure 6B (bottom). Genes that were at least 2-fold up-regulated by either Org 214007-0 or prednisolone in comparison to vehicle treated mice are shown in Figure 6A (upper part). Among these genes are, *a.o.*, *Foxo1* and bona fide GR target genes like *Fkbp51* and *Per2* (shown as an example in Fig. 6B, upper part). As visualized in Figure 6A, the fold induction of gene expression by Org 214007-0 was always lower than that caused by prednisolone, whereas fold repression of gene expression is more or less equal for Org 214007-0 and prednisolone. In other words, also *in vivo* Org 214007-0 shows a relatively low effect on induction of gene expression compared to prednisolone at dosages that are equally effective in suppression of arthritis.

Figure 7

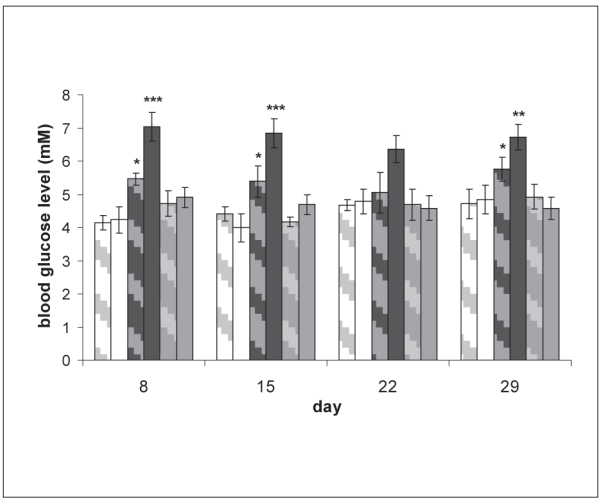

Org 214007-0 induces less fasting glucose compared to prednisolone at equi-efficacious dosages.

Mice (n=8 per group) are not treated (white bars, dashed) or treated once daily, for 28 days with either vehicle only (white bars), prednisolone 0.5 mg/kg/day (dark grey bars, dashed) or 1.5 mg/kg/day (black bars), or Org 214007-0 0.17 mg/kg/day (grey bars, dashed) or 0.5 mg/kg/day (grey bars). Both the two lowest doses of each compound are equi-efficacious in suppression of CIA as well as the two highest doses. Blood glucose levels (mean ± SEM) were measured at day 8, 15, 22 and 29, after 9 hours of fasting. * $p < 0.05$, ** $p < 0.01$, *** $p < 0.001$: significantly different (Student's t-test) from vehicle treated group.

Figure 8

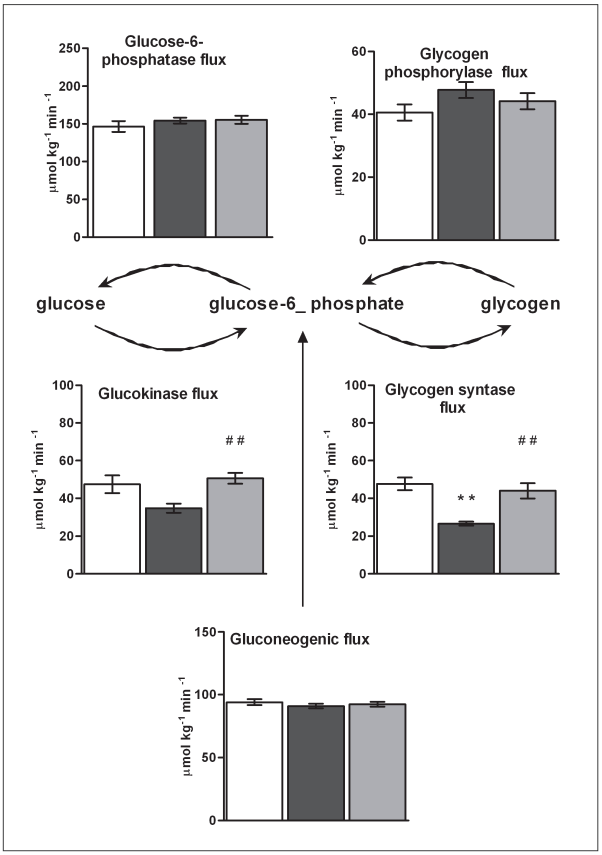

Org 214007-0 has no effect on hepatic glucose fluxes

Org 214007-0, at a dose that is equi-efficacious to prednisolone, does not effect the rates of the hepatic enzyme fluxes in mice as determined by Mass Isotopomer Distribution Analysis (MIDA). MIDA, as described in detail in Materials and Methods, was performed in mice treated p.o., once daily, for 7 days with either vehicle (white bars), 10 mg/kg prednisolone (dark grey bars) or 1.5 mg/kg Org 214007-0 (light grey bars). The glucokinase flux rate was not changed by Org 214007-0, but significantly differed from the effect by prednisolone (##: p=0.01 *vs.* prednisolone). The glycogen synthase flux rate was significantly decreased by prednisolone (**: p=0.005 *vs.* vehicle), whereas Org 214007-0 had no significant effect on this flux, but differed significantly from prednisolone (##: p=0.002 *vs.* prednisolone). Neither Org 214007-0 nor prednisolone, at equi-efficacious dosages, effects the gluconeogenic flux (*de novo* synthesis of glucose-6-phophate)

Figure 9

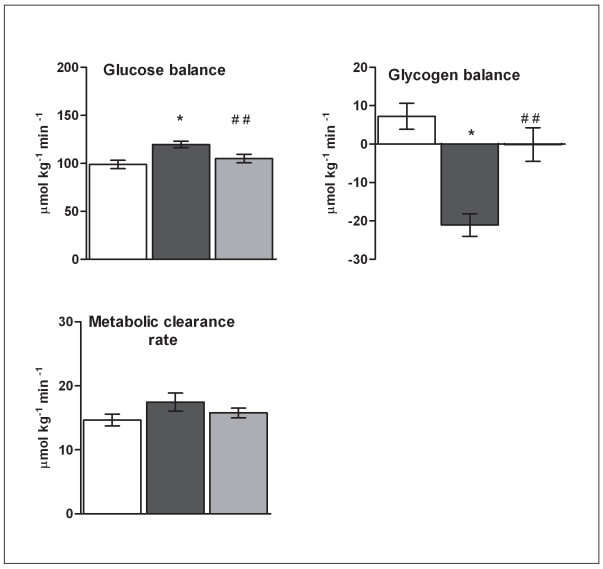

Org 214007-0, at a dose equi-efficacious to prednisolone, does not cause a shift in the glucose / glycogen balance in the liver as determined in MIDA (details in legend Figure 8). The glucose balance, which represents the difference between the glucose-6-phophatase and glucokinase flux, is not affected by Org 214007-0 treatment but is significantly changed by the prednisolone treated group (*: p=0.046 *vs.* vehicle.; ##: p=0.004 *vs.* prednisolone). The glycogen balance, representing the difference between the glycogen synthase and glycogen phophorylase flux, is not effected by Org 214007-0 treatment but is significantly changed by the prednisolone treated group (*: p=0.024 *vs.* vehicle.; ##: p=0.005 *vs.* prednisolone). Neither Org 214007-0 nor prednisolone, at equi-efficacious dosages, effects the metabolic clearance rate of blood glucose.

Finally, we assessed whether Org 214007-0 indeed has a favorable therapeutic index with respect to its (side-) effects on glucose metabolism. For this purpose, mice were treated daily with either vehicle, Org 214007-0 or prednisolone for 28 days and fasting blood glucose levels were determined at several time points. As shown in Figure 7, the fasting blood glucose levels in mice treated with prednisolone in comparison to vehicle-treated mice were already significantly elevated ($p<0.01$) from day 8 on. Interestingly, equipotent doses of Org 214007-0 did not affect fasting blood glucose levels. To evaluate the effects of the compound on hepatic glucose metabolism, a study employing a specific mass isotopomer distribution analysis (MIDA) approach was performed. Mice were dosed for 7 days with Org 214007-0 or prednisolone, again at dosages equally efficacious in inhibiting arthritis in the CIA model, or vehicle only. Also in this study, the fasting blood glucose levels in mice treated with prednisolone were significantly elevated compared to vehicle-treated mice ($p<0.05$), while Org 214007-0 did not affect fasting blood glucose level (Fig. S4). The hepatic flux rates calculated from the MIDA results are shown in Figure 8. The glucokinase and glycogen synthase flux rates were significantly decreased by prednisolone whereas Org 214007-0 had no significant effects. These differences in flux rates resulted in differences in glucose and glycogen balances as shown in Figure 9. Since prednisolone treatment caused no change in the gluconeogenic flux (from pyruvate to glucose-6-phosphate) (Figure 8) nor in the blood glucose metabolic clearance rate (Figure 9), the effect of prednisolone on the glucokinase and glycogen synthase flux rates may explain the increase in fasting glucose levels in prednisolone-treated mice. Org 214007-0 did not alter these

balances, confirming a significantly different mode of action of glucose metabolism in comparison to prednisolone.

Taken together, the *in vitro* partial GR agonistic profile of Org 214007-0 translates *in vivo* into a full anti-inflammatory compound with less adverse effects on glucose metabolism in mice. Org 214007-0 therefore represents a new class of SGRMs with an improved therapeutic index in comparison to prednisolone. This class of compounds is highly interesting for further development towards improved oral SGRMs for clinical use.

Discussion

About two decades ago, the concept of a "dissociating glucocorticoid" was defined, based on the discovery of the two different mechanisms of glucocorticoids action: transrepression versus transactivation. This concept was enforced by the finding that DNA-binding of the GR-ligand complex was not required for transrepression [5,29]. Since then, drug discovery programmes have been initiated on dissociating glucocorticoids (nowadays often referred to as SGRMs), resulting in the development of a number of compounds that indeed show improved TR/TA ratio *in vitro* (reviewed in [11]). However, only a limited number of compounds also show an dissociating profile *in vivo* when tested in preclinical animal models. This field of research and the hypothesis that an improved TR/TA ratio is beneficial in the clinic still awaits its validity, since proof of concept in man has not been shown yet. In addition it is now evident that the simple concept of TR versus TA activity requires revision based on new insights in the complexity of the mechanisms of GC action. Besides that, networks of hormonal regulation and metabolic processes are strongly interconnected [1,2,3]. Because of the complexity of GC biology, preclinical models are crucial to establish whether *in vitro* results translate into an improved profile of a SGRM *in vivo*. Most frequently, mouse models are being used to evaluate both the anti-inflammatory effects and the metabolic side effects. The latter requires specific knowledge and experimental techniques concerning (assessment of) glucose metabolism in the mouse. For example, fasting insulin and glucose levels measured in mice treated with GC clearly depend on time of fasting and time of blood sampling [30] and often seem to display patterns different from those in humans [31] .

In this paper we provide an extended *in vitro* characterization combined with specific *in vivo* data on a SGRM that belongs to a new chemical class of non-steroidal low molecular weight compounds, *i.e.*, Org 214007-0. Org 214007-0 binds with high affinity to GR, comparably to prednisolone. *In vitro*, Org 214007-0 behaved as a partial GR-selective agonist with a potency comparable to prednisolone. The maximal efficacy on induction of gene

expression by Org 214007-0, in comparison to prednisolone, is partial. The maximal efficacy on repression of inflammatory responses by Org 214007-0 is also partial but closer to that of prednisolone. This typical *in vitro* profile of Org 214007-0 was confirmed in several cell lines (HepG2, THP-1) for the total array of GC modulated genes. In addition, this unique profile of Org 214007-0 was confirmed in several types of human primary cells under different pro-inflammatory conditions.

Although Org 214007-0 binds GR with the same affinity as prednisolone, the conformation of the GR-Org 214007-0 complex leads to a lower binding affinity to the DNA GR-binding sites in comparison to the GR-prednisolone complex, as was shown by a ChIP-Seq study. These data are in agreement with the partial activity of Org 214007-0 on gene induction. Structure modeling of the GR-Org 214007-0 complex indeed indicates a conformation that changes the position of AF2 helix 12 of the GR molecule. Since co-modulator binding depends on the position of this helix, this will probably effect recruitment of co-activators and thereby gene induction activity [21,32].

The *in vivo* activity of Org 214007-0 was tested in several mouse models. Two acute inflammation models demonstrated the anti-inflammatory activity of Org 214007-0 at the level of both monocytic cells (LPS-induced TNFα model) and T cells (anti-CD3-induced IL-2 model). Strikingly, Org 214007-0 was found to behave as a potent and full GR agonistic anti-inflammatory agent in these models. Even more importantly, this strong potency and full anti-inflammatory efficacy was sustained in a chronic disease model, *i.e.*, the CIA model. Microarray analysis on muscle RNA from these mice showed that the efficacy in suppression of the CIA disease score was in line with a reduction of disease-related or pro-inflammatory genes like TLR4 ligand *S100A8/S100A9* [33] and monocyte chemotactive protein-2 (chemokine[C-C]-ligand 8 or *Ccl8*) [34]. More importantly, the partial activity of Org 214007-0 on gene induction, as observed *in vitro,* was sustained in the CIA model, since the GR-dependent induction of genes was always lower upon Org 214007-0 treatment compared to prednisolone. A large part of the induced genes are well-known GR-regulated genes like *Fkbp51*, *Foxo1*, phenylethanolamine-N-methyltransferase (*Pnmt*), *Ddit4* (or *Redd1*), *Lcn2* (or Lipocalin 2) and *Per2* [7,35]. This latter gene belongs to the class of circadian clock genes and has recently been described as a primary GR target gene involved in glucose homeostasis [36]. It is tempting to speculate that a less pronounced induction of Per-2 by Org 214007-0 compared to an equi-efficacious dose of prednisolone contributes to a better metabolic side effect profile of Org 214007-0. However, a functional metabolic side effect profile could not be derived from our CIA model, since we have not seen any induction of either glucose or insulin at a dose of 1.5 mg/kg/day prednisolone in our CIA experiments. Other groups have described increased fasting glucose or insulin levels in mice treated with prednisolone in acute inflammation models [6,37] and

in a chronic disease model [38]. Riether *et al*. [38] showed that 30 mg/kg prednisolone induced significantly elevated serum insulin levels in a mouse CIA experiment. However, the dose of prednisolone used by Riether *et al.* is much higher than the dose (1.5 mg/kg/day) that is fully efficacious in our CIA model. To gain direct insight in potentially disqualifying side effects of Org 214007-0 on glucose metabolism, we have carefully evaluated its effect on glucose metabolism in the liver, by a mass isotopomer distribution analysis (MIDA) approach. MIDA has successfully been applied to study glucose metabolism in humans [39] and was adapted for use in mice [40]. Using this method it was found that prednisolone administration of 10 mg/kg/day for 7 days significantly reduced glycogen storage in the liver by reducing glucokinase and glycogen synthase fluxes, while a dose of Org 214007-0 that was equi-efficacious in reducing arthritis did not. Surprisingly, hepatic gluconeogenesis was not affected by prednisolone treatment while the commonly accepted idea is that GCs stimulate gluconeogenesis *via* induction of genes like PEPCK (*Pck1*) and *G6pase*. However, induction of these gluconeogenic genes appears to represent an acute effect of GCs. Studies on glucose metabolism after a more chronic GC treatment in man [31,41,42] or mice [30] also showed a lack of effect on hepatic gluconeogenesis and rather point at an effect on glucose disposal. In addition, it is known that PEPCK (*Pck1*) gene expression only marginally controls the gluconeogenesis flux [43,44]. So, in contrast to prednisolone, Org 214007-0 did not have any impact on *in vivo* glucose metabolism in the mouse, since no effects on fasting blood glucose levels or on hepatic glucose metabolism were found.

Thus, Org 214007-0, is a non-steroidal SGRMs, with an improved therapeutic index compared to prednisolone. Progress in development of this new class of SGRMs could lead to future availability of effective anti-inflammatory drugs with a lower risk for metabolic side effects.

Acknowledgements

The authors wish to thank all technicians and students from the different departments of MSD Oss and of the University Medical Center of Groningen who have contributed to the work presented in this paper.

Reference list

1. Schäcke H, Döcke WD, Asadullah K (2002) Mechanisms involved in the side effects of glucocorticoids. *Pharmacol Ther*., 96: 23-43.

2. van Raalte DH, Ouwens DM, Diamant M (2009) Novel insights into glucocorticoid-mediated diabetogenic

effects: towards expansion of therapeutic options? *Eur J Clin Invest*., 39: 81-93.

3. Beck IM *et al.* (2009) Crosstalk in inflammation: the interplay of glucocorticoid receptor-based mechanisms and kinases and phosphatases *Endocr Rev*., 30: 830-882.
4. De Bosscher K, Haegeman G (2009) Minireview: Latest perspectives on antiinflammatory actions of glucocorticoids. *Mol Endocrinol*., 23: 281-291.
5. Reichardt HM *et al.* (1998) DNA binding of the glucocorticoid receptor is not essential for survival. *Cell*, 93: 531-541.
6. Schäcke H *et al.* (2004) Dissociation of transactivation from transrepression by a selective glucocorticoid receptor agonist leads to separation of therapeutic effects from side effects. *Proc Natl Acad Sci U S A*., 101: 227-232.
7. Frijters R *et al.* (2010) Prednisolone-induced differential gene expression in mouse liver carrying wild type or a dimerization-defective glucocorticoid receptor. *BMC Genomics*, 11: 359-372.
8. Ronacher K *et al.* (2009) Ligand-selective transactivation and transrepression via the glucocorticoid receptor: role of co-factor interaction. *Mol Cell Endocrinol*., 299: 219-231.
9. Kumar R, Thompson EB (2005) Gene regulation by the glucocorticoid receptor: structure:function relationship. *J Steroid Biochem Mol Biol*., 94: 383-394.
10. Belvisi MG *et al.* (2001) Therapeutic benefit of a dissociated glucocorticoid and the relevance of in vitro separation of transrepression from transactivation activity. *J. Immunol.*, 166: 1975-1982.
11. De Bosscher K, Haegeman G, Elewaut D (2010) Targeting inflammation using selective glucocorticoid receptor modulators. *Curr Opin Pharmacol*., 10: 497-504.
12. Miner JN *et al.* (2007) Antiinflammatory glucocorticoid receptor ligand with reduced side effects exhibits an altered protein-protein interaction profile. *Proc Natl Acad Sci U S A*., 104: 19244-19249.
13. Clark AR (2007) Anti-inflammatory functions of glucocorticoid-induced genes. *Mol. Cell. Endocrinol.*, 275: 79-97
14. Newton R and Holden NS (2007) Separating transrepression and transactivation: a distressing divorce for the glucocorticoid receptor? *Mol Pharmacol*., 72: 799-809.
15. Surjit M *et al.* (2011) Widespread negative response elements mediate direct repression by agonist- liganded glucocorticoid receptor. *Cell*, 145: 224 - 241.
16. Liberman AC, Druker J, Perone MJ, Arzt E (2007) Glucocorticoids in the regulation of transcription factors that control cytokine synthesis. *Cytokine Growth Factor Rev*. 1-2: 45-56.
17. Biggadike K *et al.* (2008) X-ray crystal structure of the novel enhanced-affinity glucocorticoid agonist fluticasone furoate in the glucocorticoid receptor-ligand binding domain. *J Med Chem.,* 51: 3349-3352.
18. Biggadike K *et al.* (2009) Design and x-ray crystal structures of high-potency nonsteroidal glucocorticoid agonists exploiting a novel binding site on the receptor. *Proc Natl Acad Sci U S A.*, 106: 18114-18119.
19. Kauppi B *et al.* (2003) The three-dimensional structures of antagonistic and agonistic forms of the glucocorticoid receptor ligand-binding domain: RU-486 induces a transconformation that leads to active antagonism. J Biol Chem., 278: 22748-22754.
20. De Bosscher K, Beck IM, Haegeman G (2010) Classic glucocorticoids versus non-steroidal glucocorticoid receptor modulators: survival of the fittest regulator of the immune system? *Brain Behav Immun*., 24: 1035-1042.
21. Bledsoe RK *et al.* (2002) Crystal structure of the glucocorticoid receptor ligand binding domain reveals a novel mode of receptor dimerization and coactivator recognition. *Cell*, 110: 93-105.
22. Kroe RR *et al.* (2007) Agonist versus antagonist induce distinct thermodynamic modes of co-factor binding

to the glucocorticoid receptor. *Biophys Chem*., 128: 156-164.

23. Sun Y, Tao YG, Kagan BL, He Y, Jr SS (2008) Modulation of transcription parameters in glucocorticoid receptor-mediated repression. *Mol Cell Endocrinol*., 295: 59-69.

24. Meijsing SH *et al.* DNA binding site sequence directs glucocorticoid receptor structure and activity. *Science,* 324: 407-410.

25. Wang Q *et al.* (2004) Equilibrium interactions of corepressors and coactivators with agonist and antagonist complexes of glucocorticoid receptors. *Mol Endocrinol*., 18: 1376-1395.

26. Plate R, Jans CGLM (2007) Non-steroidal compounds useful as glucocorticoid receptor modulators. WO 2007/025938

27. Kunkel EJ *et al.* (2004) Rapid structure-activity and selectivity analysis of kinase inhibitors by BioMAP analysis in complex human primary cell-based models. *Assay Drug Dev Technol*., 2: 0431-441.

28. Berg EL, Kunkel EJ, Hytopoulos E, Plavec I (2006) Characterization of compound mechanisms and secondary activities by BioMAP analysis. *J Pharmacol Toxicol Methods.*, 53: 67-74

29. Lucibello FC, Slater EP, Jooss KU, Beato M, Müller R (1990) Mutual transrepression of Fos and the glucocorticoid receptor: involvement of a functional domain in Fos which is absent in FosB. *EMBO J.* 9: 2827-2834.

30. Laskewitz AJ *et al.* (2010) Chronic prednisolone treatment reduces hepatic insulin sensitivity while perturbing the fed-to-fasting transition in mice. *Endocrinology* 151: 2171-2178.

31. van Raalte DH *et al.* (2010) Acute and 2-week exposure to prednisolone impair different aspects of beta-cell function in healthy men. *Eur J Endocrinol.* 162: 729-735.

32. Wu J, Li Y, Dietz J, Lala DS (2004) Repression of p65 Transcriptional Activation by the Glucocorticoid Receptor in the Absence of Receptor-Coactivator Interactions. *Mol. Endocrinol.* 18: 53–62

33. Ehrchen JM, Sunderkötter C, Foell D, Vogl T, Roth J (2009) The endogenous Toll-like receptor 4 agonist S100A8/S100A9 (calprotectin) as innate amplifier of infection, autoimmunity, and cancer. *J Leukoc Biol.* 86: 557-566.

34. Henningsen J, Pedersen BK, Kratchmarova I (2011) Quantitative analysis of the secretion of the MCP family of chemokines by muscle cells. *Mol Biosyst.* 7: 311-321.

35. Toonen EJM *et al.* (2011) Prednisolone induced changes in gene expression profiles in healthy volunteers. *Pharmacogenomics* (Epub ahead of print).

36. So AY, Bernal TU, Pillsbury ML, Yamamoto KR, Feldman BJ (2009) Glucocorticoid regulation of the circadian clock modulates glucose homeostasis. *Proc Natl Acad Sci U S A* 106: 17582-17587.

37. Yang BV *et al.* (2010) Dimethyl-diphenyl-propanamide Derivatives As Nonsteroidal Dissociated Glucocorticoid Receptor Agonists. *J Med Chem.* 53: 8241–8251.

38. Riether D *et al.* (2010) Nonsteroidal dissociated glucocorticoid agonists containing azaindoles as steroid A-ring mimetics. *J Med Chem.* 53: 6681-6698.

39. Hellerstein MK *et al.* (1997) Hepatic gluconeogenic fluxes and glycogen turnover during fasting in humans. A stable isotope study. *J Clin Invest*. 100: 1305-1319.

40. van Dijk TH *et al.* (2003) Quantification of hepatic carbohydrate metabolism in conscious mice using serial blood and urine spots. *Anal Biochem*. 322: 1-13.

41. Nielsen MF *et al.* (2004) Impaired basal glucose effectiveness but unaltered fasting glucose release and gluconeogenesis during short-term hypercortisolemia in healthy subjects. *Am J Physiol Endocrinol Metab.* 286: E102-110.

42. Wajngot A, Khan A, Giacca A, Vranic M, Efendic S (1990) Dexamethasone increases glucose cycling, but not glucose production, in healthy subjects. *Am J Physiol.* 259: E626-32.

43. Edgerton DS *et al.* (2009) Effects of insulin on the metabolic control of hepatic gluconeogenesis in vivo. *Diabetes* 58: 2766-2775.

44. Magnuson MA, She P, Shiota M. (2003) Gene-altered mice and metabolic flux control. *J. Biol. Chem.* 278: 32485-32488.

45. Adan RA, Cox JJ, Beischlag TV, Burbach JP (1993) A composite hormone response element mediates the transactivation of the rat oxytocin gene by different classes of nuclear hormone receptors. *Mol Endocrinol.* 7: 47-57.

46. de Groot DM *et al.* (2009) Therapeutic antibody targeting of CD97 in experimental arthritis: the role of antigen expression, shedding, and internalization on the pharmacokinetics of anti-CD97 monoclonal antibody 1B2. *J Immunol.* 183: 4127-4134.

47. Joosten LA *et al.* (1999) IL-1 alpha beta blockade prevents cartilage and bone destruction in murine type II collagen-induced arthritis, whereas TNF-alpha blockade only ameliorates joint inflammation. *J. Immunol*. 163: 5049–5055.

48. van Dijk TH *et al.* (2001) Acute inhibition of hepatic glucose-6-phosphatase does not affect gluconeogenesis but directs gluconeogenic flux toward glycogen in fasted rats. A pharmacological study with the chlorogenic acid derivative S4048. *J Biol Chem*. 276: 25727-25735.

49. Bandsma RH *et al.* (2004) Enhanced glucose cycling and suppressed de novo synthesis of glucose-6-phosphate result in a net unchanged hepatic glucose output in ob/ob mice. *Diabetologia* 47: 2022-2031.

Supporting Information

Materials and Methods

Glucocorticoid receptor binding assay

The glucocorticoid receptor (GR) fluorescence polarisation (FP) binding assay was performed using the commercially available kit from Panvera (Glucocorticoid receptor competitor assay, Green Cat# P2816). Briefly, recombinant human GR was added to a fluorescent glucocorticoid ligand (Fluormone™ GS1) in the presence of competitor test compounds in black round bottom 384 well microtitre plates for 1.5 to 2.5 hours at roomtemperature. Fluorescence polarization was measured on an Analyst with suitable 485nm excitation and 535nm emission interference filters for FP.

Assay in U2OS cells

To determine the repressive activity of GR ligands, cell line U2OS GR.G9, the human osteoblastic cell line U2OS, stably transfected with human GR, was used. Cells (104 cells/well) in Dulbecco's MEM / HAM F12 medium supplemented with 5% charcoal treated bovine calf serum (Hyclone) (v/v) and Penicillin (10 U/ml) -Streptomycin (10 µg/ml) were incubated in 384-wells plates, in the presence of 50 ng/ml TNFα (R&D systems) / 100 ng/ml IFNγ (Peprotech) and compound, for 18 hours in a humidified atmosphere at 37°C under 6.5% CO2. Hereafter, a mixture of 2.2 nM anti-hMCP-1 labeled with fluorescent donor Europium (Eu) and 16.6 nM anti-hMCP-1 labeled with fluorescent acceptor Allophycocyanin (APC) was added to each well and left at roomtemperature for 1 hour. Finally, the time-resolved fluorometric resonance energy transfer (TR-FRET) signal was measured with the Victor2TM V, 1420 Multilabel Counter (Wallac). Using 4-parameter curve fitting, IC50 values for the compounds were determined. Besides IC50, also percentage maximal efficacy of each compound related to the maximal efficacy of the reference prednisolone was given.

Assay in CHO cells

For monitoring both human steroid receptor agonistic as well as antagonistic activity of compounds, Chinese hamster ovary (CHO) K1 cells stably co-transfected with the specific human steroid receptor and its respective reporter construct were used (as previously described 45).

For human glucocorticoid receptor (GR)-specific activity CHO-GR B4.8 cells containing both recombinant human GR as well as a reporter construct consisting of the mouse mammary tumor virus (MMTV) promotor and the luciferase reporter gene, were used. Compound was incubated alone (in the agonistic setup) or with 50 nM dexamethasone (in the antagonistic setup) in microtiter white culture plates seeded with 2.4 x 104 cells / 200 µl Dulbecco's MEM/Nutrient Mix F12 medium (Gibco) supplemented with 5% charcoal treated defined bovine calf serum supplement (DBCSS, Hyclone, Utah, USA), and 10 U/ml Penicillin-10µg/ml Streptomycin (GibcoBRL) overnight at 37°C in the dark under a humidified atmosphere flushed with 5% CO2 in air. Hereafter, 200 µl medium was removed and 50 µl luciferine substrate solution from the LucLite luminescence kit (Packard, Meriden, USA) was added. After 10 minutes (when cell lysis was complete) luminescence of each sample was counted using a Topcount microplate luminescence counter. Percentage maximal agonistic efficacy was related to the maximal efficacy of dexamethasone. Percentage maximal antagonistic efficacy was related to the maximal antagonistic efficacy of reference GR antagonist Org 34116. EC50 value was calculated by 4-parameter curve fitting using the effect of 6 compound concentrations.

Similar procedures were followed for the other human steroid receptor assays containing combinations of human progesterone receptor B (PR-B) and MMTV-Luc, human androgen receptor (AR) and MMTV-Luc, human chimeric glucocorticoid-mineralocorticoid receptor (GGM, Trapp et al. (1994), Neuron 13: 1457) and MMTV-Luc, human estrogen receptor alpha (ERα) and rat oxytocin-Luc 45, and human estrogen receptor beta (ERβ) and rat oxytocin-Luc, respectively.

Gene expression profiling in HepG2 cells

HepG2-8/97-WS.5 cells were seeded at 2.105 cells/mL in a 24-well plate in DMEM/F12 medium (Gibco), supplemented with 80 U/mL penicillin, 80 µg/mL streptomycin and 5% Fetal Bovine Serum (Invitrogen). The following day, cells were washed once with PBS and medium was replaced by serum-free medium for 18 hours. Hereafter, cells were stimulated with glucocorticoid and 0.5 mM cAMP for 6 hours. RNA isolation was carried out by TRIZOL (Invitrogen) treatment. To enhance the A260/A230 ratio, samples were cleaned using the RNeasy mini kit (Qiagen) with an additional DNase step on column to ensure DNA-free RNA. RNA quantity and quality were de-

termined using the Agilent Nanodrop bioanalyzer. For all samples subjected to micro-array hybridization, the RIN (RNA integrity number) was 9.0 – 10. Double-stranded cDNA was synthesized from 1.5 µg total RNA using the One-Cycle Target Labeling Kit (Affymetrix Santa Clara, CA), and used as a template for the preparation of biotin-labeled cRNA using the GeneChip IVT Labeling Kit (Affymetrix Santa Clara, CA). Biotin-labeled cRNA was fragmented at 1 µg/µl following the manufacturer's protocol. After fragmentation, cRNA (10µg) was hybridized at 45°C for 16-17 hours to the Human Genome U133A 2.0 Array or the Human Genome U133 Plus 2.0 Array (Affymetrix, Santa Clara, CA). Following hybridization, the arrays were washed, stained with phycoerythrin-streptavidin conjugate (Molecular Probes, Eugene, OR), and the signals were amplified by staining the array with biotin-labeled anti-streptavidin antibody (Vector Laboratories, Burlingame, CA) followed by phycoerythrin-streptavidin. The arrays were laser scanned with an GeneChip Scanner 3000 6G (Affymetrix, Santa Clara, CA) according to the manufacturer's instructions. Data was saved as raw image file and quantified using GCOS (Affymetrix).

For Q-PCR, cDNA was synthesized by the use of 1 µg RNA that was added to 1 µg of random primer (Promega) in a total volume of 15 µL, heated to 70 ºC for 10 min and cooled on ice. M-MLV reverse transcriptase (200 units) (Promega), 10 nmol of each dNTP and RT buffer was added to a total volume of 25 µL and incubated for 10 min at 22 ºC, 50 min at 55 ºC and 15 min at 75 ºC. cDNA samples were stored at -20 ºC. For Q-PCR, cDNA was diluted 125 times in milliQ and 5 µL was added to 12.5 µL of SYBR green mix (Applied Biosystems cat. No. 4309155) , 2.5 µL of each primer (~20 ng/µl) and 2.5 µL of milliQ. The following primer-pairs were used: for GAPDH: 5'-CCACATCGCTCAGACACCAT-3' and 5'-CCAGGCGCCCAATACG-3'; for PEPCK (of PCK1): 5'-TCCCATTGAA-GGCATTATCTTTG-3' and 5'-GCCAGCTGAGAGCTTCATAGACT-3'; for TAT: 5'-TACAGACCCTGAAGTTACCCAG-3' and 5'-TAAGAAGCAATCTCCTCCCGA-3'; for G6Pase (of: G6PC?): 5'-TGCTGCTCAAGGGACTG-3' and 5'-GAATGGGAGC-CACTTGCTG-3'. Quantitative PCR was performed on an ABI7900HT real time thermo cycler (Applied Biosystems) and results were analyzed by SDS2.1 software.

Gene expression profiling in THP-1 cells

THP-1 cells (106 cells/ml) were incubated with a single high dose (1 µM) of either prednisolone or Org 214007-0 in the presence of either DMSO (control) or IFNγ/TNFα (220ng/ml / 375 ng/ml). After 6 hours (predetermined optimal time-point for maximal induction of most GR-regulated genes), total RNA was isolated and further processed for micro-array hybridization as described before for the HepG2 cells. For a selection of the GC-regulated genes the expression profile was confirmed. In these experiments THP1 cells were stimulated with 40 ng/ml IFNγ and 60 ng/ml TNFα and a whole dose range of prednisolone and Org 214007-0 was tested. Expression of FKBP51, DUSP1 and GILZ was measured by Q-PCR according to the same procedure as described for the HepG2 cells. In this case the following primer-pairs were used: for GAPDH: 5'-CCACATCGCTCAGACACCAT-3' and 5'-CCAGGCGC-CCAATACG-3'; for FKBP51: 5'-AAAAGGCCAAGGAGCACAAC-3' and 5'-TTGAGGAGGGGCCGAGTTC-3'; for DUSP1: 5'-GTACATCAAGTCCATCTGAC-3' and 5'-GGTTCTTCTAGGAGTAGACA-3'; for GILZ: 5'-AGTGCCTCCGGAGCCAGC-3' and 5'-ATGATTCTTCACCAGATCC-3'. Expression of MCP-1, IL-6 and IL-8 was measured by specific AlphaLISAs (PerkingElmer; #AL244C [MCP-1], #AL223C [IL-6] and #AL224C [IL-8]) according to the manufacturer manual. Briefly, 5 µL of sample was added to 20 µL of a mix (freshly prepared) AlphaLISA Anti-Analyte Acceptor beads (10 µg/mL final) and Biotinylated Antibody Anti-Analyte (1 nM final) into a 384-well white OptiPlate-384. Samples were incubated for 60 min at 23˚C. StreptAvidin-Donor beads (40 µg/mL final) were added and incubated for another 30 min at 23˚C in the dark. Plates were measured using an EnVision-Alpha Reader.

ChIP-SEQ analysis

Cells were fixed with 1% formaldehyde for 15 min and quenched with 0.125 M glycine. Chromatin was isolated by adding lysis buffer, followed by disruption with a Dounce homogenizer (cells) or motor pestle (tissue). Lysates were sonicated and the DNA sheared to an average length of 300-500 bp. Genomic DNA (Input) was prepared by treating aliquots of chromatin with RNase, proteinase K and heat for de-crosslinking, followed by ethanol precipitation. Pellets were resuspended and the resulting DNA was quantified on a NanoDrop spectrophotometer. Extrapolation to the original chromatin volume allowed quantitation of the total chromatin yield.

An aliquot of chromatin (28.5 ug) was precleared with protein A agarose beads (Invitrogen). Genomic DNA regions of interest were isolated using 4 ug antibody against GR (Santa Cruz sc-8992). Complexes were washed, eluted from the beads with SDS buffer, and subjected to RNase and proteinase K treatment. Crosslinks were reversed by incubation overnight at 65 C, and ChIP DNA was purified by phenol-chloroform extraction and ethanol precipitation.

Quantitative PCR (QPCR) reactions were carried out in triplicate on specific genomic regions using SYBR Green

Supermix (Bio-Rad). The resulting signals were normalized for primer efficiency by carrying out QPCR for each primer pair using Input DNA. ChIP and Input DNAs were prepared for amplification by converting overhangs into phosphorylated blunt ends and adding an adenine to the 3' ends. Illumina adaptors were added and the library was size-selected (175-225 bp) on an agarose gel. The adaptor-ligated libraries were amplified for 18 cycles. The resulting amplified DNAs were purified, quantified, and tested by QPCR at the same specific genomic regions as the original ChIP DNA to assess quality of the amplification reactions. Amplified DNAs (DNA libraries) were sent to Illumina Sequencing Services for sequencing on a Genome Analyzer II.

Table s1

Steroid receptor	% agonist potency	EC50 (nM)	n	% antagonist potency	IC50 (nM)	% efficacy	n
PR (B)	<0.03	>100	4	0.46 (±0.2)	19.4 (±7.6)	> 87	5
MR	<0.1	>1000	2	<1.27	>1260	> 40	2
AR	<0.13	>100	4	<3.83	>1000	na	5
ERα	<0.01	>100	5	<1.86	>1000	na	2
ERß	<0.01	>100	5	<0.9	>1000	na	5

Activity of Org 214007-0 for the other human steroid receptors, stably co-transfected with their respective reporter read-outs in CHO cells. The data are expressed as the mean (±SD) of the relative agonistic or antagonistic activity as compared to the respective reference compounds. na = not applicable; n = number of experiments

Figure s1

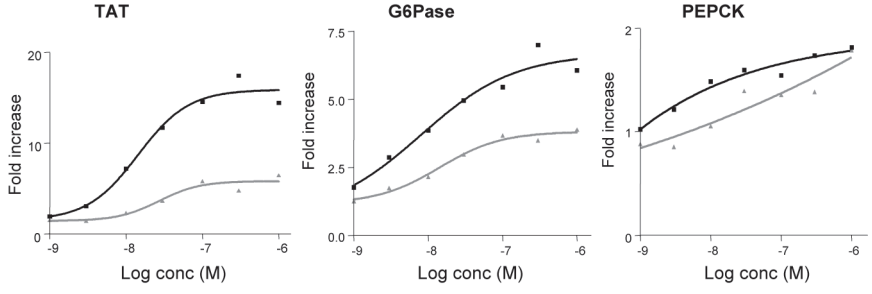

Org 214007-0, in comparison to prednisolone, partially induces expression of GC-regulated genes in the human HepG2 cell line. HepG2 cells were incubated with either vehicle, Org 214007-0 or prednisolone for 6 hours. RNA was isolated and expression of tyrosine aminotransferase (TAT), glucose 6-phosphatase (G6Pase) and phosphoenolpyruvate carboxykinase (PEPCK) was quantified by Q-PCR, expressed as fold induction in comparison to vehicle treated cells.

Table s2

	TNFα	n	IL-1β	n	IL-6	n	IL-8	n
Prednisolone	100	16	100	3	100	3	100	3
ORG 214007-0	81 (± 7)	12	64 (± 8)	3	54 (± 6)	3	49 (± 55)	3

Repressive activity of 10 µM Org 214007-0 in comparison to 10 µM prednisolone on cytokine release of human whole blood cells stimulated with LPS for 24 hours. The data are expressed as the mean percentage inhibition (±SD) by Org 214007-0 compared to that by prednisolone (set at 100%); n = number of experiments.

Figure s2

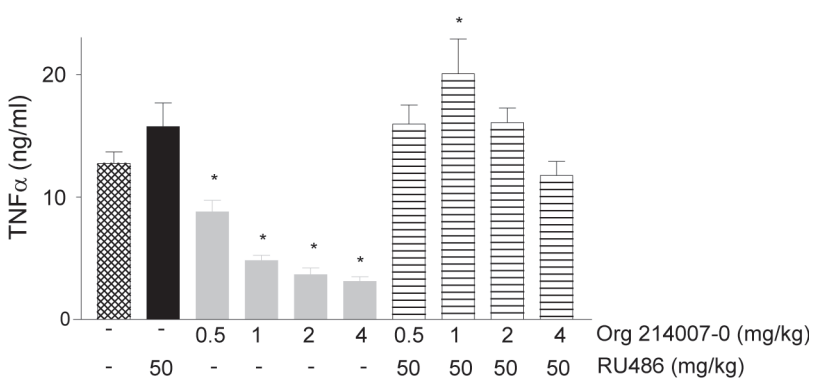

The anti-inflammatory effect of Org 214007-0 is mediated through the glucocorticoid receptor. Mice were treated p.o. either with vehicle, Org 214007-0 (0.5, 1, 2 or 4 mg/kg) in a co-treatment schedule with either a vehicle or RU486 (50 mg/kg) s.c. injection. TNFa was quantified 1.5 h after LPS challenge. Data is represented as mean ± SEM. An one way ANOVA was used for statistical analysis. An asterix (*) represents significant difference from vehicle ($p < 0.05$).

Table 5.3

	Org 214007-		Prednisolone	
	4 µmol/kg i.v.	10 µmol/kg p.o.	10 µmol/kg i.v.	20 µmol/kg p.o.
Tmax (h)		0.5		0.3
Cmax (nmol/ml)	2.19	2.12	18	11.5
T1/2 eli (h)	6.4	5.3	0.26	0.4
AUClast (h*nmol/ml)	10.1	23.2	7.1	11
AUCinf (h*nmol/ml)	10.8	24.2	7.1	11
Vz (L/kg)	3.4	3.2	0.5	1.2
Cl (L/h/kg)	0.4	0.4	1.4	1.8
MRTinf (h)	7.9	7.1	0.4	0.8
Vss (L/kg)	2.9	-	0.5	-
F (% bioavailability)	-	89.7	-	77.4

Pharmacokinetic parameters of Org 214007-0 and prednisolone in mice
For each time-point 3 female Balb/c mice are used. Tmax = Time of maximum observed concentration (in case of i.v. administration Tmax = 0 h); time is expressed in hours (h). Cmax = concentration corresponding to Tmax and expressed in nmol/ml, for i.v. dosing Cmax is extrapolated to T=0. T 1/2 eli(mination) (terminal half-life) = ln(2)/λ_z expressed in h(ours). AUClast = Area under the curve from the time of dosing (Dosing-time) to the last measurable concentration. AUCinf = predicted Area Under the Curve from the time of dosing extrapolated to infinity and expressed in "h*nmol/ml". Vz = Volume of distribution based on the terminal phase = Dose / λ_z* AUCinf and expressed inL/kg. Cl = total body clearance = Dose / AUCinf and expressed in L/h/kg. MRTinf = mean residence time (MRT) extrapolated to infinity for non-infusion models, expressed in h. Vss = gives an estimate of the volume of distribution at steady-state and is expressed in L/kg. F = % bioavailability; assuming linear kinetics, the % bioavailability after oral administration is calculated by dividing the AUCinf obtained after oral administration by the mean expected normalized AUCinf after i.v. administration of that dose (x 100%) (AUCiv = 100% by definition). The bioavailability is expressed in %. i.v. = intraveneously, p.o. = per oral.

Figure s3

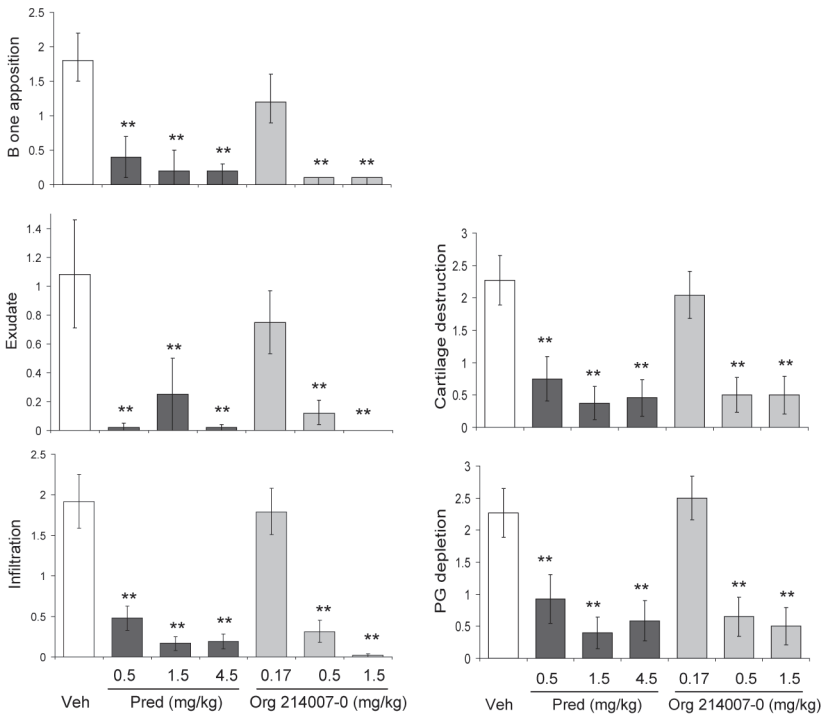

Org 214007-0 significantly reduces all parameters scored by histological examination of the knee joints of CIA mice. At the end of the CIA study (after 3 weeks of daily oral treatment with equipotent dosages of prednisolone and Org 214007-0) knee joints were fixed in 4%-buffered formaldehyde and decalcified. After decalcification the joints were washed, dehydrated and embedded in paraffin. Serial sections of at least 7 μm were stained by Hematoxylin-Eosin (for cellular infiltration and exudate formation into the joint space and bone apposition), or by toluindin blue staining (for proteoglycan depletion and cartilage and / or bone destruction of the joint). Org 214007-0, at 0.5 and 1.5 mg/kg, significantly reduced the formation of new bone (bone apposition), the infiltration of inflammatory cells in the joint cavity (exudate) or joint tissue (infiltration), cartilage destruction and proteoglycan depletion in the articular cartilage (PG depletion). Each of the histological parameters is scored at a scale of 0 – 3. Mean score of each group of mice (n=12) is indicated (± SEM). ** = significantly different from vehicle ($p < 0.01$; ANOVA-test).

Figure s4

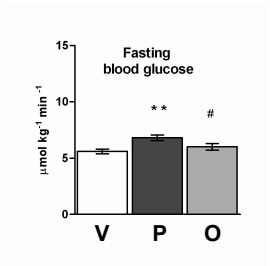

Org 214007-0, at a dose that is equi-efficacious to prednisolone, induces less fasting glucose. Mice (n=8 per group) were treated p.o., once daily, for 7 days with either vehicle (V), 10 mg/kg prednisolone (P) or 1.5 mg/kg Org 214007-0 (O). Blood glucose levels (mean ± SEM) were measured at day 8, after 9 hours of fasting. ** $p < 0.01$: significantly different (Student's t-test) from vehicle-treated group; # $p < 0.05$: significantly different (Student's t-test) from prednisolone-treated group.

6

Glucose kinetics in the collagen-induced arthritis model: an all-in-one model to assess both efficacy and metabolic side effects of glucocorticoids

Manuscript in preparation

Anke J. Laskewitz*
Erik J.M. Toonen*
Theo H. van Dijk
Aycha Bleeker
Aldo Grefhorst
Annelies E. Schouten
Ellen A.J. Bastiaanssen
Cindy van Doorn
Monique A.J. v/d Vleuten
Marie-Jose C. van Lierop
Folkert Kuipers
Albert K. Groen
Wim H.A. Dokter

*Both authors contributed equally to this study

Abstract

Prednisolone and other glucocorticoids (GCs) are potent anti-inflammatory drugs, but chronic use is hampered by metabolic side effects. Therefore, there is an urgent medical need for improved GCs that are as effective as classical GCs but have a better safety profile. A well-established model to assess anti-inflammatory efficacy is the chronic collagen-induced arthritis (CIA) model in mice, a model with features resembling rheumatoid arthritis. Models to quantify undesired effects of glucocorticoids on glucose kinetics are less well-established. Recently, we have described a model to quantify basal blood glucose kinetics using stably-labeled glucose. In the present study, we have used this blood glucose kinetic model in the CIA model treated with prednisolone to enable quantification of both efficacy and adverse effects in one animal model. Arthritis scores were decreased after treatment with prednisolone, confirming the anti-inflammatory properties of GCs. Insulin secretion and hepatic glucose production were increased, but this did not result immediately in hyperglycemia or insulin resistance, indicating a highly adaptive compensatory mechanism in these mice. In conclusion, this model allows for studying effects of (novel) GC compounds on the development of arthritis and glucose kinetics in a single animal. This integrative model provides a valuable tool for investigating (drug-induced) metabolic dysregulation in an inflammatory setting. In addition, the blood glucose kinetic model might also be useful in translational studies into metabolic side effects of GCs in RA patients.

Introduction

Prednisolone and other glucocorticoids (GCs) are very potent immunosuppressive and anti-inflammatory compounds that are among the top 10 most prescribed drugs [1]. Exogenous GCs are used in daily clinical practice to treat (chronic) inflammatory, autoimmune and allergic disorders, to attenuate organ rejection after transplantation, to treat brain edema, shock and various blood cancers [2]. Most of the effects of GCs are mediated through binding of GCs to the glucocorticoid receptor (GR), which is found in almost all human tissues.

Although very effective in reducing inflammation, prolonged treatment at medium or high dose of GCs is hampered by a wide range of metabolic side effects such as derangements of glucose metabolism, induction of insulin-resistance, beta-cell dysfunction, hyperlipidemia, fat redistribution and central obesity leading to serious conditions that are strongly associated with elevated risk for cardiovascular disease and type 2 Diabetes in humans [3-5]. The mechanisms of action underlying these metabolic side effects are largely unknown.

Seen this wide range of GC-induced side effects, there is a high medical need for improved anti-inflammatory drugs that are as effective as classical GCs but show less metabolic side effects. This type of experimental compounds are often referred to as selective GR modulators (SGRMs) [4]. Given the complexity of glucocorticoid actions, the use of animal models is required to investigate these mechanisms and several models have been applied to study the efficacy and/or metabolic side effects of new pharmaceutical compounds *in vivo* [6,7] . Preclinical efficacy of experimental GCs is often measured in collagen-induced arthritis (CIA) mice, an inflammatory model with features resembling rheumatoid arthritis (RA) [8,9]. Arthritis can be induced in susceptible strains of mice by immunization with type II collagen, the major component of articular cartilage, and has histopathologic and serological features in common with RA [10,11].

Regarding *in vivo* investigation of (compound-induced) metabolic dysregulation such as insulin resistance, a number of methods have been developed to measure glucose and insulin kinetics, of which the hyperinsulinemic euglycemic clamp (HIEC) is considered as the 'gold standard'. With respect to mice studies, the HIEC is difficult to use for longitudinal studies, since it can only be performed once in a single animal [12]. In addition, arthritic mice in the CIA model are severely ill,and therefore these mice can not be subjected to the invasive HIEC protocol. To overcome these drawbacks, a new method was developed in which stably-labeled glucose (D-[6,6-$^{2}H_{2}$]-glucose) is used in combination with a single-pool, first order kinetic model to determine blood glucose kinetics [13]. This model is especially of interest for longitudinal studies, due to the ability of repeated measurements.

An animal model to study both efficacy and glucocorticoid-induced metabolic side effects in an inflammatory setting is currently not available. Therefore, in the present study, we aim to develop an inflammatory model which can be used to investigate both efficacy and metabolic safety of GCs in the same animal at the same time by performing the blood glucose kinetics in the CIA mice model. To validate this model and to investigate the mechanisms involved in GC-induced metabolic dysfunction in an inflammatory setting, we performed two consecutive CIA experiments. First, we assessed the effects of several doses of prednisolone (0, 1.5, 10 and 30 mg/kg/day) on efficacy and metabolic safety after 0, 7 and 21 days of treatment. Secondly, in order to distinguish between GR-mediated effects of prednisolone and indirect effects on glucose kinetics resulting from its anti-inflammatory efficacy, we compared effects of prednisolone to those of ORG 37663. This compound has previously been described to be effective for the treatment of arthritis in CIA mice [6], but did not mediate its effect through the GR. Comparing the results from the prednisolone-treated subgroup to the subgroup treated with the non-GR mediated anti-inflammatory compound ORG 37663 allowed us to distinguish between GR-mediated and non-GR-mediated effects.

The results from this study revealed that it was possible to measure both efficacy and metabolic side effects of prednisolone in one experimental set-up, without affecting the severity of disease. Arthritis scores were decreased in arthritic mice after treatment with both prednisolone and ORG 37663. Concerning effects on glucose metabolism, there was a decrease in insulin sensitivity in both arthritic and non-arthritic control mice after treatment with prednisolone for three weeks, while ORG 37663 increased insulin sensitivity. These effects on insulin sensitivity were mainly due to increased insulin secretion in the prednisolone treated animals. The integration of the CIA model with the injection of D-[6,6-$^{2}H_{2}$]-glucose not only provides a valuable tool for both studying the efficacy and metabolic side-effects of experimental glucocorticoids at the same time in one model, but may prove a useful translational model for the metabolic side effects of GCs in patients suffering from RA or other (auto)immune diseases.

Methods

Animals

All experiments were approved by the Animal Welfare Committee of Merck, Oss, The Netherlands. Male DBA/1J mice were obtained from Bomholtgard (Ry, Denmark). Animals were housed and maintained at 23 °C with *ad libitum* access to water and food in a 12

hour-12 hour light-dark cycle (lights on 6 am-6 pm).

Therapeutic murine collagen-induced arthritis

The murine CIA model was performed as previously described [14]. In brief, DBA/1J mice were immunized at the base of the tail at the age of eight weeks with 200 µg bovine type II collagen in complete Freud's adjuvant enriched with 2 mg/ml *M. tuberculosis* (H37Ra). Three weeks after immunization the animals were boosted with an intra-peritoneal injection of 200 µg collagen type II, dissolved in saline. The clinical severity of arthritis (arthritis score) was graded per inflamed digit (a scale of 0 to 2 for each paw). Mice were scored on alternative days, resulting in mean scores with an overall maximum of 8 per animal. To assess the effects of treatment, the area under curve (AUC) of the mean arthritis of each animal with baseline correction (subtracting baseline AUC of arthritis score on day 0) was used. After disease onset, animals with an arthritis score ranging from 2 to 4 were divided into separate groups of 12 mice so that the mean arthritis score of all experimental groups was comparable at the start of the treatment (day 0). Mice were considered to have arthritis when significant changes in redness and/or swelling were noted in the digits or in other parts of the paws.

Treatment and experimental regimes

For the first experiment, a total of 40 arthritic animals were divided into an experimental and a control group of 20 mice each. Both groups were orally treated once a day for 21 days with placebo (0.5% gelatin and 5% mannitol in water) and arthritis development was monitored. In the experimental group (n=20) mice were subjected to a blood glucose kinetics test three times at (on day 0, 7 and 21) while mice in the control group were not subjected to the blood glucose kinetics tests.

For the second experiment, arthritic animals were treated orally once a day for 21 days with either 1.5, 10 or 30 mg/kg prednisolone in vehicle (0.5% gelatin and 5% mannitol in water) or vehicle alone. In total, 48 arthritic mice (12 per treatment group) were included. For control groups, mice were mock immunized with saline at the base of the tail at the age of eight weeks and three weeks later mock boosted with saline. Mice were further treated according the same experimental protocol and handled exactly the same as the mice that developed arthritis. In this study, these mice are referred to as non-arthritic control mice.

For the third experiment, arthritic mice were treated orally once a day for 21 days either with prednisolone (10 mg/kg) or ORG 37663 (12 mg/kg) in vehicle (0.5% gelatin and 5% mannitol in water) or placebo alone. The dose of 12 mg/kg/day for ORG 37663 was se-

lected because this dose is comparable to a dose of 10 mg/kg/day prednisolone regarding efficacy. In total, 36 arthritic mice (12 per treatment group) and 36 control mice, like described above, were included in this consecutive experiment.

All experimental treatments were conducted in a blinded fashion. At the end of the experiment, serum samples and hind knees and paws samples were obtained. Hind knees and paws were evaluated using X-ray analysis to assess bone destruction [15]. X-ray photographs were examined with a Faxitron X-ray MX-20 (0.02 mm resolution) and bone destruction was scored on a scale from 0 to 5 ranging from no damage to complete destruction [16].

Blood glucose kinetics

The fasted blood glucose kinetic test was performed three times; at day 0 (before prednisolone treatment, but after disease onset) and after 7 and 21 days of treatment. For each experiment, mice were fasted for 9 hours, body weights were measured and mice were injected intraperitoneally with a small volume of 2.0 mg D-[6,6-$^2H_2$]glucose in 0.20 ml by intraperitoneal injection (~450 µmol/kg BW) which did not cause changes in blood glucose and plasma insulin concentrations. Before and at 10, 20, 30, 40, 50, 60, 75 and 90 minutes after D-[6,6-$^2H_2$]-glucose administration, blood glucose concentrations were measured in a blood drop collected by tail tip bleeding using a glucocard X-meter (A. Menarini Diagnostics; Valkenswaard; The Netherlands). At the same time points, a small blood spot was taken on filter paper and stored at room temperature until further analysis of D-[6,6-$^2H_2$]-glucose label distribution. After the test blood samples were taken by tail tip bleeding for C-peptide measurements.

Measurements of mass isotopomer distribution by GC-MS

Whole body glucose turnover and clearance were calculated by kinetic analysis from the wash-out of injected D-[6,6-$^2H_2$]-glucose from circulation. The blood spots on filter paper were used for this. Extraction of glucose from filter paper, derivatization of the extracted compounds and gas chromatography-mass spectrometry (GC-MS) measurements of the blood were performed as previously described by Van Dijk and colleagues [17]. In short, a disk was punched out of the blood spots, glucose was extracted from the disk by incubating it in ethanol/water (10:1 v/v) and glucose was derivatized to its pentaacetate-ester. Samples were analyzed by GC-MS with positive ion chemical ionization with ammonia. The fractional isotopomer distribution measured by GC-MS (m_0-m_6) was corrected for the fractional distribution due to natural abundance of ^{13}C by multiple linear regression as described by Lee *et al.* [18] to obtain the excess fractional distribution of mass isotopomers (M_0-M_6) due to dilution of infused labeled compounds.

Table 1

Formulas for calculation of blood glucose kinetics

Eq. 1	Tracer Concentration at t	$C_t = M_t \times [glc]_t$
Eq. 2	Single-pool first-order kinetics	$C_t = C_0^{el} e^{-k^{el}t} - C_0^{ab} e^{-k^{ab}t}$
Eq. 3	Bioavailability	$F = 1 - \left(\frac{C_0^{ab} \times k^{el}}{k^{ab} \times C_0^{el}} \right)$
Eq. 4	Area under the curve	$AUC = \frac{C_0^{el}}{k^{el}} - \frac{C_0^{ab}}{k^{ab}}$
Eq. 5	Metabolic clearance rate	$MCR = \frac{F \times D}{AUC}$
Eq. 6	Apparent volume of distribution	$V = \frac{MCR}{k^{el}}$
Eq. 7	Turnover rate	$Ra = MCR \times BG$
Eq. 8	Pool size	$A = \frac{Ra}{k^{el}}$

The formulas used to calculate the concentration vs. time curves and the kinetic parameters in a first order absorption process in an one-compartment model.
C_t, D-[6,6-^{2}H]-glucose concentration at time point t; M_t, fractional contribution of D-[6,6-^{2}H]-glucose at time point t; $[glc]_t$, blood glucose concentration at time point t. $C(0)^{ab}$, initial concentration of D-[6,6-^{2}H]-glucose determined by extrapolation of the absorption period; $C(0)^{el}$, initial concentration of D-[6,6-^{2}H]-glucose determined by extrapolation of the elimination period; k^{ab}, absorption rate constant; k^{el}, absorption rate constant. D, dose D-[6,6-^{2}H]-glucose administrated; BG, average blood glucose concentration during the test; Ra = EGP

Calculation of blood glucose kinetics

For calculating the blood glucose kinetics parameters EGP (Endogenous Glucose Production) and MCR (Metabolic Clearance Rate), a single-pool, first-order kinetic model was assumed [19-21]. The excess fractional distribution of mass isotopomers (M_2)was used to calculate the first order absorption process in an one-compartment model using SAAM-II software (version 1.2.1; SAAM Institute, University of Washington, Seattle, WA, USA [22]. The formulas used to calculate the concentration *vs.* time curves and the kinetic parameters are outlined in Table 1.

C-peptide measurements

In this study we measured C-peptide concentrations as a marker for insulin production, since the half-life of C-peptide is longer when compared to the half-life of insulin. Peripheral blood samples obtained after each the experiment were centrifuged and the

retrieved serum samples were stored at -20 °C until analyzed. C-peptide concentrations were measured using a commercially available ELISA kit (mouse C-peptide ELISA; Alpco immunoassays, Salem, NH, USA).

Calculation of HOMA-IR

The Homeostasis Model Assessment for Insulin Resistance (HOMA-IR) model combines fasting glucose and insulin concentrations to calculate insulin resistance [23]. Besides using insulin, it is also possible to calculate the HOMA-IR using C-peptide concentrations Wallace 2004. The HOMA-IR expresses changes in insulin sensitivity and β-cell function relative to a population in which these parameters are considered to be normal. In this study, we assume that that the group of healthy mice, treated with placebo, had an insulin resistance (IR) of 1 (no insulin resistance). This group is used as the reference group. The reference value can be calculated from median blood glucose concentration (6.6 mM) during the blood glucose kinetics protocol and the median plasma C-peptide concentration (221 pM) at the end of the test. For this study, the value was 1459. The HOMA-IR was calculated as: $\text{HOMA - IR} = \frac{[\text{Glu}] * [\text{C - peptide}]}{1459}$

In which [Glu] is the blood glucose concentration in mM and [C-peptide] is the C-peptide plasma concentration in pM. An HOMA-IR > 1 indicates induction of insulin resistance and an HOMA-IR < 1 indicates improved insulin sensitivity.

Statistical analysis

All data are represented as mean ± SD except for the arthritis data which is represented as mean ± SEM. Data were analyzed using, where appropriate, the Student's t-test or ANOVA followed by the Tukey *post hoc* test (SPSS, Chicago, IL, USA). A p-value <0.05 was considered significant.

Results

The blood glucose kinetics test does not interfere with arthritis development

Before reliable statements could be made regarding prednisolone-induced effects on arthritis development and glucose kinetics in mice, we wanted to confirm that the blood glucose kinetics protocol itself did not influence arthritis development. Therefore, we first investigated if performing this protocol three times in arthritic mice would affect arthritis development. Figure 1 shows that a triple blood glucose kinetic test in three weeks did not affect AUC of arthritis scores and X-ray scores in the CIA mouse model.

Figure 1

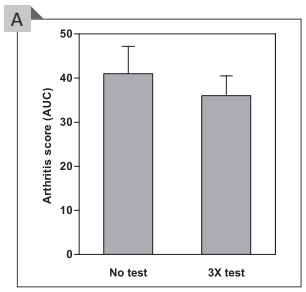

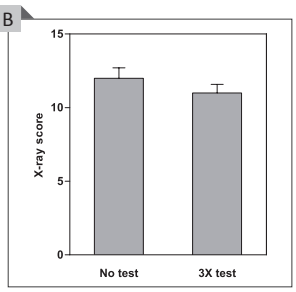

Arthritis development

Arthritis development in mice subjected to blood glucose kinetics three times and in mice in which no experiments were performed. **A,** AUC of the overall arthritis score after 21 days. **B,** X-ray analysis to assess bone destruction. Results are presented as mean ± SEM (n=20). No significant differences between the two groups was observed.

Assessing both the effects of arthritis development and prednisolone treatment on glucose kinetics

Blood glucose kinetics were used to assess both arthritis-induced and prednisolone-induced metabolic dysfunction and was performed three times: at day 0 (before prednisolone treatment) and after 7 and 21 days of treatment. Bodyweights were significantly lower in arthritic mice when compared to non-arthritic mice (p=0.0011) (Fig. 2A). This decrease in bodyweight is caused by the active inflammatory state of these arthritic mice as was previously reported [24]. Even though arthritic mice have lower bodyweights compared to control mice, treatment with several doses of prednisolone for 21 days did not have any effect on bodyweight in both groups (Fig. 2A).

Prednisolone treatment induced apoptosis of thymocytes, thereby severely reducing thymus weight dose-dependently [25]. No differences in thymus weight were observed between arthritic and non-arthritic mice. Treatment with 1.5, 10 and 30 mg/kg prednisolone per day reduced thymus weight respectively with 68%, 80% and 89% in the non-arthritic control group and with 70%, 81% and 85% in the arthritic group (Fig. 2B). These reductions are indicative for sufficient prednisolone exposure in these treatment groups.

To confirm the anti-arthritic properties of prednisolone, arthritic mice were monitored for arthritis score and X-ray score. Prednisolone dose-dependently reduced disease severity since a significant reduction of the AUC arthritis score covering the entire treatment period was observed (Fig. 2C). X-ray analysis of the arthritic joints indicate severe cartilage and bone destruction in the placebo-treated arthritic animals. In line with previous results [6], prednisolone significantly reduced the rate of cartilage and bone destruction in a dose-dependent manner (p=0.0029) (Fig. 2D). As expected, the control mice that were mock immunized with saline and three weeks later mock boosted with saline, did not develop arthritis.

No differences were observed in blood glucose concentrations between arthritic and non-arthritic mice treated with placebo for 21 days (p=0.1050) (Fig. 3A). A small but signifi-

Figure 2

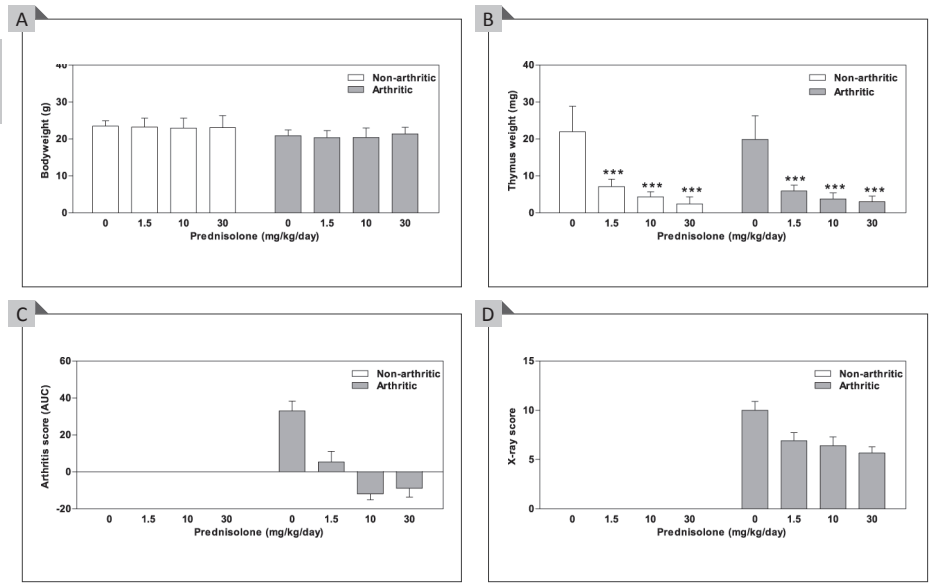

Effects of prednisolone on bodyweight, thymus weight and arthritis development after 21 days of treatment

A, Bodyweight **B,** thymus weight **C,** AUC of the overall arthritis score **D,** X-ray analysis to assess bone destruction. Results are represented as means ± SD for bodyweight and thymus weight and as mean ±SEM for AUC arthritis score and X-ray score and are outlined for each experimental group (n=12). * Significant difference p≤0.05, ** significant difference p≤0.01, *** significant difference p≤0.001

cant dose-dependent decrease in blood glucose concentrations was observed after three weeks of prednisolone treatment in both non-arthritic and arthritic mice (resp. p=0.0064 and p=0.0012) (Fig. 3A).

The glucose kinetics parameters MCR (Metabolic Clearance Rate) and EGP (Endogenous Glucose Production) were calculated by modeling the wash-out of injected D-[6,6-$^{2}H_{2}$]-glucose. EGP was not different between arthritic and non-arthritic mice (p=0.2429) before treatment. A trend towards a decreased EGP was observed after 7 days of prednisolone treatment (Table 2). After 21 days of treatment, prednisolone-treatment slightly but significant decreased EGP both in non-arthritic (p=0.006) and arthritic mice (p=0.0007) (Fig. 3C). MCR showed to be increased in placebo-treated arthritic mice (p=0.0004) when compared to non-arthritic placebo-treated mice but no differences were observed in MCR between the prednisolone treatment groups in both non-arthritic and arthritic mice after three weeks of treatment (Fig. 3B). Interestingly, even though no effects were seen upon three weeks of prednisolone treatment between the groups, MCR is lowered in both the non-arthritic groups and the arthritic groups over time (Table 2 and Fig. 3B).

Table 2

	Non-arthritic mice treated with prednisolone (mg/kg/d)				Arthritic mice treated with prednisolone (mg/kg/d)			
	0	1.5	10	30	0	1.5	10	30
Bodyweight (g) day 0	23.0±1.9	24.3±1.9	24.3±2.0	24.8±1.7	21.0±1.5#	20.7±2.5	20.5±1.5	20.3±1.6
Bodyweight (g) day 7	22.5±1.4	23.3±2.3	22.8±2.4	23.5±1.5	20.4±2.2#	20.1±2.1	20.7±1.8	20.2±1.6
Glucose (mM) day 0	5.2±1.4	4.9±1.5	5.9±1.9	6.3±2.5	5.0±1.1	4.4±1.1	5.1±1.2	4.7±2.0
Glucose (mM) day 7	6.5±1.6	5.1±1.2	4.6±1.1*	4.3±1.1*	5.4±1.0	4.7±1.0	4.7±0.9	4.3±1.7
MCR (ml/kg/min) day 0	14.4±3.2	15.2±2.6	13.4±3.5	11.7±2.2	19.1±3.3#	19.2±3.2	19.0±1.8	17.9±3.4
MCR (ml/kg/min) day 7	15.9±2.2	15.3±2.8	16.1±2.6	17.4±1.5	17.2±2.4	18.4±3.0	17.6±1.5	16.8±2.9
EGP (µmol/kg/min) day 0	71.2±10.9	72.5±22.1	75.3±24.1	72.0±27.7	94.3±24.7	82.0±12.2	95.8±19.5	90.7±7.5
EGP (µmol/kg/min) day 7	100.9±18.6	78.8±23.1	73.0±15.6*	73.1±15.2*	92.0±14.7	84.7±19.2	80.8±9.7	81.3±14.2

Table 3

	Non-arthritic mice			Arthritic mice treated		
	Placebo	Prednisolone	ORG 37663	Placebo	Prednisolone	ORG 37663
Bodyweight (g) day 0	23.5 ± 1.5	23.2 ± 1.0	25.0 ± 2.4	20.9 ± 1.3#	21.5 ± 2.9	20.8 ± 1.3
Bodyweight (g) day 7	24.3 ± 1.6	22.6 ± 1.2	23.7 ± 1.6	21.4 ± 2.2#	21.4 ± 2.7	21.7 ± 1.9
Glucose (mM) day 0	3.5 ± 1.1	4.6 ± 1.7	3.6 ± 1.8	4.8 ± 1.0	5.0 ± 1.1	4.5 ± 0.9
Glucose (mM) day 7	5.3 ± 1.9	4.4 ± 1.2	5.2 ± 1.4	5.7 ± 0.7	4.6 ± 1.0	6.0 ± 0.8
MCR (ml/kg/min) day 0	17.8 ± 9.4	18.6 ± 8.3	15.6 ± 10.2	19.0 ± 4.1	18.9 ± 2.8	13.4 ± 10
MCR (ml/kg/min) day 7	11.6 ± 5.6	14.1 ± 4.9	9.8 ± 6.3	17.0 ± 1.9#	16.7 ± 2.6	8.8 ± 6.9*
EGP (µmol/kg/min) day 0	71.1 ± 13.3	84.6 ± 16.1	68.5 ± 19.5	92.3 ± 25.5#	95.1 ± 21.5	89.9 ± 15.9
EGP (µmol/kg/min) day 7	72.7 ± 25.6	65.5 ± 13.2	65.9 ± 9.8	94.1 ± 14.3#	74.0 ± 7.7*	78.7 ± 12.2*

Treatment parameters for both non-arthritic and arthritic mice treated with prednisolone (Table 2) or ORG 37663 (Table 3) for 21 days
Both non-arthritic and arthritic mice are treated with placebo, prednisolone (0, 1.5, 10 and 30 mg/kg/day) or or ORG 37663 (12 mg/kg/day) for 21 days. Each experimental group consists of 12 mice; in total 48 non-arthritic and 48 arthritic mice were included. For Table 3 a total 36 non-arthritic and 36 arthritic mice were included.
Values represent means ± SD except for arthritis and X-ray scores which are represented in mean ± SEM. * Significant difference ($p \leq 0.05$) when compared to the placebo-treated group of that same parameter. #Significant difference ($p \leq 0.05$) when compared to the placebo-treated non-arthritic mice.

Figure 3

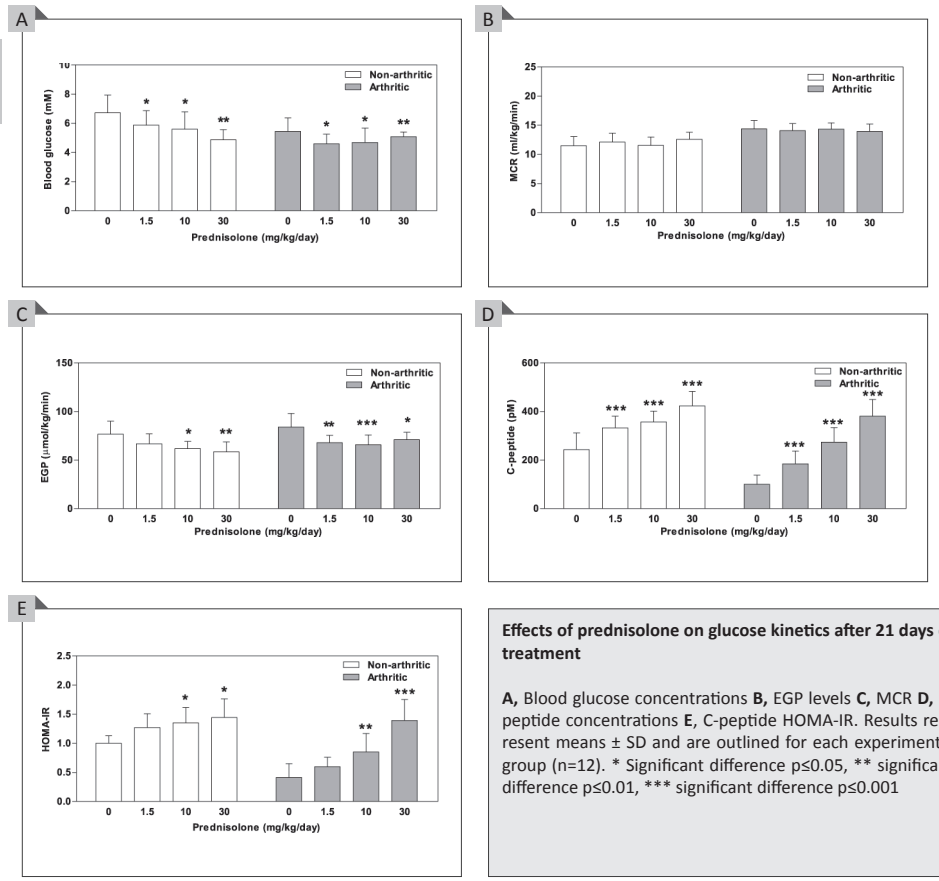

Effects of prednisolone on glucose kinetics after 21 days of treatment

A, Blood glucose concentrations **B,** EGP levels **C,** MCR **D,** C-peptide concentrations **E**, C-peptide HOMA-IR. Results represent means ± SD and are outlined for each experimental group (n=12). * Significant difference p≤0.05, ** significant difference p≤0.01, *** significant difference p≤0.001

Surprisingly, after three weeks of treatment, plasma C-peptide concentrations of placebo treated arthritic mice were significant lower than those of placebo-treated non-arthritic mice (p=0.0006) (Fig. 3D). C-peptide concentrations were strongly increased in a dose-dependent manner by prednisolone in both non-arthritic and arthritic mice, implying increased plasma insulin concentrations. This effect of prednisolone on plasma C-peptide concentrations was already observed after one week of treatment (data not shown).

From the fasting blood glucose and C-peptide concentrations, the HOMA-IR was calculated to evaluate insulin resistance. Remarkably, the HOMA-IR (Fig. 3E) suggests that placebo-treated arthritic mice are 2.3-2.5 times more insulin sensitive than placebo-treated non-arthritic animals. This decrease in HOMA-IR is the direct result of the low C-peptide concentrations as measured in the placebo-treated arthritic mice. According to the HOMA-IR data, prednisolone treatment reduced insulin sensitivity according to HOMA-IR in a dose-dependent manner in both non-arthritic (p=0.0258) and arthritic (p=0.0001) mice.

Figure 4

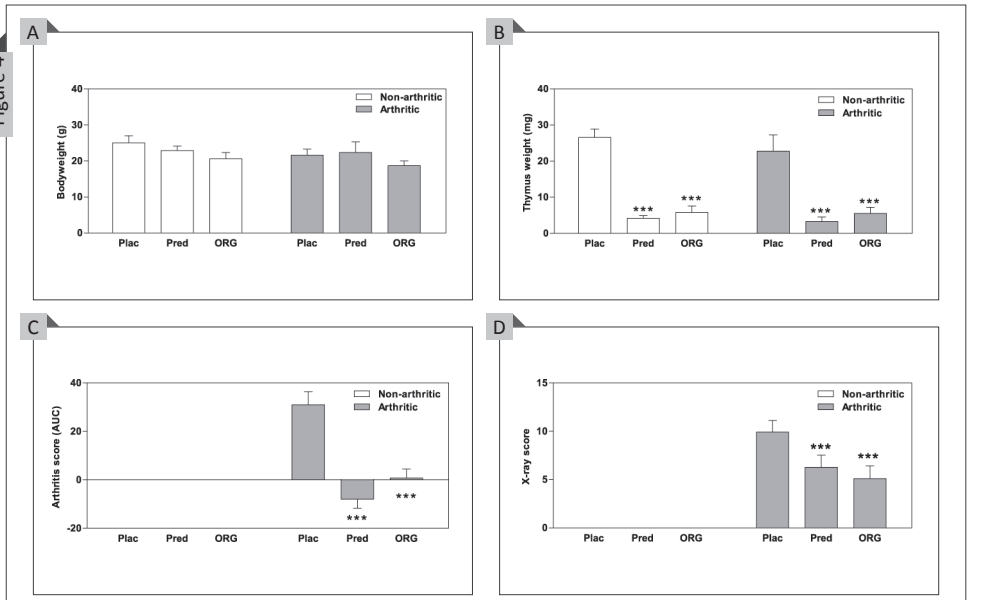

Effects of ORG 37663 and prednisolone on bodyweight, thymus weight and arthritis development after 21 days of treatment

A, Bodyweight **B,** thymus weight **C,** AUC of the overall arthritis score **D,** X-ray analysis to assess bone destruction. Results are represented as means ± SD for bodyweight and thymus weight and as mean ±SEM for AUC arthritis score and X-ray score and are outlined for each experimental group (n=12). * Significant difference p≤0.05, ** significant difference p≤0.01, *** significant difference p≤0.001

After treatment with prednisolone (30 mg/kg/d) for 21 days, both groups were equally resistant to insulin (Fig. 3E).

Assessing the effects of ORG 37663 treatment on glucose kinetics

To be able to distinguish between GR-mediated and non-GR-mediated effects, we performed a second experiment in which non-arthritic and arthritic mice were treated with ORG 37663. This compound is a steroid that was previously shown to have anti-inflammatory properties and effectively reduces arthritis in the CIA model. ORG 37663 mediates its effects through a mechanism that is independent of GR binding [6]. Therefore, ORG 37663 was used in a head-to-head comparison to prednisolone in one experiment to study to what extent effects of prednisolone on glucose kinetics are due to its anti-inflammatory properties or due to a direct effect through GR.

Similar to the first experiment, bodyweights were significantly lower in arthritic mice compared to non-arthritic mice (p=0.0001) (Fig. 4A). Non-arthritic mice showed to have lower bodyweights after treatment with prednisolone (p=0.01) or ORG 37663 (p=0.001) (Fig.

4A). No differences in thymus weight were observed between arthritic and non-arthritic mice. In the non-arthritic control group treatment with 10 mg/kg prednisolone or 12 mg/kg ORG 37663 per day reduced thymus weight respectively with 84% and 78% (Fig. 4B). In the arthritic group thymus weight was reduced with 86% and 76%, again indicative for sufficient compound exposure. In the arthritic mice, both arthritic score and X-ray score were significantly decreased ($p<0.0001$ and $p=0.0279$ respectively) after treatment with either prednisolone or ORG 37663 (Fig. 4C-D).

Arthritic mice showed slight but significant lower blood glucose concentrations after ORG 37663 treatment ($p=0.036$) (Fig. 5A). In the non-arthritic mice no statistical difference in blood glucose concentrations were detected between the treatments (Fig. 5A). Yet, EGP was decreased after treatment with either prednisolone or ORG 37663 in non-arthritic mice ($p=0.0003$), while in arthritic mice, a trend towards decreased EGP levels after both treatments was observed (Fig. 5C). Non-arthritic mice treated with prednisolone or ORG

Figure 5

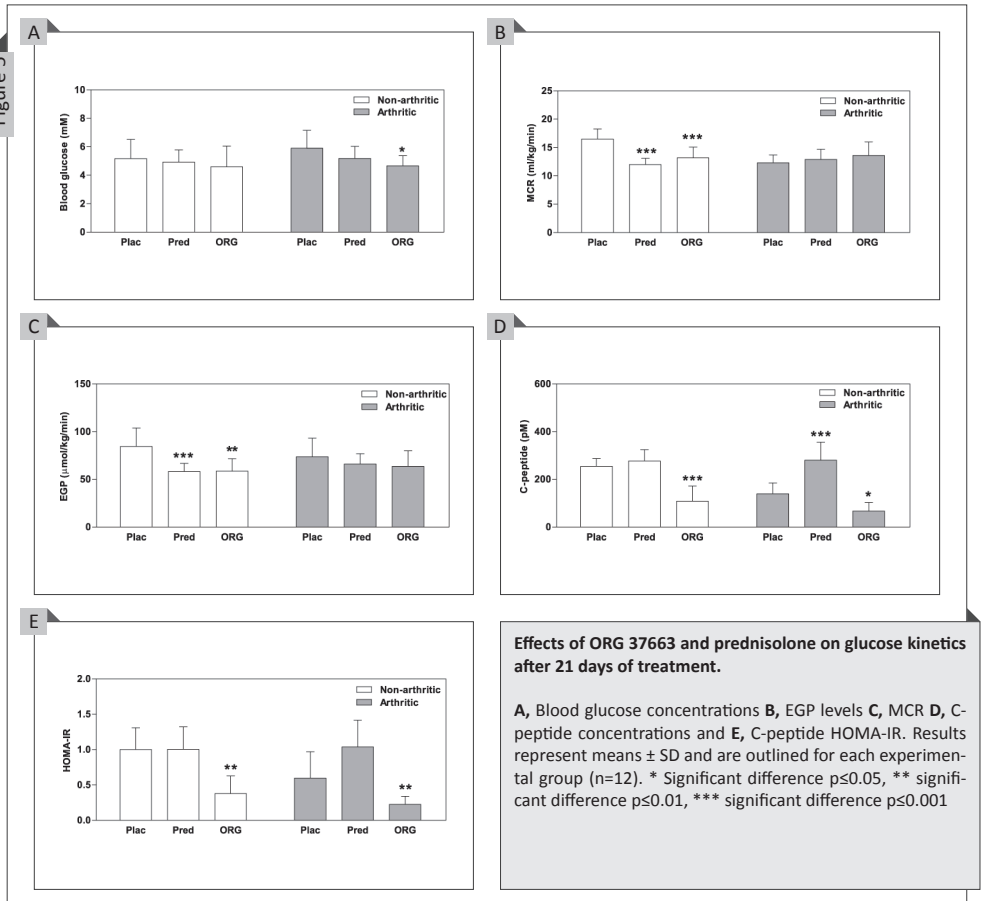

Effects of ORG 37663 and prednisolone on glucose kinetics after 21 days of treatment.

A, Blood glucose concentrations **B,** EGP levels **C,** MCR **D,** C-peptide concentrations and **E,** C-peptide HOMA-IR. Results represent means ± SD and are outlined for each experimental group (n=12). * Significant difference p≤0.05, ** significant difference p≤0.01, *** significant difference p≤0.001

37663 both had a lower MCR compared to placebo treated mice ($p<0.0001$), while this effect was not observed in the arthritic mice after treatment (Fig. 5B). As was observed in the prednisolone dose-response experiment, C-peptide concentrations from arthritic mice treated with placebo were significant lower compared to the non-arthritic mice treated with placebo after three weeks of treatment (Fig. 5D). The ORG 37663 compound caused a major decrease in C-peptide concentrations in both non-arthritic mice ($p<0.0001$) and arthritic mice ($p<0.05$) (Fig. 5D). As a consequence of the low C-peptide concentrations after treatment with ORG 37663, both arthritic and non-arthritic mice showed a tremendous increase in insulin sensitivity as calculated by the HOMA-IR (Fig. 5E). These data indicate that treatment with ORG 37663 improved insulin sensitivity in mice.

Discussion

There is an urgent need for improved GCs that are as effective as classical GCs, but have a better safety profile. However, an *in vivo* inflammatory model in which (experimental) GCs can be studied for both their effectiveness and the induction of metabolic side effects is currently unavailable. Goal of the present study was to develop such an *in vivo* inflammatory model for metabolic adverse effects. Therefore we have integrated a single-pool, first order kinetic protocol to examine blood glucose kinetics, in the well-established collagen-induced arthritis (CIA) mice model, an inflammatory model which is often used to monitor efficacy of experimental anti-inflammatory compounds. In general, trends in effects of prednisolone on glucose kinetics were similar in both arthritic mice and in the non-arthritic control group. Also the effects of ORG 37663, a non-GR mediated compound, were similar in both arthritic and non-arthritic groups. This indicates that the arthritic state of the animals does not interfere or changes the effect of prednisolone on glucose kinetics. Importantly, this also indicates that we have successfully performed blood glucose kinetics in the CIA model enabling the quantification of both efficacy and adverse effects on glucose metabolism in one animal.

This study showed that prednisolone decreased disease severity and joint destruction in arthritic mice, thereby confirming the anti-inflammatory properties of this compound. Regarding the induction of metabolic effects, prednisolone slightly decreased fasted glucose concentrations and EGP, but strongly increased insulin production (as measured by the increase in C-peptide concentrations) at the same time in both non-arthritic and arthritic mice. This resulted in an increased HOMA-IR after prednisolone treatment, indicating the induction of insulin resistance. The additive value of the applied blood glucose kinetic model, i.e., the injection of D-[6,6-$^2H_2$]-glucose, is that this allowed for discrimination of

the changes in glucose metabolism in peripheral tissues and the liver since the MCR reflects peripheral glucose metabolism and EGP (can be regarded as hepatic glucose production in fasted conditions) reflects hepatic glucose metabolism. To our knowledge, no animal model was previously described which enables quantification of both anti-arthritic efficacy and longitudinal tissue-specific metabolic adverse effects in one animal in one chronic treatment protocol. In the field of GCs and the search for compounds with improved efficacy/safety profiles (SGRMs), such a model would potentially be of great value since it closely mimics the clinical RA practice.

The 'gold standard' to investigate and quantify insulin resistance is the hyperinsulinemic euglycemic clamp (HIEC) [26]. However, seen from the perspective of laboratory animal welfare, performing such clamp studies within an inflammatory mice model such as the CIA model is impossible. Measuring glucose kinetics by modeling the wash-out of *ip* injected D-[6,6-$^{2}H_{2}$]-glucose is performed under fasted conditions whereas the HIEC utilizes steady-state insulin concentrations that are supraphysiological [13,27]. Thus, the wash-out of ip-injected glucose presumably reflects a more physiological relevant situation. In addition, unlike the HIEC the blood glucose kinetics can be applied repeatedly and is therefore applicable in longitudinal studies, such as the CIA model described here.

GCs are well known to reduce insulin sensitivity and induce β-cell dysfunction. In line with our results, several studies reported increased insulin secretion in both wild-type rodents [28] and healthy humans [29,30] after prolonged exposure to GCs. Also in RA patients an association between the use of GCs and decreased insulin sensitivity was reported [31]. To compensate for this insulin resistance, the pancreatic islets enhance their cell mass and insulin secretion. However, when the functionally expansion of islet β-cells fails to compensate for the degree of insulin resistance, insulin deficiency and ultimately GC-induced diabetes will develop. Both the non-arthritic and arthritic mice in this study were, after 21 days of prednisolone treatment, still able to compensate for their prednisolone-induced insulin resistance, resulting in no effects on blood glucose concentrations. Most likely, the treatment period (3 weeks) in this combined model is too short to study a next stage in the development of diabetes, *i.e.*, hyperglycemia and beta-cell dysfunction. Further studies will be needed to challenge this.

Both non-arthritic and arthritic mice were included in this study in order to distinguish between inflammation-induced and GC-induced metabolic dysfunction. Our results showed that arthritic mice produce less C-peptide than non-arthritic mice after treatment with placebo. This discrepancy in C-peptide production is probably due to differences in pro-inflammatory cytokine levels between healthy and arthritic mice. It is known that arthritic mice have elevated circulating levels of the pro-inflammatory cytokines TNFα and IL-1β [14].

Impaired function and cell death of both human and rodent β-cells after exposure to TNFα and IL-1β is well established [32-36]. Several potential mechanisms have been suggested for these effects including activation of MAP kinases, c-jun N-terminal kinase, p38, ERK, NF-κB and altered gene expression [36]. Recently, Muayed and co-workers reported reduced insulin secretion in murine and rat islet cells after TNFα and IL-1β mediated down regulation of ZnT8, a zinc transporter important for normal β-cell physiology [37]. Nonetheless, based upon the unchanged glucose concentrations, the untreated arthritic mice in our study were still able to compensate for the inflammation-induced reduction of insulin secretion. Both highly arthritic mice and mice treated with a high dose of prednisolone are able to compensate for reduced insulin secretion and/or reduced insulin sensitivity by keeping the MCR steady and even reduce EGP, which indicates a highly adaptive compensatory mechanism in these mice. It stresses the fact that cytokines such as TNFα and IL-1β or glucocorticoids do not operate in isolation but in a complex network of potentiating and inhibiting metabolic, inflammatory and endocrine modulating phenotypic outcome.

To be able to study to what extent effects of prednisolone on glucose kinetics are due to its anti-inflammatory properties or due to a direct effect through GR, mice were also treated with ORG 37663 and directly compared to prednisolone. ORG 37663 mediates its effects through a mechanism that is independent of GR binding. Treatment with ORG 37663 resulted in lower C-peptide concentrations when compared to prednisolone treatment in both non-arthritic and arthritic mice. This indicates that prednisolone mediates its effects on insulin secretion directly via GR and not via indirect anti-inflammatory effects.

To conclude, we successfully integrated the whole body glucose test in the CIA mice model, which enabled us to measure both efficacy and metabolic adverse effects of (experimental) GCs in an *in vivo* inflammatory setting. Thereby, it may prove a useful translational model for GC-induced metabolic derangements in patients suffering from RA or other (auto)immune diseases. This study showed that both inflammation and glucocorticoids affect insulin secretion and sensitivity but this did not lead immediately to the development of hyperglycemia and type 2 Diabetes Mellitus. This emphasizes the highly adaptive character of these mice and the complex network of several integrated mechanisms underlying the development of GC-induced and/or inflammation-induced metabolic dysfunction.

Reference List

1. Hillier, S. G. Diamonds are forever: the cortisone legacy. J. Endocrinol. 195, 1-6 (2007).
2. Rhen, T. & Cidlowski, J. A. Antiinflammatory action of glucocorticoids--new mechanisms for old drugs. N. Engl. J Med. 353, 1711-1723 (2005).
3. Schäcke, H., Docke, W. & Asadullah, K. Mechanisms involved in the side effects of glucocorticoids. Pharmacology & Therapeutics 96, 23-43 (2002).
4. Schäcke, H., Berger, M., Rehwinkel, H. & Asadullah, K. Selective glucocorticoid receptor agonists (SEGRAs): novel ligands with an improved therapeutic index. Mol Cell Endocrinol. 275, 109-117 (2007).
5. van Raalte, D. H., Ouwens, D. M. & Diamant, M. Novel insights into glucocorticoid-mediated diabetogenic effects: towards expansion of therapeutic options? Eur. J Clin Invest 39, 81-93 (2009).
6. Dulos, J. et al. Suppression of the inflammatory response in experimental arthritis is mediated via estrogen receptor alpha but not estrogen receptor beta. Arthritis Res Ther. 12, R101 (2010).
7. Thompson, C. S. Animal models of diabetes mellitus: relevance to vascular complications. Curr. Pharm. Des 14, 309-324 (2008).
8. Miner, J. N. et al. Antiinflammatory glucocorticoid receptor ligand with reduced side effects exhibits an altered protein-protein interaction profile. Proceedings of the National Academy of Sciences 104, 19244-19249 (2007).
9. Hwang, J., Rodgers, K., Oliver, J. C. & Schluep, T. Alpha-methylprednisolone conjugated cyclodextrin polymer-based nanoparticles for rheumatoid arthritis therapy. Int J Nanomedicine. 3, 359-371 (2008).
10. Courtenay, J. S., Dallman, M. J., Dayan, A. D., Martin, A. & Mosedale, B. Immunisation against heterologous type II collagen induces arthritis in mice. Nature 283, 666-668 (1980).
11. Stuart, J. M., Townes, A. S. & Kang, A. H. Nature and specificity of the immune response to collagen in type II collagen-induced arthritis in mice. J Clin Invest 69, 673-683 (1982).
12. Monzillo, L. U. & Hamdy, O. Evaluation of insulin sensitivity in clinical practice and in research settings. Nutr. Rev. 61, 397-412 (2003).
13. Laskewitz, A. J. et al. Chronic Prednisolone Treatment Reduces Hepatic Insulin Sensitivity while Perturbing the Fed-to-Fasting Transition in Mice. Endocrinology 15, 2171-2178 (2010).
14. Joosten, L. A., Helsen, M. M., van de Loo, F. A. & van den Berg, W. B. Anticytokine treatment of established type II collagen-induced arthritis in DBA/1J mice: a comparative study using anti-TNFalpha, anti-IL-1alpha/beta and IL-1Ra. Arthritis Rheum. 58, S110-S122 (2008).
15. Dulos, J., Verbraak, E., Bagchus, W. M., Boots, A. M. & Kaptein, A. Severity of murine collagen-induced arthritis correlates with increased CYP7B activity: enhancement of dehydroepiandrosterone metabolism by interleukin-1beta. Arthritis Rheum. 50, 3346-3353 (2004).
16. Joosten, L. A. et al. IL-1 alpha beta blockade prevents cartilage and bone destruction in murine type II collagen-induced arthritis, whereas TNF-alpha blockade only ameliorates joint inflammation. J Immunol. 163, 5049-5055 (1999).
17. van Dijk, T. H. et al. Quantification of hepatic carbohydrate metabolism in conscious mice using serial blood and urine spots. Anal. Biochem. 322, 1-13 (2003).
18. Lee, W. N., Byerley, L. O., Bergner, E. A. & Edmond, J. Mass isotopomer analysis: theoretical and practical considerations. Biol. Mass Spectrom. 20, 451-458 (1991).
19. Ader, M., Ni, T. C. & Bergman, R. N. Glucose effectiveness assessed under dynamic and steady state conditions. Comparability of uptake versus production components. J Clin Invest 99, 1187-1199 (1997).

20. Best, J. D. et al. Role of glucose effectiveness in the determination of glucose tolerance. Diabetes Care 19, 1018-1030 (1996).

21. Pacini, G., Thomaseth, K. & Ahren, B. Contribution to glucose tolerance of insulin-independent vs. insulin-dependent mechanisms in mice. Am J Physiol Endocrinol. Metab 281, E693-E703 (2001).

22. van Dijk, T. H. et al. An increased flux through the glucose 6-phosphate pool in enterocytes delays glucose absorption in Fxr-/- mice. J Biol. Chem 284, 10315-10323 (2009).

23. Matthews, D. R. et al. Homeostasis model assessment: insulin resistance and beta-cell function from fasting plasma glucose and insulin concentrations in man. Diabetologia 28, 412-419 (1985).

24. Kokkola, R. et al. Successful treatment of collagen-induced arthritis in mice and rats by targeting extracellular high mobility group box chromosomal protein 1 activity. Arthritis Rheum. 48, 2052-2058 (2003).

25. Compton, M. M. & Cidlowski, J. A. Rapid in vivo effects of glucocorticoids on the integrity of rat lymphocyte genomic deoxyribonucleic acid. Endocrinology 118, 38-45 (1986).

26. DeFronzo, R. A., Tobin, J. D. & Andres, R. Glucose clamp technique: a method for quantifying insulin secretion and resistance. Am. J. Physiol 237, E214-E223 (1979).

27. Muniyappa, R., Lee, S., Chen, H. & Quon, M. J. Current approaches for assessing insulin sensitivity and resistance in vivo: advantages, limitations, and appropriate usage. Am J Physiol Endocrinol. Metab 294, E15-E26 (2008).

28. Ogawa, A. et al. Roles of insulin resistance and beta-cell dysfunction in dexamethasone-induced diabetes. J Clin Invest 90, 497-504 (1992).

29. Henriksen, J. E., Alford, F., Ward, G. M. & Beck-Nielsen, H. Risk and mechanism of dexamethasone-induced deterioration of glucose tolerance in non-diabetic first-degree relatives of NIDDM patients. Diabetologia 40, 1439-1448 (1997).

30. van Raalte, D. H. et al. Acute and 2-week exposure to prednisolone impair different aspects of beta-cell function in healthy men. Eur. J Endocrinol 162, 729-735 (2010).

31. Dessein, P. H., Joffe, B. I., Stanwix, A. E., Christian, B. F. & Veller, M. Glucocorticoids and insulin sensitivity in rheumatoid arthritis. J Rheumatol. 31, 867-874 (2004).

32. Corbett, J. A. & McDaniel, M. L. Intraislet release of interleukin 1 inhibits beta cell function by inducing beta cell expression of inducible nitric oxide synthase. J Exp. Med. 181, 559-568 (1995).

33. Rabinovitch, A. & Suarez-Pinzon, W. L. Cytokines and their roles in pancreatic islet beta-cell destruction and insulin-dependent diabetes mellitus. Biochem. Pharmacol. 55, 1139-1149 (1998).

34. Xenos, E. S. et al. Effect of tumor necrosis factor alpha and of the soluble tumor necrosis factor receptor on insulin secretion of isolated islets of Langerhans. Transplant. Proc. 24, 2863-2864 (1992).

35. Xenos, E. S. et al. IL-1 beta-induced inhibition of beta-cell function is mediated through nitric oxide. Transplant. Proc. 25, 994 (1993).

36. Donath, M. Y., Storling, J., Berchtold, L. A., Billestrup, N. & Mandrup-Poulsen, T. Cytokines and beta-cell biology: from concept to clinical translation. Endocr. Rev. 29, 334-350 (2008).

37. El Muayed M. et al. Acute cytokine-mediated downregulation of the zinc transporter ZnT8 alters pancreatic beta-cell function. J Endocrinol. 206, 159-169 (2010).

7

Prednisolone treatment leads to excessive dyslipidemia in mice carrying a dimerization-defective glucocorticoid receptor

Manuscript in preparation

Anke J. Laskewitz
Alexander Rauch
Aldo Grefhorst
Holger Reichhardt
Folkert Kuipers
Jan P. Tuckerman
Albert K. Groen

Abstract

Synthetic glucocorticoids, such as prednisolone, are potent anti-inflammatory drugs. Their use, however, is limited by the severe side effects they may induce. Many of the side effects resemble features of the metabolic syndrome, such as weight gain, insulin resistance and dyslipidemia. Glucocorticoids act via the glucocorticoid receptor (GR) either in a dimeric or monomeric manner. In order to segregate monomeric from dimeric GR effects on dyslipidemia, we treated GR^{dim} mice, that carry a mutation in the dimerization loop of the DNA binding domain, with prednisolone for six days. This treatment did not influence fasting glucose levels in GR^{dim} mice, but strongly increased plasma triglyceride and cholesterol levels. This was already apparent after one day of treatment. Prednisolone treatment resulted in a dramatic 9-12 fold increase of triglycerides and free cholesterol in the VLDL-sized lipoprotein fractions of prednisolone-treated GR^{dim} mice. Surprisingly, hepatic cholesterol(ester) content did not change. The unusual lipid profile was not caused by cholestasis as plasma bile acid concentration did not increase. Hepatic gene expression levels of lipoprotein lipase *(Lpl)* were 23 times induced, but when plasma LPL activity was blocked, there was only a slight increase in VLDL-TG production. In conclusion, this study shows that prednisolone treatment in GR^{dim} mice leads to formation of an atypical VLDL particle containing high levels of triglyceride, phospholipids and free cholesterol. These results indicate an important role of monomeric GR in regulation of lipid metabolism and this may contribute to unravelling the mechanisms underlying glucocortoid-induced side effects.

Introduction

Synthetic glucocorticoids (GCs) are worldwide the most prescribed drugs for auto-immune disorders, such as inflammatory bowel disease, asthma and rheumatoid arthritis, because of their potent action to reduce inflammation [1]. However, their use is limited by the many adverse effects they induce such as osteoporosis, insomnia, depression, insulin resistance, weight gain and dyslipidemia [2,3]. Interestingly, the latter three are also components of the metabolic syndrome, a cluster of metabolically related factors that together increase the risk for cardiovascular disease and Diabetes Mellitus type II [4].

GCs act via the glucocorticoids receptor (GR), a member of the nuclear receptor family [5,6] which is ubiquitously expressed. In the cytoplasm of a target cell GCs bind to the GR, upon which the GR can be imported into the nucleus. Once in the nucleus the GR requires homodimerization to bind to glucocorticoid response elements (GRE) of target genes on the DNA, a process called transactivation. Ligand-activated GR can also reside within the cytoplasm, where it can monomerically interact with other proteins, like PI3K and JNK, to interfere in the inflammation response [7,8]. Another monomeric action of GR takes place inside the nucleus, by binding of GR monomers to pro-inflammatory transcription factors, such as NF-κB and AP-1 [9,10] causing transrepression. The ability to dissociate the transactivating effects from transrepression was shown *in vitro* [11]. Development of GR^{dim} mouse that carry a point mutation in the dimerization interface of the DNA binding domain resulting in a defective dimerization domain [12], allowed for the discrimination between monomeric and dimeric effects of the GR *in vivo* [13].

In particular GR^{dim} mice were still able to exert certain GC-induced anti-inflammatory responses, like AP-1[14] and NF-κB [15] thereby being able to prevent irritant skin inflammation, showing that these anti-inflammatory properties of GCs are acting via GR monomers. However, not all anti-inflammatory properties of GCs were preserved in GR^{dim} mice, since in GR^{dim} mice GCs do not prevent contact hypersensitivity [16], or prevent LPS-induced sepsis (Kleyman *et al*. FASEB J in press) [13] or arthritis (Baschant *et al.* PNAS in press). Traditionally dimerization-induced gene expression was attributed to side effects, due to GR dimer-induced gene expression for instance [17]. Interestingly, GCs still induced osteoporosis in GR^{dim} mice [18], whereas metabolic side effects have been poorly investigated so far. A micro-array study on mRNA expression in livers of prednisolone-treated WT and GR^{dim} mice revealed a clear dissociation of direct and indirect GR target genes [17], however there were no differences between vehicle-treated WT and GR^{dim} mice in gene-expression patterns. Upon prednisolone-treatment ~500 probe sets were significant regulated in WT mice, while only 34 probe sets were regulated in GR^{dim} mice, showing that the effects of the GR^{dim} mutation only become apparent upon stimulation with a GR ligand.

In Cushing's syndrome, *i.e.*, excess of either endogenous GCs or exogenous GCs, hepatic fat accumulation has been shown [19,20] and dyslipidemia has repeatedly been reported as an adverse effect of GC treatment [21,22]. Moreover, Lemke *et al.* revealed that hepatic GR controls expression of genes involved in fatty acid oxidation and lipolysis pathway and that dyslipidemia in *db/db* mice can be reversed by deleting hepatic GR [23]. The micro-array study of Frijters *et al*. [17] showed that genes involved in lipid and glucose metabolism were among the differentially regulated gene sets. We therefore hypothesized that the adverse effects on lipid and glucose metabolism caused by chronic prednisolone treatment should be abolished in GR^{dim} mice. In the current study we assessed the effects of prednisolone treatment in GR^{dim} mice on lipid metabolism. Surprisingly, prednisolone treatment led to excessive dyslipidemia in GR^{dim} mice.

Materials and methods

Animals and treatment

Female GR^{dim} mice [12] on a BALB/c background and their wild type littermates (n=5-7) were housed at the Leibniz Institute for Age Research, Fritz Lipmann Institute, Jena, Germany or transported to the animal facility of the University Medical Center Groningen and housed under IVC conditions, in a 12 hour-12 hour light-dark cycle (lights on 7 am-7 pm). The mice had free access to water and a standard laboratory chow (RMH-B, Abdiets, Woerden, The Netherlands). Female mice of 3 months were continuously treated with prednisolone for 7 days by subcutaneous implantation of slow-release pellets, resulting in a calculated dose of 12.5 mg/kg/day (15 mg; 60 day release; Innovative Research of America Inc.). All experiments were approved by the Ethics Committee for Animal Experiments of the State University Groningen and with permission of the responsible authorities of Thüringen.

Plasma lipid and lipoprotein analysis

Before and during prednisolone treatment orbital blood samples were taken from 4-hour fasted mice, plasma was separated and samples were stored at -20 ˚C for plasma lipid analysis. Plasma triglycerides and total cholesterol was measured by commercially available kits (Roche/Hitachi, Roche Diagnostics-GmbH, Mannheim). Plasma phospholipids, free cholesterol and non-esterified fatty acids were measured by commercially available kits from Diasys (Diagnostic Systems-GmbH, Holzheim, Germany). Plasma lipoproteins from pooled plasma samples were separated using fast protein liquid chromatography (FPLC) on a Superose 6 column (GE Healthcare, Uppsala, Sweden) [24]. In the resulting fractions triglycerides, total and free cholesterol and phospholipids were analyzed as described

above. From the FPLC fractions Apolipoprotein (Apo)A and ApoB were analyzed by western blot analysis from (Meridian) and (Calbiochem), respectively. The VLDL core:surface ratio was calculated by the sum of triglycerides and cholesterylesters (core) from the FPLC fractions 8-15 divided by the sum of free cholesterol and phospholipids (surface) of these fractions. Hepatic lipids were extracted from the liver homogenates according to Bligh and Dyer [25] and measured using similar kits for plasma lipid analysis.

VLDL production

A separate group of mice were fasted for 4 hours and injected intraperitoneally with Poloxamer 407 (1g/kg BW) dissolved in saline as previously described [26]. Orbital blood samples were taken at time points 0h, 1h, 2h, 3h and 4 hours after injection from which plasma was separated and stored at -20 ˚C until analysis of triglyceride content as described above. VLDL-TG production rate was calculated from the slope of the TG concentration *vs*. time curve from the last 2 hours, corrected for amount of plasma/kg bodyweight.

Bile cannulation

After 7 days of prednisolone or vehicle treatment mice were subjected to bile cannulation. Mice were anaesthetized by an *ip* injection of Hypnorm (1mL/kg) (fentanylcitrate 0.315 mg/mL and fluanisone 10 mg/mL, VetaPharma, Leeds, UK) and diazepam (10 mg/kg) (Centrafarm, Etten-Leur, The Netherlands). The gallbladder was cannulated as described previously [27]. For correct measurements, bile of the first 5 min was discarded after which bile was collected for 30 minutes, during which mice were placed in a humidified incubator to maintain body temperature. Bile flow was determined gravimetrically, assuming a density of 1 g/ml for bile. The collected bile was analyzed for bile acid profile, cholesterol and phospholipid content as previously described [28].

Gene expression

For analysis of hepatic gene expression, hepatic RNA was isolated from snap frozen, crushed livers using the TriReagent method (Sigma, St. Louis, MO, USA) according to manufactures protocol. Using a Nanodrop spectrophotometer the integrity and concentration of RNA was determined (NanoDrop™ 1000 Spectrophotometer, Thermo Scientific, Waltham, MA). cDNA was obtained using the reverse transcription procedure with Moloney murine leukemia virus-RT (Roche Diagnostics, Mannheim, Germany; Greiner BioOne, Alphen a-d Rijn, The Netherlands) with random primers according to manufactures protocol. cDNA levels were measured in real-time quantitative PCR amplification using an ABI PRISM 7700 sequence detector (Applied biosystems, Foster City, USA) against a calibration curve of pooled cDNA solutions. Expression levels were normalized for *Rplp0* (ribo-

somal protein, large, P0 (*36b4*)). The sequence of all primers and probes are deposited at RTPrimerDB (http://www.rtprimerdb.org).

Statistics

All data are represented as mean ± SEM. Statistical analysis for multiple comparison were performed by Kruskal-Wallis test, followed for two independent groups by Mann-Whitney-U tested, corrected for multiple testing, using SPSS for Windows software (SPSS, Chicago, IL, USA). Significance was considered at a level of $p<0.05$.

Results

GR^{dim} mice are hypersensitive for prednisolone-induced dyslipidemia

At baseline, all mice had similar bodyweights (Table 1). Seven days of prednisolone treatment reduced bodyweight in WT mice compared to baseline by almost 10% (Table 1), while in GR^{dim} mice prednisolone-treatment did not alter bodyweight. Yet, food intake was similar in all groups. Prednisolone treatment had no effect on fasting plasma glucose levels in either WT or GR^{dim} mice. However, fasting insulin levels were drastically increased by prednisolone treatment in WT mice almost 9-fold, suggestive for insulin resistance, while a lack of dimerization of the GR greatly prevented this increase in GR^{dim} mice, to

Table 1

	WT control	GR^{dim} control	WT Prednisolone	GR^{dim} Prednisolone
Bodyweight (g) day 0	21.5 ± 1.3	22.6 ± 1.4	21.9 ±1.1	21.7 ± 1.6
Bodyweight (g) day 7	22.0 ± 0.7	22.9 ± 1.4	19.9 ± 1.0*	21.5 ± 1.3
Δ bodyweight (g)	0.5 ± 0.8	0.3 ± 1.2	-1.9 ± 0.7*	0.2 ± 0.4
Food intake (g/day)	3.5 ± 0.5	3.2 ± 0.3	3.4 ± 0.2	3.5 ± 0.5
Plasma				
Glucose (mM) fasted	5.1± 0.6	5.0 ± 0.6	5.2 ± 0.5	5.2 ± 0.3
Insulin (mU/l)	9.4 ± 4.3	11.9 ± 5.7	84.7 ± 37.7*	24.9 ± 9.2$^{*\#}$
Triglycerides (mM)	0.8 ± 0.2	1.2 ± 0.3$^{\#}$	1.3 ± 0.3*	10.1 ±3.1$^{*\#}$
Total cholesterol (mM)	0.3 ± 0.2	0.6 ± 0.4$^{\#}$	0.7 ± 0.7*	1.3 ± 0.6*
NEFA (mM)	1.1 ± 0.1	1.6 ± 0.5$^{\#}$	1.4 ± 0.5	2.4 ± 0.8*
Phospholipids (mM)	1.1 ± 0.3	1.9 ± 0.9	2.6 ± 0.9*	3.4 ± 1.6*

Plasma parameters of vehicle or prednisolone-treated WT and GR^{dim} mice
* p <0.05 ctrl *vs* prednisolone; $^{\#}$ p <0.05 between genotype .

a modest 2-fold increase. At baseline, GR^{dim} mice had slightly elevated plasma levels of triglycerides, cholesterol and non-esterified free fatty acids (NEFA). Surprisingly, prednisolone treatment strongly increased plasma lipids in GR^{dim} mice; total plasma cholesterol were increased 2-fold, triglycerides as much as 8-fold compared to untreated GR^{dim} mice. In WT mice prednisolone treatment increased plasma lipid levels to a considerably lesser extent (Table 1).

In order to determine the effect of prednisolone on lipoprotein distribution, plasma samples from untreated and 7-days prednisolone-treated WT and GR^{dim} mice were pooled and fractionated by fast protein liquid chromatography (FPLC). Separation of plasma lipoproteins revealed that the majority of triglycerides in prednisolone-treated GR^{dim} mice, was present in the VLDL-sized fractions. In contrast, prednisolone treatment in WT mice appeared to reduce TG in the VLDL-sized fractions (Fig. 1A). In addition, phospholipid levels strongly increased in the VLDL-sized fractions in GR^{dim} mice treated with prednisolone,

Figure 1

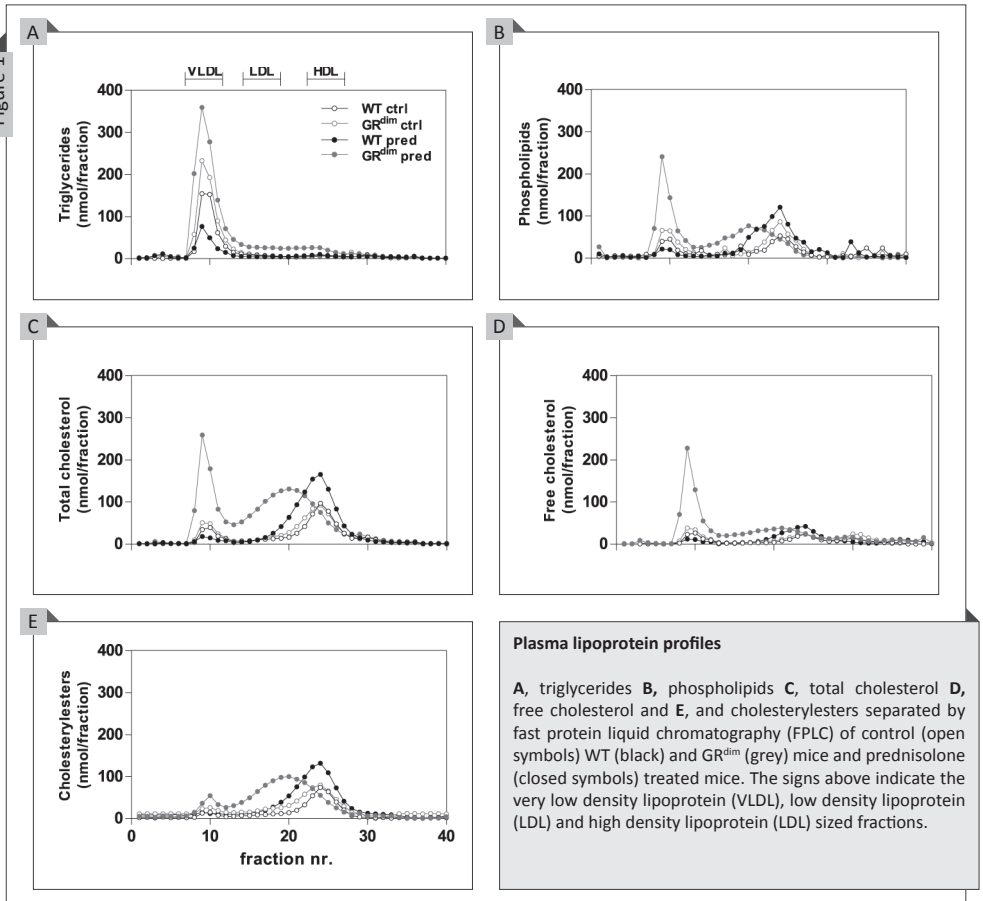

Plasma lipoprotein profiles

A, triglycerides **B,** phospholipids **C**, total cholesterol **D,** free cholesterol and **E**, and cholesterylesters separated by fast protein liquid chromatography (FPLC) of control (open symbols) WT (black) and GR^{dim} (grey) mice and prednisolone (closed symbols) treated mice. The signs above indicate the very low density lipoprotein (VLDL), low density lipoprotein (LDL) and high density lipoprotein (LDL) sized fractions.

while in WT mice most of the phospholipids were present in the HDL-sized fractions (Fig. 1B). In WT mice, prednisolone slightly increased phospholipid levels in the HDL-sized fractions. Total cholesterol levels revealed a similar pattern, *i.e.*, high total cholesterol levels in the VLDL-sized fractions of prednisolone-treated GR^{dim} mice versus a slightly increased total cholesterol level in prednisolone-treated WT mice (Fig. 1C). Cholesterol in the VLDL-sized fractions of prednisolone-treated GR^{dim} mice was mainly in its free form (Fig. 1D), while there was an increase in cholesterylesters (Fig. 1E) in the HDL-sized fractions of prednisolone-treated WT mice. In the prednisolone-treated GR^{dim} mice the peak of cholesterylesters was shifted towards the LDL-sized fractions.

Figure 2

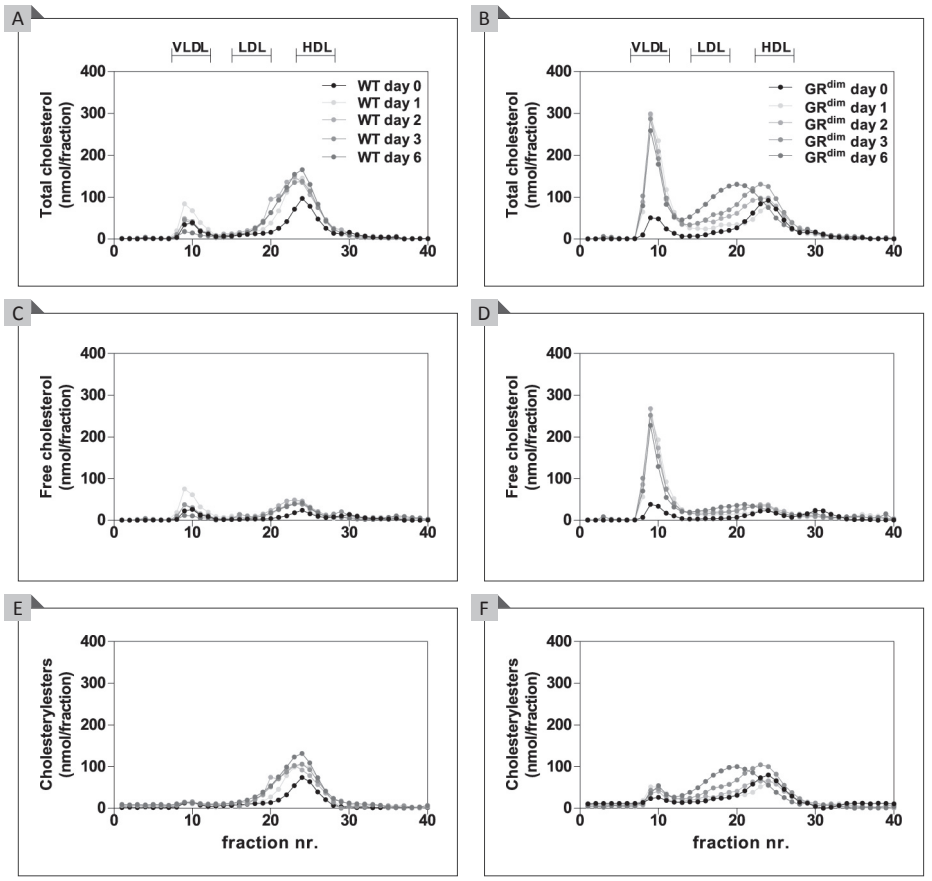

Plasma lipoprotein profiles of total cholesterol, free cholesterol, and cholesterylesters

A, total cholesterol of WT mice **B,** total cholesterol of GR^{dim} mice **C**, free cholesterol of WT mice **D**, free cholesterol of GR^{dim} mice **E**, cholesterylesters of WT mice and **F**, cholesterylesters of GR^{dim} mice separated by FPLC. Black lines indicate day 0, before treatment of each genotype and light to dark grey lines indicate day 1 to 6 of prednisolone treatment in each genotype. The signs above indicate the very low density lipoprotein (VLDL), low density lipoprotein (LDL) and high density lipoprotein (LDL) sized fractions.

In order to reveal whether the increase in VLDL-associated triglycerides, phospholipids and cholesterol levels in prednisolone-treated GR^{dim} mice were direct effects of prednisolone treatment or due to accumulation over time, we evaluated plasma samples from WT and GR^{dim} mice during the six days of prednisolone treatment. Plasma samples were taken on day 0, before treatment and at day 1, 2, 3 and 6 of treatment, after which plasma samples were pooled and fractionated by FPLC. Figure 2 shows the FPLC profiles of total cholesterol, free cholesterol and cholesterylesters from WT (Fig. 2A, C and E) and GR^{dim} mice (Fig. 2B, D and F) during prednisolone treatment. The slightly increased cholesterylester levels in the HDL-sized fractions in WT mice, were already apparent after 1 day of treatment and did not drastically change over time (Fig. 2E). In GR^{dim} mice, the increased free cholesterol peak in the VLDL-sized fractions was already present after a single day of prednisolone-treatment and remained high during the entire treatment period (Fig. 2D). In contrast, the increase in cholesterylesters in GR^{dim} mice appeared after 3 days of prednisolone-treatment and shifted towards the LDL-sized fractions upon 6 days of treatment (Fig. 2F). There is a clear temporal effect on this parameter of prednisolone treatment. The increase in triglycerides and phospholipids in the VLDL-sized fractions of GR^{dim} mice followed a similar pattern as free cholesterol, *i.e.*, after a single day of prednisolone treatment phospholipids and triglycerides were increased (data not shown).

Since apolipoprotein A-I (ApoA-I) is specific for HDL particles, a Western blot of ApoA-I was performed on the FPLC fractions that contained the highest HDL-cholesterol concentrations from plasma samples of six day prednisolone-treated WT and GR^{dim} mice in order to confirm the presence of HDL lipoproteins (Fig. 3). In WT mice, the cholesterol peak was present between fractions 20 and 27 (Fig. 1C); in these fractions ApoA-I protein levels were detectable by Western blotting, confirming the presence of HDL particles. However, in the plasma samples from GR^{dim} mice, that showed a cholesterol peak between fractions 15 and 25, no ApoA-I was detected below fraction 23, which could indicate a shift from HDL towards LDL and not the presence of very large HDL particles. In addition, plasma of

Figure 3

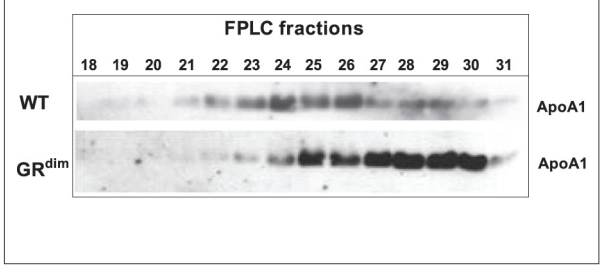

Western blot analysis of Apolipoprotein A1 (ApoA-I) from the higher FPLC fractions of WT (upper panel) and GR^{dim} mice (lower panel) treated with prednisolone for 6 days.

Numbers above indicate the fraction obtained by FPLC.

GR^{dim} mice treated with prednisolone contained a large amount of ApoA-I in fractions 27-30, indicating a high concentration of small pre-β HDL lipoproteins.

Prednisolone treatment in GR^{dim} mice does not lead to Lp-X formation

The drastic increase of free cholesterol and phospholipids in the VLDL fractions might indicate the presence of lipoprotein-X (Lp-X), which is a particle of VLDL -size that contains large amounts of free cholesterol and phospholipids. Lp-X is primarily formed during cholestasis, when hepatobiliary secretion of phospholipids and cholesterol is hampered [29]. To investigate the possible occurrence of cholestasis we determined plasma bile acids levels (Fig. 4A). Interestingly, the concentration of plasma bile acids was not significantly altered in prednisolone-treated GR^{dim} mice and even tended to be reduced (Fig. 4A). Prednisolone-treatment did not alter hepatic cholesterol and phospholipids in either genotype (table 2). Hepatic triglyceride levels were also not affected by prednisolone in WT mice either. Surprisingly, opposite to increased plasma triglyceride levels, hepatic triglyceride levels were reduced in livers of GR^{dim} mice.

Bile formation was studied in detail by performing a bile duct cannulation. 7 Days of prednisolone treatment significantly increased bile flow in WT mice, but not in GR^{dim} mice (Fig. 4B). Biliary output of cholesterol (Fig. 4C) and phospholipids (Fig. 4D) were similar in untreated mice and increased upon prednisolone treatment, independently of the genotype. Total bile acids in bile where increased in GR^{dim} mice treated with prednisolone

Figure 4

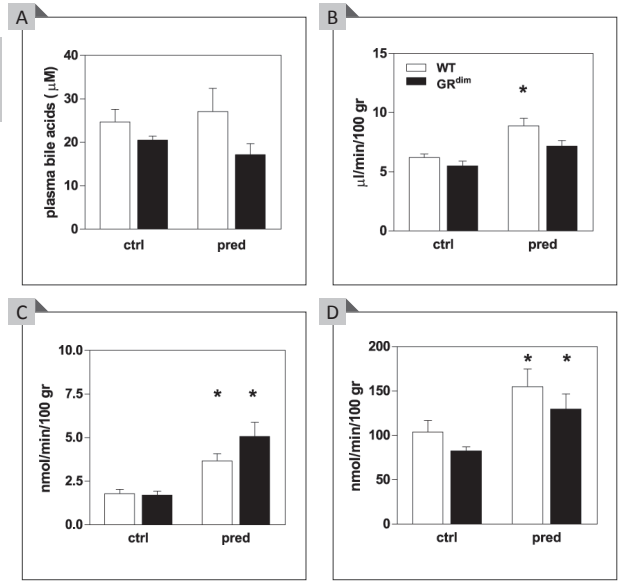

Bile acid parameters

A, Plasma bile acids **B,** bile flow **C,** biliary cholesterol output **D,** biliary phospholipid output from WT and GR^{dim} mice untreated (white bars) or treated for six days with prednisolone (black bars) after bile cannulation.

Figure 5

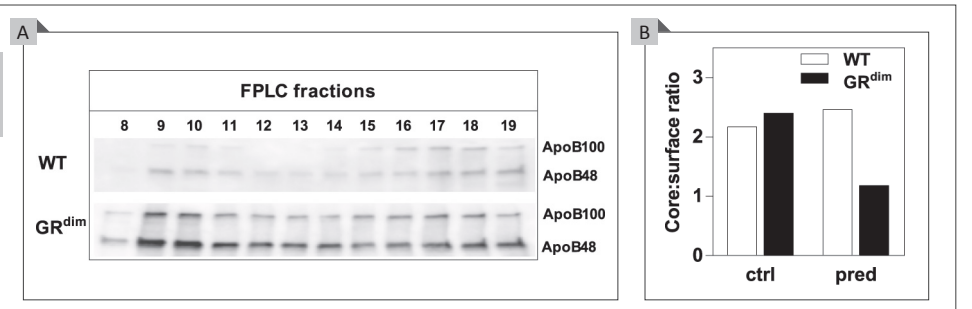

Western blot analysis of Apolipoprotein B (ApoB100 and ApoB48)

A, the lower FPLC fractions of WT (upper panel) and GR^{dim} mice (lower panel) treated with prednisolone for 6 days. Numbers above indicate the fraction obtained by FPLC. **B**, Core:surface ratio from control (white bars) and prednisolone (black bars) treated WT and GR^{dim} mice.

(Supplemental Figure 1). Upon analysis of the bile acid profile, except for ursodeoxycholic acid (UDCA), no significant differences were observed. Interestingly, prednisolone treatment increased the UDCA content considerably in both genotypes (Supplemental Figure 1). Taken together, no signs of cholestasis were found. In addition, the large amount of triglycerides in the VLDL-sized fractions is unusual for Lp-X and the therefore the lipoproteins formed in GR^{dim} mice upon prednisolone treatment, are very unlikely to represent 'classical' Lp-X.

Since the formation of Lp-X was excluded, we hypothesized that the lipoprotein particle formed in the VLDL fractions of GR^{dim} mice upon prednisolone treatment could be a result of an increased number of (smaller) VLDL particles. The amount of ApoB protein was analyzed by Western blotting (Fig. 5 A) in FPLC fractions. In the fractions 8-15 representing the VLDL-sized particles, GR^{dim} mice contained more ApoB, both ApoB48 and ApoB100, indicating the presence of more particles, since each particle only contains a single ApoB molecule. Moreover, the VLDL core-surface ratio (Fig. 5B) was reduced in prednisolone-treated GR^{dim} mice, which implicates that these particles are probably smaller in size. In addition, the appearance of more ApoB in the higher FPLC fractions of prednisolone-treated GR^{dim} mice confirms the finding of reduced ApoA-I, *i.e.*, the fact that these mice have more LDL-sized particles in their circulation.

To find the mechanism of the increased amount of ApoB in plasma, we measured hepatic expression of genes involved in lipid and cholesterol metabolism (Table 3). No differences were seen on ApoB gene expression, but this is not surprising since ApoB secretion is mostly posttranslational regulated [30]. Strikingly, in prednisolone-treated GR^{dim} mice expression of lipoprotein lipase (*Lpl*) gene was increased 23-fold compared to WT control

Table 3

	WT control	GR^{dim} control	WT Prednisolone	GR^{dim} Prednisolone
GR-targets				
Tat	1.00 ± 0.23	1.00 ± 0.15	1.15 ± 0.11	0.40 ± 0.07$^{*\#}$
Pck1	1.00 ± 0.30	1.75 ± 0.13	1.51 ± 0.27*	1.86 ± 0.17$^{\#}$
Bile production and secretion				
Abcg5	1.00 ± 0.09	1.46 ± 0.28$^{\#}$	0.91 ± 0.08	1.83 ± 0.24$^{\#}$
Abcg8	1.00 ± 0.17	1.68 ± 0.55	1.05 ± 0.20	1.51 ± 0.50
Bsep (AbcB11)	1.00 ± 0.16	0.99 ± 0.12	1.66 ± 0.13*	1.74 ± 0.31$^{*\#}$
Cyp7a1	1.00 ± 0.45	0.64 ± 0.36	0.41 ± 0.13	0.18 ± 0.08$^{*\#}$
Cyp8b1	1.00 ± 0.28	0.80 ± 0.34	0.56 ± 0.14*	1.27 ± 0.40
Fxr (Nr1H4)	1.00 ± 0.20	0.85 ± 0.16	0.70 ± 0.12	0.76 ± 0.11
Mdr2 (AbcB4)	1.00 ± 0.21	1.41 ± 0.20$^{\#}$	2.02 ± 0.41*	1.32 ± 0.37
Ntcp (Scl10A1)	1.00 ± 0.05	1.00 ± 0.12	1.16 ± 0.06*	1.57 ± 0.30$^{*\#}$
Cholesterol metabolism				
Lcat	1.00 ± 0.10	1.59 ± 0.29$^{\#}$	1.26 ± 0.22	1.20 ± 0.25
Acat1	1.00 ± 0.29	1.19 ± 0.37	0.72 ± 0.18	0.56 ± 0.12$^{*\#}$
HDL metabolism				
Abca1	1.00 ± 0.17	1.47 ± 0.2$^{\#}$	1.22 ± 0.19	1.33 ± 0.27
ApoA-I	1.00 ± 0.13	0.95 ± 0.25	1.88 ± 0.32*	1.72 ± 0.38$^{*\#}$
Pltp	1.00 ± 0.07	1.99 ± 0.45$^{\#}$	0.37 ± 0.06*	0.97 ± 0.26*
Sr-b1 (Scarb1)	1.00 ± 0.33	1.15 ± 0.20	1.55 ± 0.20*	1.15 ± 0.36
VLDL metabolism				
ApoB	1.00 ± 0.19	1.11 ± 0.17	1.07 ± 0.14	1.07 ± 0.10
Hl (Lipc)	1.00 ± 0.17	0.90 ± 0.16	0.45 ± 0.09*	0.51 ± 0.09$^{*\#}$
Lpl	1.00 ± 0.21	1.70 ± 0.64	0.66 ± 0.04	23.01 ± 11.06$^{*\#}$
Mttp	1.00 ± 0.12	1.13 ± 0.11	2.45 ± 0.19*	1.82 ± 0.09$^{*\#}$

Hepatic gene expression of control WT and GR^{dim} mice and prednisolone-treated WT and GR^{dim} mice
*, p<0.05 *vs.* sham same genotype; #, p<0.05 *vs.* sham wild-type. Results were normalized to *Rplp0* (ribosomal protein, large, P0 (*36b4*)) with data from control wild type mice defined as '1'. Values are means ± SD; n = 4-5; *, p<0.05 vs control same genotype; #, p<0.05 vs WT control; *Tat*, tyrosine amino transferase; *Pck1*, phosphoenolpyruvate carboxykinase 1, cytosolic (*Pepck*); *Abcg5*, ATP binding cassette, sub-family G, member 5; *Abcg8*, ATP binding cassette, sub-family G, member 8; *Bsep*, bile salt export pump (*Abcb11*); *Cyp7a1*, cytochrome P450, family 7, subfamily a, polypeptide 1; *Cyp8b1*, cytochrome P450, family 8, subfamily b, polypeptide 1; *Fxr*, Farnesoid-X receptor (*Nr1h4*, nuclear receptor subfamily 1, group H, member 4); *Mdr2*, multidrug resistance transporter 2 (*Abcb4*); *Ntcp*, (*Slc10a1)* solute carrier family 10 (sodium/bile acid cotransporter family), member 1; *Lcat*, lecithin-cholesterol acyltransferase; *Acat1*, acetyl-CoenzymeA acyltransferase; *Abca1*, ATP binding cassette, sub-family A, member 1; *ApoA-I*, apolipoprotein A1; *Pltp*, phospholipid transfer protein; *Sr-b1*, (*Scarb1, scavenger receptor classB, member1)*;*ApoB*, apolipoprotein B; *Hl*, *(Lipc)* lipase, hepatic; *Lpl*, lipoprotein lipase; *Mttp*, microsomal triglyceride transfer protein.

mice. In contrast, hepatic lipase (*Hl*) was decreased by prednisolone treatment in both genotypes. Prednisolone itself increased *ApoA-I* expression in both genotypes to a similar extent. Although a minor increase was found on expression of lecithin-cholesterol acyl-

Figure 6

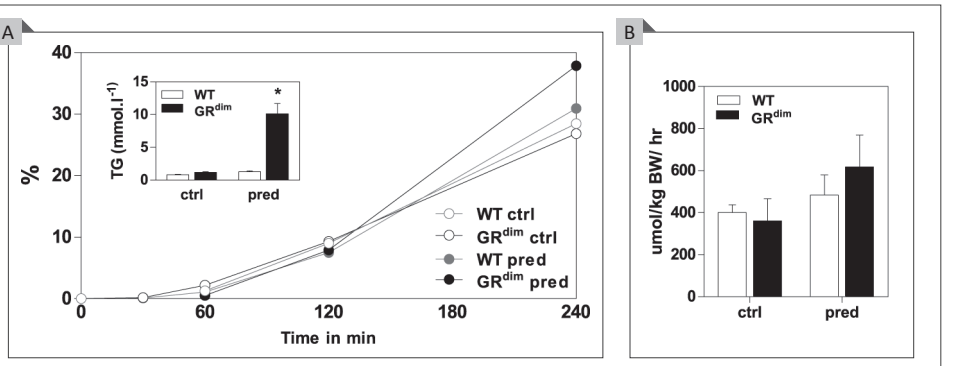

VLDL-TG secretion

A, VLDL-TG secretion of WT (grey lines) and GR^{dim} mice (black lines) after control (white bars – open symbols) or prednisolone treatment (black bars – closed symbols). VLDL secretion was measured after Poloxamer administration and is depicted as a percentage of t=0). Triglycerides levels from t=0 are depicted in the insert. **B**, VLDL-secretion rates were calculated from the slope of the curve

transferase (*Lcat)* in untreated GR^{dim} mice compared to WT controls, no differences were seen upon prednisolone treatment.

LPL exerts an important role in VLDL catabolism and the gene encoding LPL is highly induced in the GR^{dim} mice upon prednisolone treatment. Inhibition of LPL activity by Poloxamer P407 is commonly used to measure the rate of hepatic VLDL production. TG levels at the start of the experiment confirmed the excessive increase in plasma TG in prednisolone-treated GR^{dim} mice (Fig. 6A, insert). The accumulation of newly produced VLDL-TG was slightly increased in GR^{dim} mice (Fig. 6A). From the slope of t120-240 the VLDL production rate was calculated. GR^{dim} mice treated with prednisolone show a trend of increased production (p=0.054) (Fig. 6B), which could cause the increased levels of triglycerides, free cholesterol and phospholipids in the VLDL-sized fractions.

Discussion

It has been hypothesized that GR dimerization fulfils an important role in glucocorticoid-induced side effects and that lack of GR dimerization may improve the therapeutic profile of glucocorticoid treatment. Therefore, there is major interest in development of so called dissociating glucocorticoids as new pharmaceuticals [5]. So far, the glucocorticoid-induced side effects examined in these dissociating studies focused mainly on osteoporosis and insulin resistance [3,31]. In the present study we examined the effect of blocking GR dimerization on lipoprotein metabolism. Here we show that the lack of GR dimerization induces

excessive dyslipidemia in Balb/C mice, implying an important role for GR dimerization in the control of lipid homeostasis in mice.

We hypothesized that the lack of GR dimerization would reduce the adverse effects caused by prednisolone treatment. This did seem to be the case for insulin resistance, since prednisolone treatment induced fasting hyperinsulinemia in WT mice, but not in GR^{dim} mice. At the baseline of the present study we matched WT and GR^{dim} mice for bodyweight. Since the GR^{dim} mice were slightly lighter, these mice were on average 3 weeks older to result in the same bodyweight. Prednisolone treatment reduced bodyweight in WT mice, which, opposite to weight gain in humans, has been reported previously for rodents [32]. In GR^{dim} mice, prednisolone did not reduce bodyweight. Food intake was similar between all groups, indicating that prednisolone might have an effect on energy expenditure in WT mice, which was abolished in GR^{dim} mice.

In this study an abnormal lipoprotein profile was observed in prednisolone-treated GR^{dim} mice consisting of two major components. Firstly, high amounts of triglycerides, phospholipids and free cholesterol were present in the VLDL-sized fractions. Secondly, there was a shift in cholesterylesters form HDL towards LDL in GR^{dim} mice treated with prednisolone compared to WT prednisolone-treated mice. The peak of VLDL-sized triglycerides, free cholesterol and phospholipids was already apparent after a single day of prednisolone treatment, while the shift from HDL toward LDL cholesterylesters occurred over time, indicating two independent mechanisms accounting for these effects.

The high amount of VLDL-sized free cholesterol and phospholipids could indicate the presence of Lp-X, a lipoprotein particle containing high amounts of free cholesterol and phospholipids, often formed during cholestasis. Since no signs of cholestasis were found on liver lipids, plasma bile acids and bile formation, the presence of Lp-X was excluded. In addition to cholestasis, lecithin-cholesterol acyltransferase (LCAT)-deficiency could also cause the formation of Lp-X particle [33,34]. Although there were no differences on *Lcat* gene-expression levels, it could still be that LCAT activity was diminished in GR^{dim} prednisolone-treated mice. This could be due to a factor interfering with LCAT. For functional activity, LCAT requires ApoA-I to bind to the HDL-particle for cholesterol transfer. Screening of the micro-array dataset from Frijters *et al.* [17] revealed an upregulated expression of serum amyloid A1 (SAA1), a protein involved in acute inflammation. This protein is known to be able to replace ApoA-I from HDL-particles [35], thereby blocking LCAT activity. A diminished function of LCAT could explain the lack of cholesterylesters in plasma of prednisolone-treated GR^{dim} mice. In addition, we checked for ApoA-I by Western blotting, but we could not detect ApoA-I in the VLDL-sized fraction in both genotypes. In the HDL-sized fraction, however, a clear shift of ApoA-I was found towards the higher fractions in prednisolone-

treated GR^{dim} mice, indicative for a higher concentration of small pre-β HDL lipoproteins and a shift from HDL towards LDL and not the presence of very large HDL particles.

Although the high plasma TG levels point to diminished activity of LPL in plasma of prednisolone-treated GR^{dim} mice we found up-regulated gene-expression levels of hepatic *Lpl*. These data were confirmed by a Chip-Seq analysis (Rao *et al.*, unpublished data) performed on livers from vehicle and prednisolone-treated WT and GR^{dim} mice. This study revealed that, in contrast to the general assumption that dimerization of GR is essential for direct activation or repression of GR-target genes, also monomeric GR could actively induce gene-expression. The classical promoter of GR-target genes, called the glucocorticoid response element (GRE) could indeed only be activated by dimerized GR and classical target genes were not activated in GR^{dim} mice. However, in livers from prednisolone-treated GR^{dim} mice a subset of genes was up-regulated, implying that the GR with the point mutation A458T might gain some transcriptional activity depending on promoter contexts. One of the target genes from this subset was *Lpl.*

By blocking LPL, VLDL-TG secretion was measured and a small increase was found in prednisolone-treated GR^{dim} mice. In principle, this small increase could over time result in a large accumulation of VLDL-sized particles. However, the strong induction in plasma triglycerides, phospholipids and free cholesterol levels in the VLDL-sized fractions were already present after a single day of treatment and did not further increase during prolonged treatment suggesting that the increase in VLDL-like particles must have been due to inhibition of VLDL breakdown. The increased amount of ApoB could result in more and smaller particles as shown by the VLDL core:surface ratio. Possibly these smaller particles interact less with LPL inhibiting their degradation. It has been shown previously that GCs can increase the amount of ApoB proteins, both by an increased secretion and reduced clearance in rat hepatocytes treated with dexamethasone [36].

Overall, the data described in this study reveal that to our surprise prednisolone-treatment leads to excessive dyslipidemia in GR^{dim} mice, indicating an important role of monomeric GR in regulation of lipid metabolism and this may contribute to unravelling the mechanisms underlying glucocortoid-induced side effects.

Acknowledgements

This research was performed within the framework of project TI-106 of the Dutch Top Institute Pharma.

Reference List

1. Rhen, T. & Cidlowski, J. A. Antiinflammatory action of glucocorticoids--new mechanisms for old drugs. N. Engl. J Med. 353, 1711-1723 (2005).
2. Schacke, H., Docke, W. & Asadullah, K. Mechanisms involved in the side effects of glucocorticoids. Pharmacology & Therapeutics 96, 23-43 (2002).
3. Stanbury, R. M. & Graham, E. M. Systemic corticosteroid therapy--side effects and their management. Br. J Ophthalmol. 82, 704-708 (1998).
4. Walker, B. R. Cortisol--cause and cure for metabolic syndrome? Diabet. Med. 23, 1281-1288 (2006).
5. Stahn, C., Lowenberg, M., Hommes, D. W. & Buttgereit, F. Molecular mechanisms of glucocorticoid action and selective glucocorticoid receptor agonists. Mol. Cell Endocrinol. 275, 71-78 (2007).
6. Weinberger, C. et al. Identification of human glucocorticoid receptor complementary DNA clones by epitope selection. Science 228, 740-742 (1985).
7. Caelles, C., Gonzalez-Sancho, J. M. & Munoz, A. Nuclear hormone receptor antagonism with AP-1 by inhibition of the JNK pathway. Genes Dev. 11, 3351-3364 (1997).
8. Limbourg, F. P. & Liao, J. K. Nontranscriptional actions of the glucocorticoid receptor. J Mol Med. (Berl) 81, 168-174 (2003).
9. Baschant, U. & Tuckermann, J. The role of the glucocorticoid receptor in inflammation and immunity. J. Steroid Biochem. Mol. Biol. 120, 69-75 (2010).
10. Kassel, O. et al. A nuclear isoform of the focal adhesion LIM-domain protein Trip6 integrates activating and repressing signals at AP-1- and NF-kappaB-regulated promoters. Genes Dev. 18, 2518-2528 (2004).
11. Heck, S. et al. A distinct modulating domain in glucocorticoid receptor monomers in the repression of activity of the transcription factor AP-1. EMBO J. 13, 4087-4095 (1994).
12. Reichardt, H. M. et al. DNA binding of the glucocorticoid receptor is not essential for survival. Cell 93, 531-541 (1998).
13. Kleiman, A. & Tuckermann, J. P. Glucocorticoid receptor action in beneficial and side effects of steroid therapy: Lessons from conditional knockout mice. Molecular and Cellular Endocrinology 275, 98-108 (2007).
14. Tuckermann, J. P. et al. The DNA binding-independent function of the glucocorticoid receptor mediates repression of AP-1-dependent genes in skin. J. Cell Biol. 147, 1365-1370 (1999).
15. Reichardt, H. M. et al. Repression of inflammatory responses in the absence of DNA binding by the glucocorticoid receptor. EMBO J. 20, 7168-7173 (2001).
16. Tuckermann, J. P. et al. Macrophages and neutrophils are the targets for immune suppression by glucocorticoids in contact allergy. J Clin Invest 117, 1381-1390 (2007).
17. Frijters, R. et al. Prednisolone-induced differential gene expression in mouse liver carrying wild type or a dimerization-defective glucocorticoid receptor. BMC. Genomics 11, 359 (2010).
18. Rauch, A. et al. Glucocorticoids suppress bone formation by attenuating osteoblast differentiation via the monomeric glucocorticoid receptor. Cell Metab 11, 517-531 (2010).
19. Arnaldi, G. et al. Pathophysiology of dyslipidemia in Cushing's syndrome. Neuroendocrinology 92 Suppl 1, 86-90 (2010).
20. Shibli-Rahhal, A., Van Beek, M. & Schlechte, J. A. Cushing's syndrome. Clinics in Dermatology 24, 260-265 (2007).
21. Taskinen, M. R., Nikkila, E. A., Pelkonen, R. & Sane, T. Plasma lipoproteins, lipolytic enzymes, and very low density lipoprotein triglyceride turnover in Cushing's syndrome. J Clin Endocrinol. Metab 57, 619-626

(1983).

22. Wajchenberg, B. L. Subcutaneous and visceral adipose tissue: their relation to the metabolic syndrome. Endocr. Rev 21, 697-738 (2000).

23. Lemke, U. et al. The glucocorticoid receptor controls hepatic dyslipidemia through Hes1. Cell Metab 8, 212-223 (2008).

24. Rader, D. J. Molecular regulation of HDL metabolism and function: implications for novel therapies. J. Clin. Invest 116, 3090-3100 (2006).

25. BLIGH, E. G. & DYER, W. J. A rapid method of total lipid extraction and purification. Can. J. Biochem. Physiol 37, 911-917 (1959).

26. Gautier, T. et al. Hepatic lipid accumulation in apolipoprotein C-I-deficient mice is potentiated by cholesteryl ester transfer protein. J. Lipid Res. 48, 30-40 (2007).

27. Kuipers, F. et al. Altered lipid metabolism in apolipoprotein E-deficient mice does not affect cholesterol balance across the liver. Hepatology 24, 241-247 (1996).

28. Liu, Y. et al. Dexamethasone exposure of neonatal rats modulates biliary lipid secretion and hepatic expression of genes controlling bile acid metabolism in adulthood without interfering with primary bile acid kinetics. Pediatr. Res 63, 375-381 (2008).

29. Chang, P. Y. et al. Lipoprotein-X reduces LDL atherogenicity in primary biliary cirrhosis by preventing LDL oxidation. Journal of Lipid Research 45, 2116-2122 (2004).

30. Ginsberg, H. N. & Fisher, E. A. The ever-expanding role of degradation in the regulation of apolipoprotein B metabolism. J Lipid Res 50 Suppl, S162-S166 (2009).

31. Schacke, H., Docke, W. & Asadullah, K. Mechanisms involved in the side effects of glucocorticoids. Pharmacology & Therapeutics 96, 23-43 (2002).

32. Thomas, C. R., Turner, S. L., Jefferson, W. H. & Bailey, C. J. Prevention of dexamethasone-induced insulin resistance by metformin. Biochem. Pharmacol. 56, 1145-1150 (1998).

33. Nishiwaki, M. et al. Human lecithin:cholesterol acyltransferase deficiency: in vivo kinetics of low-density lipoprotein and lipoprotein-X. Arterioscler. Thromb. Vasc. Biol. 26, 1370-1375 (2006).

34. Zhu, X. et al. A novel in vivo lecithin-cholesterol acyltransferase (LCAT)-deficient mouse expressing predominantly LpX is associated with spontaneous glomerulopathy. Am J Pathol. 165, 1269-1278 (2004).

35. Xie, X. et al. Polymorphisms in the SAA1/2 gene are associated with carotid intima media thickness in healthy Han Chinese subjects: the Cardiovascular Risk Survey. PLoS. One. 5, e13997 (2010).

36. Wang, C. N., McLeod, R. S., Yao, Z. & Brindley, D. N. Effects of dexamethasone on the synthesis, degradation, and secretion of apolipoprotein B in cultured rat hepatocytes. Arterioscler. Thromb. Vasc. Biol. 15, 1481-1491 (1995).

Supporting Information

Figure s1

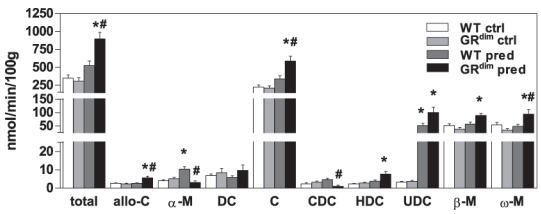

The bile acid profile from bile of control WT mice (white bars), control GR^{dim} mice (light grey bars), prednisolone-treated WT mice (dark grey bars) and prednisolone-treated GR^{dim} mice (black bars).

Total bile acids and the amount of allocholic acid (allo-C), alpha-muricholic acid (α-M), deoxycholic acid (DC), cholic acid (C), chenodeoxycholic acid (CDC), hyodeoxycholic acid (HDC), ursodeoxycholic acid (UDC), beta-muricholic acid (β-M) and omega-muricholic acid (ω-M).

8

General Discussion

Anke J. Laskewitz

General discussion

The overarching aim of the studies described in this thesis was to better understand underlying mechanisms of GC-induced metabolic derangements. We focused specifically on *in vivo* studies of insulin resistance and dyslipidemia in mice as major adverse effects associated with chronic prednisolone treatment seen in humans. For in-depth analysis of GC-induced derangements in glucose metabolism, we chose to study the effects of GCs in (genetically-engineered) mice with state-of-the-art stable isotope methods. To this purpose, multiple mouse models and methodologies to evaluate glucose metabolism have been applied. The studies described in this thesis reveal the complexity of GC-induced adverse effects in mice. In the general discussion multiple factors adding to this complexity will be discussed; these factors should be considered for future studies. Firstly, in this thesis several methods to measure insulin resistance have been applied, including a novel method introduced in chapter 2. Some pro's and con's of the methodologies described will be discussed. Secondly, there is a great variety of synthetic GCs and different modes of administration to choose as a treatment regime for mice, which should be chosen wisely. Thirdly, various mouse strains tend to respond differently to GC-treatment, therefore an overview is given of different studies analyzing the effects of GC-treatment on glucose metabolism involving different mouse strains. Then shortly the effects of glucocorticoids on lipid metabolism will be handled. Finally, there are many other factors that should be taken into account when investigating adverse effects of GCs, which will be discussed in this chapter. These discussion points then lead to the perspectives for future studies.

Choosing the proper methodology to measure insulin resistance

Insulin resistance constitutes a clinically undesired situation in which insulin-sensitive tissues, like liver, muscle and adipose tissue, have a reduced response to circulating insulin levels. Insulin resistance leads to high blood glucose levels and is usually characterized by both high glucose and insulin levels [1]. However, there are multiple methodologies to measure or diagnose insulin resistance and in this part of the discussion the advantages and disadvantages of these methodologies will be discussed. It should be realized that insulin resistance in itself is not a disease but a physiological state preceding diabetes mellitus type 2 and comprises a component of the metabolic syndrome. The metabolic syndrome, in turn, constitutes a risk for diabetes mellitus type 2 and cardiovascular disease. While diabetes mellitus type 2 in humans is diagnosed by fasting blood glucose levels >7 mM, a 2-hour plasma glucose of 11,1 mM during an oral glucose tolerance test or a HbA1c > 6,5% [2], the most commonly used manner to express insulin resistance is the **HOMA-IR**, in which fasting blood glucose and fasting plasma insulin measurements are related to each other by a formula introduced by Matthews *et al.* [3]. This HOMA-IR is relative easy to

perform, since only fasting blood glucose and insulin levels need to be collected, however it does not give detailed information on tissue specific insulin sensitivity. In this thesis multiple methods have been used to analyze glucose metabolism and tissue specific insulin resistance. In **chapter 2** an adaptation to HOMA-IR is described, which adjusts the HOMA-IR to the basal blood glucose and plasma insulin levels of mice and hence allows for the use of an HOMA-IR in mice. Two traditional techniques to more specifically study insulin resistance by the effects of insulin action are the **oral glucose tolerance test (OGTT)** and **the insulin tolerance test (ITT)** [4]. These techniques involve stimulation of glucose metabolism, either by administering an oral high bolus of glucose (for the OGTT), or by a single *ip.* injection of insulin (for the ITT), after which glucose levels are monitored to result in a glucose curve. The area under this curve is a measure for insulin resistance. As a pilot experiment we performed oral glucose tolerance tests in mice treated with prednisolone for four weeks (Fig. 1, not published). The high dose of prednisolone (10 mg/kg/d) clearly increased fasted blood glucose levels (Fig. 1A), suggesting insulin resistance. However, the glucose curve of the OGTT from prednisolone treated mice peaked at a lower glucose level, resulting in a reduced area under the curve which implies increased insulin sensitivity. As Fig. 1B shows, there were no differences in glucose curve on day 0 before treatment, while the 10 mg/kg/day prednisolone treatment reduced the glucose curve at day 7 (Fig. 1C), which was still present at day 21 (Fig. 1D). To make a validated statement on insulin resistance, one should take blood samples during the OGTT to determine insulin levels. At the time of this pilot study, this was technically not possible because the amount of blood

Figure 1

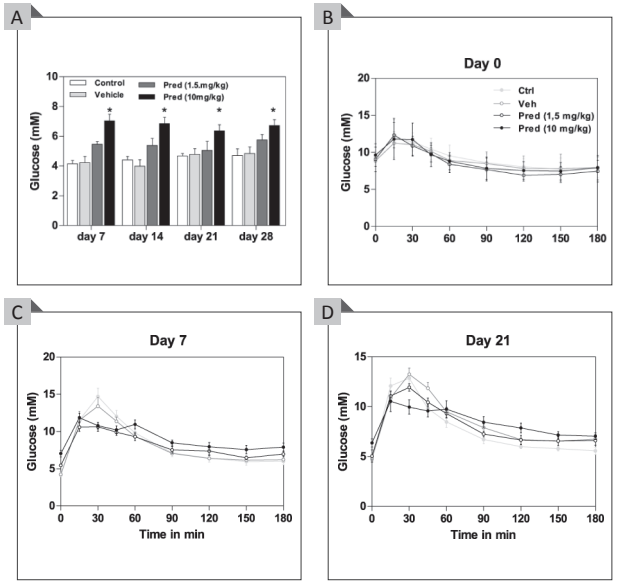

Effects of 4-week prednisolone op glucose levels

A, Fasting glucose levels during four week treatment **B**, glucose curve of oral glucose tolerance tests on day 0 (before treatment) **C,** glucose curve of oral glucose tolerance tests on day 7 and **D**, glucose curve of oral glucose tolerance tests on day 21

needed to be collected for insulin measurements was too high for mice. However, due to improvement of sensitivity of insulin measurement techniques this problem has been overcome nowadays.

To study insulin resistance in detail, the **hyperinsulinemic euglycemic clamp (HIEC)** is regarded as the 'gold standard' [5,6]. The HIEC, adapted for use in mice in our laboratory [7], was used in **chapter 3 and 4** to evaluate GC-induced effects on insulin sensitivity in C57BL/6J mice in detail. By continuous infusion of insulin a high plasma insulin level is created (hyperinsulinemic). Simultaneously, glucose is infused to maintain blood glucose at a steady level (euglycemic). In this protocol the infusion rate of glucose (GIR) is a measure for insulin sensitivity as insulin sensitive tissues take up more glucose. And therefore more glucose is needed to maintain euglycemia. By adding glucose tracers to this protocol (*i.e.*, stable isotopes) one can discriminate between fluxes into and out of hepatic and peripheral tissue (muscle, adipose tissue) [8], divided in hepatic glucose production and metabolic clearance rate. In order to more specifically analyze hepatic glucose metabolism we used Mass Isotopomer Distribution Analysis (MIDA) [8,9] in **chapter 4** and **5**, which is a technique for in-depth analysis of hepatic glucose fluxes of (part of the) glycolysis, glycogenolysis, and gluconeogenesis. This measurement has been previously described for analysis of hepatic glucose fluxes in a 9-hours fasted state [10,11], but in order to acquire knowledge of hepatic glucose fluxes during hyperinsulinemia, we combined the standard HIEC with the MIDA in **chapter 4**.

In addition to the generally accepted methods to evaluate insulin resistance, we developed a simple stable isotope based technique to assess glucose kinetics under 9-hours fasted conditions. This method is described in **chapter 2** and used in **chapter 3, 4** and **6**. Using this method we were able to measure glucose metabolism in a stable, fasted state with limited inconvenience for the experimental animals. The test can be repeated in a single animal multiple times, leading to a significant reduction in numbers of animals used per experiment. For the analysis of fasted blood glucose kinetics, mice were injected *ip.* with a small amount of stably-labeled glucose (D-[6,6-$^{2}H_{2}$]glucose, ~500 µmol kg^{-1} BW), after which blood glucose levels are measured and blood spots are taken on filter paper every 10 minutes for the next 90 minutes. From the wash-out of injected D-[6,6-$^{2}H_{2}$]-glucose from the circulation the whole body glucose turnover and clearance rates can be calculated by kinetic analysis. This method does not disturb fasting glucose metabolism or insulin secretion; therefore one single measurement of plasma insulin levels after the test is sufficient to make a validated statement on insulin resistance, that can be related to calculated values of glucose production and glucose clearance (HGP and MCR, respectively). However, one should realize that although the basal blood glucose kinetics together with the prevailing insulin levels gives good insight in glucose metabolism insulin resistance.

However, because insulin is a hormone that is secreted upon stimulation of the pancreatic beta-cells after feeding, the meaning of increased insulin concentrations in a fasted state is debatable, since these levels are often still below the insulin concentration after a meal. Therefore, the method of fasted blood glucose kinetics also had it's disadvantages and is not a perfect method for analyzing insulin resistance. In a situation of insulin resistance fasted insulin levels might still play an active role. The HOMA-IR, the fasting blood glucose kinetics and the MIDA methods are measurements performed during a basal, *i.e.*, fasted state. It should be realized that the perfect method probably does not exist as each method has its advantages and disadvantages.

The methods described above all yield a measure for insulin resistance. Many papers describe a good correlation between the surrogate indices, such as the HOMA-IR, with the GIR during hyperinsulinemic euglycemic clamp studies in humans [12,13]. For rodent models developed to resemble human metabolic diseases, comparisons of the correlation between surrogate indices, such as HOMA-IR, and the HIEC are scarce. The group of Quon showed that the correlation between HOMA-IR and the GIR during HIEC is very moderate in mice as well as in rats [14,15]. The studies described in **chapter 3** and **4** reveal that the HOMA-IR and HIEC are disconnected for prednisolone-treated C57BL/6J mice, therefore the HOMA-IR is not a good predictive value for insulin resistance in mice.

Choosing a glucocorticoid treatment protocol

The most commonly used GCs in clinical practice are prednisolone and dexamethasone. While dexamethasone is a very potent anti-inflammatory drug, often used to treat acute sepsis, prednisolone is less potent but the preferred GC for treatment of chronic inflammatory diseases, such as rheumatoid arthritis and inflammatory bowel diseases. The focus of the experiments described in this thesis is on prednisolone, because we aimed to approach the human situation as much as possible and it is during chronic treatment that side effects on glucose and lipid metabolism cause major problems.

The mode by which the GCs are administered to the animal is subject to debate. In many studies, GCs were injected intraperitoneally, however, this way of administration is undesirable in patients. For continuous administration in animal studies, GCs can also be administered *via* long-term continuous release pellets, which also reduce the stress of dosing and handling. These pellets are implanted subcutaneously, where matrix-driven delivery takes place. The idea behind this method is that the pellet would release a constant and continuous dose of prednisolone. However, in our hands, the levels of prednisolone retrieved in plasma of pellet-implanted animals varied highly. Moreover, a pilot study to test continuous prednisolone administration via osmotic pumps in rats also did not

result in administration of a constant dose (M-J. van Lierop, MSD, personal communication). In the clinic, prednisolone is given orally, usually once a day. Therefore, we chose to administer prednisolone daily by gavage in a vehicle solution containing 0.5% gelatin/5% mannitol. To make sure that this vehicle containing a sugar alcohol has no effect on glucose metabolism, it was first compared to water (Fig. 1). Compared to an oral bolus of water, the vehicle had no effect on glucose metabolism as measured by fasting blood glucose levels and oral glucose tolerance test. Nevertheless, a major drawback of this mode of treatment is the daily handling and the stress mice perceive while being strained for oral gavage. In addition, timing of treatment dosing can affect the circadian rhythm in a different manner, which will be discussed further on. Overall, it is clear that the mode of administering can have a great effect on treatment outcome.

Choosing the right mouse model

The fact that GCs exert their effects in many different organs and tissues, which, in addition, show complex interaction with each other, makes it difficult to evaluate GC-induced effects on various aspects of metabolism in artificial *in vitro* models. Several descriptive studies have been performed in healthy human volunteers [16-18] and in patients [19-21], but more in-depth, fundamental research requires application of animal models. Rodents comprise the most widely used animal species, thanks to their fast reproduction rates, their relative small size and easy housing. Since the introduction of genetic modification, mice are more and more preferred over rats. In addition, in our laboratory, state-of-the-art stable isotope methods to quantify glucose and lipid metabolism for use in mice have been developed and extensively tested. Therefore, we have chosen to assess GC-induced adverse effects on glucose and lipid metabolism in mice.

Our goal was first to assess GC-induced adverse effects in 'normal' mice, with the possibility to take it one step further in arthritic mice or in transgenic mice. We choose the C57BL/6J mouse strain as our 'normal' mice, because this strain is one of the most extensively used mouse strains for metabolic studies. Moreover, C57BL/6J mice are known to be susceptible to diet-induced obesity and insulin resistance. Unfortunately, within the C57BL/6J mice, there are still quite some differences between breeding lines from different suppliers (*e.g.*, Harlan *vs.* Charles River). Mice described in this thesis are C57BL/6J mice from Harlan. We also used mice from the DBA/1J strain, which is the only strain susceptible to collagen-induced arthritis (CIA), in order to test the effects of sustained prednisolone treatment in an inflammation model. Finally, experiments were done in GR^{dim} mice on a BALB/c background, since this transgenic model is not viable on a C57BL/6J background. The results of evaluation of prednisolone-induced effects on insulin sensitivity in these different mouse strains are summarized in Table 1, in which also an overview

of multiple published studies is given in which the effects of GCs on glucose metabolism and insulin resistance have been assessed in different mouse strains.

Experimental animal models of GC-induced insulin resistance

Many studies have been performed in animals in which dexamethasone has been used to induce insulin resistance, however, most of these experiments have been performed in rats as mentioned in the introductory **chapter 1**. Although Stojanovska *et al*. describe that dexamethasone treatment in rats causes insulin resistance [30], some results obtained

Table 1

Mouse strain	Treatment	Fasting glucose	Fasting insulin	Insulin resistance	Ref.
C57BL/6J	Prednisolone(O) 10 mg/kg/day	↑	↑	HIEC ↔ WBGT ↑ MIDA ↔ / ↑ OGTT ↔	22 [4] Lierop [5] [UD]
DBA/1J	Prednisolone (O) 10 mg/kg/day	↓	↔ C-pep↑	WBGT ↔ OGTT ↔	Toonen [6] [PC]
FVB	Prednisolone (p) 12.5 mg/kg/day	↔	↑	ITT ↑	* [PC]
BALB/c	Prednisolone (p) 12.5 mg/kg/day	↔	↑	WBGT ↑	[UD] [7]
Aston colony (1 *ob* gene)	Dexamethasone 2.5 mg/kg/day, (*ip*)	↑↑	↑↑	ITT ↑	23
A^{vy}/a (yellow viable) and a/a (control)	Dexamethasone (p) 1.5 mg/kg/day	A^{vy}/a ♂↓ A^{vy}/a ♀↑ a/a ♀↔ a/a ♂↔	A^{vy}/a ♂↓ A^{vy}/a ♀↑↑ a/a ♀↑ a/a ♂↑		24,25
C57BL/6J On HF diet	Dexamethasone 3x 11 mg/kg in 5 d	↔	↔	HOMA-IR ↑ OGTT ↔	26
$LDLR^{-/-}$ mixed background	Dexamethasone 1 mg/kg 5 months	↑	↑↑	OGTT ↑ ITT ↑	27
C57BL/KsJ$^{+/+}$ C57BL/6J$^{+/+}$ C57BL/KsJ$^{db/db}$ C57BL/6J$^{db/db}$	Dexamethasone, 0.125 mg/kg/day	↔ ↔ ↓ ↔	↑ ↑ ↔ ↑		28
C57BL/6	Dexamethasone Methylprednisolone 20 mg/kg/day			OGTT ↑ OGTT ↔	29

Effects of glucocorticoids on glucose metabolism in different mouse models and strains

Fasting glucose levels or insulin resistance remained similar ↔, reduced ↓or increased ↑ upon prednisolone treatment. *[PC] Personal communication from A. Rauch (Leibniz Institut Jena) data from WT GR^{dim} mice on a FVB background, [UD]- unpublished data, [#] – chapter number in this thesis, (O)- adminatration by oral gavage, (p)- administration by subcutaneous pellet. Yellow viable – Obese mice, A^{vy}/a ♂ were already hyperglycemic.

with dexamethasone in rats are debatable; one study showed insulin resistance to be due to a dexamethasone-induced reduction in muscle specific glucose uptake, while no physiological signs of insulin resistance were present, either at fasting glucose or insulin levels, nor was insulin resistance assessed by OGTT or HIEC [31]. Moreover, Severino *et al.* claimed that dexamethasone treatment is a good model to study GC-induced insulin resistance, but only showed a small effect on insulin levels and no effect blood glucose levels and do not assess insulin resistance in more detail [32]. Nevertheless, daily treatment of rats with 1 mg/kg of dexamethasone is generally accepted to induce insulin resistance.

A similar model for mice has not been published yet as a generally accepted model for GC-induced insulin resistance. Table 1 gives an overview of multiple studies in which the effects of GCs on glucose metabolism and insulin resistance have been assessed in different mouse strains. From this overview it is clear that the effects of GCs on glucose metabolism in mice are highly variable. Besides the experiments described in this thesis and personal observations (first four lines of Table 1), the only published study in which (methyl)-prednisolone was used, showed no effects of the drug on outcome of the oral glucose tolerance test [29]. All other studies published have been performed using dexamethasone. Moreover, the 'gold-standard' HIEC has, to our knowledge, not been performed in GC-treated mice, probably because the HIEC is a technically complex method to perform in mice.

In the studies presented in Table 1, insulin resistance is mostly evaluated by OGTT or ITT. These methods deliver valuable information on the uptake and clearance of glucose and insulin, respectively. Nevertheless, interpretation of these tests can be complicated. Gounarides *et al.* treated high fat-fed mice with dexamethasone for 5 days [26]. These authors performed an OGTT before and after treatment in dexamethasone- and saline-treated mice and represent their data as the difference between baseline and post-treatment values of both groups. This resulted in a large difference between saline and dexamethasone treatment (~ Δ-100 mM vs. ~ Δ80 mM, saline *vs.* dex at t=120) however, closer analysis of the data revealed a peculiar great difference before and after saline treatment (glucose value of ~520 mM *vs.* ~420 mM at t=120, pre *vs*. post saline treatment; ~500 mM vs. ~580 mM at t=120, pre *vs*. post dexamethasone treatment), which underlies a great part of the overall difference between dexamethasone and saline treatment. In this study dexamethasone did not increase plasma insulin levels, while in several other studies [27,28] dexamethasone treatment did result in elevated plasma insulin levels, like prednisolone-treatment did. However, this increase in insulin levels does not necessarily mean that these mice were insulin resistant, as shown in **chapter 3** and **4**. It could be that there is a shift in the homeostatic balance, meaning that at an increased insulin set-point, all tissues respond in a similar manner.

Figure 1

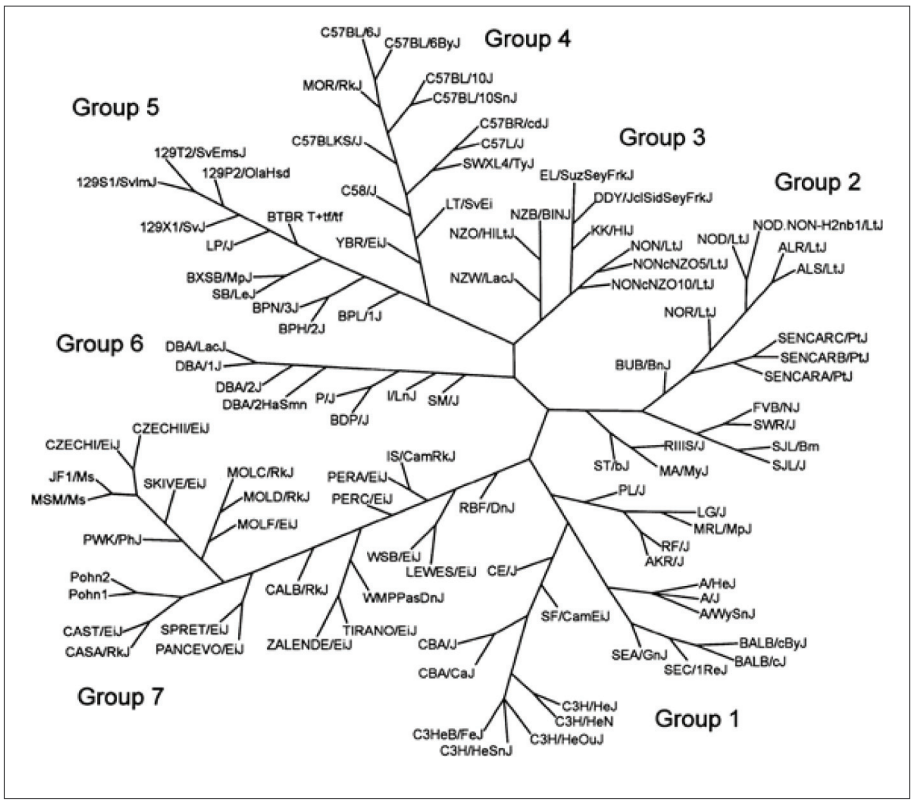

Genetic tree off inbred mouse strains. Adapted from [33]

Table 1 also reveals that in mice on a diabetes-prone background, like the female A^{vy}/a mice or the $LDLR^{-/-}$ mice, GCs appeared to be able to induce insulin resistance. In addition, there is a great difference between the different strains of inbred mice. Figure 2 shows the family tree of inbred mouse strains, in which the mouse strains described in this thesis are circled, thereby showing how these three mouse strains are genetically related each other.

From this family tree, which is based on genetic screening of different inbred mouse strains, it is obvious that the three mouse strains used in this thesis are very distinct from each other, which might underlie the differences in susceptibility to GC-induced adverse effects on glucose metabolism. Another genetic screening, focusing specifically on the susceptibility for diet-induced obesity (DIO) and insulin resistance in multiple inbred mouse strains with a great variety in the genetic background, very well describes different mouse strains that are susceptible for DIO [34,35]. This revealed that the C57BL/6J mouse

strain is highly sensitive to develop DIO, while the BALB/c strain that originates from A/J mice, resistant to DIO. Similarly, the DBA/1J strain is also not sensitive to DIO [34]. These different susceptibilities for diet-induced insulin resistance might reflect the differences in susceptibility for GC-induced effects on glucose metabolism, although induction of insulin resistance via GCs most likely involves different pathways than induction of insulin resistance via high fat diet feeding.

Retrospectively, C57BL/6J mice might not have been the perfect mouse strain to evaluate GC-induced insulin resistance. However, as Table 1 shows, none of the strains tested so far would qualify as such. The ideal follow-up would be an extensive screening with prednisolone and dexamethasone in different mouse strains with one type of assessment of insulin resistance, for which the hyperinsulinemic euglycemic clamp would be the method of choice.

Also take into account…

Besides carefully choosing the method to analyze insulin resistance, the GC treatment and the animal model, one should take into account that many other factors are involved in GC action and glucose metabolism.

First of all, the development of diabetes mellitus type 2 is not solely a result of insulin resistance in insulin sensitive organs, but more specifically the failure of the **pancreas** to compensate for the lack of effect of the prevailing insulin concentrations. When insulin resistance evolves and insulin sensitive tissues, like liver, muscle and adipose tissue, do not respond adequate to the prevailing insulin levels, the pancreas will compensate for this lack of insulin action by secretion of more insulin. The pancreas consists for a large part of exocrine mass producing digestive enzymes, in which the islets of Langerhans reside that function as an endocrine gland [36]. The islets of Langerhans account for 1-1.5 % of the total pancreas and consist of 4 different cell types: α-cells producing glucagon, PP-cells releasing pancreatic polypeptide, δ-cells producing somatostatin and β-cells producing insulin. However, over time as the metabolic tissues become more insulin resistant, the β-cells will get exhausted and will be unable to continue increasing their insulin secretion. This process is referred to as β-cell dysfunction. β-cells also express glucocorticoid receptors (GR) [37] and the effects of GCs on β-cell function are highly contradictory. Like GC-induced insulin resistance, most studies on the effects of GC on β-cell function have been performed in dexamethasone-treated rats. Dexamethasone treatment leads to an increased glucose-stimulated insulin secretion (GSIS) of isolated pancreatic islets of Langerhans from rats treated for several days [38-40]. In a personal observation, we saw that islets from 7 day prednisolone treated C57BL/6J also showed increased GSIS. However, isolated islets from

conventional and *Ob/Ob* mice, cultured with dexamethasone demonstrated reduced GSIS [41,42], which has also been shown for isolated rats islets cultured with dexamethasone [43]. In addition, aged mice over-expressing pancreatic GR had impaired β-cell function [44]. There is a clear difference between direct and indirect effects of GCs on insulin secretion by islets, as shown by the *in vitro* studies in which islets were cultured with GCs and *in vivo* studies in which the animals were treated with GCs. Moreover, the *in vivo* studies were short-term which could imply that β-cell function is increased to overcome the peripheral insulin resistance in the first period and that the β-cells are still able to compensate. It could be that prolonged GC treatment would finally lead to exhausted islets and lead to β-cell dysfunction. Overall, these data show that GCs have an effect on the pancreas that need to be further studied, but still needs to be taken into-account when studying GCs induced insulin resistance.

Secondly, besides the metabolic tissues (liver, muscle and adipose tissue) and the pancreas, the **brain** plays an important role in GC-regulated energy metabolism and food intake, and thereby glucose metabolism and insulin resistance. The hypothalamus is an important region in the brain, linking the nervous system to the endocrine system and plays a major role in the GCs system [36]. The hypothalamus is involved in metabolic functions such as blood pressure homeostasis, temperature regulation and food intake, but also in memory processes, emotion and day night rhythm, since the suprachiasmatic nuclei (SCN) which is regarded as the central clock, is localized in the hypothalamus [45]. Here the effects of GCs on circadian rhythm and neuro-endocrine regulators of food intake will be discussed.

It is known that the **circadian clock** induces a circadian rhythm in cortisol secretion, while on the other hand changes in GC homeostasis alter the circadian rhythm. This is clear by the fact that one of the side effects in patients on GC treatment is insomnia [46]. In addition, it has been shown that GR binds actively to the promoter of the Period 1 (*Per1)* gene, an important regulator of the circadian clock [47] and *Per1* knockout mice have a disturbed rhythm in cortisol secretion [48]. In addition, to add to the complexity and interrelating effects of GCs and circadian rhythm, it has been shown that GR expression shows a circadian rhythm in adipose tissue, but not in liver and muscle [49]. GC treatment reduces the endogenous cortisol production by the negative feedback route of the HPA-axis, thereby taking over the circadian rhythmicity of cortisol production. Cortisol in humans normally peaks early in the morning, therefore timing of GC-treatment is essential to not interfere in the circadian rhythm [50]. Besides GCs, food intake also has a considerable effect on circadian rhythm [51]. Food intake is regarded as a dominant clock regulator (Zeitgeber) [52]; when nocturnal animals only had access to food during day time, they inverted their peripheral circadian rhythm. Moreover, GC are known for their ability to increase appetite, resulting

in increased food intake [53] in humans also at night, thereby interfering with the circadian rhythm. When studying GC-induced alterations of glucose metabolism, one should take the circadian rhythm into account. Treatment timing should compensate the reduced cortisol levels, preferably dosing GC just before normal peak levels would occur. Additionally, it would be very elegant to monitor circadian differences of activity and time of food intake. In the studies described in **chapter 3** and **4**, prednisolone was administered at 13:00 pm, being a bit early for replacements of normal corticosterone levels, which peaks just before the dark (active) period at 18:00 [54]. In addition, we monitored activity and food intake during prednisolone treatment, while the mice were subjected to the calorimetric cages in **chapter 4**, although no significant differences were found.

In **chapter 3,** it was revealed that increased fasting glucose levels were more a result of an altered feeding-fasting response than caused by GC-induced insulin resistance, making the nutritional status an important factor when studying GC-induced effects on insulin sensitivity and glucose metabolism. The nutritional status is dependent on the (timing of) food intake in mice. Besides the hyperglycemic clamp, all experiments analyzing glucose metabolism in this thesis were performed in overnight fasted mice, to ascertain a similar nutritional status. Nevertheless, hormones involved in the neuro-endocrine regulatory network of food intake, such as insulin and leptin were increased upon prednisolone treatment. These neuro-endocrine factors execute part of their role in the hypothalamus.

Although it has been assumed that the brain is insulin insensitive, it is now known that insulin receptors are expressed in many regions, especially in the hypothalamus, hippocampus and cerebral cortex [55]. Insulin can cross the blood-brain barrier via active receptor-mediated transport. Central insulin does not affect glucose uptake in the brain itself, but mediates whole body energy balance via a complex neuro-peptidergic signaling network in the hypothalamus [56]. In addition, central insulin seems to play a role in memory performance and locomotor activity [57,58]. Moreover, there is evidence that central insulin resistance can evolve, as shown by a study of Hallschmid *et al.* in which intranasal insulin treatment reduced bodyweight in normal-weight, but not in overweight subjects [59]. Even though central insulin resistance is a highly unexplored field, it might be that GCs might alter central insulin sensitivity. Zakrzewska *et al.* have shown that central administration of dexamethasone in rats clearly increased plasma insulin levels three-fold [60].

In chapter 4 we show that prednisolone increased plasma leptin levels. In this same study from Zakrzewska, leptin was found to be induced four-fold in rats treated with dexamethasone intracerebroventricularly (i.c.v.) [60]. Leptin is a hormone produced by adipocytes and typically present in circulating levels proportional to the adipose mass [61]. Leptin is involved in regulation of appetite and energy metabolism and suppresses appetite via the leptin

receptor on neuropeptide Y (NPY) secreting neurons in the hypothalamus [62]. GCs and leptin have counter regulatory effects and are highly interacting; not only central GCs, but also peripheral GCs increase leptin secretion independently of the amount of adipose tissue as described by us in **chapter 4** and others [63]. The *Ob* gene regulating leptin levels contains an GRE [64] and GC treatment increases *Ob* gene expression [65]. On the other hand, leptin treatment was able to increase corticosterone levels upon stress [66] and acutely reduces corticosterone in mice [67,68]. These data show that GCs are highly interacting with other hormone signaling pathways and have counter-regulatory effects, most of which take place in the hypothalamus.

Lastly, in **chapter 3** and **4** we found that fibroblast growth factor 21 (FGF21) was increased by prednisolone treatment. FGF21 has been discovered in 2000 as a novel member of the fibroblast growth factor family [69], although recently it has been found that FGF21 functions as an endocrine factor instead of a growth factor by Inagaki and colleagues [70]. FGF21 is predominantly expressed mostly by tissues involved in regulation of metabolism, such as the liver [69], brown adipose tissue [71,72], muscle [73] and pancreas [74]. FGF21 plays a dominant role in energy regulation during fasting [70,75,76]. It has also been suggested that FGF21 might function as a neuro-endocrine regulator, since central administration of recombinant human FGF21 improves insulin sensitivity in diet-induced obese rats [77]. These data show that FGF21 plays an important role in processes in which GCs also interact. We were the first to report the effect of GCs on increasing FGF21 expression and plasma concentrations. This opens a completely new field to explore GC-related effects on glucose metabolism via FGF21.

Overall, the data described above show that there are complex interactions between GCs, circadian rhythms, food intake and hormonal regulation. In order to study one of these mechanisms, as was done in this thesis for the effects of GCs on glucose metabolism, one should make sure that the other factors are not affected. Especially when evaluating insulin resistance by HOMA-IR, it should be taken into account that the relationship between fasting glucose levels and plasma insulin levels only has meaning for insulin sensitivity when other metabolic regulators, like FGF21 and leptin, remain unaffected.

Future implications

As discussed above, there are differential effects between prednisolone treatment in humans and mice, not only on the induction of insulin resistance, but also on changes in bodyweight. While visceral obesity and weight gain are among the many side effects of chronic GC treatment in humans [78,79], mice do not gain weight upon GC treatment but,

in contrast, even lose weight [23] (and personal observation after 4 weeks of prednisolone treatment), which is also the case in rats [80]. In multiple humans studies, insulin resistance has been assessed by the hyperinsulinemic euglycemic clamp [16,18], in healthy volunteers treated with GCs clearly proving GC-induced insulin resistance. This was also shown in patients [81]. Unfortunately, as the studies in this thesis describe, the effects of GCs on glucose metabolism remain partly unclear, although it is obvious from the HIEC studies in **chapter 3** and **4** that prednisolone-treatment does not lead to 'classical insulin resistance'.

On the other hand, in humans GC-induced insulin resistance is also variable. First of all, not all patients receiving chronic GCs develop insulin resistance. A recent study by Hoes *et al.* showed that chronic rheumatoid arthritis (RA) patients receiving GCs are equally insulin sensitive and glucose tolerant as RA patients that do not receive GCs [82]. Moreover, not all patients react similar to GC treatment, with the one patient having no or hardly any side-effects, while in the other patient, treatment had to be stopped because of extreme side effects [83]. This might be due to the effect of genetic background which varies highly between humans, as was also seen in GC treatment in mice between different strains. In addition, GC resistance is a rare hereditary disease highly dependent on genetic background of patients, determining the outcome of GC treatment. For some of these patients polymorphisms in the GR have been found [84,85]. It has been hypothesized that GR polymorphisms underlie GC-induced adverse effects on glucose and lipid metabolism. Herein lies the future for personalized medicine

Overall, the *in vivo* studies performed in this thesis contribute to an improved understanding of GC-induced effects on glucose metabolism; however, we could not confirm 'classical insulin resistance' induced by GCs in mice according to the 'gold standard' measurement by the HIEC. This leads to the question whether mice are the right model to study GC-induced metabolic adverse effects. For fundamental research questions, in which insights of molecular pathways are involved, mice are still a preferred animal model, due to the possibility of genetic engineering. However, the studies described in this thesis did not suggest an optimal mouse model for GC-induced metabolic adverse effects, focussing on physiological resemblance of adverse affects as seen in humans. Nevertheless, to our knowledge these studies are the first to provide in-depth analysis of the effects of GCs on glucose metabolism and insulin resistance in mice. Many techniques were used to assess insulin resistance under different conditions, to ascertain that 'classical insulin resistance' was not detected in prednisolone-treated C57BL/6J mice. Moreover, this last chapter gives a valuable overview of studies published so far on the effects of GCs on glucose metabolism in mice. The studies described in this thesis provide an important step in the recognition of the value of mice studies in GC-related adverse effects. For future studies one should carefully choose the proper animal model, depending on the research question.

Reference List

1. Ascaso, J. F. et al. Diagnosing insulin resistance by simple quantitative methods in subjects with normal glucose metabolism. Diabetes Care 26, 3320-3325 (2003).
2. American Diabetes Association Standards of medical care in diabetes--2011. Diabetes Care 34 Suppl 1, S11-S61 (2011).
3. Matthews, D. R. et al. Homeostasis model assessment: insulin resistance and beta-cell function from fasting plasma glucose and insulin concentrations in man. Diabetologia 28, 412-419 (1985).
4. Antuna-Puente, B. et al. How can we measure insulin sensitivity/resistance? Diabetes & Metabolism 37, 179-188 (2011).
5. DeFronzo, R. A., Tobin, J. D. & Andres, R. Glucose clamp technique: a method for quantifying insulin secretion and resistance. Am. J. Physiol 237, E214-E223 (1979).
6. Bergman, R. N., Prager, R., Volund, A. & Olefsky, J. M. Equivalence of the insulin sensitivity index in man derived by the minimal model method and the euglycemic glucose clamp. J. Clin. Invest 79, 790-800 (1987).
7. Grefhorst, A. et al. Differential effects of pharmacological liver X receptor activation on hepatic and peripheral insulin sensitivity in lean and ob/ob mice. Am. J Physiol Endocrinol Metab 289, E829-E838 (2005).
8. Hellerstein, M. K. et al. Hepatic gluconeogenic fluxes and glycogen turnover during fasting in humans. A stable isotope study. J Clin Invest 100, 1305-1319 (1997).
9. Hellerstein, M. K. & Neese, R. A. Mass isotopomer distribution analysis at eight years: theoretical, analytic, and experimental considerations. Am. J. Physiol 276, E1146-E1170 (1999).
10. van Dijk, T. H. et al. Acute inhibition of hepatic glucose-6-phosphatase does not affect gluconeogenesis but directs gluconeogenic flux toward glycogen in fasted rats. A pharmacological study with the chlorogenic acid derivative S4048. J. Biol. Chem. 276, 25727-25735 (2001).
11. van Dijk, T. H. et al. Quantification of hepatic carbohydrate metabolism in conscious mice using serial blood and urine spots. Anal. Biochem. 322, 1-13 (2003).
12. Chen, H., Sullivan, G. & Quon, M. J. Assessing the predictive accuracy of QUICKI as a surrogate index for insulin sensitivity using a calibration model. Diabetes 54, 1914-1925 (2005).
13. Katz, A. et al. Quantitative insulin sensitivity check index: a simple, accurate method for assessing insulin sensitivity in humans. J. Clin Endocrinol. Metab 85, 2402-2410 (2000).
14. Muniyappa, R. et al. Comparison between surrogate indexes of insulin sensitivity/resistance and hyperinsulinemic euglycemic clamp estimates in rats. American Journal of Physiology - Endocrinology And Metabolism 297, E1023-E1029 (2009).
15. Lee, S. et al. Comparison between surrogate indexes of insulin sensitivity and resistance and hyperinsulinemic euglycemic clamp estimates in mice. American Journal of Physiology - Endocrinology And Metabolism 294, E261-E270 (2008).
16. Pagano, G. et al. An in vivo and in vitro study of the mechanism of prednisone-induced insulin resistance in healthy subjects. J. Clin. Invest 72, 1814-1820 (1983).
17. van Raalte, D. H. et al. Acute and 2-week exposure to prednisolone impair different aspects of beta-cell function in healthy men. Eur. J Endocrinol 162, 729-735 (2010).
18. van Raalte, D. H. et al. Low-dose glucocorticoid treatment affects multiple aspects of intermediary metabolism in healthy humans: a randomised controlled trial. Diabetologia (2011).
19. van der Goes, M. C. et al. Monitoring adverse events of low-dose glucocorticoid therapy: EULAR recommendations for clinical trials and daily practice. Annals of the Rheumatic Diseases 69, 1913-1919 (2010).

20. Burt, M. G., Johannsson, G., Umpleby, A. M., Chisholm, D. J. & Ho, K. K. Impact of acute and chronic low-dose glucocorticoids on protein metabolism. J. Clin. Endocrinol. Metab 92, 3923-3929 (2007).

21. Burt, M. G., Roberts, G. W., Guilar-Loza, N. R., Frith, P. & Stranks, S. N. Continuous Monitoring of Circadian Glycemic Patterns In Patients Receiving Prednisolone For COPD. Journal of Clinical Endocrinology & Metabolism 96, 1789-1796 (2011).

22. Laskewitz, A. J. et al. Chronic Prednisolone Treatment Reduces Hepatic Insulin Sensitivity while Perturbing the Fed-to-Fasting Transition in Mice. Endocrinology 15, 2171-2178 (2010).

23. Thomas, C. R., Turner, S. L., Jefferson, W. H. & Bailey, C. J. Prevention of dexamethasone-induced insulin resistance by metformin. Biochem. Pharmacol. 56, 1145-1150 (1998).

24. Yen, T. T., Gill, A. M., Powell, J. G. & Sampson, B. M. Ciglitazone prevents and reverses dexamethasone-induced hyperglycemia in female viable yellow mice. Int. J Obes. Relat Metab Disord. 16, 923-933 (1992).

25. Gill, A. M., Leiter, E. H., Powell, J. G., Chapman, H. D. & Yen, T. T. Dexamethasone-induced hyperglycemia in obese Avy/a (viable yellow) female mice entails preferential induction of a hepatic estrogen sulfotransferase. Diabetes 43, 999-1004 (1994).

26. Gounarides, J. S. et al. Effect of dexamethasone on glucose tolerance and fat metabolism in a diet-induced obesity mouse model. Endocrinology (2007).

27. Bernal-Mizrachi, C. et al. Dexamethasone induction of hypertension and diabetes is PPAR-alpha dependent in LDL receptor-null mice. Nat. Med. 9, 1069-1075 (2003).

28. Orland, M. J. & Permutt, M. A. Genetic susceptibility to diabetes in inbred strains of mice: measurements of proinsulin mRNA and response to dexamethasone. Diabetologia 30, 934-939 (1987).

29. Zhao, R. et al. Exenatide improves glucocorticoid-induced glucose intolerance in mice. Diabetes Metab Syndr. Obes. 4, 61-65 (2011).

30. Stojanovska, L., Rosella, G. & Proietto, J. Evolution of dexamethasone-induced insulin resistance in rats. Am. J. Physiol 258, E748-E756 (1990).

31. Ruzzin, J., Wagman, A. S. & Jensen, J. Glucocorticoid-induced insulin resistance in skeletal muscles: defects in insulin signalling and the effects of a selective glycogen synthase kinase-3 inhibitor. Diabetologia 48, 2119-2130 (2005).

32. Severino, C. et al. Low-dose dexamethasone in the rat: a model to study insulin resistance. Am. J. Physiol Endocrinol. Metab 283, E367-E373 (2002).

33. Petkov, P. M. et al. An Efficient SNP System for Mouse Genome Scanning and Elucidating Strain Relationships. Genome Research 14, 1806-1811 (2004).

34. Clee, S. M. & Attie, A. D. The genetic landscape of type 2 diabetes in mice. Endocr. Rev. 28, 48-83 (2007).

35. Lee, K. T. Y., Karunakaran, S., Ho, M. M. & Clee, S. M. PWD/PhJ and WSB/EiJ Mice Are Resistant to Diet-Induced Obesity But Have Abnormal Insulin Secretion. Endocrinology (2011).

36. Nussey, S. S. a. W. S. A. L. T. &. F. & c2001 Endocrinology, An integrated approach. Taylor & Francis, London (2001).

37. Delaunay, F. et al. Pancreatic beta cells are important targets for the diabetogenic effects of glucocorticoids. J. Clin. Invest 100, 2094-2098 (1997).

38. Holness, M. J., Smith, N. D., Greenwood, G. K. & Sugden, M. C. Interactive influences of peroxisome proliferator-activated receptor alpha activation and glucocorticoids on pancreatic beta cell compensation in insulin resistance induced by dietary saturated fat in the rat. Diabetologia 48, 2062-2068 (2005).

39. Giozzet, V. A., Rafacho, A., Boschero, A. C., Carneiro, E. M. & Bosqueiro, J. R. Dexamethasone treatment in vivo counteracts the functional pancreatic islet alterations caused by malnourishment in rats. Metabolism 57, 617-624 (2008).

40. Barbera, M. et al. Dexamethasone-induced insulin resistance and pancreatic adaptive response in aging rats are not modified by oral vanadyl sulfate treatment. Eur. J. Endocrinol. 145, 799-806 (2001).

41. Khan, A., Ostenson, C. G., Berggren, P. O. & Efendic, S. Glucocorticoid increases glucose cycling and inhibits insulin release in pancreatic islets of ob/ob mice. Am. J. Physiol 263, E663-E666 (1992).

42. Lambillotte, C., Gilon, P. & Henquin, J. C. Direct glucocorticoid inhibition of insulin secretion. An in vitro study of dexamethasone effects in mouse islets. J Clin Invest 99, 414-423 (1997).

43. Zhang, X. et al. Inhibition of Forkhead Box O1 Protects Pancreatic +¦-Cells against Dexamethasone-Induced Dysfunction. Endocrinology 150, 4065-4073 (2009).

44. Davani, B. et al. Aged transgenic mice with increased glucocorticoid sensitivity in pancreatic beta-cells develop diabetes. Diabetes 53 Suppl 1, S51-S59 (2004).

45. Balsalobre, A. et al. Resetting of circadian time in peripheral tissues by glucocorticoid signaling. Science 289, 2344-2347 (2000).

46. Chrousos, G. P. & Kino, T. Glucocorticoid signaling in the cell. Expanding clinical implications to complex human behavioral and somatic disorders. Ann. N. Y. Acad. Sci. 1179, 153-166 (2009).

47. Yamamoto, T. et al. Acute physical stress elevates mouse period1 mRNA expression in mouse peripheral tissues via a glucocorticoid-responsive element. J Biol. Chem. 280, 42036-42043 (2005).

48. Dallmann, R., Touma, C., Palme, R., Albrecht, U. & Steinlechner, S. Impaired daily glucocorticoid rhythm in Per1 (Brd) mice. J. Comp Physiol A Neuroethol. Sens. Neural Behav. Physiol 192, 769-775 (2006).

49. Yang, X. et al. Nuclear receptor expression links the circadian clock to metabolism. Cell 126, 801-810 (2006).

50. Ross, R. J. & Rostami-Hodjegan, A. Timing and type of glucocorticoid replacement in adult congenital adrenal hyperplasia. Horm. Res. 64 Suppl 2, 67-70 (2005).

51. Mendoza, J. Circadian clocks: setting time by food. J Neuroendocrinol. 19, 127-137 (2007).

52. Schibler, U., Ripperger, J. & Brown, S. A. Peripheral circadian oscillators in mammals: time and food. J Biol. Rhythms 18, 250-260 (2003).

53. Tataranni, P. A. et al. Effects of glucocorticoids on energy metabolism and food intake in humans. Am. J. Physiol 271, E317-E325 (1996).

54. Véniant, M. M. et al. Time of the day for 11beta-HSD1 inhibition plays a role in improving glucose homeostasis in DIO mice. Diabetes Obes. Metab 11, 109-117 (2009).

55. Ketterer, C. et al. Insulin sensitivity of the human brain. Diabetes Res. Clin Pract. 93 Suppl 1, S47-S51 (2011).

56. Morton, G. J., Cummings, D. E., Baskin, D. G., Barsh, G. S. & Schwartz, M. W. Central nervous system control of food intake and body weight. Nature 443, 289-295 (2006).

57. Tschritter, O. et al. The cerebrocortical response to hyperinsulinemia is reduced in overweight humans: A magnetoencephalographic study. Proceedings of the National Academy of Sciences 103, 12103-12108 (2006).

58. Dzoljic, E., van Leeuwen, R., de Vries, R. & Dzoljic, M. R. Vigilance and EEG power in rats: effects of potent inhibitors of the neuronal nitric oxide synthase. Naunyn-Schmiedeberg's Archives of Pharmacology 356, 56-61 (1997).

59. Hallschmid, M., Benedict, C., Schultes, B., Born, J. & Kern, W. Obese men respond to cognitive but not to catabolic brain insulin signaling. Int J Obes 32, 275-282 (2007).

60. Zakrzewska, K. E. et al. Induction of obesity and hyperleptinemia by central glucocorticoid infusion in the rat. Diabetes 48, 365-370 (1999).

61. Friedman, J. M. Leptin at 14 y of age: an ongoing story. Am J Clin Nutr. 89, 973S-979S (2009).

62. Valassi, E., Scacchi, M. & Cavagnini, F. Neuroendocrine control of food intake. Nutr. Metab Cardiovasc. Dis. 18, 158-168 (2008).

63. Licinio, J. et al. Human leptin levels are pulsatile and inversely related to pituitary-adrenal function. Nat. Med. 3, 575-579 (1997).

64. Gong, D. W., Bi, S., Pratley, R. E. & Weintraub, B. D. Genomic structure and promoter analysis of the human obese gene. J Biol. Chem 271, 3971-3974 (1996).

65. de, V. P., Saladin, R., Auwerx, J. & Staels, B. Induction of ob gene expression by corticosteroids is accompanied by body weight loss and reduced food intake. J Biol. Chem 270, 15958-15961 (1995).

66. Heiman, M. L. et al. Leptin inhibition of the hypothalamic-pituitary-adrenal axis in response to stress. Endocrinology 138, 3859-3863 (1997).

67. Clark, K. A., Shin, A. C., Sirivelu, M. P., Mohankumar, S. M. & Mohankumar, P. S. Systemic administration of leptin decreases plasma corticosterone levels: role of hypothalamic norepinephrine. Brain Res. 1195, 89-95 (2008).

68. Vrang, N., Kristensen, P., Tang-Christensen, M. & Larsen, P. J. Effects of Leptin on Arcuate Pro-Opiomelanocortin and Cocaine-Amphetamine-Regulated Transcript Expression Are Independent of Circulating Levels of Corticosterone. Journal of Neuroendocrinology 14, 880-886 (2002).

69. Nishimura, T., Nakatake, Y., Konishi, M. & Itoh, N. Identification of a novel FGF, FGF-21, preferentially expressed in the liver. Biochim. Biophys. Acta 1492, 203-206 (2000).

70. Inagaki, T. et al. Endocrine Regulation of the Fasting Response by PPARalpha-Mediated Induction of Fibroblast Growth Factor 21. Cell Metab 5, 415-425 (2007).

71. Chartoumpekis, D. V. et al. Brown adipose tissue responds to cold and adrenergic stimulation by induction of FGF21. Mol. Med. 17, 736-740 (2011).

72. Hondares, E. et al. Hepatic FGF21 expression is induced at birth via PPARalpha in response to milk intake and contributes to thermogenic activation of neonatal brown fat. Cell Metab 11, 206-212 (2010).

73. Izumiya, Y. et al. FGF21 is an Akt-regulated myokine. FEBS Letters 582, 3805-3810 (2008).

74. Fon Tacer, K. et al. Research Resource: Comprehensive Expression Atlas of the Fibroblast Growth Factor System in Adult Mouse. Mol Endocrinol 24, 2050-2064 (2010).

75. Badman, M. K., Koester, A., Flier, J. S., Kharitonenkov, A. & Maratos-Flier, E. Fibroblast growth factor 21-deficient mice demonstrate impaired adaptation to ketosis. Endocrinology 150, 4931-4940 (2009).

76. Berglund, E. D. et al. Fibroblast growth factor 21 controls glycemia via regulation of hepatic glucose flux and insulin sensitivity. Endocrinology 150, 4084-4093 (2009).

77. Sarruf, D. A. et al. Fibroblast Growth Factor 21 Action in the Brain Increases Energy Expenditure and Insulin Sensitivity in Obese Rats. Diabetes 59, 1817-1824 (2010).

78. Schacke, H., Docke, W. & Asadullah, K. Mechanisms involved in the side effects of glucocorticoids. Pharmacology & Therapeutics 96, 23-43 (2002).

79. Stanbury, R. M. & Graham, E. M. Systemic corticosteroid therapy--side effects and their management. Br. J Ophthalmol. 82, 704-708 (1998).

80. Saad, M. J., Folli, F., Kahn, J. A. & Kahn, C. R. Modulation of insulin receptor, insulin receptor substrate-1, and phosphatidylinositol 3-kinase in liver and muscle of dexamethasone-treated rats. J. Clin. Invest 92, 2065-2072 (1993).

81. Willi, S. M. et al. Troglitazone antagonizes metabolic effects of glucocorticoids in humans: effects on glucose tolerance, insulin sensitivity, suppression of free fatty acids, and leptin. Diabetes 51, 2895-2902

(2002).

82. Hoes, J. N. et al. Glucose tolerance, insulin sensitivity and +¦-cell function in patients with rheumatoid arthritis treated with or without low-to-medium dose glucocorticoids. Annals of the Rheumatic Diseases (2011).

83. Barnes, P. J. Corticosteroid resistance in airway disease. Proc. Am. Thorac. Soc. 1, 264-268 (2004).

84. CHARMANDARI, E. V. A. N., KINO, T. O. M. O. & Chrousos, G. P. Familial/Sporadic Glucocorticoid Resistance: Clinical Phenotype and Molecular Mechanisms. Annals of the New York Academy of Sciences 1024, 168-181 (2004).

85. van Rossum, E. F. C. et al. A Polymorphism in the Glucocorticoid Receptor Gene, Which Decreases Sensitivity to Glucocorticoids In Vivo, Is Associated With Low Insulin and Cholesterol Levels. Diabetes 51, 3128-3134 (2002).

A

Appendices

English summary
Nederlandse samenvatting
Author list
Dankwoord
Biography

Summary

Synthetic GCs such as prednisolone have potent anti-inflammatory actions and are widely prescribed for treatment of chronic inflammatory diseases such as rheumatoid arthritis and inflammatory bowel diseases. Unfortunately, these drugs can elicit severe adverse effects, many of which resemble features of the metabolic syndrome such as weight gain, hyperglycemia, insulin resistance and dyslipidemia. The combination of these symptoms is also referred to as Cushing's syndrome. The work described in this thesis focuses on the metabolic effects of prednisolone treatment in mice and how these adverse effects are brought about.

In order to evaluate *in vivo* glucose metabolism and insulin resistance repeatedly in a basal, fasted condition, a method in which blood glucose kinetics can be assessed without perturbing glucose homeostasis, is described in chapter 2. This model, in which glucose kinetics are described by single-pool, first order kinetics, was performed in mice in which insulin resistance was induced by feeding a high fat diet for 5 weeks. We confirmed that a 5 week high fat diet induced insulin resistance by hyperglycemia and hyperinsulinemia, resulting in increased HOMA-IR. In addition, a high fat diet reduced glucose clearance rate, the disposition index and both hepatic and peripheral insulin sensitivity (IS). To compensate for this insulin resistance, β-cell function was slightly increased. In conclusion, **chapter 2** describes a novel method in which it is possible to combine the calculated insulin sensitivity in fasting conditions with blood glucose kinetics in the same situation.

This novel method was employed in **chapter 3** focusing on the consequences of chronic prednisolone treatment on insulin sensitivity and blood glucose kinetics in C57BL/6J mice. Prednisolone treatment led to hyperglycemia and hyperinsulinemia, resulting in an increased HOMA-IR, but this apparent reduced insulin sensitivity could not be confirmed with a hyperinsulinemic euglycemic clamp. Application of our newly developed method revealed that prednisolone-treated mice show an increased hepatic glucose production under basal conditions at higher insulin levels, indicative for reduced insulin sensitivity. In addition, prednisolone-treated mice had higher plasma FGF21 concentrations in the fed and fasted condition and showed hardly any reduction in blood glucose levels upon fasting, revealing that the apparent insulin resistance induced by prednisolone-treatment was more likely due to an altered feeding-to-fasting transition.

Insulin resistance can be induced by a western type diet, therefore in **chapter 4** we investigated whether adverse effects of prednisolone are aggravated in mice with compromised glucose metabolism due to high fat diet feeding. Prednisolone treatment aggravated fasting hyperglycemia and hyperinsulinemia caused by high-fat feeding, resulting in a higher

HOMA-IR. In addition, basal glucose kinetics revealed a similar glucose production and clearance rate at high insulin levels, implying reduced insulin sensitivity. Remarkably, using hyperinsulinemic-euglycemic or hyperglycemic clamp techniques, neither hepatic nor peripheral insulin resistance was enhanced in the group that was additionally treated with prednisolone. Yet, analysis of hepatic glucose metabolism revealed that prednisolone did alter glycogen balance by reducing glycogen synthase flux, under hyperinsulinemic as well as hyperglycemic conditions. In addition to elevated insulin levels, prednisolone-treated mice showed a major rise in plasma leptin and FGF21 levels. These data indicate that prednisolone-induced adverse effects on glucose metabolism in high-fat diet fed mice do not reflect impaired insulin action but may be caused by changes in the hormonal regulatory network controlling glucose metabolism.

In view of the severe adverse effects of prednisolone and dexamethasone in humans, the development of new GC with less or no adverse effects is highly desirable. **Chapter 5** describes a non-steroidal glucocorticoid receptor (GR)-selective compound (Org 214007-0) with a binding affinity to GR similar to that of prednisolone. Using various cell lines and primary human cells, we showed that Org 214007-0 acts as a partial GC agonist, since it repressed inflammatory genes and was less effective in induction of metabolic genes. More importantly, *in vivo* studies in mice indicated that Org 214007-0 retained full efficacy in acute inflammation models as well as in a chronic collagen-induced arthritis (CIA) mouse model to reduce inflammation. Gene expression profiling of muscle tissue derived from arthritic mice showed a partial activity of Org 214007-0 at an equi-efficacious dosage of prednisolone, with an increased ratio in repression versus induction. Finally, prednisolone, but not Org 214007-0 induced elevated fasting blood glucose levels in mice, a phenotype accompanied by a shift in the hepatic glucose / glycogen balance. These data demonstrate that Org 214007-0 belongs to the new class of selective glucocorticoid receptor modulators (SGRM's) with an increased therapeutic index compared to prednisolone that could contribute to effective anti-inflammatory therapy with a lower risk for metabolic side effects.

For evaluation of novel GCs, it is highly preferable to be able to measure both efficacy and metabolic safety in the same animal. Preclinical efficacy of newly developed compounds can be assessed in DBA/1J mice with collagen-induced arthritis (CIA), a model with features resembling rheumatoid arthritis in humans. However, adverse effects on metabolism of novel GCs have never been tested in this disease model. Therefore the method described in chapter 2 was applied in the CIA model. Arthritis scores were decreased after treatment with prednisolone, confirming the anti-inflammatory properties of GCs. Insulin secretion and hepatic glucose production were increased, but this did not result immediately in hyperglycemia or insulin resistance, indicating a highly adaptive compensatory

mechanism in these mice. In conclusion, this model allows for studying effects of (novel) GC compounds on the development of arthritis and glucose kinetics in a single animal. This integrative model provides a valuable tool for investigating (drug-induced) metabolic dysregulation in an inflammatory setting.

Finally, in order to discriminate between dimeric and monomeric actions of the GR upon activation by prednisolone in the development of metabolic adverse effects, GR^{dim} mice were applied in **chapter 7**. These transgenic mice have a defect in the dimerization domain, abrogating dimeric GR gene-controlled transcription. GR^{dim} mice were treated with prednisolone for six days, which did not influence fasting glucose levels but strongly increased their plasma triglyceride and cholesterol levels, *i.e.*, a dramatic 9-12 fold increase for triglycerides and free cholesterol in the VLDL-sized lipoprotein fraction. Surprisingly, hepatic cholesterol and phospholipids levels did not change. The unusual lipid profile was not caused by cholestasis as plasma bile acid concentration did not increase. Hepatic gene expression levels of lipoprotein lipase *(lpl)* were 23 times induced, yet when LPL activity was blocked by Polaxamer, there was only a slight increase in VLDL secretion. The study described in this chapter showed that sustained prednisolone treatment in GR^{dim} mice leads to formation of atypical VLDL particles. These results indicate an important role for monomeric GR in regulation of lipid metabolism and may contribute to unravelling the mechanisms underlying GC-induced side effects.

Overall, the studies described in this thesis show that the effects of prednisolone on the induction of insulin resistance in mice is not as straight-forward as reported in humans and rats. Chapter 8 discusses this aspect extensively. Prednisolone treatment caused hyperglycemia and hyperinsulinemia in C57BL/6J mice, but 'classical insulin resistance' according to the HIEC could not be documented. Prednisolone-treatment of DBA/1J or BALB/c mice did lead to hyperinsulinemia without hyperglycemia; yet, in these mice the HIEC was not performed. Nevertheless, blood glucose kinetics in the fasted situation did implicate reduced insulin sensitivity and prednisolone did alter hepatic glucose metabolism and lipid metabolism. In addition, the studies described in this thesis revealed that feeding status and hormonal regulation are important factors which have to be taken into account when studying GC's induced insulin resistance. Taken together, these results showed that GCs both alter glucose and lipid metabolism, but GC-induced insulin resistance in mice is not as straightforward as reported in humans. For future analysis of metabolic adverse effects of GC in mice, prior evaluation of the specific research question should lead the choice for an optimal animal model. The studies described in this thesis provide a first step in this direction.

Nederlandse samenvatting

Korte inleiding

De term glucocorticoïden is een verzamelnaam voor hormonen en medicijnen die werken via de glucocorticoïd receptor (GR). Het belangrijkste glucocorticoïd in mensen is cortisol. cortisol wordt ook wel een stress hormoon genoemd, omdat het in verhoogde mate in het bloed wordt uitgescheiden tijdens stressvolle situaties. Cortisol wordt geproduceerd door de bijnier onder invloed van de hypothalamus-hypofyse-bijnier as. De hypothalamus is een gebied in de hersenen dat de stressvolle situatie registreert en daarop de stof corticotropin releasing hormone (CRH) uitscheidt. CRH stimuleert de hypofyse die vervolgens adrenocorticotropic hormoon (ACTH) uitscheidt. In de bijnier activeert ACTH de omzetting van cholesterol in cortisol. Dit proces heeft een negatieve terugkoppeling, wat betekent dat de aanwezigheid van cortisol in de hersenen de uitscheiding van CRH verlaagt en daardoor de productie van cortisol door de bijnier afremt. In stressvolle situaties zorgt cortisol voor een verhoogde energiehuishouding door het glucose en lipide metabolisme te beïnvloeden. Dit verloopt via binding aan de cortisol receptor in meerdere organen en weefsels, waaronder de lever, spieren en vetweefsel. De energie die vrijkomt kan gebruikt worden voor bijvoorbeeld de 'vecht-of-vlucht' reactie. Cortisol beïvloedt ook het immuun systeem en de bloeddruk. Glucocorticoïden werken op bijna alle weefsels, want de GR komt vrijwel overal tot expressie.

Gebaseerd op de rol van glucocorticoïden in regulering van het immuun-systeem zijn meerdere medicijnen ontwikkeld die de immuunreactie kunnen onderdrukken. Dit worden synthetische glucocorticoïden genoemd. Dexamethason en prednisolon worden het meest gebruikt. Deze medicijnen worden sinds de jaren 50 veelvuldig toegepast voor de behandeling van auto-immuun ziekten, zoals reuma, de ziekte van Crohn en astma. Helaas heeft het gebruik van glucocorticoïden vele vervelende bijwerkingen. De meest bekende zijn de zichtbare bijwerkingen, zoals gewichtstoename (met name rond de buik), een rond gezicht, acne en versnelde haargroei. Echter, de minder zichtbare bijwerkingen kunnen nog vervelender zijn, zoals osteoporose (botontkalking), hyperglycemie (verhoogde bloedsuiker waarden), dyslipidemie (verstoorde vethuishouding in het bloed) en de ontwikkeling van insuline resistentie.

Insuline is een belangrijk hormoon voor de glucose-huishouding. In een glucose-rijke situatie (bijvoorbeeld na een maaltijd) stimuleert insuline de opname van glucose vanuit het bloed naar de weefsels waar glucose opgeslagen kan worden. In de lever kan glucose opgeslagen worden als glycogeen; spieren kunnen glucose direct benutten, maar ook opslaan als glycogeen. Het vetweefsel heeft echter de grootste opslagcapaciteit, maar

daarvoor moet glucose eerst omgezet worden in vetten. Deze opslag vindt plaats onder invloed van insuline. In een glucose-arme situatie zijn de insuline spiegels laag. In samenwerking met andere hormonen, stimuleert dit de lever tot de productie van glucose voor onder andere de hersenen, die glucose als belangrijkste energiebron gebruiken.

Insuline resistentie is een voorfase van diabetes mellitus type II. De cellen van de belangrijkste organen in het glucose metabolisme, zoals lever, spieren en vetweefsel, zijn in het geval van insuline resistentie minder gevoelig voor insuline. Hierdoor is er meer insuline nodig om de cellen even sterk te stimuleren om glucose op te nemen. Dit is echter een vicieuze cirkel, waardoor er steeds meer insuline nodig is. De alvleesklier produceert insuline en kan deze verhoogde vraag niet altijd aan waardoor de glucose concentratie in het bloed toch oploopt. Dan is er sprake van diabetes type II. In een latere fase van diabetes type II raakt de alvleesklier zo overbelast dat de insuline secretie stopt. De type II gaat dan als het ware over in type I diabetes.

Doel van het onderzoek

Bij langdurige medicatie met glucocorticoïden zoals prednisolon, kunnen insuline resistentie en dyslipidemie als bijwerkingen voorkomen. Het doel van het onderzoek beschreven in dit proefschrift was het achterhalen van de manier waarop deze bijwerkingen ontstaan. Met behulp van muismodellen werd het effect van prednisolon op het glucose metabolisme, insuline resistentie en dyslipidemie bestudeerd. Hiervoor werd onder andere gebruik gemaakt van methoden waarbij gebruik gemaakt werd van stabiel gemerkte isotoop verbindingen.

Samenvatting dit proefschrift

Na een inleiding en een overzicht van de inhoud van dit proefschrift in **hoofdstuk 1**, staat in **hoofdstuk 2** staat een nieuwe methode beschreven om het glucose metabolisme te bestuderen in een gevaste situatie, als er dus relatief weinig glucose in het bloed aanwezig is. De methode maakt gebruik van een eenmalige injectie met stabiel gelabeld glucose. Dit houdt in dat tussen het reeds in het lichaam aanwezige glucose het geïnjecteerde glucose door middel van het label terug gevonden kan worden. Hierdoor kan de klaring van het glucose uit het bloed gereconstrueerd worden. Dit levert een mooie curve op. Aan de hand van deze curve kan de glucose productie (door de lever) en de glucose opname (met name door spieren en vet) worden berekend. Het vernieuwende van deze methode is dat het een vrij simpel uit te voeren techniek is, die voor de dieren veel minder belastend is vergeleken met bestaande methoden. In combinatie met gemeten insuline waarden, geven de berekende waarden een waardevolle indicatie over de mate van insuline resist-

entie. In hoofdstuk 2 werd een 'normale' groep muizen vergeleken met een groep muizen die een vorm van insuline resistentie kregen door middel van een hoog-vet dieet.

De methode werd in **hoofdstuk 3** gebruikt in muizen die 7 dagen met prednisolon behandeld waren. Deze muizen hadden verhoogde gevaste glucose en insuline waarden, wat insuline resistentie deed vermoeden. Ook was de glucose productie (gemeten met de methode beschreven in hoofdstuk 2) in deze muizen verhoogd. Echter, de gouden standaard voor het aantonen van insuline resistentie is de hyperinsulinemische euglycemische clamp. Voor deze redelijk bewerkelijke en belastende methode kregen de muizen gedurende enkele uren een insuline infuus (hyperinsulinemie). Dit zorgt voor een daling van de bloed glucosewaarden. Om een hypoglycemie (te lage bloedsuikerwaarden) te voorkomen, werd gelijktijdig een aangepast glucose infuus gegeven en de glucose waarden gemeten om de glucose spiegel stabiel te houden (euglycemisch). De hoeveelheid glucose die geïnfundeerd moet worden om glucose spiegels stabiel te houden, is een maat voor de insuline gevoeligheid. Voor prednisolon behandelde muizen was eenzelfde hoeveelheid glucose nodig als voor de controle dieren, wat aangeeft dat ze even insuline gevoelig waren. Hiermee werd 'klassieke' insuline resistentie uitgesloten. Er was echter opgemerkt dat de prednisolon behandelde muizen in de gevoede toestand een lagere glucosespiegel hadden. Hierop werden de muizen 24 uur gevast, waaruit bleek dat de prednisolon behandelde muizen een veranderde 'gevoed-gevast' overgang hadden. Daarnaast bleek dat FGF21, een recentelijk ontdekt hormoon dat sterk betrokken is bij de energiehuishouding gedurende een vasten-periode, sterk verhoogd was in prednisolon behandelde dieren. Deze resultaten samen geven aan dat de vermoede insuline resistentie, klaarblijkelijk een effect was van de veranderde voeden-vasten regulatie.

Zoals ook beschreven in hoofdstuk 2 kan insuline resistentie opgewekt worden door een hoog-vet dieet, dat ook gebruikt werd in **hoofdstuk 4**. Er werd verwacht dat de combinatie van een hoog-vet dieet bovenop prednisolon therapie, de effecten van prednisolon zou versterken. Door de combinatie van een hoog-vet dieet met prednisolon therapie werden de glucose en insuline spiegels sterk verhoogd. Echter, ook nu bleek uit de hyperinsulinemische euglycemische clamp dat de muizen op een hoog-vet dieet met prednisolon therapie even insuline resistent waren als de muizen met alleen een hoog-vet dieet. Dit was ook het geval gedurende een hyperglycemische clamp, waarin een glucose infuus gegeven werd om de bloedsuikerwaarden te verhogen tot 17 mM. Het lichaam reageert hierop door insuline aan te maken. Hier is de hoeveelheid glucose die toegediend moet worden een maat voor de insuline uitscheiding en gevoeligheid. Dit was onveranderd in muizen behandeld met prednisolon of alleen met het oplosmiddel. Het hoog-vet dieet daarentegen induceerde wel de verwachte verlaging in insuline gevoeligheid. Met behulp van de stabiele isotoop techniek MIDA (massa isotopomeer distributie analyse) werd de

enzymatische omzetting van glucose en bijproducten (de glucose fluxen) in de lever gemeten. Hieruit bleek dat, ook al waren de prednisolon behandelde muizen niet insuline resistent, de glucose fluxen in de lever wel veranderd waren. Met name de omzetting van het glucose tussenproduct glucose-6-fosfaat in glycogeen (de opslag vorm van glucose) was verminderd. Daarnaast bleek dat niet alleen de insuline spiegels in het bloed verhoogd waren, maar ook de spiegels van leptine en FGF21, beide hormonen die betrokken zijn bij de energiehuishouding. Op grond hiervan werd geconcludeerd dat veranderingen in het glucose metabolisme door prednisolon therapie met een hoog-vet dieet niet het directe gevolg waren van insuline resistentie, maar een verandering in het regulatie systeem van de energiehuishouding op hormoon niveau.

Door de bijwerkingen van prednisolon is het van groot belang dat er nieuwe middelen ontwikkeld worden die net zo ontstekingsremmend werken, maar minder neveneffecten hebben. In **hoofdstuk 5** staat een nieuw glucocorticoid beschreven, ORG 214007-0. Het idee van het achterliggende mechanisme van dit nieuwe middel is dat het wel bindt aan de GR en daarmee interacties met andere eiwitten in de cel uitvoert, maar dat het directe effect op de expressie van genen die betrokken zijn bij het ontstaan van de bijwerkingen verminderd is. Dit noemt men dissociërende effecten en dit type middelen worden selectieve GR modulators (SGRM's) genoemd. Allereerst werd in cellijnmodellen (*in vitro*) gekeken naar het effect op genexpressie van verschillende genen. Het effect op de genen die betrokken zijn bij bijwerkingen was minder met ORG 214007-0 dan met prednisolon. Het effect op de genen die betrokken zijn bij de ontstekingsremmende werking was echter bijna net zo goed als met prednisolon. In muisstudies (*in vivo*) werd gekeken naar de effectiviteit om ontstekingen te kunnen remmen in een muismodel voor reumatoïde artritis. Hieruit bleek dat ORG 214007-0 zelfs bij een lagere dosis effectiever was in het remmen van de ontsteking. Daarna werd gekeken naar het glucose metabolisme in een ander muismodel. Net als in de vorige hoofdstukken beschreven, verhoogde prednisolon ook in deze studie de gevaste glucose waarden; dit was met eenzelfde effectieve dosis van ORG 214007-0 niet het geval. Met behulp van de MIDA methode zagen we dat prednisolon wederom de glucose fluxen veranderde; ORG 214007-0 deed dit niet. Dit leidde tot de conclusie dat ORG 214007-0 een dissociërend glucocorticoïd is en dat dit middel zou kunnen bijdragen aan een verbeterde behandeling met gelijkwaardige ontstekingsremmende capaciteiten, maar met minder bijwerkingen.

In hoofdstuk 5 werden de metabole bijwerkingen en de ontstekingsremmende capaciteiten van glucocorticoïden bestudeerd in twee verschillende modellen. In **hoofdstuk 6** werd gestreefd naar optimalisatie van de analyse van bijwerkingen en effectiviteit in één diermodel. Hiervoor werd het collageen-geïnduceerde artritis model gebruikt. Deze muizen worden echter erg ziek en belastende methoden, zoals de hyperinsulinemische eugly-

cemische clamp, kunnen niet in deze muizen uitgevoerd worden. Daarom hebben we de bloed glucose kinetiek methode uit hoofdstuk 2 in deze muizen met artritis uitgevoerd. Behandeling van artritis muizen met prednisolon verlaagde de artritis scores, waarmee de ontstekingsremmende werking van de gebruikte dosis prednisolon bevestigd werd. In deze muizen was de insuline uitscheiding, gemeten aan de hand van C-peptide, verhoogd, even als de hepatische glucose productie. Echter, dit leidde niet tot een hyperglycemie of tot insuline resistentie, wat aangeeft dat er een sterk compensatie mechanisme aanwezig is in deze muizen.

Naast insuline resistentie heeft prednisolon ook minder bekende effecten op de vet-huishouding. Dyslipidemie, een verstoring van zowel cholesterol als triglyceride homeostase in het bloed, wordt ook als bijwerking van prednisolon gerapporteerd. Om meer inzicht te krijgen in het mechanisme werd het onderzoek in **hoofdstuk 7** uitgevoerd in transgene muizen. Normaal gesproken werkt prednisolon via de GR. Na binding met de receptor in de cel gaat dit complex van ligand (prednisolon) en receptor naar de celkern. In de celkern zijn telkens 2 receptor-complexen (dimeer) nodig om aan het DNA te binden en als transcriptiefactor genen te activeren (of te onderdrukken). Dit noemt men dimerisatie. Echter, wanneer een gebonden receptor alleen blijft (monomeer) kan het nog steeds verschillende effecten hebben, zoals binding aan andere transcriptiefactoren of eiwitten. Het idee is ontstaan dat de dimeren voornamelijk de bijwerkingen veroorzaken, terwijl de monomeren ontstekingsremmend werken. Hiervoor werd in hoofdstuk 7 gekeken naar het effect van prednisolon op dyslipidemie in muizen waarin geen dimerisatie plaatsvindt; zogenaamde GR^{dim} muizen. Wildtype en transgene muizen werden met prednisolon of oplosmiddel behandeld gedurende 6 dagen. Zowel in prednisolon behandelde wildtype als transgene muizen was geen effect op glucosespiegels in het bloed te zien. Prednisolon behandeling in wildtype muizen zorgde voor een lichte verhoging van plasma cholesterol en triglyceriden. Echter, in transgene muizen was dit effect van prednisolon enorm versterkt. Met name plasma triglyceriden en cholesterol spiegels waren 9 tot 12 keer verhoogd. Verassend genoeg had dit geen effect op de triglyceride en cholesterol concentraties in de lever en de muizen waren ook niet cholestatisch (vernauwing van de galwegen), want de concentratie van galzouten in plasma was normaal. Een interessante observatie was dat expressie van het lipoproteïne lipase gen in de lever 23 keer was verhoogd. Dit gen is betrokken bij de triglyceride afbraak. De zoektocht naar de precieze oorzaak van het ontstaan van deze extreme dyslipidemie in GR^{dim} muizen moet nog verder uitgebreid worden, maar het is duidelijk dat monomeer GR hierbij een belangrijke rol speelt.

Conclusie

Concluderend duiden de resultaten uit de hoofdstukken beschreven in dit proefschrift

erop dat de effecten van prednisolon op de ontwikkeling van insuline resistentie en dyslipidemie in muizen niet zo eenduidig is als gerapporteerd in mensen. De verschillende factoren die hierop van invloed kunnen zijn, worden uitgebreid bediscussieerd in **hoofdstuk 8**. Deze factoren variëren van de behandelmethode en de duur van de behandeling, de verschillen tussen de verscheidene muizen stammen, tot de methode waarop insuline resistentie gemeten wordt en de effecten van overige organen en hormonen in het glucose metabolisme.

Prednisolon therapie veroorzaakte hyperglycemie en hyperinsulinemie in C57BL/6J muizen, maar de 'klassieke' insuline resistentie werd niet aangetoond met behulp van de 'gouden standaard' de hyperinsulinemische euglycemische clamp methode. In de muizenstammen DBA/1J en BALB/c werd een hyperinsulinemie gevonden, zonder een hyperglycemie. In deze muizen is helaas geen hyperinsulinemische euglycemische clamp uitgevoerd. Echter, uit de gevaste bloed glucose kinetiek experimenten en de MIDA experimenten bleek dat het hepatische glucose metabolisme toch veranderd was door prednisolon behandeling. Daarnaast bleek uit meerdere studies beschreven in dit proefschrift dat de voedingsstatus en de hormonale regulatie belangrijke factoren zijn waar rekening mee gehouden moet worden wanneer de bijwerkingen van prednisolon op het metabolisme bestudeerd worden. Samenvattend bleek uit de resultaten dat glucocorticoïden zowel het glucose- als het lipide-metabolisme veranderen, maar dat prednisolon-geïnduceerde insuline resistentie in muizen niet zo eenvoudig ligt en niet zo duidelijk gezien wordt als in mensen. Voor toekomstig onderzoek van metabole bijwerkingen van prednisolon in muizen, moet eerst het optimale diermodel gekozen worden. De resultaten beschreven in dit proefschrift voorzien in een eerste stap in deze richting.

Author list

Bastiaansen, E.A.J.[1] Boer, T.S.[2]
Bleeker, A.[3] Bloks, V.W.[3]
Dokter, W.H1[1,4] Grefhorst, A.[3,5]
Groen, A.K.[3] Kuipers, F.[2,3,6]
Laskewitz, A.J.[3] Rauch, A.[7]
Reichardt, H.[8] Reijngoud, D-J.[2]
Schreurs, M.[9] Schouten, A.E.[1]
Toonen, E.J.M.[10] Tuckermann, J.P.[7]
Van der Vleuten, M.A.J.[1] Van Dijk, T.H.[2,3]
Van Doorn, C. [1] Van Lierop, M-J.C.[1,11]

1. Department of Immune Therapeutics, MSD Research Laboratories, Oss, The Netherlands
2. Department of Laboratory Medicine, University Medical Center Groningen, University of Groningen, Groningen, The Netherlands
3. Department of Pediatrics, University Medical Center Groningen, University of Groningen, Groningen, The Netherlands
4. Present address: Synthon Research Laboratories, Nijmegen, The Netherlands
5. Present address: Department of Internal Medicine, Erasmus MC, Rotterdam, The Netherlands
6. Current position: Dean of the Medical Faculty, University Medical Center Groningen, University of Groningen, Groningen, The Netherlands
7. Tissue-specific hormone action, Leibniz Institute for Age Research, Fritz Lipmann Institute, Jena, Germany
8. Department of Cellular and Molecular Immunology, University of Göttingen Medical School, Göttingen, Germany
9. Department of Pathology & Medical Biology, Molecular Genetics, University Medical Center Groningen, University of Groningen, Groningen, The Netherlands
10. present address: Department of Internal Medicine, Radboud University Nijmegen Medical Centre, Nijmegen, The Netherlands.
11. Present address: PK-PD MSD, Oss, The Netherlands

Een ongeluk zit in een klein hoekje…

Geluk zit hem in de rest!

Dankwoord

En dan is het eindelijk zover. Wat begon als colloquium onderwerp, ligt hier nu in de vorm van een proefschrift. Van te voren wist ik dat het een roerig traject zou worden, want ik ken geen enkel promotieproject dat geen ups en downs kent, maar dat het zo'n heftige periode zou worden, had niemand denk ik kunnen vermoeden. Het overlijden van Harmen en Anniek W. heeft mij ontzettend geraakt en deed me beseffen dat 'genieten' je belangrijkste taak in het leven is. Na mijn eigen ongeluk is dit alleen nog maar duidelijker geworden. Ik ben ontzettend blij dat ik na de ellende van 2009 toch in staat ben om dit dankwoord te kunnen schrijven, maar dat had ik niet kunnen doen zonder de steun, hulp en liefde van heel veel mensen. Met dit dankwoord kan ik waarschijnlijk mijn naasten nooit genoeg bedanken, maar ik ga toch een poging wagen.

Allereerst wil ik graag van deze gelegenheid gebruik maken om iedereen te bedanken die tijdens mijn ziekhuis- en herstelperiode kaartjes, berichtjes, bloemen en e-mails hebben gestuurd. Die steun, vaak vanuit onverwachte hoek, heeft mij heel erg goed gedaan.

Geachte Prof. dr. F. Kuipers, beste Folkert, ik ben erg dankbaar voor jouw vertrouwen om mij aan te stellen op een project bij een subsidiegever die nog niet eens bestond. Tijdens de eerste TiPharma meetings, waar ik de enige Aio was tussen alle professoren, leerde ik al gauw jouw sterke onderhandel kwaliteiten kennen. Bovendien ontdekte ik dat je als echte Groninger een man van weinig woorden bent, maar dat ieder woord raak is. Ik heb ontzettend veel van je geleerd, al moest ik in het begin wel een beetje wennen aan je manier van communiceren en je kritische vragen. Deze vragen stimuleerden me altijd weer om verder te zoeken, dieper te graven en langer na te denken. Nadat je decaan bent geworden, heb je Bert het vertrouwen over mijn project gegeven, maar ik ben blij dat je in de laatste maanden toch weer nauw betrokken was bij het afronden van dit proefschrift. Bedankt voor je begeleiding, de efficiënte besprekingen, goede discussies en je snelle en tekstueel briljante manier van redigeren.

Geachte Prof. dr. A.K. Groen, beste Bert, nadat je Folkert zijn positie als hoofd van het lab kindergeneeskunde had overgenomen, hebben we elkaar volgens mij 2 á 3 keer gesproken vóór mijn ongeluk. Tijdens mijn herstelperiode heb ik je leren kennen als een sociale, geïnteresseerde en spirituele man. Ik heb jouw interesse in mijn project zeer gewaardeerd. Je hebt me nog niet kunnen overtuigen dat cholesterol het aller leukste vakgebied is, maar ik heb veel van je geleerd en hoofdstuk 7 is toch in mijn boekje gekomen. Bedankt voor alle steun, begeleiding, je persoonlijke interesse en je vertrouwen dat ik een goede KCio zal worden.

Beste Dr. van Dijk, Theo, ik had het geluk toen ik begon dat jij en Aldo al enig voorwerk hadden verricht. Hierdoor ben je vanaf het begin af aan bijzonder nauw betrokken geweest bij mijn project. Door de vele tripjes naar TiPharma meetings in Oss en de vele uren op ADL8 waarbij we bestaande technieken nog verder optimaliseerden, hebben elkaar beter leren kennen en dat is uitgegroeid tot wat ik als een bijzondere samenwerking beschouw. Ik wil je graag bedanken dat ik je 's ochtends vroeg voor een experiment nog even kon bellen met de laatste vraagjes en je geduld en stimulerende woorden om mij alle handelingen tijdens dierexperimenten te leren. Ik denk dat jouw kennis en kunde door sommigen in ons lab wordt onderschat. En Theo, bedankt voor gezelligheid en goede gesprekken tijdens de vele bakjes koffie, de dure biertjes in Rome, de sushi in Amsterdam en de friet bij jou en Jenny en voor het puppy knuffelen. Kun je in de toekomst de weg wel vinden zonder AnkeAnke? Ik denk dat ik nu wel in je vergane glorie map kan.

Beste Dr. Grefhorst, Aldo, net zoals Theo was je al eerder met mijn project bezig dan ikzelf, met dit verschil dat jij in Texas zat toen ik begon. Maar toen je terugkwam was je direct weer bij mijn project betrokken. Ik heb je praktische hulp zeer gewaardeerd, vooral in de overgangsfase tussen Folkert en Bert en bij de begeleiding van Christine. Ik heb diep respect voor jouw manier van denken, bij ieder resultaat weet je gelijk wel weer een leuk experimentje te bedenken om dieper te graven; ik denk dat deze eigenschap jou tot een zeer goed onderzoeker maakt. Bedankt voor je interesse in mijn project en je snelle nakijk werk van mijn stukken.

Beste Dr. Reijngoud, Dirk-Jan, wie had ooit gedacht dat ik in je voetsporen zou treden. Nu die onuitputtelijke biochemische kennis nog. Ik wil je bedanken dat je deze kennis altijd hebt willen delen en voor je andere kijk op mijn stukken. Dankzij jouw vernieuwende inzichten is hoofdstuk 4 een mooi stuk geworden. Met jou wil ik ook graag Rebecca bedanken voor jullie hulp in mijn weg naar klinisch chemicus in opleiding.

Bij deze zou ik ook graag de leden van de leescommissie, Prof. dr. Michaela Diamant, Prof. dr. Jan Tuckermann, Prof. dr. Gertjan van Dijk willen bedanken. Daarnaast wil ik de overige leden van kindergeneeskunde, Henk-Jan (voor wijs advies), Peter, Pieter, Edmond, Uwe, Barbera, Torsten (bedankt voor alle keren dat je me mee de grens over wilde nemen in ruil voor M&M's), Hans, Robert, Klary en Frans S., bedanken voor hun kritische vragen en input tijdens de dinsdagmorgen meetings. Dolf bedankt voor al je hulp met het papierwerk.

Mijn project was onderdeel van het TiPharma project 'Glucocorticoid-induced insulin resistance' waardoor ik met veel verschillende afdelingen samen heb gewerkt. Beste Dr. Doktor, Wim, jouw leiding over dit project heb ik als zeer aangenaam ervaren en jouw efficiënte manier van vergaderen maakten de TiPharma bijeenkomsten zeer succesvol.

Bedankt voor het opzetten en leiden van ons project en dat je ons altijd aan het belang van dosis-respons curves hebt herinnerd. Ook bedankt voor je hulp bij onze stukken.

Dankzij dit project heb ik in vele samenwerkingen mogen participeren. De grootste van deze samenwerkingen was toch wel met Organon/Shering Plough/MSD, ook al waren het roerige tijden. Beste Marie-José, bedankt voor alle antwoorden op de praktische vragen vooral in het begin en je input in mijn stukken. Ik duim nog steeds voor ons PNAS-stuk. Monique, bedankt voor de overnachting in 'Hotel van der Vleuten' en de vele pakketjes prednisolone die je verstuurd hebt. Annelies, ik ken geen enkele bio-technicus die zo snel is als jij. Erik, jij kwam als laatste als postdoc bij ons project en dit heeft de samenwerking nog meer versterkt. Ik heb onze telefoontjes als ik niet 'somewhere in Germany' was zeer gewaardeerd. Ik vind het knap van ons dat 'even bellen?' toch bijna altijd minstens een half uur werd. Ik heb goede hoop voor ons CIA-stuk!

Daarnaast wil ik de andere projectleden van TiPharma project T1-106 bedanken. Door de mix van *in vitro* in het LUMC via *in vivo* in het UMCG naar humane studies in het AMC, UMCU en VU waren de TiPharma meetings erg gevarieerd. Bedankt voor jullie input en discussies en de blik op de klinische relevantie. Daniël en Margot, ik vond het mooi om met jullie op de EASD in Rome te staan.

Ook wil ik de organisatie TiPharma, met in het bijzonder Prof. dr. Crommelin, Karin en Patricia, bedanken voor een mooi PhD-project. Omdat ik een van jullie eerste promovendi was, kreeg ik de mogelijkheid mijn enthousiasme voor het onderzoek te delen met de buitenwereld, zowel in de promotie-film, het interview in intermediair, op het Ecopa congres in Alicante en in het gesprek met minister Ab Klink, al heeft dat laatste helaas niet geholpen. Daarnaast wil ik jullie bedanken voor jullie persoonlijke betrokkenheid na mijn ongeluk.

Another great collaboration was with the Tuckermann-lab from the Leibniz Institute in Jena. Dear Prof. dr. Tuckermann, Jan, I'm glad I could work with you on the GR^{dim} mice. I learned a lot from you on GR-dimerization and glucocorticoid function. I've really appreciated your input in meetings and your structured supervision of the project. Thank you for a nice collaboration and for being in my reading committee. Alex, thank you for a good collaboration, sending data and mice. I hope chapter 7 will lead to a nice publication. De derde partij in deze samenwerking was met het lab van Prof. dr. Stunnenberg; beste Henk, Nagesha en Melysia, ik ben altijd erg onder de indruk geweest van de Chip-seq methode, al was de data niet altijd even makkelijk te begrijpen. Bedankt voor de interessante meetings, waar ik veel over bio-informatica van jullie geleerd heb.

De laatste samenwerking was niet zo ver van huis, maar op de andere gang. Beste Dr. de Vos, Paul, Maaike (Smelt) en Bart. Ondanks een prettige samenwerking, heeft het eilandjes isoleren helaas geen mooie resultaten opgeleverd, maar Maaike, gelukkig wel een vriendschap. Bedankt voor jullie hulp en het stug volhouden, helaas was 3x geen scheepsrecht. Leonie, bedankt voor je hulp bij de Luminex meting.

Zonder de vakkundige verzorging van 'mijn' muizen had geen enkel hoofdstuk dit proefschrift gehaald. Daarvoor wil ik alle medewerkers van het CDP enorm bedanken en in het bijzonder Diana (als ze vechten, moeten ze wel van Anke zijn), Ralph, Ar, Harm, Lucas (in herinnering), Maurice, Mark, Annemiek, Andrea, Angela, Flip (bedankt voor je persoonlijke interesse), Arie, Wiebe, Miriam, Cathrien, Hester, Marcia, Annet, en niet te missen (daar waar de muziek is) Ramon.

Ondanks de vele Aio's en post-docs bij het lab kindergeneeskunde zijn het de analisten die het lab draaiende weten te houden. Daarvoor wil ik Rick, Vincent, Aycha, Renze (bedankt voor je hulp met de galzouten), Trijnie, Henk (bedankt voor je humor en muziek), Nicollete & Janny (ik heb jullie gemist bij het liedjes maken), Wytse, Juul & Angelika (bedankt voor alle histologie) en Marleen enorm bedanken. De specialistische kunde van een aantal mensen hebben een grote bijdrage aan dit proefschrift geleverd en deze vorm van technische assistentie beschouw ik als zeer waardevol. Daarnaast leveren sommige van jullie een belangrijke en gezellige bijdrage aan de half 12 lunch groep. Hilde & Gea, bedankt voor jullie secretariële ondersteuning en alle nieuwtjes.

Beste Rick, jouw specialistische kunde op het gebied van de microchirurgie is erg waardevol geweest voor meerdere hoofdstukken. Ik heb jouw aanwezigheid altijd als zeer prettig ervaren en ik geloof niet dat er ooit een minuut stilte valt als wij samenwerken. Bedankt voor je hulp, de gezellige tripjes naar Heidelberg, Jena en Hannover en de mooie avondjes bij FC Groningen of bij jullie voor de houtkachel.

Beste Vincent, ik denk dat net zoals bij Theo jouw waarde voor het lab nogal eens onderschat wordt. Gelukkig heb ik veel van je mogen leren over statistiek, micro-arrays en andere analytische details waar ik als bioloog soms geen oog voor had. Ook al worden jij en Theo soms als Waldorf en Statler neergezet, ik denk dat die beiden ook eigenlijk hele lieve mannen zijn. Bedankt voor al je hulp, je luisterend oor en dat je mijn 'kleine' leescommissie wilde zijn.

Beste Aycha en Marleen, naast dat ik jullie beide super leuke meiden vind, denk ik dat het lab kindergeneeskunde blij mag zijn zo'n enthousiaste jonge garde analisten erbij te hebben. Aycha, bedankt voor al je hulp en de vele metingen die je hebt gedaan tijdens mijn laatste jaar. Die meiden etentjes houden we erin.

Naast werken op het lab kindergeneeskunde, heb ik ook vele uurtjes in het lab van metabole ziekten zitten. Theo B, bedankt voor de vele GC-MS metingen en je hulp en geduld om mij wegwijs te maken in de wereld van de GC-MS. Ook Klaas wil ik hiervoor bedanken. Tineke, bedankt voor je hulp bij mijn metingen. Pim&Pim en Albert, bedankt dat jullie altijd een antwoord hadden op mijn praktische vragen. Ook alle andere mensen van het metabole lab wil ik bedanken voor het accepteren van mijn enorme hoeveelheid vieze buizen en het in bezet houden van het warmte blok. Fjodor, bedankt voor je regelmatige bezoekjes aan het chocoladelaatje.

Toen ik in 2006 op het lab kwam voelde ik me al snel thuis, dit was mede dankzij een grote groep slimme, hardwerkende maar ook erg gezellige collega Aio's. Jelske, Esther, Leonie, Niels en Maaike (Oosterveer); ik was blij dat ik niet bij jullie in het kippenhok zat, maar wel voor de gezelligheid kon langskomen. Alle oud Aio's bedankt voor de vele bieravondjes, waarna of flinke stapavondjes (Maaike: Folkert zou trots op ons zijn) of gezellige logeerpartijtjes volgden (Leonie: alleen XX) en leuke uitjes met de meiden (wadlopen of sauna). Maxi, bedankt voor de vele feestjes, ze leverden mooie foto's met pompoenen, snorren en pruiken op. Maxi en Leo, ik heb goede herinneringen aan de 'boat' in happypants met een goede film, lekkere wijn en altijd wel iemand die in slaap viel. Hilde en Sabina, ik heb ook erg goede herinneringen aan de gezellige avondjes met z'n drieën met spelletjes (lekker spanken die monkey), picknicken in het plantsoen en leuke dansavondjes. Sabina, ik ben blij dat we dat samen in Philly (I love the city!!!) nog een keer hebben overgedaan. Op de feestjes mis ik jou en Frans C. als Ray & Anita. Yan, thanks for sharing the stress hormone. Marijke en Maaike, de fameuze M&M, bedankt voor al jullie glucose hulp en gezelligheid. Maaike, waai je de volgende keer als een wervelwind weer eens langs? Lieve Marijke, enorme vraagbaak die alle antwoorden wel ergens netjes in een map heeft staan, ontzettend bedankt voor alle hulp, zowel de korte vragen als wel je praktische hulp in het lab. Door de vele uren die we samen in het lab hebben gestaan, heb ik veel van je geleerd. Keystone was mooi samen met jou!.. Ik wens je heel veel geluk met je 2^{e} carrière als mama erbij. Annelies, (INTJ-tje) bedankt dat jij altijd het overzicht en de kalmte bewaart. Ik ben blij dat ik samen met jou de loopbaanoriëntatie cursus heb gedaan. De updates en etentjes met Marije houden we erin. En dan waren er nog de echte doktoren onder ons: Frans C. (superpresentator), Jaap, Hester, Anniek K, en Anniek W (in herinnering). Anniek K. (supermama), ik heb grote bewondering voor jouw energie (haal je die uit koekjes?) en ontzettend bedankt voor je hulp in Haren. Jaap, jij bent voor mij de rust en precisie zelve, bedankt voor je hulp.

In bijna 6 jaar Y2.117 heb ik heel wat kamergenootjes versleten. Ondanks dat het misschien een 'ongeluks' kamer was, was, is en blijft(?) Y2.117 voor mij de leukste kamer van KG dankzij Janine, Thierry, Antonella, Laura, Marijke, Hilde, Harmen (in herinnering),

Gemma, Elise (stille kracht!), Jurre (moleculaire allesweter), Marije, Carolien, Jelena en Brenda. Meiden, ik hoop voor jullie dat er weer een vrouw in de chickies room komt! Bedankt voor de gezelligheid, goede gesprekken, adviezen, hulp bij experimenten, gezellige etentjes, de vele koppen koffie, eerst dankzij de Senseo (bedankt Hilde) en nu lekker luxe beneden (Marije, Jelena, Gemma; do I owe you one?). Gemma and Marije, after more than 3 years in the same 6 m2 I think we build up something more than just being colleagues. Gemma I loved sharing cheasy movies, either watching them together or by sms. Marije, bedankt dat je me geïntroduceerd hebt in de bakvissen wereld van Twighlight en ik ben blij dat je met me mee wilde naar Snow Patrol (ik hoop dat ik niet tè luid meegezongen heb). I really enjoyed the positive vibes you both send. I hope and think we will stay close for many more years. Carolien, buuv, we komen elkaar vast nog tegen. Succes met de rest van je MD/PhD project. Jelena, bedankt voor alle inside-information voor promovendi. Brenda, ik zou zeggen 'break a leg' voor een voorspoedig aio-schap, maar een schouder is denk ik wel voldoende.

Daarnaast wil ik de andere aio's en postdocs van het lab kindergeneeskunde bedanken voor een prettige werksfeer en succes wensen bij hun onderzoek: Jan-Freark (onze eigen oh oh Cherso was leuk)(heb je al een datum?), Gijs (nieuwe MIDA-man), Karen, Arne (Sinterklaas?), Wijtske (laat die mannen ook eens voor jou werken), Maurien, Jaana, Mark, Karin, Fiona, Agnes, Elodie, Jolita, Wei-lin (ik heb niks te klagen), Matthijs, Janine. En als laatste maar zeker niet de minste de meisjes van Verkade; Willemien, Marjan, Margot (nog even volhouden, NY is waiting for you), Nienke, Mariëtte (grote organisator van de Ladies night!) en Andrea (4:04!). Bedankt voor een mooie tijd!

Ook wil ik graag de buren op het lab, MDL, bedanken voor een prettige werksfeer en altijd de mogelijkheid om jullie pipetboy/plakband/stikstof hengelaar/etc. te lenen. Daarnaast wil ik de mensen van het Hofker-lab bedanken voor goede samenwerkingen en interessante meetings.

Annemieke & Hilde, Marijke, Theo en Annelies, bedankt dat ik bij jullie mocht oefenen in het buigen. Ik vond het een grote eer om als paranimf naast een ieder van jullie te staan.

De keuze voor het onderzoek is voor mij aangewakkerd door stimulerende voorbeelden tijdens mijn studie. Beste Prof. dr. Bos, Nico, ik heb een mooie en zeer leerzame periode bij jou op het lab gehad en bedankt dat je me hebt voorgedragen als student bij Mecky, dat was een levensveranderende ervaring voor mij. Dear Prof. dr. Pohlschröder, Mecky, I am very grateful for the opportunity you gave me to work in your lab as a student in Philadelphia. You're a lighting example for me for successful women in science. Your motivating and stimulating supervision made me decide to get my PhD and last June I was

happy to have such good and stimulating conversations again. Thank you for being you! Dear Maria, working with you in Mecky's lab in Philly was a great pleasure for me, I hope I can visit Argentina again. Maaike (Stoel), ook jij was voor mij een voorbeeld om Aio te worden, maar ik heb vooral veel waardering voor de manier waarop jij een zwaar promotie traject en een misschien nog wel zwaardere postdoc project hebt afgerond. Bedankt voor de mooie tijd in Philly.

Buiten het lab kon ik mijn energie en soms frustratie kwijt in sporten en voornamelijk het volleybal. Zowel bij Veracles week dames 2 als bij Oranje Nassau dames 8 heb ik een ontzettend leuke tijd gehad. Wd2, bedankt voor de leuke trainingen, de vele gezellige stapavondjes en bonenavondjes en een mooie vakantie in Portugal. ON d8, bedankt dat jullie me zo snel in jullie hechte club opnamen, ik vond het erg gezellig! Volgend jaar sinterklaas???

Daarnaast waren er een aantal lieve vriendinnetjes bij wie ik het ook eens ergens anders over kon hebben dan werk. Mijn sociale contacten lieten af en toe te wensen over, maar bij echte vriendinnen maakt het niet uit hoe vaak je elkaar ziet, het blijft altijd fijn als je elkaar ziet. Lieve Tanja, bij jou kan ik echt zeggen dat we 'way-back' gaan. Sinds de peuterschool ben jij een vaste waarde in mijn leven en daar ben ik heel dankbaar voor. Lieve Anniek, niet van de peuterschool, maar wel sinds de middelbare school. Ik denk dat we in vele dingen tegenpolen zijn, maar desalniettemin is het altijd gezellig, ook al moet je de zigeuners van je af slaan ;-). Christa, ik kom echt in 2012 naar Londen! Kim en Selena, ik zie jullie (en die kleine mannen) echt veel te weinig, maar bedankt voor alle gezelligheid en jullie steun toen ik in het ziekenhuis lag. Niet veel mensen komen vanuit Rotterdam (en Easterwierum) voor bezoek van een half uurtje, dat heb ik heel erg gewaardeerd.

Irma en Marc, bedankt voor jullie hulp en de vele etentjes tijdens de laatste fase.

Dan zijn er natuurlijk nog vriendinnetjes bij wie het wel vaak over de biologie gaat. Lisa, Saskia, Hilde, Marianne en Betty; zoals Hilde al beschreef zijn we super verschillende persoonlijkheden, maar wel een mooi stel biologen bij elkaar. Meiden, bedankt voor vele gezellige avondjes, dinertjes & ontbijtjes, filmpjes kijken, het delen van mannen (en vrouwen) perikelen, uitjes, boottripjes en festivals. Lisa, we zijn de Groninger leftovers, maar ik ben blij dat ik nu het vaakst van jouw uitbundigheid en kookkunsten mag genieten. Saskia, ik heb grote bewondering voor het avontuur dat je met Huub, Jort en … (en natuurlijk Ingrid) aangaat in Australië. Ik mis je. Betty en Marianne, collega´s(!), dank jullie wel voor het delen van promotieperikelen en voor jullie enthousiasme over de klinische chemie. Hilde, wat kan ik zeggen. Dat ik je mis weet je al.

Ik ben blij dat ik al vanaf het begin van mijn studie biologie zulke lieve vrienden heb

gevonden, en onderdeel mag zijn van het JAAH-gezelschap. We hebben ontelbare keren samen gegeten (in het begin op vaste avonden na het BOMmen) en mooie weekendjes weg gehad. Met niemand kan ik zo lachen als met jullie (pwaap!). Lieve Hilde, niet alleen ben je een super goede vriendin, ik heb ook het voorrecht gehad om bijna 4 jaar je collega en kamergenootje te mogen zijn. Je hebt me geleerd dat ik bij pyruvaat rechtsaf moet. Ik heb grote bewondering voor jouw ambitie en passie voor de wetenschap en je vermogen om hier vol voor te gaan. Daarnaast heb ik je altijd als een wijze, lieve en attente vriendin gezien, bij wie ik altijd terecht kan, ook al was het midden in de nacht (omdat de politie mijn huis afgezet had). Ik hoop dat je heel succesvol zult zijn in Boston (voor mij ben je dat al!) en daarna weer snel terug komt. Niet alleen voor mij, maar ook voor mijn familie ben jij een bijzonder grote steun geweest na mijn ongeluk. Lieve Jan, ik ben met veel plezier je huisgenootje geweest en we hebben lief en leed gedeeld. Helaas kan email de trap toch niet helemaal vervangen, maar ik ben blij dat het altijd als vanouds is. Daar waar Hilde, Miek en ik net klaar zijn, begin jij net aan je promotietijd, maar in de tussentijd ben je al hard op weg om gynaecoloog te worden. Ik denk dat dit deze carrière switch heel goed bij jou past en ik wens je daarbij veel succes toe. Lieve Annemieke, je bent voor mij als super lieve, attente vriendin een vaste waarde in Groningen, waar ik altijd van op aan kan. Ik ben blij dat ik met jouw in dezelfde fase zit, zowel in de twijfelfase vooraf en nu tijdens de promotiefase. Bedankt dat ik ook bij jou mocht oefenen met buigen en dat jij mijn paranimf wilt zijn en alle antwoorden op mijn vragen hebt. Ik hoop dat ik mijn zenuwen net zo goed in bedwang hou. Ik ben trots op je, dat jij de jeugd van tegenwoordig aan gaat pakken! Hilde en Miek, ik keek uit naar jullie dagelijkse bezoekjes aan mij in het ziekenhuis, toevallig altijd net als ik liep, zodat ik vol trots aan jullie mijn vorderingen kon tonen.

Ze zeggen wel eens, je vrienden kun je kiezen maar je familie niet. Gelukkig niet, want ik zou niet weten waar ik zo'n fijne familie zou kunnen vinden. Met een klein clubje kan ik ze gelukkig allemaal bedanken voor hun steun en liefde. Lieve oma, Janny en Ina, bedankt voor jullie stimulerende woorden, steun toen ik in het ziekenhuis lag, interesse in mijn onderzoek en jullie bijdrage om mijn studie te halen. Oma, zonder jou zou Philadelphia niet mogelijk geweest zijn. Lieve John & Miriam, bedankt voor jullie interesse in mijn werk en de ontspannende bootvaarten. Rob & Willeke, bedankt voor jullie steun en de hulp met de jurken-issues.

Liebe Judith und Lieber Stephan, gerne will ich Euch danken für die schönen Wochenenden in Eickhof und die Möglichkeit die Ihr mir gegeben habt dort in aller Ruhe an meiner Doctorarbeit zu arbeiten. Dear Anne und Tano, I would also like to thank you for all the nice times where I could relax from work, either in Eickhof, Genua, Frabosa, Bogliasco or at the Rennsteig. I hope we'll visit your renewed place in Bogliasco soon! Anne, I also would like to thank you for the nice times in Philly and introducing me to your brother ;-).

Lieve Sybren en Debora, ik vind het gezellig dat jullie nu ook in Groningen wonen (leuk huis!). Sybren, kleine zusjes worden groot, maar wie anders kon mijn hand vast houden toen ik het ziekenhuis weer uit liep dan mijn grote broer. Ik ben blij dat wij uit zo'n hecht gezin komen en bedankt dat je als puber je kleine zusje overal mee heen nam. Dankzij jou mocht ik veel. We moeten maar weer een broer-zus-zus tripje plannen.

Lieve Fardau en Bertus, bedankt dat jullie mij gedurende mijn promotietijd als jullie inboedel wilden hebben. Het was erg fijn altijd bij jullie aan te kunnen schuiven en op de bank te kunnen ploffen. Bertus, wat hebben we een boel leuke films gezien als Fardau sliep hè. Fardau, ik ben zo blij dat jíj mijn zusje bent, je staat altijd voor me klaar, kan mijn buien hebben (en ik de jouwe) en we hebben vaak aan een half woord genoeg (en anders zeggen we het tegelijk). Zoals ik al beschreef kan ik jou nooit genoeg bedanken voor alle steun toen ik in het ziekenhuis lag, je wilde alles wel voor me doen. Ik ben je briefje met 100 redenen kwijt, maar dat is niet erg want ze zitten in mijn hoofd voor jou. Ook al ben je mijn kleine zusje, je bent mijn grote steun en toeverlaat. Wij zijn zusjes!

'*KVK Kelken*'

Lieve papa en mama, ik voel me gezegend dat ik jullie dochter ben. Jullie manier van opvoeden, ongedwongen, open en vrij, maar stimulerend en warm, heeft me gemaakt tot wie ik ben. Zonder jullie was ik nergens. Jullie hebben me altijd gestimuleerd dat ik moest doen wat ik leuk vond en ik denk dat jullie daarin zeer geslaagd zijn. Jullie huis blijft altijd een thuis, niet alleen voor mij, maar voor een ieder die daar binnen stapt. Ik kan jullie nooit genoeg bedanken voor jullie goede zorgen, iedere dag de hele dag bij me in het ziekenhuis en daarna 3 maanden thuis. Pap, wat was ik blij met jouw verplegende kunde. Ook al weet ik dat het voor jullie de normaalste zaak van de wereld is, dat is het niet. En ook nu ik in Leeuwarden werk, staan jullie vaak voor me klaar. Dankzij en voor jullie is dit proefschrift nu af.

'want je kunt het niet alleen'

Lieve Christoph, er zijn niet genoeg woorden om te beschrijven wat ik voor je voel, maar ik weet wel dat jij mijn alles bent. Jouw rust en kalmte heb ik echt nodig en ik ben blij dat je af en toe op de stopknop drukt. In jouw armen voel ik me veilig en thuis. Van 600 km, via 450 km, nu op 100 km afstand, hoop ik dat het in 2012 0 km zal worden. Ik kijk er naar uit samen met jou de toekomst tegemoet te gaan. Ich liebe dich!

'*Everything is better together*'

Liefs Anke

Biografie

Anke Jourika Laskewitz werd geboren op 9 februari 1982 te Leeuwarden. Aan het Piter Jelles Montessori (voormalig Slauerhoff college) in Leeuwarden behaalde zij in 2000 haar VWO-diploma, waarna ze aan de studie Biologie begon aan de Rijksuniversiteit Groningen. Na een specialisatie in de richting Medische Biologie volgden twee afstudeer stages. De eerste werd uitgevoerd bij de afdeling Immunologie & Histologie van de afdeling celbiologie van het Universitair Medisch Centrum Groningen onder leiding van Prof. dr. Nico Bos. De bevindingen van deze stage werden geraporteerd in een verslag getiteld 'Inductie van CD70-gemedieerde apoptose in multiple myeloma'. De tweede stage werd uitgevoerd bij het Department of Biology aan de University of Pennsylvania onder leiding van Prof. dr. Mecky Pohlschröder. Deze stage leide tot een auteurschap de publicatie in het Journal of Bacteriology (feb 2006; 188(4):1251-9), getiteld 'Archaeal and bacterial SecD and SecF homologs exhibit striking structural and functional conservation'. Vervolgens werd de studie afgesloten met een scriptie bij de afdeling medische biologie onder leiding van Prof. dr. Ingrid Molema en een colloquium bij de afdeling kindergeneeskunde bij Prof. dr. Folkert Kuipers.

Na het behalen van het doctoraal Medische Biologie in januari 2006, begon zij aan een promotieonderzoek op TiPharma project 'glucocorticoïd-geïnduceerde insuline resistentie' in het laboratorium van de afdeling kindergeneeskunde met als promotores Prof. dr. Folkert Kuipers en Prof. dr. Bert Groen. De bevindingen van dit onderzoek staan beschreven in dit proefschrift. Vanaf 1 december 2011 is Anke in opleiding tot klinisch chemicus bij stichting KCL Leeuwarden verbonden aan het Medisch Centrum Leeuwarden.

Biography

Anke Jourika Laskewitz was born on the 9th of february 1982 in Leeuwarden, the Netherlands. In 2000 she graduated from high school (Piter Jelles college Montessori) and started a Master degree in Medical Biology at the University of Groningen. As an undergrad student she worked in the department of Immunology and Histology at the University Medical Center Groningen under supervision of Prof. dr. Nico Bos on CD70-induced apoptosis in Multiple Myeloma. A second internship was performed at the Department of Biology at the University of Pennsylvania in the lab of Prof. dr. Mecky Pohlschröder. This internship resulted in an authorship on the paper 'Archaeal and bacterial SecD and SecF homologs exhibit striking structural and functional conservation' in the Journal of Bacteriology (feb 2006; 188(4):1251-9). This study was finished with a Master thesis at the department of medical biology under supervision of Prof. dr. Ingrid Molema and a colloquium at the Department of Pediatrics under supervision of Prof. dr. Folkert Kuipers at the University Medical Center Groningen.

After obtaining her masters degree in Medical Biology in 2005, she started a PhD in the Laboratory of Pediatrics at the University Medical Center Groningen under supervision of Prof. dr. Folkert Kuipers and Prof. dr. bert Groen. This project was financed by the TiPharma. The results obtained in this research project are described in this thesis. On the first of December 2011 Anke started as a clinical chemist in training at the clinical chemistry laboratory at the Medical Center Leeuwarden.